

PLASTIC DERIVED BITUMEN MODIFIERS (W-BINDER) FROM PYROLYSIS
IN SUSTAINABLE ROAD CONSTRUCTION

CHARLOTTE LOUISE ABDY

Doctor of Philosophy

ASTON UNIVERSITY

June 2023

©Charlotte Louise Abdy, 2023

Charlotte Louise Abdy asserts their moral right to be identified as the author of
this thesis

This copy of the thesis has been supplied on condition that anyone who
consults it is understood to recognise that its copyright belongs to its author and
that no quotation from the thesis and no information derived from it may be
published without appropriate permission or acknowledgement.

Aston University

Plastic Derived Bitumen Modifiers (w-Binder) from Pyrolysis in Sustainable Road Construction

Charlotte Louise Abdy

Doctor of Philosophy

2023

Thesis Summary

There are current largescale efforts within the paving industry to move towards the use of sustainable binder alternatives to bitumen, which is a non-renewable and highly impacting resource. The use of waste plastics as binder materials within asphalt concrete is considered as a practical and cost-effective alternative, especially as the growth of new recycling capacities is becoming more crucial. Furthermore, plastic-derived bitumen modifiers from the thermochemical treatment of plastics could be a viable solution to the current limitations associated with plastic bitumen modifiers (PMB), while producing asphalt with enhanced rheological properties and failure resistances.

This study provides a novel contribution to outlining the potential of high-density polyethylene (HDPE) thermal pyrolysis waxes in the modification of bitumen (w-binder) and subsequent hot mix asphalt (HMA) mixtures (w-asphalt), as well as in reclaimed asphalt (RAP) rejuvenation. In the interest of product and process optimisation, it establishes key relationships between pyrolysis process parameters, the chemical and thermal properties/ mechanisms of the wax modifiers and the rheological and mechanical performance of the modified binders/mixtures. Finally, dense graded asphalt concrete modified with an optimal HDPE pyrolysis wax (6 wt% of the binder) and 20% RAP was produced and its resistance to key pavement deterioration modes was determined.

The optimal wax was produced at higher pyrolysis temperatures and nitrogen flowrates (having the lowest vapour residence times.) Such process parameters had a crucial role in the resultant wax chemistry and thermal ageing behaviours. Oxidation and polymerization reactions were key mechanisms identified during wax thermal ageing and their effect on the resultant binder and mixture properties were highlighted. The asphalt mixtures produced had enhanced or unaffected resistance to the key failure modes studied, with the RAP + HDPE pyrolysis wax mixture showing superior performance. The HDPE pyrolysis wax acted as a sufficient rejuvenating agent to mitigate the otherwise adverse effects to fatigue resistance of high RAP content in HMA mixtures. This application of plastic pyrolysis wax could help to reduce the amount of non-renewable materials used for HMA production, increasing the usage of recyclable and secondary materials within flexible pavements in the effort to approach a circular economy.

Keywords: Waxes; High-density polyethylene; Thermal degradation; Hot mix asphalt; RAP rejuvenators

Dedication

To Tori Abdy, Lisa Abdy, Jake Hunt & Luna, for their constant love and support.

Acknowledgments

I would like to express my sincere gratitude to my main supervisor, Dr. Yuqing Zhang for this research opportunity and his constant guidance and support over the years. From him I have learnt many valuable technical skills within pavement engineering and sincerely appreciate this time under his supervision. Thank you for your teaching, advice, and continuous effort to ensure that I had all the necessary resources to complete the work required for this thesis.

I would also like to sincerely thank my associate supervisor, Dr. Jiawei Wang for his continuous support and valuable suggestions and comments on my work. Thank you for stepping in as main supervisor in my final year and always being available to provide advice, especially regarding career opportunities and next steps. Many thanks to my viva voce examiners, Dr. Nick Thom, and Dr. Zhentao Wu, for their insightful comments on my work.

I appreciate the financial support provided by Aggregate Industries to make this combined research effort possible. Many thanks to Ignacio Artamendi, Bob Allen as well as Chris Allpress and everyone at the AI labs who welcomed me during my week visit and their help with mixture design and formulation. My appreciation is extended to Elisha Francis for her support within the Aston labs.

I also would like to express my sincere appreciation to my current and former colleagues who made my PhD journey smoother and more enjoyable; many thanks to Dr. Huan Xiang, Hanyu Zhang, Dr. Eman Lafta Omairey, Dr. Yangming Gao and Dr. Linglin Li for their support and encouragement.

My deepest gratitude goes to my mother and sister for their selfless love and endless support. Special thanks to Mr. Jake Hunt and Luna, for their love, patience, and encouragement.

I appreciate the additional financial support provided by Aston University via a PhD studentship to make this research possible.

This doctoral thesis consists of the following publications:

1. C. Abdy, Y. Zhang, J. Wang, Y. Yang, I. Artamendi, and B. Allen, "Pyrolysis of polyolefin plastic waste and potential applications in asphalt road construction: A technical review," *Resources, Conservation and Recycling*, vol. 180, p. 106213, 2022.
2. C. Abdy, Y. Zhang, J. Wang, Y. Cheng, I. Artamendi, and B. Allen, "Investigation of high-density polyethylene pyrolyzed wax for asphalt binder modification: Mechanism, thermal properties, and ageing performance," *Journal of Cleaner Production*, vol. 405, p. 136960, 2023.
3. C. Abdy, Y. Zhang, J. Wang, Y. Cheng, I. Artamendi, and B. Allen, "High-Density Polyethylene Pyrolysis Wax in Asphalt Binder 'w-binder' Modification," *Under Review*
4. C. Abdy, Y. Zhang, J. Wang, Y. Cheng, I. Artamendi, and B. Allen, "Pyrolysis Wax Binder Additives from High-Density Polyethylene in Hot Mix and Reclaimed Asphalt Mixtures: A Laboratory Study," *Under Review*

Table of Contents

Thesis Summary	2
Dedication	3
Acknowledgments	4
Table of Contents	6
List of Figures.....	10
List of Tables.....	13
CHAPTER 1: Introduction.....	14
1.1 Background.....	14
1.2 Problem Statement	16
1.3 Research Aim & Methodology.....	18
1.4 Thesis Outline	19
CHAPTER 2: Literature Review	22
2.1 Background.....	22
2.2 Plastic Waste Management	25
2.3 Pyrolysis of Polyolefin Plastics.....	28
2.3.1 Polyolefins in Plastic Solid Waste Streams	28
2.3.2 Plastic Recycling via Pyrolysis.....	30
2.3.3 Pyrolysis Mechanism	35
2.3.4 Pyrolysis of Polyolefin Plastics for Oil & Wax Production	36
2.4 Asphalt Pavement.....	40
2.4.1 Bitumen	42
2.5 Pavement Failures	45
2.5.1 Fatigue Cracking.....	46
2.5.2 Rutting	46
2.6 Polyolefin Plastics in Road Construction.....	47
2.6.1 Flexible Road Materials	47
2.6.2 Polyolefin Modified Asphalt Binders.....	49
2.6.3 Polyolefin Modified Asphalt Binder Performance	52
2.6.4 Polyolefin Modified Asphalt Mixture Performance	54
2.6.5 Technical Limitations	56
2.6.6 Life Cycle Analysis and Cost Assessment.....	58
2.7 Pyrolysis Polyolefins in Road Construction.....	60

2.7.1 Wax in Bitumen	63
2.7.2 Wax Technologies in Asphalt Pavement	64
2.7.2.1 Warm-Mix Asphalt	64
2.7.2.2 Reclaimed Asphalt Pavement	66
2.7.3 Plastic Pyrolysis Wax: Established & Potential Applications.....	68
2.8 Summary	71
CHAPTER 3: Experimental Programme	74
3.1 Introduction	74
3.2 Materials	74
3.2.1 High-Density Polyethylene.....	74
3.2.2 Asphalt Binder	75
3.3 Thermal Pyrolysis of HDPE	75
3.4 w-Binder Production.....	77
3.5 Wax and Binder Characterisation	78
3.5.1 Gas Chromatography-Mass Spectroscopy (GC-MS).....	78
3.5.1.1 Mass Response Factor (RF) Calculation.....	80
3.5.2 Thermogravimetric Analysis (TGA).....	81
3.5.3 Differential Scanning Calorimetry (DSC)	83
3.5.4 Wax Ageing Experiment	84
3.5.5 Fourier Transform Infrared Spectroscopy (FTIR).....	85
3.5.5.1 FTIR Calculation for Oxidative Ageing Indexes	86
3.5.6 Penetration Test	88
3.6 Binder Performance Tests	89
3.6.1 Dynamic Shear Rheometer	89
3.6.2 Rolling Thin Film Oven Test (RTFO)	94
3.6.3 Pressure Ageing Vessel (PAV) Test.....	95
3.6.4 Frequency Sweep (FS) Test.....	96
3.6.4.1 Master Curve Construction.....	96
3.6.4.2 Black Diagram	98
3.6.4.3 Complex Viscosity	98
3.6.5 Rutting factor	100
3.6.6 Shear Fatigue Tests	102
3.6.6.1 Linear Amplitude Sweep (LAS) Test	103
3.6.6.2 Time Sweep (TS) Test.....	104
3.6.6.3 Mechanistic Modelling of Crack Growth	105

3.6.7 Dispersity – Optical Microscope	106
3.7 Asphalt Mixture Formulation	107
3.7.1 Asphalt Binder	107
3.7.2 Aggregates	108
3.7.3 Mixing and Compaction	109
3.8 Asphalt Mixture Performance Tests	111
3.8.1 Indirect Tensile Stiffness Modulus (ITSM) Test	111
3.8.2 Indirect Tensile Fatigue Test (ITFT).....	113
3.8.2.1 Mechanistic Modelling of Cracking Damage.....	114
3.8.3 Repeated Load Axial Test (RLAT).....	115
3.8.4 Indirect Tensile Strength (ITS) Test.....	117
3.9 Summary	119
CHAPTER 4: High-Density Polyethylene Pyrolyzed Wax: Mechanism, Thermal Properties, and Ageing Performance	120
4.1 Overview	120
4.2 Pyrolysis Yields.....	120
4.3 Wax Chemical Characterisation.....	123
4.3.1 FTIR Analysis	123
4.3.2 GC-MS Analysis	124
4.4 Wax Thermal Characterisation.....	128
4.4.1 TGA Analysis	128
4.4.2 DSC Analysis.....	129
4.5 Thermal Ageing of Waxes.....	131
4.5.1 Mass Loss	131
4.5.2 Chemical Characterisation.....	132
4.6 Summary	137
CHAPTER 5: High-Density Polyethylene Pyrolysis Wax in Asphalt Binder ‘w-Binder’ Modification.....	138
5.1 Overview	138
5.2 w-Binder Rheological Testing	138
5.2.1 Needle Penetration	138
5.2.2 Frequency Sweep Test Analysis	140
5.2.3 Black Space Diagrams	142
5.2.4 Complex Viscosity	145
5.3 w-Binder Fatigue Performance	146

5.3.1 LAS and TS Tests.....	146
5.3.2 Crack Growth Modelling	148
5.4 w-Binder High-Temperature Performance	149
5.5 Chemical Characterisation	151
5.5.1 Modification Mechanism	151
5.6 Ageing Performance	153
5.6.1 Rheological properties of aged w-Binders	153
5.6.2 Mass Loss during Ageing	155
5.6.3 Ageing Indexes from FTIR.....	156
5.7 w-Binder Dispersity	159
5.8 Summary	161
CHAPTER 6: Pyrolysis Wax Binder Additives from High-Density Polyethylene in Hot Mix and Reclaimed Asphalt Mixtures	163
6.1 Overview.....	163
6.2 Compactability	163
6.3 Indirect Tensile Stiffness Modulus Test (ITSM).....	165
6.4 Indirect Tensile Fatigue Test (ITFT).....	167
6.5 Repeated Load Axial Tests (RLAT)	170
6.6 Indirect Tensile Fatigue (ITS) Test & Moisture Resistance	173
6.7 Summary	174
CHAPTER 7: Conclusions and Recommendations	176
7.1 Conclusions	176
7.2 Recommendations	178
References.....	180
Appendices.....	204

List of Figures

Figure 1.1	Research Workflow	21
Figure 2.1	Design from Recycling Concept Key Aspects, adapted from [45].	24
Figure 2.2	Plastic solid waste management methods including four valorisation routes, adapted from [52, 53].	27
Figure 2.3	Schematic diagram of the intermediate pyrolysis system (1) Feeder; (2) Feed Inlet; (3) The Pyrolysis Reactor; (4) Heating Jackets; (5) Outer Screw; (6) Inner Screw; (7) Vapour Outlet; (8) Stands; (9) Char Outlet and Char Pot; (10) Motor; (11) Shell and Tube Condenser; (12) Liquid Vessel; (13) Electrostatic Precipitator [90].	31
Figure 2.4	Radical mechanism of the thermal degradation of polyethylene, taken from [65, 106].	36
Figure 2.5	Typical cross-section of a conventional flexible pavement [114].	41
Figure 2.6	The colloidal structure of SARA fractions in bitumen, adapted from [120].	42
Figure 2.7	Typical molecular structure of the saturate fraction in bitumen [121].	43
Figure 2.8	Typical molecular structure of the aromatic fraction in bitumen [121].	43
Figure 2.9	Typical molecular structure of the aromatic fraction in bitumen [121].	44
Figure 2.10	Possible molecular structures present within the asphaltene fraction [121].	44
Figure 2.11	Pavement response to traffic loading, adapted from [124].	45
Figure 2.12	Fatigue ‘alligator’ cracking in asphalt pavement [126].	46
Figure 2.13	Figure 2.12 Rutting in asphalt pavement [127].	47
Figure 2.14	Thermal degradation stirred reactor system for pyrolysis PP, used by Al-Hadidy et al [192].	61
Figure 2.15	Established and on-going researched applications/upgrading routes for plastic pyrolytic waxes within the petrochemical and industries.	70
Figure 3.1	Schematic diagram of the bench scale pyrolysis reactor system used in this study.	76
Figure 3.2	w-Binder production program summary.	77
Figure 3.3	Typical GC-MS instrument configuration, [217].	78
Figure 3.4	Typical chromatogram for paraffin wax, [218].	78
Figure 3.5	Thermogravimetric Analyser.	81
Figure 3.6	Typical TGA/DTG curves obtained for HDPE [222].	81
Figure 3.7	A typical DSC experimental configuration, [224].	82
Figure 3.8	A typical DSC thermogram of heat absorbed versus temperature for polymers, adapted from [225].	83
Figure 3.9	Pyrolysis waxes in ceramic crucibles for short-term ageing test.	84

Figure 3.10	FTIR-ATR principle of operation.	85
Figure 3.11	Typical FTIR spectrum obtained for long-term aged bitumen, demonstrating key functional groups for oxidation assessment and different band area integration methods. Adapted from [228].	87
Figure 3.12	The penetration test: configuration and set-up, adapted from [232].	88
Figure 3.13	Basic principle of the Dynamic Shear Rheometer (DSR), [167].	89
Figure 3.14	Phase lag between the applied sinusoidal strain and stress response, adapted from [236].	90
Figure 3.15	Relationship between the complex shear modulus, storage modulus (elastic component), loss modulus (viscous component) and phase angle.	92
Figure 3.16	DSR test equipment with plate geometries.	93
Figure 3.17	RTFO oven.	94
Figure 3.18	RTFO sample bottles.	94
Figure 3.19	PAV sample pan.	94
Figure 3.20	PAV test set-up.	94
Figure 3.21	A typical master curve and its construction, adapted from [247].	95
Figure 3.22	A typical black diagram for bitumens modified with different chain length Fischer-Tropsch waxes, [197].	97
Figure 3.23	A typical isochronal plot of the $\log \eta^*$ versus temperature and log-log plot of the η^* versus ω , [253].	99
Figure 3.24	Typical plot of $G^*/\sin\delta$ as a function of temperature, adapted from [259].	100
Figure 3.25	The (G_0^*) and (δ_0) determined from LAS test results, [261].	102
Figure 3.26	A typical stress versus strain curve obtained from the LAS test, [266].	103
Figure 3.27	Typical results of time sweep (TS) test, from which (G_N^*) and (δ_N) may be obtained [261].	103
Figure 3.28	Evolutions of crack length for bio-oil modified bitumen, [264].	104
Figure 3.29	OSTEC RAMOS S120 microscope.	105
Figure 3.30	Example of glass slide samples.	105
Figure 3.31	(Top) Target particle size distribution of the mixtures used in this investigation; (Bottom) RAP particle distribution.	108
Figure 3.32	(Left) Mechanical asphalt mixer; (Right) Laboratory Roller Compactor.	109
Figure 3.33	The configuration of the ITSM test in the UTM-HDY machine.	111
Figure 3.34	The configuration of the ITFT test in the UTM-HYD machine.	112
Figure 3.35	Configuration of the RLAT test in the UTM-HYD machine.	115
Figure 3.36	Typical raw data from the RLAT for asphalt mixtures.	115
Figure 3.37	Configuration of the ITS test in the UTM-HYD machine.	117

Figure 3.38	Typical data presentation for the ITS and TSR for asphalt mixtures, [280].	117
Figure 4.1	Yields (wt%) of wax with respect to the reactor operating conditions.	121
Figure 4.2	FTIR Spectra for HDPE Pyrolysis Waxes. ('450-2' stands for pyrolysis wax produced at 450 °C using a 2 L min ⁻¹ nitrogen flowrate, etc.)	123
Figure 4.3	Representative TGA and DTG thermograms for each pyrolysis wax thermal degradation as a function of pyrolysis conditions ('450-2' stands for pyrolysis wax produced at 450 °C using a 2 L min ⁻¹ nitrogen flowrate, etc.)	128
Figure 4.4	Mass loss of pyrolysis waxes with thermal conditioning.	131
Figure 5.1	Penetration points of the control and wax modified asphalt binders at 25 °C. (450-6%' stands for a 6 wt% dosage of the pyrolysis wax produced at 450 °C.)	138
Figure 5.2	Master curves for the complex shear modulus ($ G^* $) of the control binder and pyrolysis wax modified binders. (450-6%' stands for a 6 wt% dosage of the pyrolysis wax produced at 450 °C.)	141
Figure 5.3	Black diagrams of neat and pyrolysis wax blended binders, from 30-70°C utilising frequency sweep test parameters.	143
Figure 5.4	Complex viscosity as a function of temperature.	145
Figure 5.5	Binder crack length evolution curve of the RTFO+PAV aged neat and w-binders.	148
Figure 5.6	The $ G^* /\sin\delta$ of the neat and w-binders after short-term ageing.	149
Figure 5.7	Neat bitumen infrared spectrum, identifying main functional chemical groups.	151
Figure 5.8	FTIR spectra of the unaged neat and w-binders.	151
Figure 5.9	Master curve of the $ G^* $ for the control binder and pyrolysis wax modified binders in the: (a) short-term (RTFO) aged (b) long-term (RTFO+PAV) aged condition.	153
Figure 5.10	The mass loss of the neat and w-binders after RTFO ageing.	155
Figure 5.11	Ageing indices of the neat and w-binder at different stages of ageing: (a) Sulfoxide Index, (b) Carbonyl Index.	157
Figure 5.12	Optical microscope images of the control and w-binders for evaluation of dispersity in the unaged condition: (a) 40/60, (b) 450-6%, (c) 450-12%, (d) 500-6%, (e) 500-12%, (f) 550-6%, (g) 550-12%.	159
Figure 6.1	Frequency distribution of air void content of the control and test mixtures.	164
Figure 6.2	ITSM master curves for the stiffness modulus of the control and test mixtures.	166
Figure 6.3	The average number of cycles to failure (N_f) for each mixture, determined by the peak of the E_{ratio} vs. N curve.	168
Figure 6.4	(Top) The damage density (169

Figure 6.5	Averaged RLAT results of the control and test mixtures at test. temperature 40 °C.	171
Figure 6.6	Calculated creep rate, f_c of the control and test mixtures.	171
Figure 6.7	Average ITS values of unconditioned (dry) and conditioned (wet) specimens from each mixture and TSR values.	173

List of Tables

Table 2.1	Chemical structures, properties, and examples of applications for polyolefins HDPE, LDPE, and PP, collated from [69, 70].	29
Table 2.2	Summary of example studies investigated as a chemical treatment for virgin/waste polymers in laboratory micro-, bench and pilot scale.	32
Table 2.3	Key advantages and limitation for the pyrolysis of PSW.	34
Table 2.4	Pyrolysis technologies and parameters used in literature for polyolefin pyrolysis with resultant product wax yields.	39
Table 2.5	Existing studies using virgin or waste Polyolefins HDPE/LDPE/PP in Polymer-Modified Bitumen Binders (PMBs) and Asphalts (PMAs.)	50
Table 3.1	Grade designation properties of Azalt® 40/60 asphalt binder.	74
Table 3.2	Pyrolysis conditions.	75
Table 3.3	Grade designation properties of Azalt® 70/100 asphalt binder.	106
Table 4.1	Distribution in weight percentage of hydrocarbons in each pyrolysis wax sample and percentile distribution in gasoline and high MW categories, as well as class of components.	124
Table 4.2	Onset and peak melting points of the pyrolysis waxes using DSC.	130
Table 4.3	Distribution in weight percentage of molecular weight and class of hydrocarbons in pyrolysis waxes (450-2, 500-2 and 550-2) after thermal conditioning at 170 °C from 0-6 hours.	135
Table 5.1	Phase angle of neat and w-binders at loading frequency of 1.59 Hz for two different temperatures.	154
Table 6.1	Descriptive statistics for the air void content of the control and test mixtures.	164

CHAPTER 1: Introduction

1.1 Background

Recently, plastomers such as High-Density Polyethylene (HDPE) have contributed to a significant increase in disposable medical waste as a result of the COVID-19 pandemic [1]. The identification of sustainable valorisation routes for 'end-of-life' plastic waste such as this is becoming more crucial. One emerging trend in research and an application that is considered both practical and cost-effective is the incorporation of these plastics into asphalt binders as a partial replacement, typically at modification levels between 3% and 5% weight of the binder [2,3]. The material performance enhancements achieved with polyethylene-modified bitumen can include an improved resistance to rutting and fatigue cracking; lowered thermal, degradation, moisture and stripping susceptibility; and an enhanced Marshall stability [4]. Yet, this approach has not yet gained widespread acceptability in practise and commercialisation due to its associated technical limitations. These can include higher binder viscosity and reduced workability, thus raising the production temperature and energy requirements; poor low temperature performance; low chemical compatibility and poor storage stability; poor dispersion of the plastic modifiers in bitumen, with high mixing times and temperatures that lead to excessive aging; and the indeterminate performance of higher blend ratios [2, 4-7].

Bituminous asphalt binders naturally contain microcrystalline and amorphous waxes containing branched, alicyclic, and aromatic components [8]. Due to current refinery processes of straight run bitumen, this wax is low in content and does not particularly influence the binder or subsequent asphalt properties. However, commercial waxes have gained recent attention as binder viscosity improvers, especially for high viscosity/low workability binders such as polymer-modified and rubberised bitumen, as well as mixtures that contain reclaimed (RAP) binders and aggregates. Their purpose is to reduce the process temperature and energy requirement, in turn lowering both production cost as well as emissions [9-12]. When utilised as a warm-mix asphalt (WMA)

technology, they have been observed to achieve reduced process temperatures of 100-140 °C. Furthermore, achieving a lower void content due to improved compaction would make pavements denser and more robust. Typical viscosity lowering additives used for bitumen are Fischer-Tropsch (FT) paraffin, polyethylene and Montan waxes [8]. In particular, polyethylene wax is a low molecular weight binder additive that has previously been incorporated into polymer-modified WMA and reported to enhance the fatigue, moisture, and temperature cracking resistances, as well as rutting in some instances [15-17]. Waste polyolefin plastics can be treated via thermochemical processes such as pyrolysis to produce value-added products including polyethylene waxes.

Pyrolysis involves the heating of plastics to moderate-severe temperatures (<800 °C) in an inert atmosphere. At moderate process temperatures (500 °C), aliphatic waxes are the primary product as well as pyrolytic oil containing high contents of heavy hydrocarbon waxes [18, 19]. Literature review work conducted within this thesis has highlighted the current scope of established applications for these wax products, with a general lack identified outside of the alternative fuel and chemical feedstock industries [4]. Comprehensive research is necessary to fully explore the potential of polyethylene pyrolysis wax within asphalt binder modification, to ensure commercial viability and profitability for this circular economy application. As a hot-mix asphalt (HMA) binder additive, it may negate the technical limitations of plastic modifiers. Furthermore, it may provide rejuvenating as well as similar technical advantages to current commercial viscosity reducing waxes, when used as an additive with RAP.

Previously, blends of pyrolysis oils and waxes from waste rubber and plastic feedstocks have been incorporated at 5 wt% into bitumen, enhancing the workability and mechanical properties of the binders and increasing resistance to rutting, fatigue and low-temperature cracking [12]. Pyrolyzed low-density polyethylene (LDPE) has been incorporated at 2-8 wt% into bitumen, demonstrating increased compatibility with the bitumen to an extent. The resultant admixtures had improved resistances to temperature, permanent deformation, and moisture, as well as increased Marshall stability [20]. The

pyrolysis wax produced from fresh and waste HDPE has been used in a composite binder (polymer-modified binder, styrene-butadiene-styrene (SBS) and other functional additives) at a 2 wt% dosage. The composite wax modified binder had a reduced the binder viscosity and while increasing the $|G^*|$, it also reduced the δ values and had an improved rutting resistance [21].

Within this context, this thesis aims to further provide a baseline of understanding of the interactions between HDPE pyrolysis process parameters, the product wax characteristics and resultant HDPE pyrolysis wax modified binder ('w-binder') performance in HMA. These key relationships have not yet been fully explored by the previous works described within this particular scope of research. This baseline may then be applied for the pyrolysis waxes obtained from other end-of-life materials, providing a full understanding of the benefits of this application, from a circular economy perspective. Furthermore, extensive characterisation of the waxes can provide an insight into their use as RAP rejuvenating agents, when used in conjunction within the current standard type of rolled mixed asphalt.

1.2 Research Questions

Literature review work within this thesis details the current scope of established applications for the main wax product obtained from plastic thermal pyrolysis, with a sizeable research gap identified outside of petrochemical and chemical feedstock industries [2]. This gap in literature can be attributed to a lack in the extensive characterisation for this product to match it with potential applications. Furthermore, there is a large absence of research knowledge in the sole capacity of fully degraded polyolefin pyrolysis products and their capacities as flexible pavement materials, such as in asphalt binder and mixture modification. Additionally, there has also been no comprehensive attempt to form relationships between the pyrolysis parameters used and the resultant effects of pyrolysis products on the asphalt binder performance, from chemical/thermal and mechanical/rheological standpoints.

With further consideration of the desired application, conventional flexible roads are prone to deterioration as a result of multiple factors, namely traffic loading, construction practices and thermal susceptibility of the asphalt materials [31,32]. Therefore, the addition of plastic-derived wax products and reclaimed materials should be adopted with the aim of enhancing bitumen and subsequent HMA performance over the service temperatures and timescales associated with the main modes of pavement failure.

With these identified research gaps and considerations, the key research questions of this study have been selected:

1. How can pyrolysis process conditions effect the quality of the product waxes from pure HDPE pellets, in terms of chemical composition and thermal characteristics. Moreover, how can the resultant wax chemistry impact the thermal ageing mechanisms that occur to both the wax upon its incorporation into bitumen, as well as the wax modified bitumen throughout its service life (in terms of evaporation, oxidation, and polymerization reactions.) Identifying such relationships are in the interest of product and process optimisation. Likewise, this point of investigation may highlight the requirement of additional stabilising additives within this practical application.
2. As a result of the chemical and thermal ageing characteristics, can the pyrolysis waxes be effectively added to bitumen at reduced blending times and temperatures to typical polymer-modified bitumen production, achieving good dispersity. Furthermore, how can these properties impact the rheological, mechanical, thermal and workability performance of the resultant w-binders. This investigation will determine if the plastic-derived waxes negate the technical limitations of conventional polymer-modified binders, especially in terms of high and low temperature performance.
3. Finally, in the interest of waste management and circular economy, can HDPE pyrolysis waxes be paired with end-of-life road materials (RAP) to increase the total amount of recyclables used within asphalt flexible pavements, while improving vital failure resistances. This will determine if HDPE pyrolysis wax

may be suitable for RAP rejuvenation applications. A selected wax dosage will be selected for this investigation, dependent on optimum enhancement to the bitumen as demonstrated by the previous research outcomes.

1.3 Research Aim & Methodology

This work aims to provide a baseline of understanding of the interactions between HDPE pyrolysis process parameters, the product wax characteristics and resultant plastic pyrolysis wax modified binder ('w-binder') performance in HMA. This baseline of understanding may then be applied for waxes from other plastics as well as waste plastics, further increasing the amount of recyclable material within flexible pavements to approach a circular economy. To achieve this research aim, the study was divided into three phases (which are further illustrated in Figure 1.1,) each with their own research objectives:

Phase 1: Establish the thermal pyrolysis mechanisms of HDPE and the relationships between the process operating parameters and resultant wax chemical and thermal properties. Also, determine the thermal stability and ageing mechanisms that occur to the waxes upon incorporation and blending with the bitumen. This will enable the suggestion of a suitable blending protocol for the w-binders and later aid in providing an understanding of the wax's behaviour as a modifier material, from a chemical perspective.

Phase 2: Produce w-binders with a lower (6wt%) and higher (12wt%) modification level of HDPE pyrolysis wax, using the suitable blending protocol suggested in Phase 1. Determine the relationships between the chemical and thermal properties of the waxes and their rheological and mechanical performance via the utilization of rheological, chemical, and thermal characterisation techniques. This will also allow for the selection of an optimal wax/wax dose to take forward for w-asphalt formulation.

Phase 3: Investigate the resistance of HDPE pyrolysis wax modified asphalt mixtures (w-asphalt) to the key modes of failure within HMA. This will be achieved through a series of mechanical performance mixture tests. Additionally, establish

the rejuvenating capacity of the pyrolysis wax modified binders when incorporated into HMA with 20% RAP.

1.4 Thesis Outline

This thesis is composed of two journal papers that have been published and two papers that have been submitted for review. The contents of these papers have been modified and dispersed throughout the document into relevant chapters to ensure article flow and avoid repetitions. Additional information was included in the literature review and methodology to further expand on the research scope and testing principles. The thesis includes seven chapters and is organised as follows:

Chapter 1 presents an introduction, including background, problem statement, research objectives/workflow and thesis outline.

Chapter 2 presents a comprehensive technical review which: introduces current plastic waste management methods; the thermal pyrolysis of plastic waste polyolefins, with a heavy focus on wax production; exploration into the current use of polyolefin plastics in HMA, including the achievable property enhancements of PO plastic asphalt (binder) modification, the associated limitations from a technological and environmental standpoint, as well as life cycle and economic assessment data; provides a discussion on plastic wax-based warm mix asphalt (WMA) technologies and the potential use of PO plastic-derived wax products from pyrolysis as a modifier with similar properties in HMA. The technical review in this chapter has been published as a paper in *Resources, Conservation and Recycling*, [2].

Chapter 3 presents the laboratory experimental work performed in this study. It details the materials used, followed by the experimental principles, setups, and data analyses.

Chapter 4 presents the thermal pyrolysis of HDPE, in which pyrolysis mechanisms and wax yields are described, and relationships between the process operating parameters and resultant wax chemical and thermal properties

are established. It additionally focuses on the thermal properties and ageing performance of the waxes, especially with regards to volatile loss and the proposed ageing mechanisms that occur. These characterisations allow for the selection of optimal waxes to be taken forward to the next phase for blending with bitumen. The optimum blending conditions are also suggested. This chapter is a paper published in the *Journal of Cleaner Production*, [33].

Chapter 5 presents the relationships between the chemical and thermal properties of the waxes and their rheological and mechanical performance, allowing for the selection of an optimal wax to take forward for w-asphalt formulation. An extensive investigation using shear fatigue tests and a DSR based crack growth model (DSR-C) is employed. The ageing mechanisms of the w-binders are explored as a continuation of the investigation into the thermal and oxidative stability of the waxes within this application.

Chapter 6 presents the laboratory performance investigation of HMA mixtures with the incorporation of high-density polyethylene (HDPE) wax that has been obtained via thermal pyrolysis and up to 20% RAP. Mixture resistances to the key modes of failure within HMA are investigated using standard procedures including mixtures' stiffness, fatigue, rutting, fracture, and moisture susceptibility.

Chapter 7 presents the summaries and conclusions from the thesis as well as recommendations for future studies.

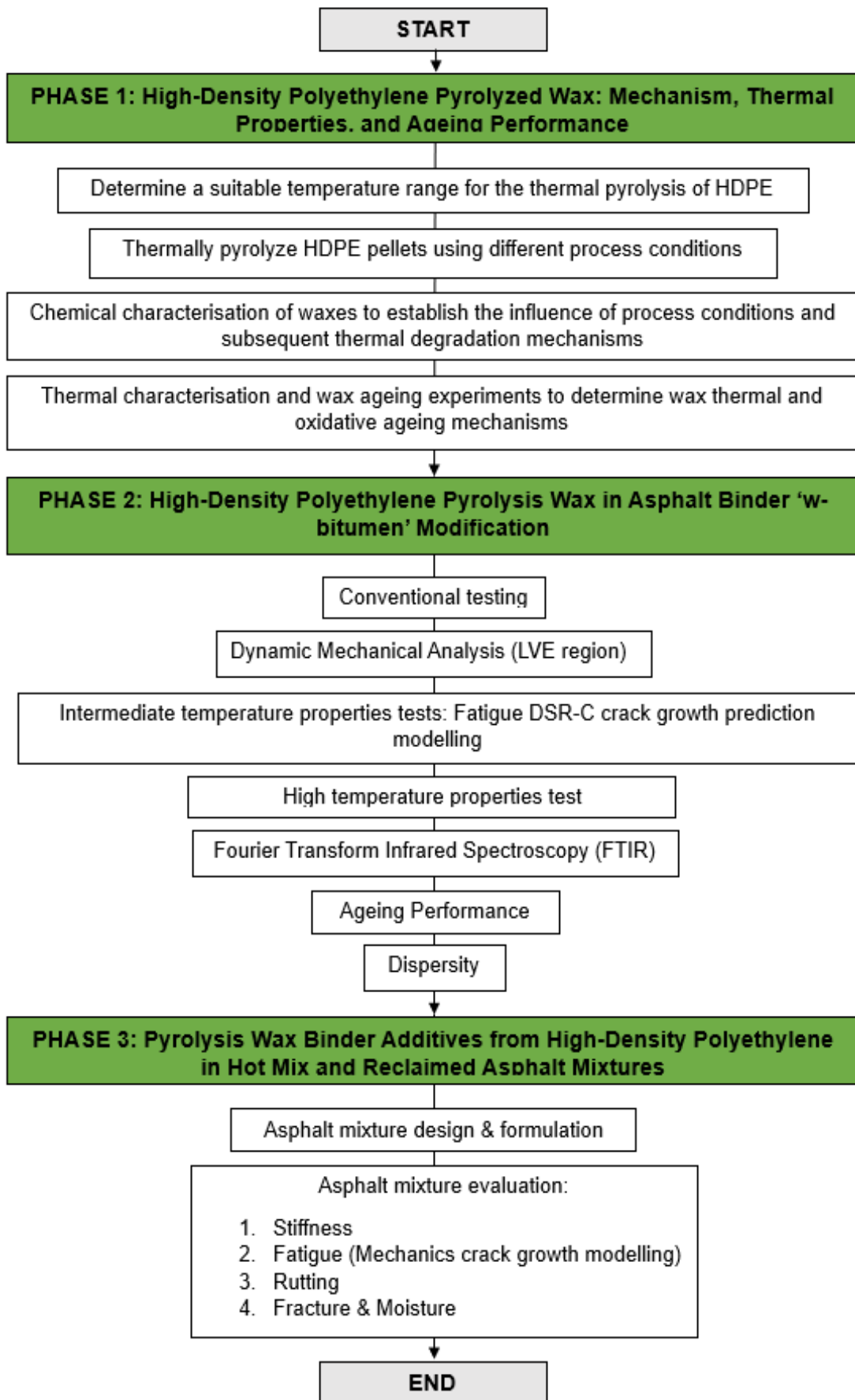


Figure 1.1 Research Workflow.

CHAPTER 2: Literature Review

2.1 Background

To increase Europe's sustainability and resource efficiency as part of the European Commission's Circular Economy Plan (CEP), concepts such as Industrial Symbiosis have recently been promoted. Industrial symbiosis is the process by which wastes, or by-products of an industry or industrial process become the raw materials to be used in a more sustainable way [34, 35]. Moreover, the document published by the European Commission entitled 'Roadmap to a Resource Efficient Europe' emphasises the role that waste should play in boosting the economy and viewing it as a resource by the year 2020 [36]. Therefore, there is increasing importance in the investment of research examining the innovative ways of using wastes such as recycled plastics as a resource. In 2018, global plastics production reached 359 million tonnes, with Europe producing 61.8 million tonnes of that total. Correspondingly, of the 29.1 million tonnes of European post-consumer plastic waste collected in the same year, only 32.5% of the waste was sent to recycling facilities [37].

A major portion of the plastic produced each year is used to make disposable items of packaging or other short-lived 'single use' products that are discarded within a year of manufacture [38]. Polyolefin (PO) plastics such as High-Density Polyethylene (HDPE), Low-Density Polyethylene (LDPE) and Polypropylene (PP) make up the majority of municipal plastic waste streams and have had a recent demand surge due to their versatility in single-use medical applications, mainly due to the COVID-19 pandemic [39]. Plastic is a petroleum-based material, and its rising demand has led to the increased depletion of the non-renewable fossil fuel, indicating that our current use of plastics is not sustainable [40]. With the rising demand and consumption of this inexpensive, non-biodegradable material and its recycling still at a low rate, the sheer accumulation and disposal of end-of-life plastic solid waste (PSW) is now a great problem. In 2019, the EU exported 1.5 million tonnes of plastic waste mostly to recycling facilities in Turkey and Asian countries. This share of exported plastic

waste to countries such as China has recently fallen significantly due to the adoption of restrictions on the import of plastic waste in 2018 [41]. Additionally, as of 2021 the export of hazardous plastic waste and plastic waste that is hard to recycle from the EU to non-member countries of the Organisation for Economic Co-operation and Development (OECD) has been banned. Therefore, new sustainable recycling capacities must grow to accommodate the new tonnages of plastic waste, diverting from incineration and landfill and equally fulfilling the new EU recycling targets [42].

The potential of thermochemical technologies such as pyrolysis for the conversion of waste polyolefins to value-added products and feedstocks/new materials for other industries makes it a suitable and viable waste management route, as well as a possible contributor to achieving industrial symbiosis in the future for the plastic industry and others. A concept relevant to examining application routes for plastic wastes and advocated for by recent review works is Design from Recycling [43, 44]. This concept was adapted from the Design for Recycling schematic promoted within the framework of the CEP and entails that the secondary raw materials originating from the recycled polymer waste of a previous products end of life (EoL) is the new starting point of new product development. Its key aspects are shown in Figure 2.1, adapted from [45]. Pyrolysis could become increasingly crucial in the future as a strategy for upgrading plastics to products that can be extensively characterised and matched with applications throughout different industries.

On the other hand, following a recent push from governments and road authorities to become more sustainable, there has been an increasingly prominent trend within the pavement industry in using waste materials in hot mix asphalt (HMA) roading applications. This is in response to the need of reducing consumption of both costly virgin and increasingly scarce materials and avoiding landfilling [46]. The use of waste polyolefin plastics in asphalt modification are well documented to impart enhanced service properties over a wide range of temperatures in road paving applications, especially improving rutting resistance at high in-service temperatures as well as temperature and stripping susceptibility

[47, 48]. However, using these waste materials doesn't come without limitations, from both technical and environmental standpoints [46].

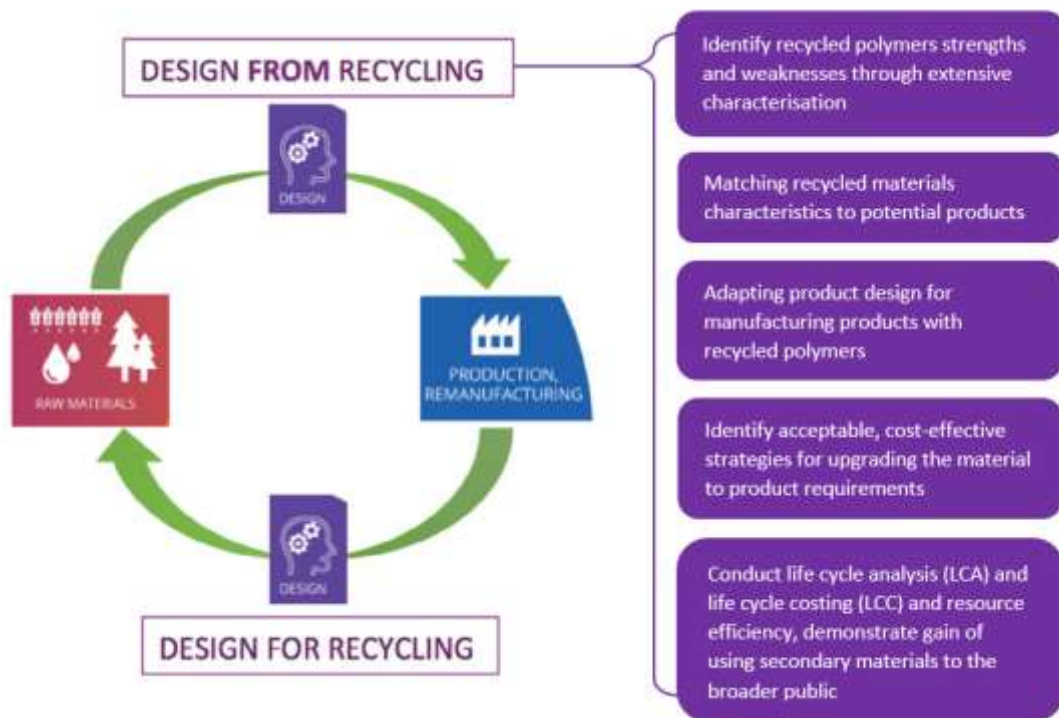


Figure 2.1 Design from Recycling Concept Key Aspects, adapted from [45].

Based on the research gaps discussed in the problem statement of this thesis and as part of phase one of the project, a literature review was conducted with the following objectives:

- 1) Discuss the current plastic waste management methods and the need for new sustainable recycling capacities.
- 2) Investigate the thermal pyrolysis process for the most abundant plastic waste polyolefins, low-density polyethylene (LDPE), high-density polyethylene (HDPE) and polypropylene (PP), with a focus on the heavy wax products.
- 3) Explore the current use of recycled PO plastics in the hot mix asphalt (HMA) layers of flexible roads as an alternative binder material and aggregate. However, its use in binder modification via wet process manufacturing techniques is mainly considered.
- 4) The achievable property enhancements of PO plastic asphalt (binder) modification, the associated limitations from a technological and

environmental standpoint, as well as life cycle and economic assessment data will be examined.

- 5) Provide a discussion on plastic wax-based warm mix asphalt (WMA) technologies and the potential use of PO plastic-derived wax products from pyrolysis as a modifier with similar properties in HMA and HMA containing reclaimed asphalt (RAP).

2.2 Plastic Waste Management

Landfilling plays an important role in current plastic solid waste (PSW) management strategies; however, this method is a non-sustainable and questionable option as the plastics remain as a lasting environmental burden. The continuous disposal of PSW and its accumulation in landfill sites has been associated with significant effects that are detrimental to both environmental quality and human health [49]. Recycling and re-use play considerable roles in the 2019 Zero Waste Europe hierarchy for achieving circularity and sustainability goals [50]. Recycling is an important PSW management method as it avoids the environmental burdens associated with landfill, while minimizing the consumption of energy and finite resources as well as reducing emissions associated with plastic production [51]. There are currently four recycling methods outlined for PSW, which are shown in Figure 2.2 as part of the plastic production chain, adapted from [52, 53].

Re-extrusion (primary) recycling is a closed loop recycling scheme that is considered as an efficient solution for industrial PSW process scrap [54]. The scrap is mechanically reprocessed into a product with equivalent properties through its re-introduction into the heating cycle of the processing line, in order to increase production [38]. This type of recycling requires semi clean, non-contaminated waste which is the same type as the virgin resin to which the degraded plastic will partially substitute. Increasing the recycled plastic fraction may save on market prices compared with the virgin counterparts as well as reduce processing costs and waste generated by plastic converters, however, the feed mixture decreases the quality of the overall product [55]. Mechanical

(secondary) recycling is the most common method for the recycling of plastic wastes. This is an open-loop recycling scheme that involves the mechanical reprocessing of PSW into new lower-value products. The mechanical recycling of PSW can only be performed on single-polymer waste, thus needing an extensive number of pre-treatment and preparation steps (collection, sorting, washing, grinding) that are discussed in detail elsewhere [45]. This creates the challenge of high energy demand and utilities associated with process operation. Multiple re-processing steps (heating and mechanical shearing) also result in molecular damage mechanisms, reducing the integrity of the final product [43, 56]. Open-loop recycling can be considered as a form of cascading into ever lower-valued applications and the consumer demand for high end products makes investment in these types of recycling schemes non-profitable [57]. Alternatively, energy recovery via incineration (quaternary recycling) is a well-supported treatment method for municipal solid waste with high PSW content in Europe by associations such as ISOPA (European Diisocyanate & Polyol Producers Association). The high calorific value (CV) of plastics match that of conventional fuels and therefore PSW can be used in incinerators to give energy via electricity generation, district heating or combined heat and power schemes [58]. This method is an effective way to reduce the volume of PSW, however, results in the loss of valuable raw materials as all waste is converted to energy. It is also considered ecologically unacceptable due to the production of airborne highly toxic substances (furans, dioxins, acid gases) and groundwater pollution as a result of the plastic content in the processed waste and process conditions [5]. The EU has established directives (2000/76/EC) for emission limits and guidelines for incineration plants, however, reducing hazardous components dramatically increases operation costs [55].

The discussed challenges faced by the current PSW recycling methods lead to them being unacceptable to the principles of sustainable development and consequently, there has been a large growing research interest surrounding chemical (tertiary) recycling. Chemical recycling is the process in which polymers are converted into smaller hydrocarbon molecules via a change to their chemical structure using a chemical reaction or heat. It is based on a number of

technologies that can generate pure value-added products for various industrial and commercial applications [45]. These technologies include both chemical and thermo-chemical techniques, such as catalytic cracking, glycolysis, gasification, hydrogenation, methanolysis, pyrolysis, amongst others. Pyrolysis and gasification are thermochemical methods that are especially under extensive research and development for the establishment of suitable conditions, due to recent works demonstrating the potential of the products from PSW as alternative fuels [59-61]. The increased global effort in this area of research has particularly been demonstrated in recent bibliometric analysis [62]. Monomer recovery is another product destination that has received research interest from these techniques, involving feedstock recycling in closed cycle material flows for certain plastic-wastes, thus reducing the demand on petroleum for virgin plastic production [63, 64]. Chemical recycling has a high potential for heterogeneous and contaminated PSW when separation is not economical or technically feasible. Furthermore, the depolymerisation technologies utilised in chemical recycling can result in a very profitable and sustainable industrial scheme, providing high product yields with minimum residual waste. The research and development of such technologies would increase the incentive to recycle polymers, as well as decouple the plastic industry from fossil feedstock [52, 65].

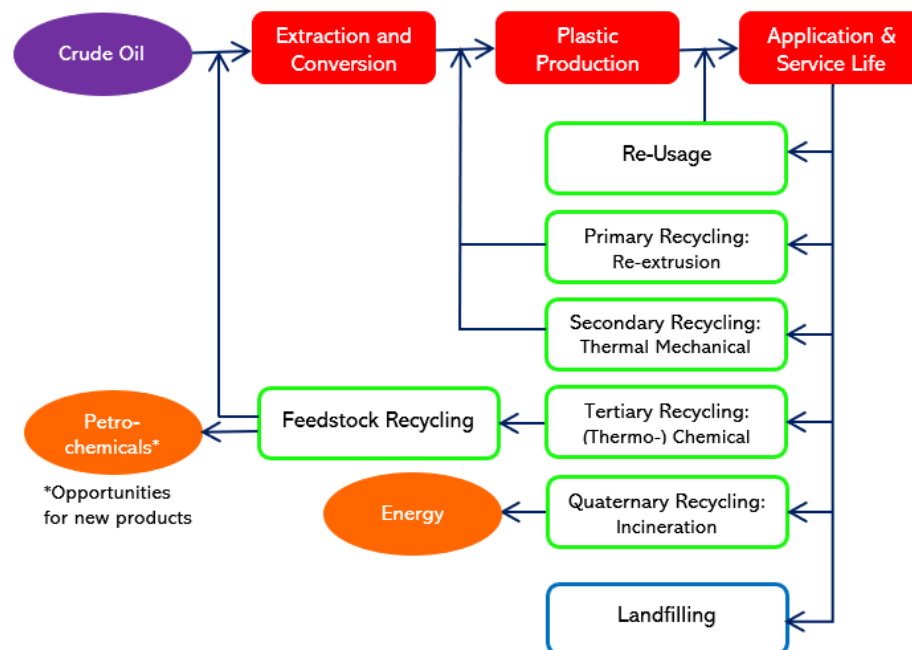


Figure 2.2 Plastic solid waste management methods including four valorisation routes, adapted from [52, 53].

2.3 Pyrolysis of Polyolefin Plastics

2.3.1 Polyolefins in Plastic Solid Waste Streams

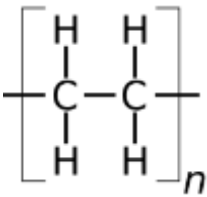
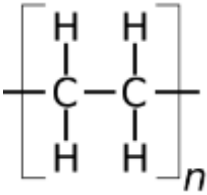
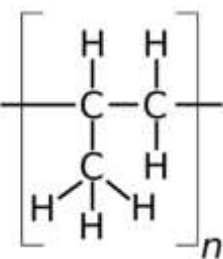
Thermoplastics are materials that can be melted when heated and hardened when cooled. Due to this susceptibility to change and molecular reformation with heat exposure, currently about 80% of consumed plastics in western Europe are thermoplastics, especially polypropylene (PP), low-density polyethylene (LDPE), high-density polyethylene (HDPE), polyvinyl chloride (PVC), polyethylene terephthalate (PET) and polystyrene (PS) [57]. Polyethylene alone makes up around 40% of the plastic total in plastic waste streams, thus the majority of solid plastic wastes are of polyolefin (PO) nature. In fact, due to their versatility towards many applications (packaging, bags, foils, toys, storage, etc.), within municipal solid waste streams; LDPE, HDPE, and PP account for around 65% of waste stream PSW [6].

Plastics have been thoroughly studied over the years with major research focus on their valorisation through thermochemical processes from low grade recycled plastics into petrochemical feedstock. More recently, pyrolysis particularly has been extensively applied on various scales and has been presented as a promising technique for such purposes. The suitability of plastic as a feedstock has also been demonstrated and its viability is clear, especially for polyolefins such as polyethylene, polypropylene, and polystyrene [66]. This is due to their capability for the production of somewhat clean distillates by comparison to other organic feedstock materials. As well as this, unlike biomass, polyolefins in particular have little oxygen content, thus a higher carbon efficiency as well as higher margin products can be obtained [45].

This literature review has focused its scope on the pyrolysis of polyolefins namely LDPE, HDPE, and PP, as they are most abundant in plastic waste streams and have very similar composition, such that the same valorisation routes may be applied to them [67]. They are suitable as a feedstock with high carbon and volatile matter contents, and low ash content. Due to these properties, the capacity for production of valuable pyrolysis tar products has been demonstrated extensively in literature, making pyrolysis a favoured treatment and method of

choice for the thermochemical treatment (TCT) of plastics [40, 57, 68] The chemical structures, properties and examples of each polyolefin is shown in Table 2.1, collated from [69, 70].

Table 2.1 Chemical structures, properties, and examples of applications for polyolefins HDPE, LDPE, and PP, collated from [69, 70].

Plastic	Chemical Structure	Properties	Applications
High Density Polyethylene (HDPE)	 $\left[\begin{array}{cc} \text{H} & \text{H} \\ & \\ -\text{C} & -\text{C}- \\ & \\ \text{H} & \text{H} \end{array} \right]_n$	<ul style="list-style-type: none"> ❖ Melting range: 250-260°C ❖ Softening range: 90°C (approx.) ❖ Clear, tough, solvent resistant, barrier to gas and moisture 	Shopping bags, household articles, bottle caps
Low Density Polyethylene (LDPE)	 $\left[\begin{array}{cc} \text{H} & \text{H} \\ & \\ -\text{C} & -\text{C}- \\ & \\ \text{H} & \text{H} \end{array} \right]_n$	<ul style="list-style-type: none"> ❖ Melting range: 120°C (approx.) ❖ Softening range: 80-90°C (approx.) ❖ Soft and flexible, translucent, easily scratched 	Shopping bags, bin bags, cosmetic and detergent bottles, milk pouches
Polypropylene (PP)	 $\left[\begin{array}{cc} \text{H} & \text{H} \\ & \\ -\text{C} & -\text{C}- \\ & \\ \text{H} & \text{H} \\ & \\ \text{H} & \text{H} \end{array} \right]_n$	<ul style="list-style-type: none"> ❖ Melting range: 140-160°C (approx.) ❖ Softening range: 95-110°C (approx.) ❖ Hard, translucent, versatile, solvent resistance 	Detergent wrapping, bottle caps and fasteners, food and vapour packaging, microwave food trays

2.3.2 Plastic Recycling via Pyrolysis

Pyrolysis is a thermochemical conversion technology that can be considered a 'feedstock recycling' process, in which the thermal degradation of long chain organic materials in an inert atmosphere occurs at temperatures of around 500 °C [71, 72]. The hydrocarbon content in the waste is converted into gases, oil and chars of different proportions and compositions depending on multiple process operational factors that have been comprehensively studied throughout plastic pyrolysis literature. These commonly include the feedstock used, e.g. co-pyrolysis of plastic mixtures and the use of virgin or real-life plastic waste [73, 74], the reactor technology [57, 75, 76], variable reactor operating parameters such as the temperature [6, 58, 77], reaction or residence time [40, 78, 79], as well as the presence of chemical agents [80-83], or catalysts [83-88], used in the reaction. The process is considered flexible such that it is capable of treating many different solid hydrocarbon wastes, producing clean fuel gas of high calorific value [89]. The solid char contains both carbon and mineral content of the original feed material, while the tar fractions consist of a complex of organic compounds and can be very rich in aromatics [54].

The pyrolysis process varies between authors in terms of cracking technologies, conditions, catalysts, and units used, depending largely on the selected feedstock and targeted products. However, the principle depolymerisation cracking reactions and subsequent recovery of valuable hydrocarbon products remain analogous. An example pyrolysis system is the cylindrical screw reactor depicted in the schematic shown in Figure 2.2. During operation, feedstock continuously enters the system via a screw feeder and conveyed through the reactor via an inner screw conveyor. The pyrolysis vapour leaves the reactor and passes through a shell and tube condenser, where the pyrolysis vapour is condensed to form pyrolysis liquid. The permanent gases pass through an electrostatic precipitator system for aerosol removal. After further fibre cartridge filtration, the final cleaned gas is sent to a flare system. Char from the pyrolysis is collected in a char pot [90].

Pyrolysis has long been investigated as a viable recycling route for wastes such as biomass and rubber and more recently has received increasing attention for PSW treatment. Surveying the literature reveals an extensive number of studies on virgin and PSW polyolefin pyrolysis at micro-, bench and pilot scales, some articles are summarised in Table 2.2 for example. It is important to note that pyrolysis experiments are dominantly operated at laboratory scale (micro- and bench scale). Availability of information is more limited for larger scale processes; however, many countries and business entities are developing processes for waste polymer pyrolysis [75].

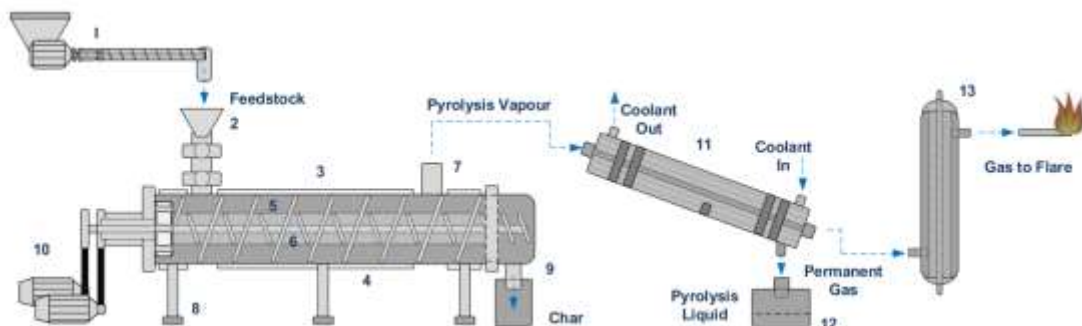


Figure 2.3 Schematic diagram of the intermediate pyrolysis system (1) Feeder; (2) Feed Inlet; (3) The Pyrolysis Reactor; (4) Heating Jackets; (5) Outer Screw; (6) Inner Screw; (7) Vapour Outlet; (8) Stands; (9) Char Outlet and Char Pot; (10) Motor; (11) Shell and Tube Condenser; (12) Liquid Vessel; (13) Electrostatic Precipitator [90].

Table 2.2 Summary of example studies investigated as a chemical treatment for virgin/waste polymers in laboratory micro-, bench and pilot scale.

Author	Scale	Feedstock	Process Conditions	Products	Summary
Al-Salem et al [91]	Micro	LLDPE	20-800 °C, heating rates of 5, 10, 15, 20, 25 °C/min	Gases	Thermal degradation kinetics and stability investigated via non-isothermal thermogravimetric analysis.
Al Salem et al [92]	Micro	HDPE	500-800 °C, heating rate 5 °C/min, nitrogen gas flow rate 20 ml/min	Oil, waxes, gases, solid chars	Isothermal pyrolysis including a comprehensive gas chromatography (GC) analysis of both liquid and gaseous products. Proposed model for degradation kinetics of parallel first order reactions.
Horvat et al [65]	Bench	HDPE, LDPE, waste PE	400-460 °C, 4-hour reaction time, nitrogen flowrate 5-75 mL/min	Oil, polymer residue (waxes), gases, coke	Pyrolysis in a semi-batch pyrolysis reactor, followed by hydrogenation of product oils into liquid fuel fractions.
Mastellone et al [93]	Bench	Recycled PE	300-450 °C, residence time 60-180 s	Gases, Liquid, Solid (not degraded PE), Solid (tar)	Pyrolysis in a fluidised bed reactor. Process yields with differing fluidizing velocities, bed temperatures, residence times were reported.
Miskolczi et al [94]	Pilot	Waste LDPE	250-400 °C, 60 min	Liquid oil, gases, solid residue	Pyrolysis using a ZSM-5 catalyst, feed capacity 9.0 kg/hr. The

			reaction time		composition of product gasoline and light oil fractions produced using the catalyst were advantageous for fuel-like applications.
Csukás et al [75]	Pilot	Waste HDPE	465-545 °C	Gases, Naphtha, middle distillates , heavy oil	Pyrolysis in a tubular reactor with distillation unit, feed capacity range 0.04-1.2 kg/h. Dynamic simulation model developed for pyrolysis of plastics wastes based on a four-step degradation scheme.

So far, pyrolysis has been developed to a commercial scale [55]. In 2018, there were 15 companies operating 87 plants worldwide to produce petrochemical and chemical feedstocks from plastics [95]. For example, the Recycling Technologies pilot plant located in the UK operating an advanced fluidised reactor system that converts non-recycled plastic, such as those commonly used in the packaging industry for film, into the low sulphur hydrocarbon Plaxx™. This can be refined into a low sulphur alternative to heavy fuel oil, slack wax or as a feedstock for more plastics. The system is being upscaled to process 7,000 tonnes per annum (tpa) of plastic waste [95]. In the US, Renewology pyrolyzes mixed plastics and packaging materials (grade 3-7) in a continuous auger kiln reactor calibrated to produce naphtha or a middle distillate suitable for diesel use at refineries. With current 10 tonnes per day (tpd) modules, the company will be commencing ‘Renew Pheonix’ in 2021 for a 6,000,000 lbs annual target capacity commercial plant [76, 96, 97]. In Europe, Plastic Energy’s recycling plant in Spain has a processing capacity of 5,000 tonnes of plastic waste (including PE, PP and PS) per annum. The PSW is recycled via their thermal anaerobic conversation (TAC) process in a continuous stirred-tank reactor at moderate temperatures to produce

TACCOIL™ chemical feedstock, sold to the petrochemical industry to convert to virgin plastic, oil, or transportation fuels [76, 98]. Further information on other commercial pyrolysis processes and advanced technologies can be found elsewhere [54, 71].

Numerous authors have published articles for the purpose of presenting various thermochemical recycling technologies for the conversion of PSW, with a number of technologies including pyrolysis concluded to be robust enough to warrant further research and development [57, 99, 100]. Such review articles frequently offer similar analyses of PSW recycling technologies, both conventional and thermochemical, with a research focus on comparisons of environmental impacts, such as greenhouse gas (GHG) emissions, energy consumption and waste reduction between technologies [45, 54, 57, 67, 101]. Other authors have utilised specific waste management strategies using evaluation tools for comparison, such as life-cycle assessments (LCA) and Technology Readiness Levels (TRL) [55, 102]. A common trend in these research analyses is the comparison of current waste management in Europe with the pyrolysis of waste plastics to produce petrochemicals including propane, butane, and gasoline [103]. Table 2.3 presents key advantages and limitations for the pyrolysis of PSW, gathered from the analyses mentioned.

Table 2.3 Key advantages and limitation for the pyrolysis of PSW.

Advantages	Limitations
Technical	
<ul style="list-style-type: none"> • Simple Technology • Suitable for lower quality/mixed wastes • High efficiency and product yield • High capacity for electricity and valuable products from waste • Capable of continuous operation • TRL range 7-9 for production of liquid fuels 	<ul style="list-style-type: none"> • Insufficient understanding of reaction pathways • Subsequent problems with scaling up reactions • Requires handling of char co-product • Sensitivity to feedstock
Environmental	
<ul style="list-style-type: none"> • Lower GHG emissions and consumption of fossil fuel resources (compared to other TCTs and conventional recycling methods) 	<ul style="list-style-type: none"> • Landfilling of residues: char, silica (sand) and bottom ashes

<ul style="list-style-type: none"> • Dioxins not formed due to inert reaction atmosphere 	
Cost	
<ul style="list-style-type: none"> • Few pre-treatment steps required • Lower operating temperatures compared to other TCTs 	<ul style="list-style-type: none"> • High energy requirement • Products often need upgrading

2.3.3 Pyrolysis Mechanism

Polyolefin pyrolysis proceeds via a complex degradation mechanism, yielding a broad spectrum of products (C_1 - C_{30}), yet the primary devolatilization reaction yields mainly wax-like materials with a typical carbon number range of C_{20} - C_{50} [104]. Wax is the main product obtained by thermal pyrolysis of polyolefins at lower temperatures and its formation is an attractive route to minimise energy requirements. The pyrolytic waxes from polyolefin feedstocks are aliphatic, mostly long-chain unbranched alkanes, with a chemical composition that is very similar to that obtained for commercial paraffinic waxes, as demonstrated by [105]. However, significant differences include the olefinic groups present in pyrolytic waxes due to radical degradation mechanisms, as well as the alkyl chains being much less branched [29, 105].

Polyolefin pyrolysis consists of a set of free-radical reaction mechanisms, predominantly yielding a broad product spectrum of lower molecular paraffins and α -olefins (C_1 to C_{50}). The plastic degradation mechanism has been previously described to involve three main steps that occur sequentially, being initiation, propagation, and termination [56, 64]. During the initiation reaction, the polymer chain undergoes a random homolytic scission, initiating the mechanism by producing primary radicals. Moreover, hydrogen abstraction and β -scission are considered as the propagation steps and are associated particularly with the degradation of PO plastics [69]. Hydrogen abstraction (intermolecular) entails the transfer of hydrogen between the primary radicals and hydrocarbon chains to produce new hydrocarbon products as well as more stable radicals. β -scission involves the scission of paraffin, olefin and diolefin radicals to produce olefin or diolefin products, as well as a new radical. The thermal degradation is completed by a recombination reaction which generates a smaller residual polymer chain

[29, 105]. The radical chain mechanisms can be seen in Figure 2.3. Typically, waxy materials in the C₂₀-C₅₀ range are produced in the primary devolatilization reaction of pyrolysis. These primary products are cracked further in secondary reactions to yield mainly olefinic hydrocarbons. Though, the gaseous products are highly reactive and thus further tertiary reactions take place to form more stable compounds, including aromatics. The process may also yield additional products such as hydrogen, methane, and coke when the product stream undergoes a long residence time [102, 105].

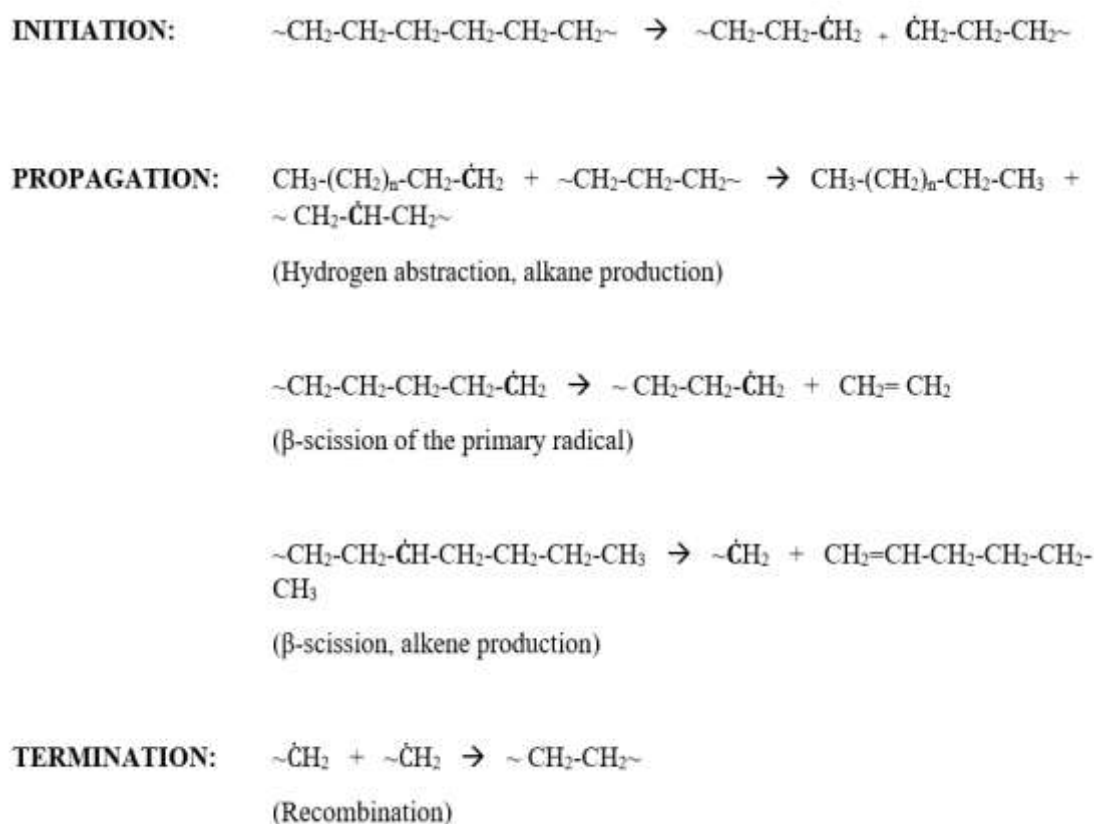


Figure 2.4 Radical mechanism of the thermal degradation of polyethylene, taken from [65, 106].

2.3.4 Pyrolysis of Polyolefin Plastics for Oil & Wax Production

A prominent trend in polyolefin pyrolysis literature is the thermal and catalytic pyrolysis of PE and PP into oils with heating values similar to conventional diesel and high aromatic content (BTX-benzene, toluene, and xylene aromatics) to be used as a petrochemical feedstock or fuel oil [107, 108]. Others have also

considered the light and heavy wax co-products for their suitability as feedstock for steam and catalytic crackers to be upgraded into products for both chemical and petrochemical industries [29, 109]. Pyrolysis experiments are dominantly operated at laboratory scale, however, the range of reactor technologies used with a focus on polyolefin wax production, or the wax co-product analysis is diverse. Prevalent technologies include fluidised bed and conical spouted bed (CSBR) reactors. Kaminsky et al pyrolysed pure and mixed polyolefins (PE, PP and PS) in a fluidised bed reactor at 510 °C to produce aliphatic waxes. The wax product fractions were categorised as light waxes (bp between 300-500 °C, *n*-C₁₈₋₃₇, and *i*-C₂₁₋₅₀) and heavy waxes (bp > 500°C, > *n*-C₃₇ and > *i*-C₅₀) to give a total wax yield of 84 wt% for PE and 57.5 wt% for PP. No interaction between the two polymers PE and PP was indicated in fluidised bed pyrolysis [109]. Williams et al pyrolysed LDPE between 500-700 °C in a fluidised bed reactor, obtaining a 45.3 wt% wax yield [110]. It should be noted that this yield in comparison to results from other authors highlights the inconsistency that can be found in literature regarding wax product categorisation and methods of reporting yield data [109]. In this instance, for conditions below 600 °C, the distinction between the oil and wax phases were less clear and the product oil was classed as a low viscosity waxy material.

Alternatively, in more recent works Aguado et al utilised a conical spouted bed reactor (CSBR) for the selective obtaining of wax by polyolefin (HDPE, LDPE, and PP) pyrolysis. The design of this alternative technology negates the limitations of the fluidised bed reactor that can lead to bed defluidization, such as particle agglomeration which can be serious when handling solids of irregular texture and/or sticky nature and with size distribution. No differences were observed between the results for the two types of PE, both producing very similar wax products, with a maximum yield of 80 wt% at the lowest temperature of 450 °C [104]. Arrabiourrutia et al received very similar results using the same technology, obtaining a maximum wax yield of 80 wt% at 450 °C for both HDPE and LDPE. However, a notable trend in these studies is the highest wax yield coming from PP, obtaining 92 wt% at 450 °C. Higher wax yields at lower temperatures for PP were deduced to be due to a more branched structure in PP

compared to that of PE [29]. Other authors have utilised vacuum pyrolysis in a batch reactor, in which the energy of evaporation of the primary macromolecules formed in the radical initiation reactions is lower than the activation energy required to trigger further radical initiation reactions, yielding fewer light organics and gases. Chaala et al obtained a 71.3 wt% wax yield in a bench scale reactor at 20 kPa reduced total pressure from electric cable wastes [105]. Additional pyrolysis reactor technologies to note include batch and auger reactors, in which authors have previously obtained >75 wt% and 93.2 wt% wax yields respectively from thermal pyrolysis at lower to moderate process temperatures [36, 111]. Table 2.4 can be referred to for further comparison of pyrolysis technologies in literature and resultant wax yield capacities and further technologies and their analysis can be found throughout review articles in current literature [40, 67].

In terms of pyrolysis parameters, the wax yield decreases dramatically at higher process temperatures. The temperature is the main parameter that controls the cracking reaction of the polymer chain and high temperatures support the cleavage of C-C bonds, resulting in the increased cracking of macromolecules into lighter organic oil fractions, and at higher temperatures to gases [73, 110]. An increase in reaction time will also decrease the yield of wax due to the increased conversion of the primary products [40, 112]. Furthermore, studies have been carried out with the focus to produce wax from plastic waste, investigating the effect of these pyrolysis parameters on the resultant wax quality and comparing the wax products to industrial standards. This was done using indicators such as wax melting point and penetration degree and clearly demonstrated that with careful control of both temperature and pyrolysis time, waxes with the properties of both commercial paraffinic and microcrystalline wax can be produced. It has also been indicated that plastic waste dyes do not affect the quality indicators of the PE pyrolysis wax [111, 112]. Additionally, at low pressures with short residence time of vapours in the reactor, it has been seen in the pyrolysis of mixed PE wastes that the major reaction to take place is the disproportionation of the primary macroradicals, forming n-paraffins and olefins at moderate temperatures [113]. Or when operating under vacuum conditions,

low cleavage of the macromolecular chain ends occurs, resulting in lower yields of light organics and gases, with increased soft and hard wax products [105].

Table 2.4 Pyrolysis technologies and parameters used in literature for polyolefin pyrolysis with resultant product wax yields.

Author	Type of Pyrolysis	Reactor	PO Plastic	Pyrolysis Temperature (°C)	Pyrolysis Time (s)	Wax Yield (wt %)	
Arabiourruti et al [29]	Thermal Pyrolysis	Conical Spouted Bed (CSBR)	LDPE	450 500 600	-	80 69 51	
			HDPE	450 500 600	-	80 68 49	
			PP	450 500 600	-	92 75 50	
Chaala et al [105]	Vacuum Pyrolysis	20 kPa Bench	Electric cable waste (mainly XLPE)	450	-	71.3	
Predel et al [109]	Thermal Pyrolysis	Fluidised Bed	PE	510	-	84 83.7 76	
			PE/PP (60:40)	510	-	71.5	
			PE/PP (40:60)	510	-	56.2	
			PP	510	-	57.5	
Williams et al [110]	Thermal Pyrolysis	Fluidised Bed	LDPE	500	-	45.3 * 35.4 24.8 12.1 4.0	
				550			
				600			
				650			
				700			
Aguado et al [104]	Thermal Pyrolysis	Conical Spouted Bed (CSBR)	LDPE	450	1-1080	80 69 57 51	
				500			
				550			
				600			
			HDPE	450		1-1080	80 68 61 49
				500			
				550			
			PP	450		1-1080	92 75
				500			

				550 600		67 50
Al-Salem et al [36]	Thermal Pyrolysis	Auger	PSW (PE majority)	500	-	93.2
Ademiluyi et al [111]	Thermal Pyrolysis	Batch	Waste PE sachets	130-150	18,00-2,400	>75

* Excluding results for 'Oil and Wax' product mixtures.

2.4 Asphalt Pavement

Hot mix asphalt (HMA) is a composite material commonly used within flexible pavements, consisting largely of mineral aggregates bound by a bituminous binder. Within flexible pavements, traffic loading is transferred to a soil sub-grade via points of contact between aggregates in a granular structure [114]. Due to this, wheel loads acting on the pavement are distributed to a wider area and thus flexible pavements typically consist of multiple layers to utilize this mode of stress distribution. Conventionally, the multi-layered systems of flexible pavements place high quality materials in the top layers, as this is where stress is the highest. The lower layers experience lower stress magnitudes and therefore are formulated using lower-quality materials. Aside from sealant, tack and prime coats that waterproof the pavement and ensure proper bonding between the upper courses, the typical layers of conventional flexible pavements are depicted in Figure 2.4 and include:

- **Surface Course**

This course (also known as the wearing course) is constructed using high quality bituminous materials including dense graded asphalt concrete, as it is in direct contact with traffic loads. It must be waterproof, skid-resistant, and highly resistant to deformation and distortion as a result of loading.

- **Binder Course**

This layer is similar to the surface course, however, consists of lower quality, larger aggregates, and less bitumen binder. The binder course is responsible for distributing loads from the surface to the base courses.

- **Base Course**

The base course typically consists of larger aggregates in a granular asphalt structure and/or hydraulically bound (such as concrete,) as well as crushed stone, slag, and other untreated materials. It provides additional structural support and sub-surface drainage while further transferring loads from the upper to the subbase and subgrade courses.

- **Sub-Base Course**

A layer of material beneath the base course that provides additional structural support and drainage. In the case of low quality and stiffness sub-grade courses, it acts as a barrier to prevent fines from entering the pavement structure, as well as a filler for the base course when it is open graded. If the pavement design includes a stiff, high quality sub-grade layer the sub-base course may not be needed.

- **Sub-grade**

The bottom foundational layer of the pavement, consisting of natural soil that is compacted to a particular density to ensure it can endure the stresses transferred to it from the upper courses. This layer transfers the traffic loads from the upper material layers to the ground.

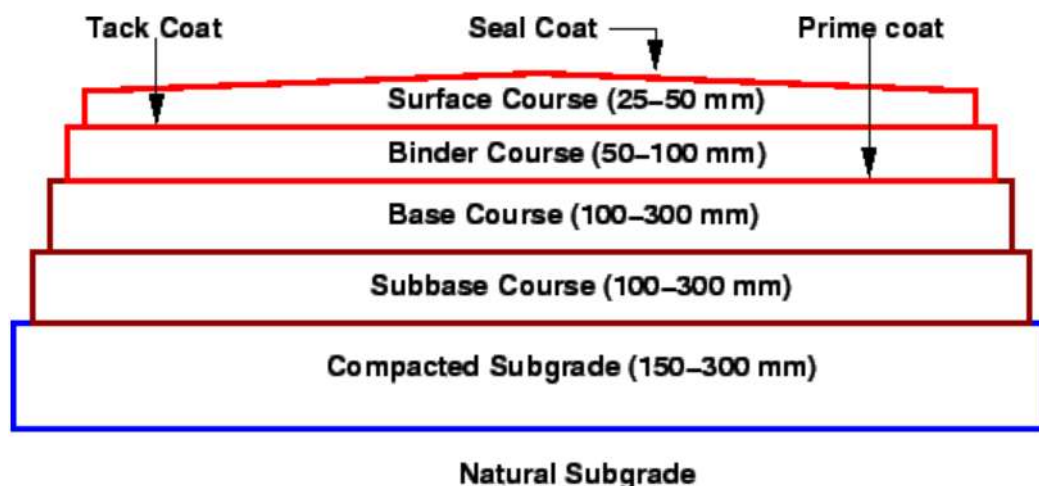


Figure 2.5 Typical cross-section of a conventional flexible pavement [114].

2.4.1 Bitumen

Bitumen is a by-product of vacuum distillation in petroleum oil refineries (or can be found in natural deposits) and is a viscoelastic, rheological, and non-magnetic material [115]. Possessing waterproof and adhesive properties, it is a black or brown substance that is non-volatile and gradually softens when heated [116]. Elemental analysis of bitumen manufactured from a variety of crude oils shows that most bitumens contain: carbon 82-88%, hydrogen 8-11%, sulphur 0-6%, oxygen 0-1.5% and nitrogen 0-1% [117]. The complexity of both the chemical composition and structure of bitumen gives explanation to its complex physio mechanical and physiochemical behaviours [118]. Its characterisation can be split into four main constituents: saturates (5-15 wt%), aromatics (30-45 wt%), resins (30-45 wt%) and asphaltenes (5-20 wt%), otherwise known as SARA fractions. The exact composition of each chemical family depends on the crude origin [115, 119]. These constituents together form a colloidal structure, as depicted in Figure 2.5.

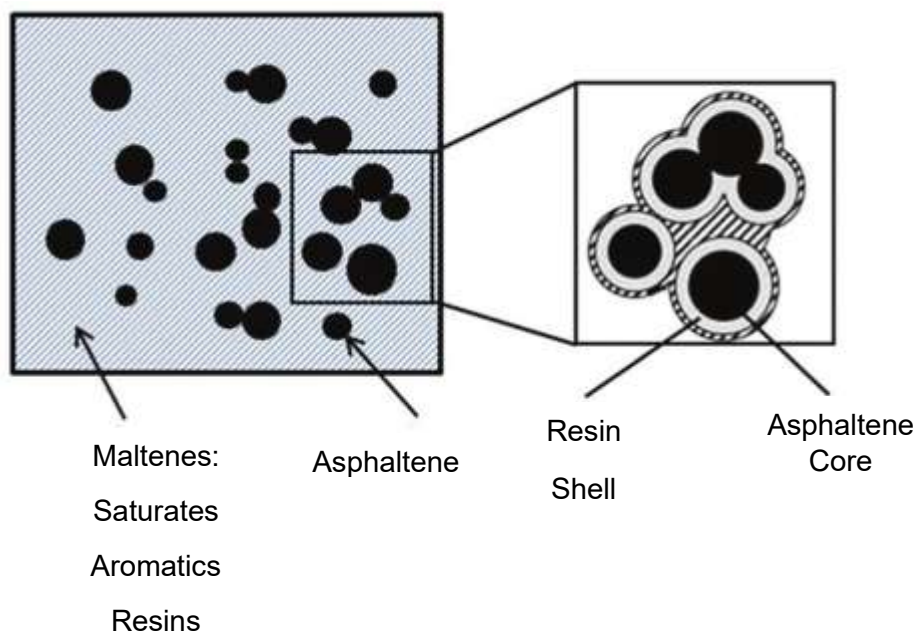


Figure 2.6 The colloidal structure of SARA fractions in bitumen, adapted from [120].

Descriptions of the main SARA fractions in bitumen are as follows:

- **Saturates** are colourless/white, non-polar and viscous oils with an average molecular weight 600 g mol^{-1} [121]. They mainly consist of straight and branched-chain aliphatic hydrocarbons with some heteroatoms and aromatic rings, as seen in Figure 2.6. Softer bitumens generally contain more saturates and have the increased ability to restore broken bonds [32].

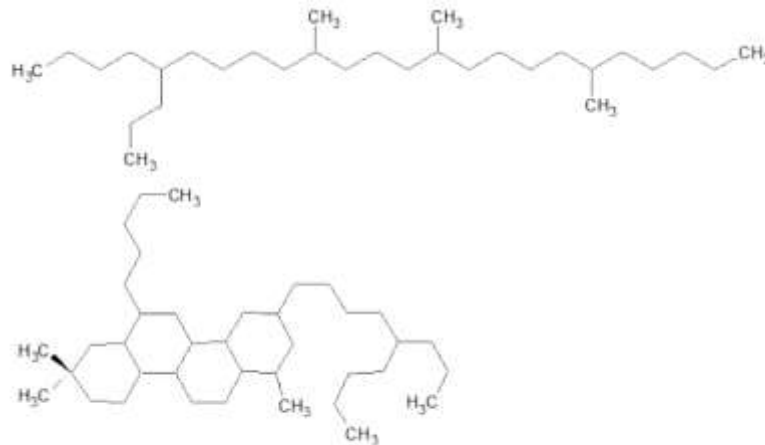


Figure 2.7 Typical molecular structure of the saturate fraction in bitumen [121].

- **Aromatics** are black/brown in colour and are more viscous than saturates with a molecular weight of 800 g mol^{-1} [121]. They are composed of lightly condensed aromatic and naphthenic rings with side chains. The function of the aromatic fraction in the colloidal structure is as a plasticiser as well as solvent for the asphaltene and resin fractions. Its typical molecular structure is presented in Figure 2.7.

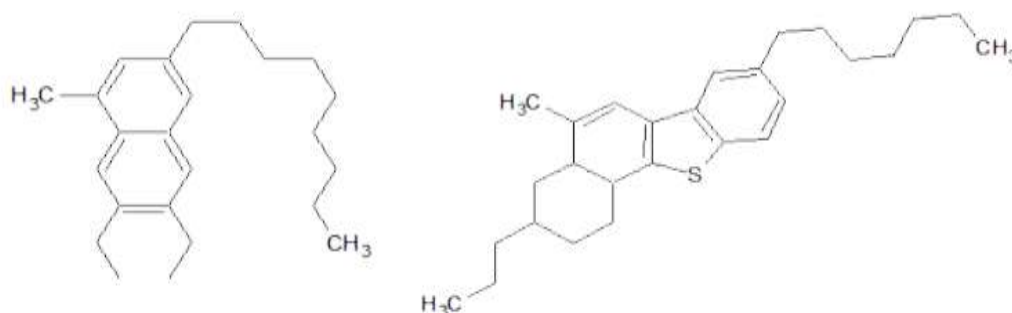


Figure 2.8 Typical molecular structure of the aromatic fraction in bitumen [121].

- **Resins** are polar aromatics which are dark in colour, heavy semisolids/solids at room temperature. They have an average molecular weight of 1100 g mol^{-1} , become brittle when cold and act as a disperser for the asphaltene colloidal structure to form a homogeneous liquid [32]. Alongside asphaltenes, resins can govern the rheological properties of the bitumen [121]. Their typical molecular structure is exhibited in Figure 2.8.

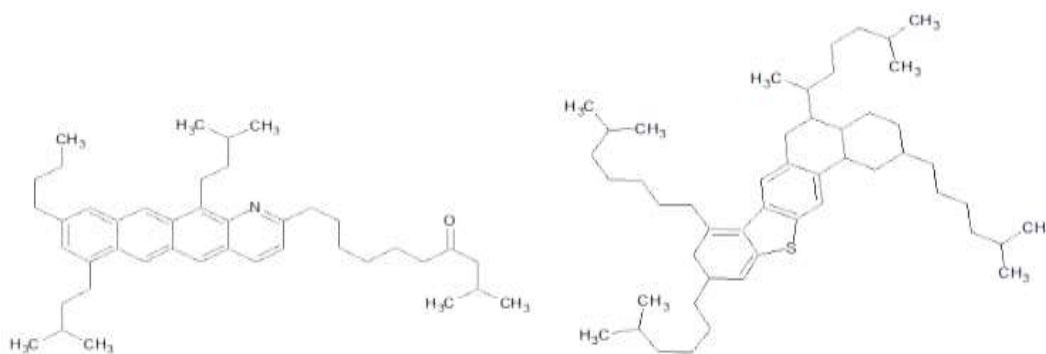


Figure 2.9 Typical molecular structure of the aromatic fraction in bitumen [121].

- **Asphaltenes** are described as dark brown/black friable solids that have the greatest influence on the properties of bitumens, increasing their viscosity, hardness, brittleness and softening point [122, 123]. They have molecular weights estimated to be 250 to 3500 g mol^{-1} [121]. Possible molecular structures that can be identified in asphaltene are polyaromatic units, alkyl chains, heteroatoms (nitrogen, oxygen, and sulphur) and metal porphyrins (vanadium, nickel, and iron), as exhibited in Figure 2.9.

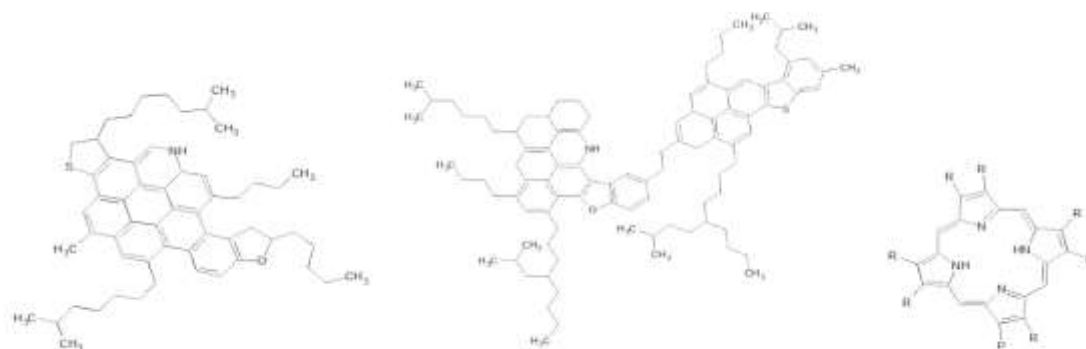


Figure 2.10 Possible molecular structures present within the asphaltene fraction [121].

2.5 Pavement Failures

Within flexible pavements, major modes of deterioration and eventual failure include fatigue cracking and rutting. When the multi-layer material is being subjected to wheel loading, the layers will bend which causes tensile stresses/strains in the horizontal direction (at the bottom of each bound course) and compressive stresses/strains in the vertical direction (in the bulk section of the material.) This is depicted in Figure 2.10. Repetitive loading characteristic of vehicle traffic and these resultant stresses/strains can cause fatigue cracking at the bottom of the bound course as well as rutting within the vertical section. These major modes of pavement deterioration will be described in this section.

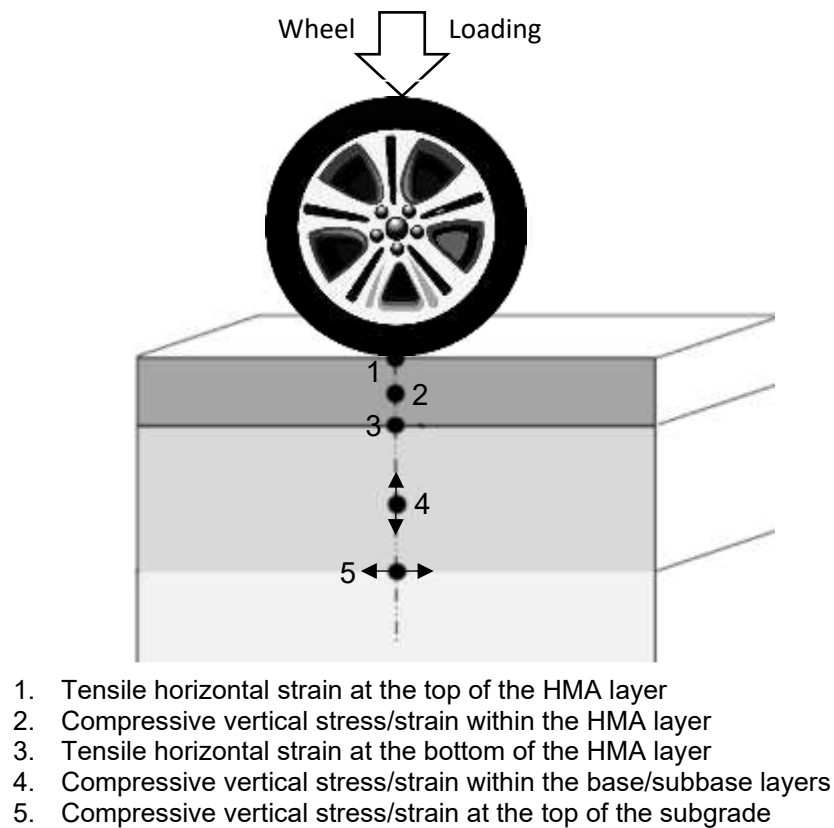


Figure 2.11 Pavement response to traffic loading, adapted from [124].

2.5.1 Fatigue Cracking

At intermediate temperatures between 10-40 °C, the main distress within flexible pavement structures is fatigue cracking. It entails two phases of degradation processes, the first corresponding to damage that is uniformly distributed throughout the material via the initiation and propagation of 'micro-cracks,' which reduce the stiffness of the material. The second phase involves the coalescence of the 'micro-cracks' and the appearance of 'macro-cracks,' which propagate through the material bound layers (as seen in Figure 2.11) until material failure [125]. When 20% of the pavement surface is cracked, it is considered to be failed [32].



Figure 2.12 Fatigue 'alligator' cracking in asphalt pavement [126].

2.5.2 Rutting

At temperature conditions above 40 °C, the asphalt binders within flexible pavements become softer and more viscous. The main failure mode exhibited at these conditions is permanent deformation or rutting. Rutting mainly occurs due to high volumes of traffic and therefore load repetitions, causing plastic deformation of the materials within the multi-layer pavement structure. It can be observed by extreme consolidation of the pavement along the wheel path (as seen in Figure 2.12) possibly due to a reduction of air voids within the asphalt layer, or the permanent deformation of the base or subgrade layers. Possible causes of rutting may include insufficient manufacturing and compaction of the

HMA layer allowing for plastic lateral flow; a higher binder content reducing internal friction between aggregates; the use of rounded aggregates; the use of softer binder in warmer regions. The material is considered to be failed if a rut depth of 20 mm is reached.



Figure 2.13 Rutting in asphalt pavement [127].

2.6 Polyolefin Plastics in Road Construction

2.6.1 Flexible Road Materials

In order for an application to be viable for the reuse of plastic waste, it would need to have the capacity for incorporating high volumes of plastic. As well as this, very little cost should be involved in the preparation. Using waste plastic directly in HMA pavement structures is considered as a practical application with the large volumes of both plastics and roads produced [11]. In a literature analysis conducted by Zhao et al out of the articles evaluated between 2014-2019 studying plastics as a waste solid material in pavement engineering, polyolefins PE and PP were two of the most studied plastics [128]. It is noted that the plastics are predominantly evaluated in literature for the application as a modifier or 'reinforcement' in the pavement material, more specifically via incorporation into the bituminous binders. Throughout its service life, HMA requires durability over a range of climate conditions and traffic loads. The engineering performance of its constituent materials such as the neat bitumen binders may not be satisfactory under all possible climates. Therefore, cost effective and alternative binder

materials such as waste plastics are increasingly being investigated to boost binder performance and extend service life, while decreasing the use of bitumen [129, 130].

Waste polyolefin (PO) plastics are good candidates as a cheaper material for asphalt binder modification. The melting point ranges of polyolefin plastics are below the temperature range that is commonly used in the production of HMA (usually varying between 150-180 °C); therefore, these materials can be readily incorporated into the bitumen [10]. Plastics may be directly introduced via the wet process into the hot asphalt binder (polymer modified bitumen, PMB.) This is done prior to being used in the production of modified asphalt mixtures (polymer modified asphalt, PMA [131].)

Alternatively, the plastics can be added via the dry process to the hot mineral aggregates before the asphalt binder as another aggregate. The dry process promotes simplicity and requires no process modification within the asphalt plant, facilitating the use of waste plastics via this modification technique [10]. In this way, authors have investigated varying percentage replacements of mineral aggregates with waste polymeric materials in different asphaltic mixture fractions. Many have reported improved asphalt mixture properties such as Marshall stability, indirect tensile strength (ITS), indirect tensile strength ratio (TSR), resistance to permanent deformation and fatigue [132-136]. This method can utilise a higher amount of waste plastic in comparison to the wet process (by weight of the total mix) and result in a reduction in the bulk density of the compacted mix, proving advantageous in terms of haulage costs [132]. Additionally, upon adding the plastics directly with the hot aggregates, they can soften and coat the aggregates, improving aggregate linkage as well as the adhesiveness between the binder and aggregates.

However, the dry process has been reported to have the limitation of performing inconsistently when using high plastic content in the asphalt mixtures [131, 132]. The majority of published studies prefer the use of the wet process, as this leads to a larger degree of modification and therefore to a better use of the waste

plastics for property improvement [10]. Due to this, studies modifying bitumen binders and subsequent asphalt with waste plastics via the wet process will be primarily reviewed in *Section 2.6.2*.

2.6.2 Polyolefin Modified Asphalt Binders

Polymers are one of the most important and widely used additives for the improvement of asphalt properties. Synthetic and virgin polymers have been used in asphalt as a binder modifier as early as 1843 for improving asphalt resistance against permanent deformation related to temperature changes [137]. However, they are well documented to impart enhanced service properties over a wide range of temperatures in road paving applications [47, 48]. The use of virgin polymers is uneconomical due to their high cost, thus can only be used in small amounts to enhance asphalt binder properties. With the current challenge of minimizing plastic waste and finding sustainable routes for its valorisation and re-use, a large number of research works have emerged for the incorporation of waste plastics into bitumen and studying the effect of these additives on the properties of the modified asphalt. It has been shown throughout numerous studies that the modification of bitumen with recycled polymers gives analogous results in enhancing the properties of bitumen as compared to virgin polymers [138-140]. This can be seen further in Table 2.5, which details the studies that have used both virgin and waste plastics as binder modifiers, obtaining similar conclusions that will be further discussed in *Sections 2.6.3-2.6.5*.

The percentage of polymer added to the binder can vary between 1-10 wt%, the most common being between 3-5 wt% [10]. The majority of authors employ the wet process to incorporate plastic additives into bitumen, using high shear mixing at a particular temperature until a homogenous blend is achieved. However, this mixing can be done using a variation of process parameters. In Table 2.5 it can be seen that both virgin and waste PO plastics are typically added at temperatures of 150-190 °C, blended for 0.5-2 hours at a blending speed of 200-8200 rpm. The structure and properties of PMBs can be a function of blending conditions, mainly the temperature and blending time. Optimum blending parameters are chosen by

evaluating certain blend characteristics including the waste plastic dispersion and storage stability, microstructure, and performance properties of the PMBs [47, 141].

Table 2.5 Existing studies using virgin or waste Polyolefins HDPE/LDPE/PP in Polymer-Modified Bitumen Binders (PMBs) and Asphalts (PMAs.)

Author	Base Binder (pen. grade)	Plastic Modifier	Blending Method	Conclusions
Attaelmanan et al [140]	80/100	<ul style="list-style-type: none"> • HDPE: 1,3,5,7 wt% 	Mixed at 170 °C using a high-speed stirrer, 3000 rpm, 2 h	<ul style="list-style-type: none"> • Raised softening point and decreased penetration • Modified binders less susceptible to temperature and more favourable for hot climates (higher rutting resistance) • Increase in adhesion between aggregate and bitumen, decrease stripping of HMA and moisture susceptibility
Casey et al [142]	200 and 150	<ul style="list-style-type: none"> • Waste PP, LDPE, HDPE powder: 2,3,4,5 wt% • Waste PP mulch: 2,3,4,5 wt% • Blends 4 wt% HDPE/LDPE with 2wt% 	Heat the base binder to 160 °C, add additive and mix for 60 min, add the plastic, mix for a further 90 min	<ul style="list-style-type: none"> • Storage stability not achievable from PP powder and mulch blends • 4% LDPE/HDPE concentrations minimises mixture disassociation with improved performance

		<p>DETA/ 0.8 wt% PPA</p> <ul style="list-style-type: none"> • Additives: Diethylenetriamine (DETA) Phosphoric Acid (PPA) 		<ul style="list-style-type: none"> • Addition of 0.8 wt% PPA further enhanced performance levels while improving storage stability of blends
Ait-Kadi et al [143]	159/200	<ul style="list-style-type: none"> • HDPE: 1,3,5 wt% • Blends HDPE/EPDM (90/10): 1,3,5 wt% • Additives: Ethylene-Propylene-Diene terpolymer (EPDM) 	Prepared at 170 °C using high shear mixing element in jacketed reactor, stored in metallic containers at -4 °C	<ul style="list-style-type: none"> • HDPE and HDPE/EPDM results in increased low frequency viscosity and storage modulus • The presence of chemical additives like EPDM result in a more stable emulsion
Hinislioğlu et al [144]	AC-20*	<ul style="list-style-type: none"> • Waste HDPE: 4-6 and 8 wt% 	Vertical shaft mixer, 200 rpm, 145-155 and 165 °C, 5-15 and 30 min	<ul style="list-style-type: none"> • 4% HDPE binder prepared at 165 °C for 30 min has the highest Marshall Stability • HDPE mixes highly resistant to permanent deformation (rutting) in asphalt
Fang et al [145]	90A#*	<ul style="list-style-type: none"> • Waste PE (WPE): 4 wt% 	High shear emulsifier, 3750 rpm, 150, 170, 190 °C, 0.5, 1, 1.5, 2 h, particles added over 5 min	<ul style="list-style-type: none"> • Optimum WPE dispersion in the mixture is achieved at 150 °C after 1.5 hours of shearing • Relatively good storage stability achieved • Decreased temperature sensitivity of

				modified bitumen
--	--	--	--	------------------

* Sinopec Xi'an Petrochemical Company, Styrene-butadiene rubber (SBR) Modified Asphalt.

2.6.3 Polyolefin Modified Asphalt Binder Performance

A wide application of standard rheological parameter tests such as penetration, softening point, ductility, and viscosity (typically used to characterise neat bitumen grades) have been employed to characterise the performance of waste PO modified bitumen mixtures in literature. A prominent trend in bitumen modification with PO plastics is the decreasing penetration point (increasing stiffness) and increasing softening point of the binder as the proportion of polymer is increased [10, 139, 140, 146]. However, it is noted that some authors such as Casey et al have observed lower variations of penetration and softening point values for PP than those for PE [142]. Moreover, a substantial rise in viscosity has been observed by authors once more with increasing plastic dosage.

HDPE modified asphalt binders have relatively higher viscosities than its LDPE and PP counterparts and have been seen to exceed the Superpave Performance Grade (PG) defined limit of 3000 cP at 135 °C at lower percentage addition. This can be attributed to its more crystalline and higher density structure, with strong forces of attraction between molecules [137, 147, 148]. Additionally, the ductility of the PO modified binders can remain at a minimum range (100 cm) of the specification up to certain percentages, which is important at low winter temperatures [149]. Al-Ghannam et al observed this up to 8% addition of polyethylene, after which the ductility sharply decreased at further higher percentages [150]. From the observed trends in standard rheological parameters, it has been established that the addition of PO plastics and their wastes improves thermal susceptibility as well as the resistance to permanent deformation (rutting) at high temperatures [151]. Therefore, the use of waste polymers could help to extend the service life of pavements with high traffic loads and those placed in hot climates [10, 146, 152]. Naskar et al explored the enhancement of binder thermal stability through a number of thermal degradation

characteristics, observing enhancements up to 5 wt% waste plastic addition [153]. This was attributed to better swelling of the waste plastic by bitumen light components (paraffinic and aromatic compounds), disrupting the crystallinity of the polymer and improving interaction between plastic and bitumen matrix.

The viscoelastic properties of PO modified asphalt binders can additionally be characterised by the complex (stiffness) modulus (G^*) and phase angle (δ), which are obtained from a dynamic shear rheometer (DSR). Yu et al modified bitumen using 4 wt% waste LDPE and LLDPE and when compared with the original base binder, the G^* of the modified binders was increased, showing that the non-deformability of modified asphalt binders is enhanced. The phase angle (δ) of the modified binders was smaller than that of the base binders, which, combined with the enhanced G^* parameter, the storage modulus (G' , equals $G^* \cdot \cos\delta$) of the modified binders increased, indicating an increase in the elastic component [48]. Cardone et al also observed that the presence of a polymer network in 2-6 wt% plastic modified bitumen leads to an increase in stiffness (G^*) and the elastic properties of the material (lower phase angle [152].) Abdullah et al blended 1.5-6 wt% waste plastic with a 60/70 bitumen binder and focused on the rutting factor $G^*/\sin(\delta)$ obtained from DSR, finding that a higher percentage of plastic waste will result in a higher rutting resistance [146]. To further compare the rutting behaviour of short-term aged binders, the recoverable strain (R) and non-recoverable creep compliance J_{nr} are also measured from the Multiple Stress Creep and Recovery (MSCR) test. Authors have demonstrated a reduced total strain with higher dosages of PO plastics. The PMBs have higher R values and lower J_{nr} values with increased dosages, as the inclusion of polymeric chains in the asphalt binder restricts and thus improves resistance to permanent deformation [154-156].

An asphalt binder will have higher resistance to fatigue cracking if it is more elastic and not too stiff [157]. Multiple authors have conducted recent popular tests (the Linear Amplitude Sweep test, for example) to determine the fatigue life of long-term aged, modified binders by calculating the damage accumulation. In a study conducted by Amir Khanian et al, it was shown that the addition of PE

improves binder fatigue life in comparison to the base binders, regardless of the PE type, content, and applied shear strain [156]. Roja et al showed that a 3-5 wt% addition of lower molecular weight (M_w) LDPE will improve the fatigue life of the binder, due to increased chain mobility [155]. Despite this, some authors have alternatively found that PO plastics fail to improve the elastic recovery and stress relaxation of the binder, indicating the potential for thermal and fatigue cracking at low in-service temperatures [158]. Isacson et al found that the addition of PE failed to significantly improve the low-temperature flexibility of bitumen [159]. This was attributed to its regular long chain structure, the PE molecule is prone pack closely and crystallize, which could lead to a lack of interaction between the bitumen and polymer and result in instability of the modified bitumen.

2.6.4 Polyolefin Modified Asphalt Mixture Performance

The stability of an asphalt mixture verifies its performance under loading. A prominent trend in literature is that the addition of recycled PO plastic can substantially increase the stiffness and thus stability of the asphalt mixture, but only up to certain percentages, after which the stability will decrease. For example, authors have determined the highest Marshall stability values to be at a 4% dosage for HDPE [144, 160]. Hınısliođlu et al saw a stability increase in the range of 3-21% using 1-4 wt% HDPE in asphalt concrete formulated via the wet process, with other authors seeing similar results [161, 162]. The higher stabilities have been suggested to be attributable to higher cohesion of the binder and internal friction due to the plastic addition, indicated by lower flow values for modified specimens [144]. In comparison, Zoorob et al applied the dry method for the formulation of 'Plastiphalt', replacing 29.7 wt% of aggregates with LDPE and found a Marshall stability of approximately 2.5 times the control mix [136]. The recorded flow values were also lower, indicating that the mixes were both stronger and more elastic. The Marshall Quotient (MQ) is largely used as an indicator of the resistance against deformation of asphalt. Higher stability and lower flow values of Marshall specimens modified with PO plastics seen in various studies supports the increase in MQ values. This has been used to

conclude that mixes blended with PO plastics are highly resistant to rutting at high temperatures [144, 161-163].

The dynamic creep has been widely used to characterise the permanent strain behaviour of paving mixtures at relatively high temperatures where the flexible pavements are more susceptible to rutting distress [164]. The influence of PO plastics on the Marshall properties of asphalt provides an increase of the service life under repeated creep testing [160, 165]. Nejad et al saw such results with the addition of 5 wt% HDPE into the bitumen binder [166]. It was also observed that moisture increased the rutting potential the least for the modified binders, indicating a decreased moisture susceptibility. Tapkin et al observed a substantial increase in the service life of PP fibre-reinforced asphalt specimens under repeated loading, to the extent that the control specimens entered the tertiary stage of creep at the loading rate corresponding to the primary stage of creep for the modified mixes [162]. However, it is importantly noted by some authors that due to the stiffening effect of the polymers, mixtures with the highest polymer percentage are rather incompressible and have lower workability [134, 165]. This is an important consideration in terms mixture pumpability and the potential increase in energy and emissions required for the PMA formulation. This also may present a limit on the amount of each plastic that can be added to the flexible pavement via this production technique. Especially when plastics used in the 'wet' process already account for a very small percentage of the overall mass, given that bitumen is approximately 5% of the total mix [46]. Care must also be exercised with very high stiffness mixes due to their lower tensile strain capacity to failure. Such mixes are more likely to fail by cracking, particularly when laid over foundations which fail to provide adequate support [136]. Regardless, multiple authors have agreed in fatigue life studies for PO modified asphalt that for a thick pavement that is evaluated in the constant stress mode of testing, increasing stiffness of the asphalt binder causes a better fatigue life in the asphalt mixture [166, 167]. Nejad et al saw the fatigue life of 5 wt% HDPE asphalt mixtures to be 1.16 times the control mixture when conducting Indirect Tensile Fatigue (IFT) tests [166]. Other authors have found an improvement in tensile strength and related properties of mixtures containing polymer fibres, especially

polypropylene. Tapkin et al [136] found that a 0.3-1% addition of polypropylene fibres into asphalt concrete on a dry basis prolonged the fatigue life with less reflection cracking.

Flexible pavements are additionally susceptible to the damaging effects of moisture, causing the displacement of the bitumen film from the aggregate surface in the presence of water. In literature it has been demonstrated via various techniques (Indirect Tensile Strength (ITS) and Tensile Strength Ratio (TSR), Marshall Stability ratio of 'wet and 'dry' specimens) that PO plastics improve binder-aggregate adhesion as higher moisture resistance is gained. Therefore, PO modified PMAs will have higher durability and service life with potentially lower construction and maintenance costs [140, 166, 168, 169]. In addition, Haider et al found that PE modified asphalt mixtures through the wet process showed better adhesion and moisture resistance than those modified through the dry process [170]. However, plastic coated aggregates have too been demonstrated to favour the impact, crushing, stripping and abrasion resistance of aggregates [171].

2.6.5 Technical Limitations

Modifying bitumen binders and the subsequent asphalt with waste PE and PP plastics is an attractive option for the low-cost improvement of asphalt concrete mixes at 3-5 wt% of bitumen [172]. However, despite the advantages of PO modification, there are several potential challenges that could limit its future development and commercialisation. Some are related to the chemical compatibility between waste plastics and bitumen, leading to phase separation and poor storage stability that has been reported in various works [142, 145, 173]. The tendency for long chain PO plastics to pack closely and crystallise can lead to a lack of interaction with the bitumen and result in the instability of the modified binder. Compatibility can also be poor due to the non-polar nature of the polymers, making them completely immiscible with the bitumen [174, 175]. Other factors such as viscosity and density differences, the molecular weight distribution, melt flow index (MFI), concentration, and the degree of branching of

the polymers as well as the aromaticity and asphaltene content of the base binders have additionally been linked to determining the compatibility of PMB mixtures [130, 173, 176].

A popular solution is the use of polyolefin-based copolymers that can have polar components and are either inert or reactive with the asphalt binder. Elastomers such as ethylene-vinyl acetate (EVA) and ethylene-propylene-diene (EPDM) have received much research attention for steric emulsion stabilization and can be effective (as seen in some of the studies included in Table 2.5.) The copolymers can additionally enhance binder properties that the polyolefin plastics cannot improve alone [139, 143, 151, 177]. However, as reported by Pérez-Lepe et al, upon mixing various (EPDM/PE) blend compositions, these materials are not always efficient due to not being able to entangle sufficiently with the polyolefins in the absence of cross-linking promoters, therefore the stabilising effect is not fulfilled [173]. Alternatively, reactive compatibilizer agents that modify the olefinic chain with additional functional groups can improve the miscibility of the polymer and bitumen and enhance binder characteristics further, for example maleic anhydride (MA), glycidyl methacrylate (GMA), polyphosphoric acid (PA) and reactive ethylene terpolymers (RET) [10, 151, 178, 179]. Despite this, the use of compatibilizers could limit the economic benefits of using recycled materials and in some cases, reactive additives do not always result in sufficient enhancements to obtain a homogeneous and stable mix [151]. Another unknown is whether the enhanced material properties e.g., increased rutting resistance, less temperature susceptibility, and elevated adhesion, will remain being enhanced when the PSW mixing weight is at a higher percentage (greater than 10% of bitumen.)

Other authors have focused more on the environmental aspects that mixing bitumen with waste plastics could pose, such as fuming, emissions during production, contamination and microplastics [46]. If waste plastics or other organic recycled material will be used in asphalts, more research is needed to assess their effects on workers' exposure and health, due to mutagenic potency. The sorting of plastics before possible use in asphalt may also be important in

order to remove plastics that decompose to hazardous compounds in heating, for example the noxious HCl gas from Polyvinyl Chloride (PVC) [180, 181]. The potential of waste plastic fragmentation into microplastics upon introduction in asphalt pavement layers and their role as a pollutant with potentially serious ecological impacts is also in need of further research [182]. Additionally, there are rising concerns regarding the future recyclability of the asphalt and whether this could be hindered by the incorporation of waste materials [183]. The increased viscosity of PMB blends unfortunately results in the decreased workability of the binder, needing to increase the mixing and compaction temperatures for manufacturing. This increases in energy consumption are undesirable and creates environmental concerns about emissions generated [184].

2.6.6 Life Cycle Analysis and Cost Assessment

The potential environmental effects of using waste materials in road pavement applications must be quantitatively evaluated and numerous life cycles assessment (LCA) studies have been conducted in literature for this purpose [185, 186]. Santos et al conducted a LCA investigating the impact of recycling waste plastics from local processing facilities in asphalt mixes when incorporated via the wet and dry method [46]. It showed that for the conditions and assumptions considered in the study, recycling PE plastics (as a substitute of virgin plastics) using the wet method (up to 8% addition) can be beneficial for the environment by reducing greenhouse gas (GHG) emissions up to approximately 16%. However, the use of PMB is more environmentally burdensome than the use of standard bitumen due to the fact that asphalt binder modification implies the consumption of at least one additional material. However, as discussed by Zhu et al, environmental benefits are expected to be observed in the other pavement life cycle phases in terms of reduced maintenance costs as a result of increased pavement failure resistances and greater adhesion between asphalt binder and aggregates over the service life [187]. On the other hand, the production of asphalt mixes via the dry method consumes a larger quantity of recycled plastic, however, the environmental benefits of this technique are diminished. The GHG

emissions increased by 160% when 20% recycled plastic was included in the mixes as a replacement of virgin quarry aggregate. The increase in certain impact categories is due to a greater energy demand required to produce the recycled plastic pellets. Though, it was seen that using a lower percentage aggregate replacement can still use a sizable amount of waste plastic without significantly increasing the number of emissions generated [46].

The LCA conducted by Oreto et al also concluded that wet and dry plastic modification of asphalt mixtures does entail additional environmental burdens compared to the traditional HMA binders [188]. This was attributed to factors such as the plastic pelletization process and long transportation distances. However, human carcinogen toxicity was lowered through the reduction of particulate matter and polycyclic aromatic hydrocarbons emitted during the recycling and production of plastic pellets compared to industrial modification of bitumen with virgin polymers. The predicted service life (using the Boussinesq theory and the calculation of the stress-strain state of each pavement structural layer, in compliance with the fatigue damage and rutting accumulation laws) demonstrated the use of recycled polymers in HMA binder and base layers improved the service life compared to traditional HMA without significantly affecting the environmental burdens.

In terms of cost effectiveness, binder modification using recycled plastic in PMA is considered cost effective as this is a cheaper resource than virgin polymers, while reducing bitumen use. However, the cost of recycled plastic aggregates needs further evaluation as it could potentially be much higher than that of quarry aggregate due to pelletization production processes required [46]. Alghrafy et al conducted an economic study in terms of initial cost and performance for various recycled PE modified binders [137]. The authors found that in general, 2% and 1% in the initial cost of binder can be saved when using 6% LDPE and 2% HDPE to modify virgin asphalt. Furthermore, the cost could be further substantially decreased up to 29% when modifying sulphur extended asphalt with recycled PE plastics. Furthermore, Souliman et al divided the expected performance (predicted number of fatigue cycles to failure) by the mixture unit cost of one mile

for unmodified and polymer modified asphalt [189]. The cost effectiveness value of the PMA was 105.2 cycles per cost of one mile in comparison to 41.2 cycles for the unmodified mixture.

2.7 Pyrolysis Polyolefins in Road Construction

As discussed in *Section 2.3.2*, waste PO plastics can be thermally cracked into smaller molecular products via thermochemical technologies such as pyrolysis. It has been common in the past for authors to use pyrolysis for waste material treatment prior to the preparation of bio-binders/bio-asphalt, especially for biomasses, crumb rubbers and cooking oils [190, 191]. Pyrolysis could easily be applied in the same way as an acceptable strategy for upgrading waste plastics for this product application, through the concept of Design from Recycling. In this way, PO pyrolysis products could have large potential as a plastic derived additive for HMA. The idea of using pyrolysis plastics in asphalt binder and subsequent mixture modification is not entirely new but is currently not widely researched in literature.

Al-Hadidy et al proposed the use of pyrolysis PP as a new modifier material, which was thermally degraded at 308 °C and grinded into powder before being incorporated into 40/50 grade bitumen at 1-8 wt% [149]. The pyrolysis plastic was mixed for 7 minutes at 150 °C, which is a substantially smaller time in comparison to raw recycled PP, as can be seen in Table 2.5. It was determined that the plastic is well dissolved into the binder and compatible to an extent. Similar to PP modification, the penetration points decreases while the binder stiffness, softening point, and resistance to temperature susceptibility increases. The modified asphalt mixture showed an increase in Marshall stability and decrease in flow up to 2% PP content. From the indirect tensile strength test, it was concluded that the addition of pyrolysis PP increases the adhesion between aggregate and asphalt, indicating increased stripping resistance. The pyrolysis PP enhanced the resistance to permanent deformation and rutting. Later, Al-Hadidy et al conducted a similar study using pyrolysis PP with an aim to produce a homogeneous a storage stable PMB [192]. The PP was pyrolysed at 400 °C

for 2 hours, producing a brown coloured monomer material with a lower density and melting point range of 153-157 °C. This was mechanically ground and incorporated at 1-11 wt% into 50/60 grade bitumen at 160 °C for 5 minutes by slow speed shearing. The study produced analogous conclusions to [149].

The same authors then proposed to use pyrolysis LDPE as a modifier material in the stone mastic asphalt (SMA) layer of flexible pavements [13]. The LDPE was subjected to thermal degradation at 406 °C in a stirred batch reactor set-up, depicted in Figure 2.13. The reactor was heated using an internal heater connected to a temperature controller with corresponding temperature thermocouples. Upon heating, the feedstock was stirred, and upon cracking, left the system and entered a storage tank for collection. The pyrolysis LDPE was incorporated into bitumen at 2-8 wt% using a high-speed stirrer at 160 °C and 1750 rpm for 3-5 minutes. It was demonstrated that the pyrolysis LDPE can be well dissolved in the asphalt matrix and that it was compatible to an extent. The modified binders were less susceptible to temperature and had improved resistance to deformation. The Marshall stability increased with a decreasing flow up to 6 wt% LDPE addition. It was shown that the modified SMA specimens did not weaken when exposed to moisture and that the pyrolysis LDPE was effective in preventing excessive drain down of the mixtures (bleeding phenomenon.) It was speculated that after thermal degradation, LDPE contains a larger number of activated groups which made the chemical reaction with bituminous molecules easier and contributed to the indicated improvements in resistance to deformation. In addition, the pyrolysis LDPE reduced cracking potential at low temperatures (-10 °C.)

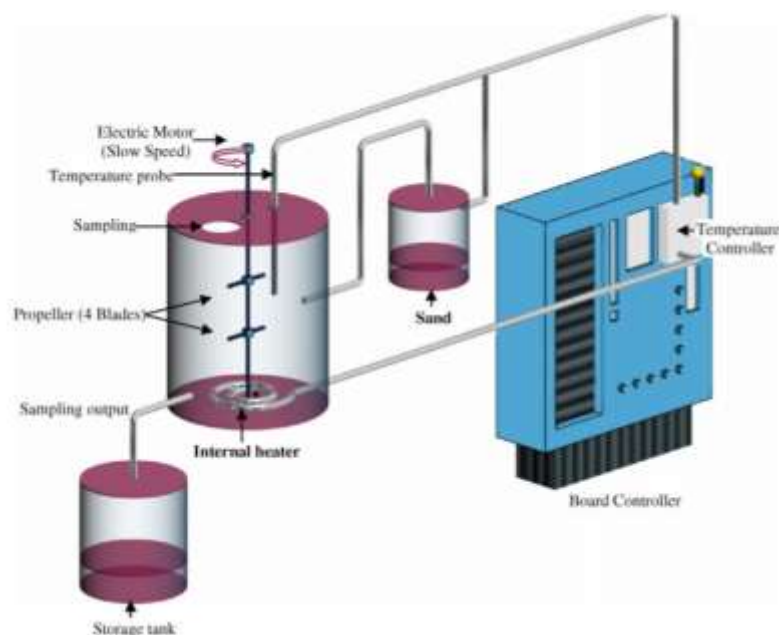


Figure 2.14 Thermal degradation stirred reactor system for pyrolysis PP, used by Al-Hadidy et al [192].

So far, pyrolysis PO plastics in asphalt binder and mixture modification has mainly resulted in very similar results to raw recycled plastic modification (see *Section 2.6.3-2.6.4.*) From the publications reviewed, an issue arises being whether the additional cost and further process environmental burdens associated with using pyrolysis plastics outweigh the advantages of using this new modifier material. A clear advantage is the ability to use lower mixing times and temperatures while achieving seemingly good mixture homogeneity, as the lower density and molecular weight additives can be completely dissolved in the bitumen. Despite this, rising mixture viscosities with an increase in pyrolysis plastic addition could still be a concern, as this suggests potential issues associated with blend workability or a limit on the amount of pyrolysis plastic that can be used. It is noted that the pyrolysis temperatures used in the works discussed are much lower than those commonly used in plastic pyrolysis literature (*Sections 2.3.2, 2.3.4.*) Looking at the thermogravimetric curves for the PO plastics, they typically completely thermally degrade at higher temperatures [193, 194]. This serves as explanation for the monomer materials produced with a melting point range of 153-157 °C that could be mechanically ground in certain studies [149]. Therefore, the extent of cracking of the plastics may not have been

enough to allow for any real changes to be seen, in comparison to the parent polymers.

Ling et al produced pyrolysis oils and waxes from waste rubber and plastic feedstock. Blends of these pyrolysis products were incorporated at 5 wt% into bitumen at 115 °C for 10 minutes. The waste-derived additive enhanced the workability and mechanical properties of the binders, increasing resistance to rutting, fatigue and low-temperature cracking [17]. Martinho et al thermally pyrolysed fresh and waste HDPE at 430-500 °C, using the resultant wax in a composite binder (polymer-modified binder, styrene-butadiene-styrene (SBS) and other functional additives) at a 2 wt% dosage. The composite wax modified binder exhibited a lower penetration point and higher softening point in comparison to the polymer-modified binder. The pure wax reduced the binder viscosity and while increasing the $|G^*|$, it also reduced the δ values and had an improved rutting resistance [195].

More research in this area that can provide more detailed pyrolysis processes and degraded product characterisation, as well as exploration into the modification mechanism between this new modifier and bitumen is needed. Additionally, further studies into the extent of compatibility of pyrolysis plastics and binders are needed to determine whether there are outstanding concerns with the storage stability of plastic-derived modifiers. Furthermore, LCA and cost assessments including the pyrolysis process to upgrade recycled plastics for use in HMA production will be beneficial in the future.

2.7.1 Wax in Bitumen

Bitumen naturally contains macrocrystalline, microcrystalline and/or non-crystalline waxes that contain branched, alicyclic, and aromatic components with heteroatoms [196]. The wax content and type within bitumen is highly dependent on the source and production process utilised. Such that, bitumens that originate from crude oil and naphthenic sources tend to contain microcrystalline and amorphous type waxes. Due to the chemical composition and structure of these,

performance problems associated with the crystallization and melting points seen within n-alkane microcrystalline waxes are negated. However, nowadays due to current refinery processes of straight run bitumen, wax is generally low in content and does not tend to negatively impact the binder or subsequent asphalt properties.

2.7.2 Wax Technologies in Asphalt Pavement

2.7.2.1 Warm-Mix Asphalt

Recently it has been suggested that due to the drawbacks associated with the waste plastic modification of asphalt binders, they instead be incorporated into warm mix asphalt (WMA) technologies. WMA mixtures have lower production temperatures of 100-140 °C (as opposed to HMA >150 °C) and therefore reduce the required energy, cost, fuel consumption and hazardous fumes, without compromising the performance of the mix [15]. There are various additives and foaming technologies that have been developed for WMA, one of which is organic additives. Organic additives function by reducing the viscosity of the base asphalt binder due to the presence of waxes and have been widely applied to improve the workability of high viscosity asphalt binders such as rubberised asphalt [16, 17].

A popular wax additive applied in literature from wax studios such as Sasol is the “Fischer-Tropsch” (Sasobit) paraffin waxes, produced synthetically from syngas [197]. While they reduce the viscosity of the bitumen at mixing and compaction temperatures, depending on the wax chain length, they can also generate stiffer materials at in-service conditions. Studies have shown an improved resistance of the mixtures against permanent deformation as well as improved interaction between modifiers (such as crumb rubber) and base asphalt [18-20]. Polyethylene wax is a lower molecular weight by-product of the polymerization process and is also widely studied for its application as a WMA additive [21, 196]. Authors have reported its incorporation in the form of fine-grained powder or granules into asphalt binder for mixture formulation [198]. The waxes have been seen to improve the moisture resistance of warm asphalt mixes; however, it is

recommended by some authors to be used as a warm mix additive at lower compaction temperatures and implemented in colder regions due potential rutting distress [21].

PE wax-based WMA additives have additionally been studied for its influence on polymer and rubber modified WMA mixtures, that provide high rutting resistance yet require higher mixing and compacting temperatures due to higher viscosities. Kim et al compared polymer modified, stone mastic HMA and WMA (with 1.5% polyethylene wax additive) and concluded that the polymer modified WMA with the wax additive had better performance characteristics [199]. The modified WMA had superior moisture, rutting, fatigue, and low temperature crack resistance than the modified HMA. Another publication to note is that by Shang et al, using pyrolysed wax from recycled crosslinked polyethylene as a WMA additive for crumb-rubber modified asphalt [200]. The pyrolysed wax was incorporated into the asphalt binder at 1-7% at 150 °C for 30 minutes. Its addition increased the softening point as well as the penetration point of the asphalt, while reducing the ductility negligibly. The addition of the wax also improved the rutting resistance parameter. The production of warm mix asphalt (WMA) has been a topic of discussion for many years within the paving industry yet has not become the standard for types of rolled asphalt mixes. The complete estimation of the potential economic benefits of using WMA technologies still needs to be explored and may not be feasible if not jointly evaluated with environmental regulations and additional costs and offsets of WMA production [17, 201].

Furthermore, at HMA production temperatures, Roja et al demonstrated that a 1% addition of PE wax to LDPE modified binders improved the dispersion of low melt flow index polymers [155]. The addition of PE wax reduced viscosity of the blends as well as the strain response and non-recoverable creep compliance of the mixtures (however, not to the extent of the binders with only LDPE additives.) The addition of the PE wax alone deteriorated the fatigue life of the binders, except when blended with low molecular weight LDPE with increased polymer chain mobility. Zhang et al reported an important relationship between the molecular weight (M_w) of LDPE and HDPE waxes and the modifying process

[202]. As the M_w of the waxes increases, the viscosity, moisture and low temperature resistance capacity of the wax modified asphalt mixtures increases, while the storage stability decreases. The high temperature resistance capacity of the PE wax modified mixtures was improved at higher M_w waxes also. A clear benefit of using plastic waxes in both hot and warm mix asphalt binders and subsequent mixes is the significantly lower mixing times (10-30 minutes [17, 200]) and/or temperatures (reduced from 20-60 °C [201].) Therefore, there is a lower cost of manufacturing, especially in comparison to raw plastic modification blending methods (see Table 2.5.)

2.7.2.2 Reclaimed Asphalt Pavement

As part of the Waste Framework Directive 2008/98/EC on waste, re-use is the second order in the hierarchy [203]. Such that, when the most favourable 'prevention/repair' route is no longer possible, asphalt can be reclaimed from the road at the end of its service life. After intermediate screening processes such as crushing and sieving, the aggregates and aged bitumen binders can be re-used in the production of new pavements. In the European Asphalt Pavement Association (EAPA) 2020 report, the total amount of reclaimed asphalt (RAP) available in the European reporting countries was 46 Mt [204]. Two key benefits of using RAP are the economic savings and environmental benefits, due to conserving energy, the reduction of virgin materials usage (resource preservation) and lower transportation costs associated with obtaining virgin materials. It also reduces the amount of construction waste that is sent to landfill. In general, the RAP level achievable in batch plants for hot mix recycling is 10-40% using the cold method (the RAP is heated by the virgin aggregates prior to mixing) and 30-80% using the hot method (the RAP is directly preheated in a separate drum.) Other batch and continuous RAP operations, as well as guidelines and standards are detailed elsewhere [203]. Researchers are exploring the potential of raising RAP content further, from 20-30%, to 40-50% and even 100% [205]. However, the most critical technical limitation in using RAP within HMA is the high stiffness of the mixtures and resultant low workability. This can lead to improper compaction in the field and ultimately lead to premature

material failure [27]. Studies have shown that the incorporation of RAP into HMA will make the mixture stiffer and more brittle due to the addition of aged binder [25]. A high stiffness will improve rutting resistance, yet negatively impact the fatigue performance of the mixture.

Recently, rejuvenators and soft binders have been researched for the modification of asphalt mixtures that contain RAP, improving their engineering properties. A rejuvenator contains a higher proportion of maltenes (or petrolenes), which are a mixture of small molecular weight resin and oil components [206]. The aim of using these additives is to re-balance the chemical composition of the aged and oxidized mixtures, which lose their maltenes during the ageing processes that occur during construction and service life [28]. Some rejuvenating agents used in literature include refined rape seed oil-based additives and tall oil from lignin depolymerization [198].

Higher usage of RAP is also reported to be feasible via the WMA wax technologies mentioned in *Section 2.7.2.1*, with ongoing research into new additives and rejuvenators [207]. Valentová et al utilised bio-based sugar cane, Fischer-Tropsch and polyethylene waxes in the modification of paving grade bitumen for use in an asphalt surface course containing up to 30% RAP. Upon evaluating the stiffness modulus, fracture toughness and indirect tensile strength (when subjected to water and frost), the study commented that this application of natural and synthetic waxes allows for the reduction of compaction temperature, while maintaining the quality of common HMA mixtures. This improves the favourability of recycling RAP which would typically have to be heated to extremely high temperatures, therefore excess thermal degradation of mixtures can be avoided [198]. Wanga et al conducted a performance investigation on recycled binders containing up to 70% artificial RAP binder with the incorporation of WMA additives. Of the WMA additives studied, it was demonstrated that the RAP + polyethylene wax mixture especially can offset the disadvantages of each other in fatigue and rutting resistance respectively, while reducing susceptibility to low temperature cracking. Moreover, the percentage of RAP binder can be increased with WMA technologies such as this [24]. However, the production of

WMA has been discussed for a while within the paving industry and has not yet become the standard type of rolled mix asphalt. An extensive valuation of the economic benefits of using these technologies still needs to be conducted, considering environmental regulations, the additional costs and offsets of WMA production, etc. [17, 201].

Considering the uses of pyrolysis products from other waste materials and blends in flexible pavements, multiple authors have noted the potential of pyrolysis oils as a rejuvenator for aged bitumen to reduce stiffness [17, 90]. Due to their softening effect, bio-oils have been widely studied in the recycling of RAP. They offer a double advantage of greater RAP amount in the asphalt mix and superior recycled asphalt functioning. It is observed that the majority of literature surrounding this topic utilises oils largely derived from sources such as biomasses and cooking/vegetable oils [208, 209]. This may be attributed to the large potential of PO plastic pyrolysis oils as alternative fuels, diverting research attractiveness. Further research into the effectiveness of PO plastic pyrolysis oils and waxes as sole rejuvenators for RAP could be conducted, apart from works that have previously studied combined polymer modified bio-derived rejuvenators [210]. Alternatively, recent publications have been conducted demonstrating the viability of biochar (derived from biomasses) for use in asphalt mixtures as bitumen modifiers and cement-based composites as nanoparticle fillers [211-213]. Such investigations are again limited for such plastic pyrolysis products, highlighting a research gap in the full understanding of plastic pyrolysis products as flexible road materials.

2.7.3 Plastic Pyrolysis Wax: Established & Potential Applications

It is typical in the pyrolysis of municipal plastics wastes (MPWs) that contain a high fraction of polyolefin polymers that aliphatic waxes are the main product at temperatures of around 500 °C and that the pyrolytic oil obtained also has a high content of wax in the form of heavy hydrocarbons. The undesirable qualities of this low-grade wax-oil mixture have attracted research attention around its potential as a cracking feedstock, upgrading the pyrolysis wax-oil into high-value

fuels and petrochemicals [29, 85]. Currently, catalytic degradation using solid acid catalysts such as zeolites, silica-alumina, fresh FCC catalysts and MCM-41 is the most commonly used method. HZSM-5 catalysts especially are well documented for the upgrading of pyrolytic wax-oils [84, 214]. Furthermore, it has been established in literature the suitability of different pyrolytic wax fractions for different upgrading processes. Light product waxes with a boiling point below 500 °C are typically planned for use as a (co-) feed in a steam cracker to yield monomers for polymer production, whereas the waxes with a boiling range above 500 °C are planned for use in fluid catalytic crackers (FCC-process) to yield petrochemical products, as aforementioned [109]. A commercial example of using paraffinic wax as a feed for refineries or steam crackers is the BP Polymer Cracking Process pilot plant, utilising a feedstock of mixed plastic wastes [215]. The higher heating value (HHV) analysis of pyrolytic waxes produced from cracking at 600 °C have been determined as comparable to original polymers and not much lower than gasoline or natural gas. Although an increase in olefin nature has been observed at higher processing temperatures, the HHV values are in the same order as standard fuels [29].

Alternatively, the direct combustion of pyrolytic waxes for energy is a suggested option if there is no commercial interest for their use as raw materials for production of fuels or chemicals. It has also been suggested that the product waxes could be gasified to hydrogen to make them more commercially beneficial [6]. Additionally, properties such as the freezing point of polyethylene (PE) wax from degradation do not in some cases make it feasible for gasoline and it would be more profitable to convert to wax compositions alike to commercial PE wax. Commercial PE wax has a wide application field including lubricants, additives in polyolefin processing, dyes, inks, antioxidants, candles, toys. Most commercial waxes such as this are produced from PE resins, making production cost high and the world market in short supply. Therefore, a technology such as pyrolysis has large potential and very strong competitive capability for the production of PE wax especially [112].

Multiple studies have been conducted for the investigation of pyrolysis parameters influence on waste polyethylene, to determine the applicability of this thermochemical technology for the production of waxes of ASTM commercial standard. With the careful control of parameters, waxes within the same melting point ranges as paraffinic and microcrystalline waxes and with penetration points close to the material standard range can be achieved [111, 112]. Compositional analysis has shown that degradation waxes are less branched and more olefinic than commercial waxes. Few authors have demonstrated that the application properties of waxes are only influenced to a minor extent by the olefinic groups, yet perhaps further investigation into their suitability for certain commercial applications may be necessary [104, 105].

In terms of commercialisation, the first waste packaging plastic conversion pyrolysis facility opened in 2019 by Trifol in Ireland for the target production of 'Envirowax'. This product is estimated to remove up to two tonnes of plastic waste with each tonne of wax produced and can be used for the production of cosmetics, candles, lubricants and chewing gum [216]. This commercialisation is significant as the technology is readily available for scaling up when further applications within other industries are identified for pyrolytic polyolefin wax. All established and on-going researched applications for pyrolytic waxes from waste polyolefin pyrolysis within the petrochemical and chemical industries have been summarised in Figure 2.14. With the current commercialisation of plastic pyrolysis waxes for use in typical commercial PE wax applications, as well as research and pilot plant-based investigations into the production of feedstocks for the petrochemical and chemical industries, it is yet still noted that this trend in research is less prominent than that for the production of pyrolysis oils from waste plastics for use in fuels. As well as this, outside of the applications stated, there is a general lack in knowledge of the known applications of pyrolysis wax outside of these industries.

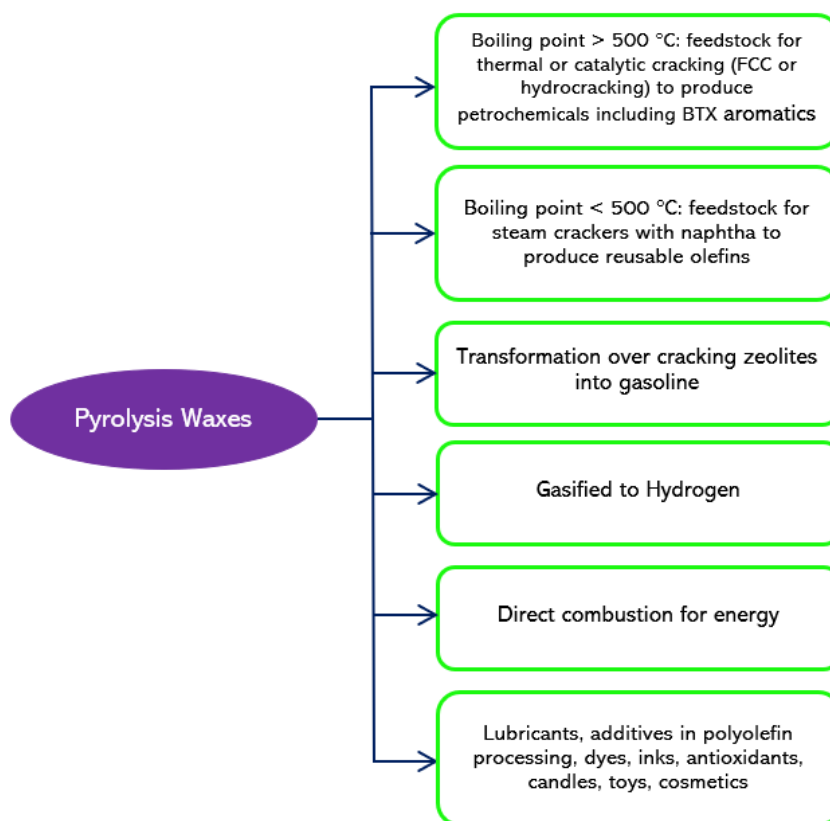


Figure 2.15 Established and on-going researched applications/upgrading routes for plastic pyrolytic waxes within the petrochemical and industries.

2.8 Summary

As part of the first phase of the project, in this chapter a comprehensive review of the pyrolysis of the abundant polyolefins found in municipal waste streams for the production of heavy wax products has been conducted. The use of these plastics as alternative materials in flexible pavements was investigated, specifically in asphalt binder and mixture modification. Furthermore, the use of plastic wax-based technologies in WMA and as modifiers in HMA was presented, providing discussion for the potential future use of PO plastics-derived wax products from pyrolysis as a modifier material in HMA.

Pyrolysis is a promising thermochemical technology for the treatment of plastic wastes that still largely go to landfill. From an environmental perspective, a multitude of author reviews and assessments indicate its advantage when compared to conventional recycling methods. It additionally has the capacity for

much future research and development to overcome its technological limitations. Furthermore, its current commercialisation for waste plastic treatment to fuel oils and waxes implies that the technology is readily available for adaptation and scaling up. In terms of the heavy wax fraction that is a main product of polyolefin thermal pyrolysis, a general lack in knowledge of its known applications outside of the fuel and chemical feedstock industries was identified.

The use of recycled polyolefin plastics in flexible pavements is a practical route as it has the capacity for incorporating high volumes of plastics, as well as reducing the cost of virgin materials. Their use in the modification of asphalt binders and subsequent mixtures, manufactured via the wet process, was mainly evaluated due to its prevalence in literature. These recycled modifiers offer a multiplicity of enhanced service properties over a wide range of temperatures, especially improving rutting resistance at high in-service temperatures as well as temperature and stripping susceptibility. LCA and cost assessment data from literature also support its use as opposed to the use of virgin plastics. However, it is not indicated as beneficial when compared to the traditional use of virgin binders due to the associated cost and environmental burdens with extra process steps and materials. It is recommended that extended investigation into the environmental and cost savings over the service life of the modified pavements needs to be conducted in the future, considering the increased service life and lesser maintenance costs. Nevertheless, the technical limitations with storage stability of polymer modified blends as well as environmental concerns of contamination, microplasticity and fuming remain as major hindrances to its future development and commercialisation. Such problems bring restrictions to the overall amount of waste plastic that can be used in this particular application, using either manufacturing method.

Alternatively, the use of polyolefin pyrolysis products was considered in asphalt modification. However, from the available publications that were reviewed, a query arises being whether the additional cost and further process environmental burdens associated with using pyrolysis plastics outweigh the similar results obtained for this new modifier material in comparison to raw plastic modifiers.

Future research is important to provide more detailed pyrolysis product characterisation and exploration into the modification mechanism between this new modifier and bitumen. Additionally, further studies into the extent of compatibility of pyrolysis plastics and binders are needed to determine whether there are outstanding concerns with the storage stability of plastic-derived modifiers. Furthermore, LCA and cost assessments including the pyrolysis process to upgrade recycled plastics for use in HMA production will be beneficial in the future.

The use of plastic-based waxes in warm mix technologies are seen to be beneficial from the perspective of performance, as well as the cost and time savings associated with manufacturing. A wax-based additive derived from the pyrolysis of recycled PO plastics for possible use in unmodified and modified HMA, WMA and RAP recycled asphalt applications could potentially be a viable solution to the current limitations associated with raw plastic modifiers. This may also offer environmental and economic benefits that are associated with wax-based modification and the increased use of recyclable materials in the flexible roads. At the moment, there is little comprehensive understanding of the full capacity for this pyrolysis product (and others) in industries such as infrastructure and construction and is worth more research, as part of Design from Recycling concepts.

CHAPTER 3: Experimental Programme

3.1 Introduction

This chapter details the laboratory experimental work performed for this study. A description of the materials used is provided as well as the experimental configurations utilised for pyrolysis wax production, w-binder, and asphalt mixture characterisation and performance testing. The main principles and techniques for data analysis are discussed for each test.

3.2 Materials

3.2.1 High-Density Polyethylene

High-density polyethylene (HDPE) was sourced from Sigma-Aldrich in the form of approximately 2 mm diameter clear round pellets (injection moulding grade). The materials physical properties were declared as density ($\rho = 0.952 \text{ g/mL}$), melt index (MI; 12 g/ 10 min), visca softening point (125 °C), and melting point (125-140 °C). HDPE was selected as it is one of the most abundant polyolefins in plastic waste streams today and has a very similar composition to its LDPE counterpart, such that the same valorization may be applied to them to produce very similar wax products (see *Section 2.3.4.*) Additionally, it decomposes into a relatively simple spectrum of hydrocarbons (waxes, oils, and gases) and due to the oxygen-free atmosphere, has much reduced emissions (dioxins, carbon dioxide) in comparison to other thermal treatment methods. Furthermore, its durable and rigid chemical structure allows it to withstand higher temperatures than LDPE, therefore requiring higher blending times and temperatures for raw plastic modification of bitumen. The findings of this study may act as a baseline and be translated to other pyrolysis configurations for the processing of HDPE and other plastics, as well as waste.

3.2.2 Asphalt Binder

The asphalt binder utilised was the Total Energies UK Azalt® 40/60 penetration grade binder. It is a commonly used bitumen grade in the UK, especially for heavily trafficked roads. Its grade designation properties are displayed in Table 3.1.

Table 3.1 Grade designation properties of Azalt® 40/60 asphalt binder.

Property	Units	Grade Designation	Test Method
Penetration @ 25 °C	dmm	40 – 60	EN 1426
Softening Point	°C	48 – 56	EN 1427
Resistance to hardening @ 163 °C	% max +/-	0.5	EN 12607 – 1
- Change in mass	min %	50	
- Retained penetration	min °C	49	EN 1427
- Softening point after hardening			
Flash point	min °C	230	EN 22592
Solubility in Toluene	min % (m/m)	99.0	EN 12592
Kinematic Viscosity @ 135 °C	min mm ² /s	325	EN 12595

3.3 Thermal Pyrolysis of HDPE

The HDPE pellets were pyrolysed using a bench scale system at 450-550 °C to examine the influence of operating temperature on product wax yield and properties. As seen in Figure 3.1, the system consisted of a fixed-bed reactor vessel containing a metal crucible that was first filled with 20 g of metal balls to provide improved heat transfer within the crucible, followed by 25 g of HDPE pellets for every batch pyrolysis reaction. The dimensions of the reactor tube were 50.8 mm diameter and 150 mm length. A Carbolite electric furnace model EVT 12/150B with a power capacity of 750 watts was used as the external heating source. Prior to each experimental run, the system was purged with nitrogen (N₂) gas to eliminate the presence of oxygen. Upon exiting the pyrolysis reactor, the gases passed through a 5 °C water condenser and further glassware for wax product condensation and collection. A cotton wool filter was in place to

capture any escaping vapours and the non-condensable gases were vented. Using this reactor configuration, the HDPE pellets were thermally degraded gradually, achieving the final temperature using a heating rate of 10 °C min⁻¹. Volatile products were purged from the reactor tube using two nitrogen flowrates (2 and 4 L min⁻¹) to additionally observe the influence of vapour residence time on the yield and properties of the pyrolysis wax products. The vapour residence times were estimated using the ideal gas law for the carrier gas and can be found in Table 3.2. The condensed wax product was collected after >2 hours of pyrolysis reaction time without separating the light and heavy fractions. All experiments were conducted in triplets. The product waxes were named according to the pyrolysis parameters used, for example the pyrolysis wax produced at 450 °C with a 2 L min⁻¹ carrier gas flowrate is referenced to as sample 450-2, and so on.

Table 3.2 Pyrolysis conditions.

Pyrolysis Temperature (°C)	Nitrogen (N ₂) Flowrate (L min ⁻¹)	Vapour Residence Time* (s)
450	2	3.76
	4	1.88
500	2	3.52
	4	1.76
550	2	3.30
	4	1.65

*Superficial, vapour residence time was estimated using Ideal Gas Law.

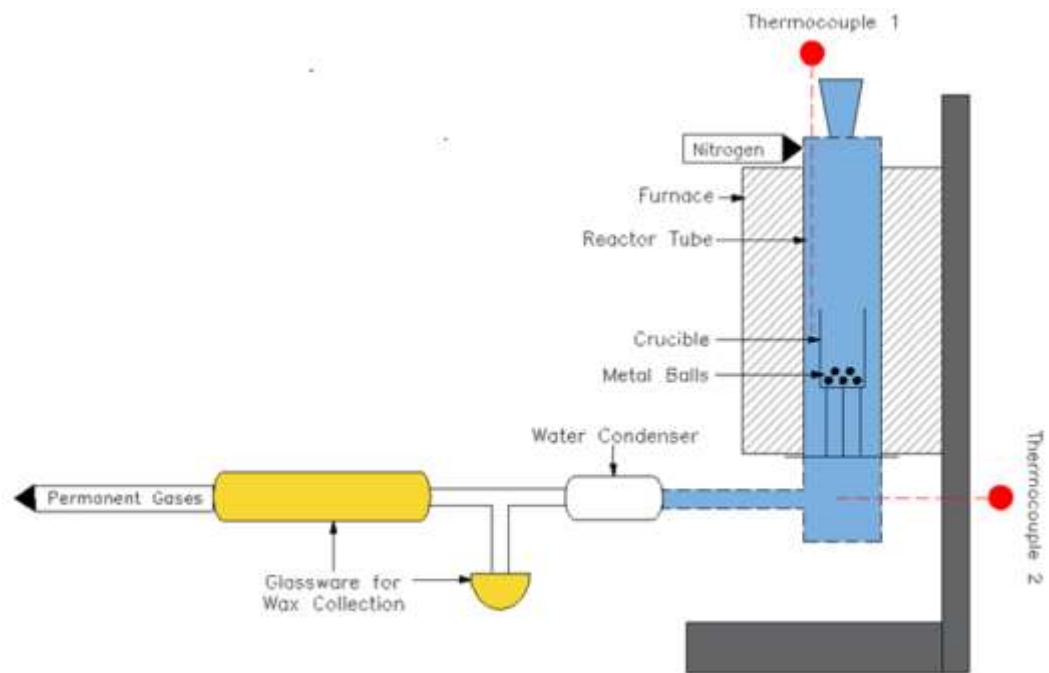


Figure 3.1 Schematic diagram of the bench scale pyrolysis reactor system used in this study.

3.4 w-Binder Production

Based on the experimental findings in Chapter 4, three waxes produced at 450, 500 and 550 °C using a constant nitrogen flowrate of 2 L min⁻¹ and resultant variable vapour residence times (Table 3.2) were selected for production of the w-Binders. The pyrolysis wax modified asphalt binders (w-binder) were prepared by blending the waxes produced at different pyrolysis conditions and 40/60 neat binder using a high-speed shear mixer at 150 °C with a rotation speed of 500 rpm for 15 minutes [9]. The mixing temperature, time and speed were recommended to minimize binder aging and reduce wax volatile loss in Chapter 4 [33]. The dosages of the wax modifiers were 6 wt% (typical plastic modification level in literature) and 12 wt% (high modification level.) 300 g of each w-binder was prepared with each batch blending. Figure 3.2 illustrates a summary of the production program for the w-binders. For simplicity, throughout the study the w-binder samples are referred to using the process temperature used to produce the HDPE pyrolysis wax, followed by the wax dosage, 'temperature (°C)-

modification level (%)'. For example, '450-6%' refers to a 6 wt% dosage of the pyrolysis wax produced at 450 °C.

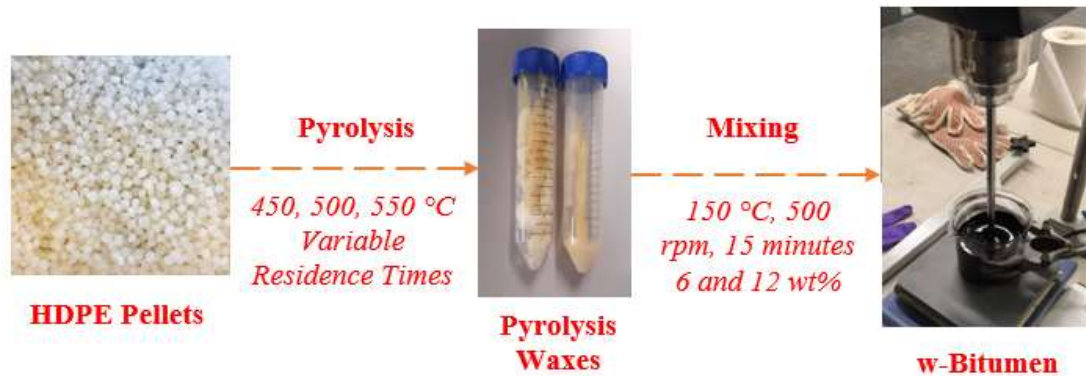


Figure 3.2 w-Binder production program summary.

3.5 Wax and Binder Characterisation

3.5.1 Gas Chromatography-Mass Spectroscopy (GC-MS)

- **Principle**

Gas Chromatography-Mass Spectroscopy is an analytical technique for the separation and identification of components within chemical mixtures, on a molecular level. The sample is vaporised, and its gaseous components are injected into a capillary column that is coated in a stationary solid or liquid phase. The sample components are carried through the column by an inert gas and elute at different retention times based on their interaction with the stationary column coating and mobile carrier gas phases (as a function of boiling point and polarity.) They are then ionized via a high energy electron beam and fragmented in the mass spectrometer, separating based on their mass-to-charge (m/z) ratios. Upon acceleration through the MS column, the ion fragments hit a detection plate, allowing for their relative abundance to be calculated and thus the components identified using commercial mass spectra libraries. A typical configuration of a GC-MS instrument is displayed in Figure 3.3.

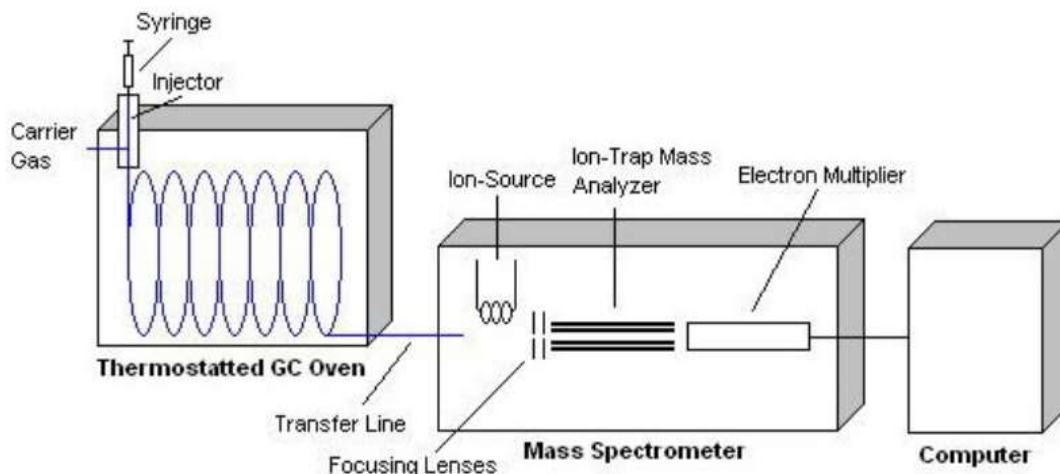


Figure 3.3 Typical GC-MS instrument configuration, [217].

- **Testing Protocol**

In this study, the wax samples were submitted for GC-MS chemical analysis. Prior to submission, the waxes were dissolved in toluene and filtered using PTFE 0.2µm filters to remove any undissolved solids that could affect the operation of the GC column. A Shimadzu GC-MS-QP2010 SE model was used for the analysis using a GC program of 50 °C to 300 °C with a heating rate of 10 °C/min [36]. The results are typically presented in chromatograms of the retention time of each sample component versus their relative abundance, a typical chromatogram for paraffin wax is displayed in Figure 3.4.

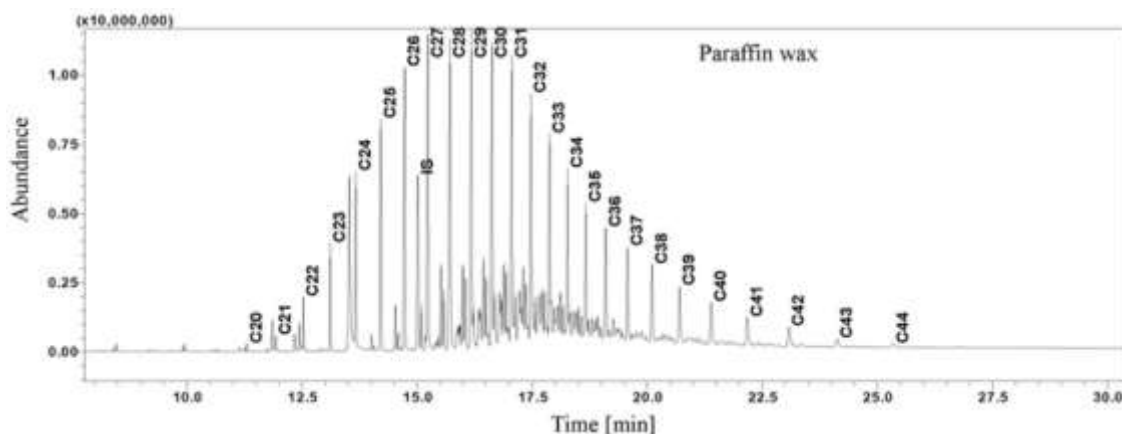


Figure 3.4 Typical chromatogram for paraffin wax, [218].

3.5.1.1 Mass Response Factor (RF) Calculation

To facilitate product analysis via GC-MS, the concepts of effective carbon numbers (ECN) and subsequent response factors (RF) for volatile organic compounds (VOCs) were utilised to obtain the relative mass% of each component within the waxes. The ECN is the sum of the carbon number (and equivalent for each molecular descriptor,) multiplied by the number of occurrences within the molecular structure of each compound, as exemplified in Equation (1) [219]:

$$\begin{aligned} \text{ECN} = & I^*(\text{CNE C}) + J^*(\text{CNE H}) + K^*(\text{CNE O}) + L^*(\text{CNE-CH}_3) \\ & + M^*(\text{CNE-CH}_2-) + N^*(\text{CNE-O-}) + O^*(\text{CNE>C=O}) \\ & + P^*(\text{CNE-CHO}) + Q^*(\text{CNE-CO}_2\text{H}) + R^*(\text{CNE Benzene ring}) \\ & + S^*(\text{CNE>C=C<}) \end{aligned} \quad (1)$$

Where I, J, K, L, M, N, O, P, Q, R and S are the occurrence number of each descriptor within each wax component's molecular structure. The ECN approach was then used to calculate the relative response factor for each wax component, where:

$$\text{RF} = m^*(\text{ECN}) + b \quad (2)$$

m and *b* were taken from Szulejko et al, a dataset of RF versus ECN for relevant VOCs in an experimental setup correlating to the one used in this study [219]. As the response factor is defined as the ratio between the concentration of a compound and the response of the GC-MS detector to that compound, the relative mass% could then be obtained:

$$\text{mass\% component} = \frac{\text{Peak Area}}{\text{RF}} \quad (3)$$

The mass fractions for each component with the pyrolysis waxes are categorised into carbon number distribution and component class and utilised to establish the existing relationships between pyrolysis process conditions and wax composition. They are also used to investigate the pyrolysis wax chemical composition before and after thermal ageing to determine ageing mechanisms.

3.5.2 Thermogravimetric Analysis (TGA)

- **Principle**

Non-isothermal thermogravimetric analysis (TGA) is a common methodology to examine the thermal properties of materials. It determines the fractional weight loss of volatiles in an inert environment of a sample as a function of temperature or time. Information about the temperature at which pyrolysis is initiated, when the rate of devolatilization is maximum, and the temperature at which the process is completed for plastic samples can be determined (onset to end-set temperatures.) Reactor design and operating temperatures can also be selected based on this analysis [220].

- **Testing Protocol**

Initially, TGA was utilised to confirm the selected range of pyrolysis temperatures to use within this study for the obtaining of waxes. It was then used to examine the thermal characteristics of the pyrolysis wax materials. Additionally, it was applied as an indicator for the thermal stability of the waxes for potential applications such as within asphalt pavements as alternative binder materials at 150-170 °C. A plastic/wax sample of 10mg was placed into a ceramic crucible. A Perkin Elmer Pyris 1 TGA (Figure 3.5) was used to analyse the pyrolysis waxes from 20-600 °C with a heating rate of 10 °C min⁻¹ under a constant flow of pure nitrogen (N₂) gas at 30 mL min⁻¹.



Figure 3.5 Thermogravimetric Analyser.

Typical weight loss versus temperature curves for HDPE show single step thermal decomposition in nitrogen, as shown in Figure 3.6, with decomposition generally ranging around 400-500 °C. Any residual masses noted tend to be attributed to the charring of the plastics under pyrolytic conditions and the presence of commercial additives [91, 221]. Likewise, a derivative thermogravimetric (DTG) curve can be utilised to observe the rate of change of mass with respect to temperature or time (rate of decomposition,) as also observed in Figure 3.6 for HDPE.

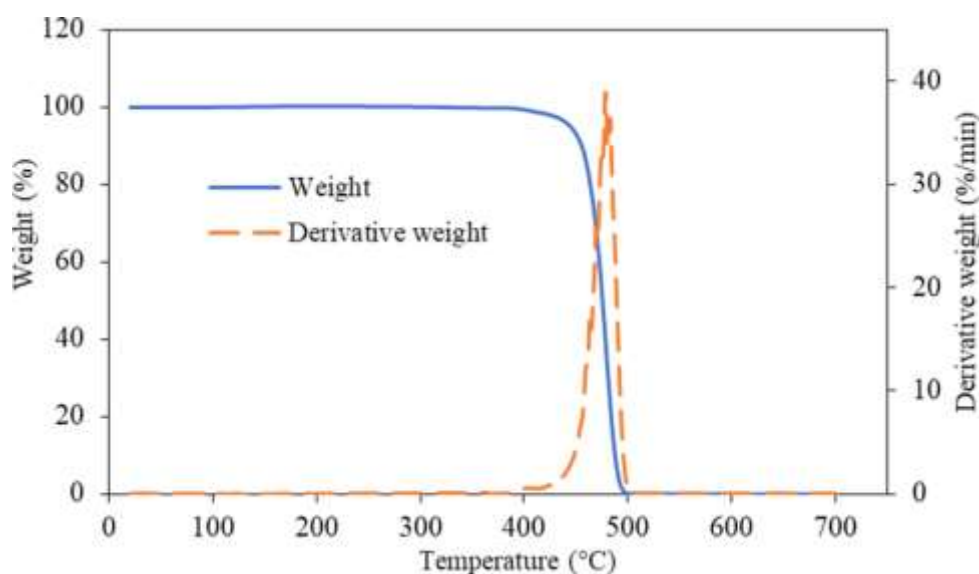


Figure 3.6 Typical TGA/DTG curves obtained for HDPE [222].

3.5.3 Differential Scanning Calorimetry (DSC)

- **Principle**

Differential Scanning Calorimetry (DSC) can be used in the thermal analysis of materials through the observation of how their heat capacity (C_p) changes with temperature in a controlled, inert atmosphere. It entails a sample of known mass to be heated/ cooled and its subsequent heat capacity recorded as changes in heat flow. Through this, the detection of key material transitions can be observed, such as melting temperature, glass transition and phase changes [223]. The experimental set-up involves two sample pans (the sample is placed in the first pan and the second pan is empty.) The two pans are placed on heaters within the DSC unit and the temperature is increased at a constant rate. When conformational changes happen within the sample material, more/ less heat flow is required from the heater to perform such transitions. In order for the heat flow of the sample pan to match that of the reference pan, the heat is adjusted accordingly and is recorded by the DSC. A typical DSC experimental configuration is shown in Figure 3.7.

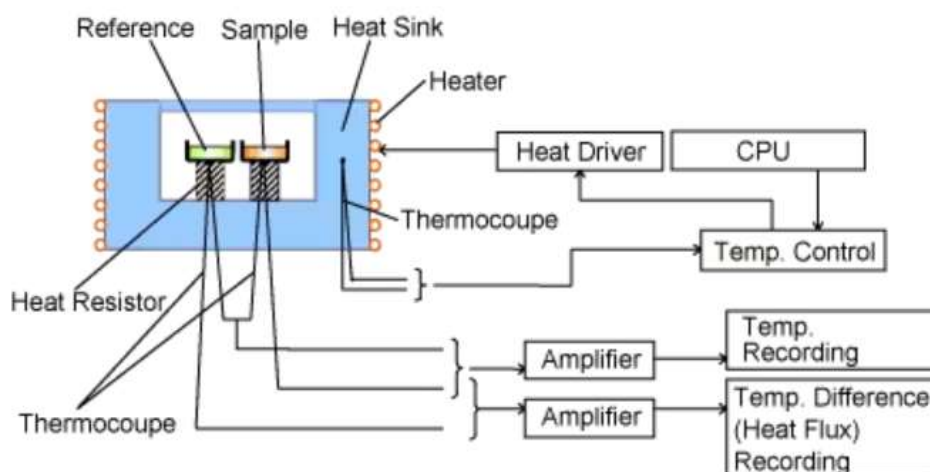


Figure 3.7 A typical DSC experimental configuration, [224].

- **Testing Protocol**

Waxes are made up of molecules of different size and nature, therefore do not have a characteristic melting point as in the case of pure substances. The melting temperature range (on-set and peak) of the plastic pyrolysis waxes in this study

were obtained via DSC. A sample of 10 mg was placed in a sealed hermetic aluminium pan. The thermal analysis was performed in a Mettler Toledo DSC 1 from 25-200 °C with a heating rate of 5 °C min⁻¹, in a nitrogen atmosphere. A typical results thermogram of heat absorbed versus temperature for polymers is shown in Figure 3.8.

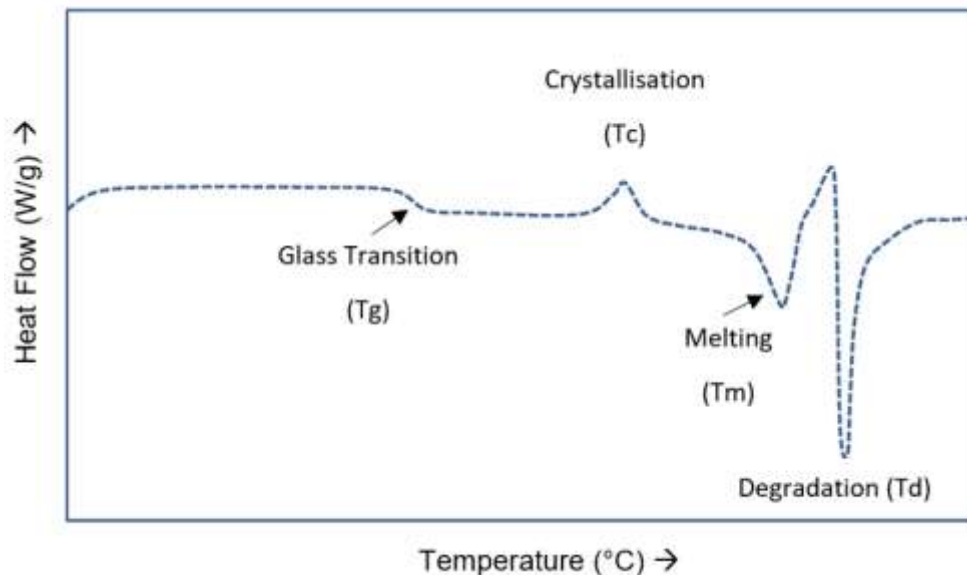


Figure 3.8 A typical DSC thermogram of heat absorbed versus temperature for polymers, adapted from [225].

3.5.4 Wax Ageing Experiment

To provide further interpretation of the results obtained from both TGA and DSC analyses for the pyrolysis waxes, an additional experimental setup was arranged for the thermal conditioning of the waxes in an ashing oven set at 170 °C for 1, 3, and 6 hours. 10 mg of the waxes were tested in ceramic crucibles (Figure 3.9.) The loss of volatiles was calculated from the mass loss. GC-MS and FTIR techniques (*Sections 3.5.1 and 3.5.5*, respectively) were utilised to show the effects of somewhat short-term ageing on the wax chemical composition. This was also utilised as an indicator for the suitability of pyrolysis waxes in asphalt pavement production, in which the bitumen binders are heated for prolonged times during mixing and storage. All ageing experiments were repeated three times.



Figure 3.9 Pyrolysis waxes in ceramic crucibles for short-term ageing test.

3.5.5 Fourier Transform Infrared Spectroscopy (FTIR)

- **Principle**

FTIR spectroscopy was employed in attenuated total reflectance mode (ATR), to allow for sample analysis in the solid or liquid state without further preparation. During the sampling, an infrared (IR) light is passed through a potassium bromide (KBr) crystal window, on which the sample is placed. Regions of the IR spectrum will be attenuated where the sample absorbs energy at this crystal-sample interface. The attenuated beam is directed via the crystal to a detector in the spectrometer, which uses this signal to generate an FTIR spectrum. This is further exemplified in Figure 3.10. The produced spectrum displays the measurement of IR absorption at different wavelengths (or wavenumbers, the reciprocal of wavelengths), which corresponds to the presence of certain functional groups within the samples [226]. FTIR spectra allow for the identification of organic, polymeric and some inorganic compounds while giving reliable information about the chemical aliphaticity and aromaticity of samples [227].

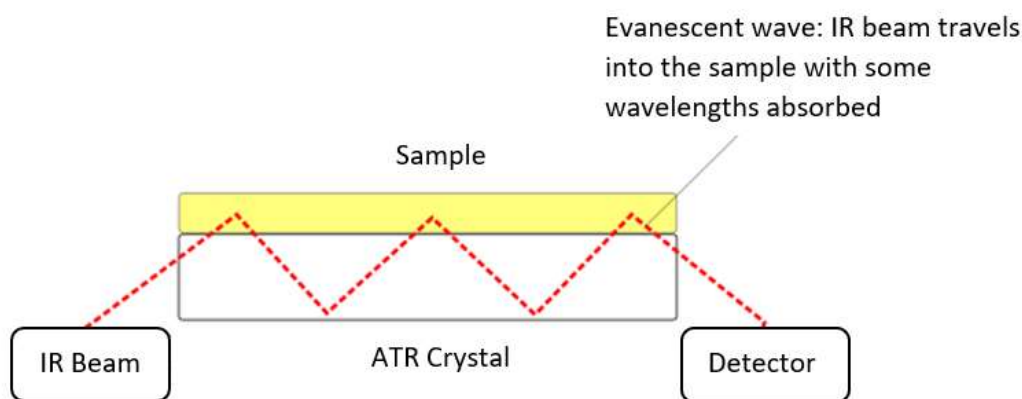


Figure 3.10 FTIR-ATR principle of operation.

- **Testing Protocol**

Within this study, FTIR was utilised to qualitatively identify the vibrational bands of chemical functional groups in both unaged and aged pyrolysis waxes. This may be used to determine their chemical and thermal stability in terms of chemical functional groups. It was also used to demonstrate the repeatability of the wax products between pyrolysis batches. Additionally, it was utilised to investigate the modification of the pyrolysis waxes upon incorporation into the bitumen binder. It was applied quantitatively to investigate oxidative ageing that takes place within the binders, as will be discussed in the next *Section 3.5.4.1*. A PerkinElmer Frontier Spectrometer was utilised to record the FTIR spectra between the wavelengths of 400 and 4000 cm^{-1} , performing 32 scans with a 4 cm^{-1} resolution. For analysis of the control and w-binders, the samples were heated, homogenized, and left to cool to ambient temperature. The analysis was carried out at room temperature, with the samples placed directly onto the ATR crystal window of the FTIR [228].

3.5.5.1 FTIR Calculation for Oxidative Ageing Indexes

The FTIR test has been applied to qualitatively and quantitatively analyse the oxidation reactions occurring to the unaged and (short-term and long-term) aged asphalt binders [227, 229]. For ageing tests, see *Sections 3.6.2-3.6.3*. Studies in literature provide the quantitative calculations for oxidation analysis using band areas [230]. The band areas are calculated using integration methods which

consider the area below the spectrum around a band maximum value, using baseline or tangential approaches. Hofko et al noted that between the two band integration methods, the tangential method has significantly worse reproducibility [228]. Therefore, the baseline approach was taken, and band areas were calculated using OMNIC Software. A typical FTIR spectrum obtained for long-term aged bitumen, demonstrating the key functional groups for the assessment of oxidation, as well as the different band area integration methods can be seen in Figure 3.11.

Functional group indexes that are typically used to characterise the oxidative aging of asphalt binders are the carbonyl (C=O) and sulfoxide (S=O) indexes. These are calculated via the following Equations (4-5):

$$\text{Carbonyl Index: } I_{\text{C=O}} = \frac{AR_{1,700}}{\sum AR} \quad (4)$$

$$\text{Sulfoxide index: } I_{\text{S=O}} = \frac{AR_{1,030}}{\sum AR} \quad (5)$$

Where AR comprises of the band areas for certain bond indexes: 1,700 cm^{-1} (C=O), 1,030 cm^{-1} (S=O), 1,035, 1,120 and 1,214 cm^{-1} (C-O), 1,465, 2,850, 2,920 cm^{-1} (CH_2) and 1,375 and 2,960 cm^{-1} (CH_3).

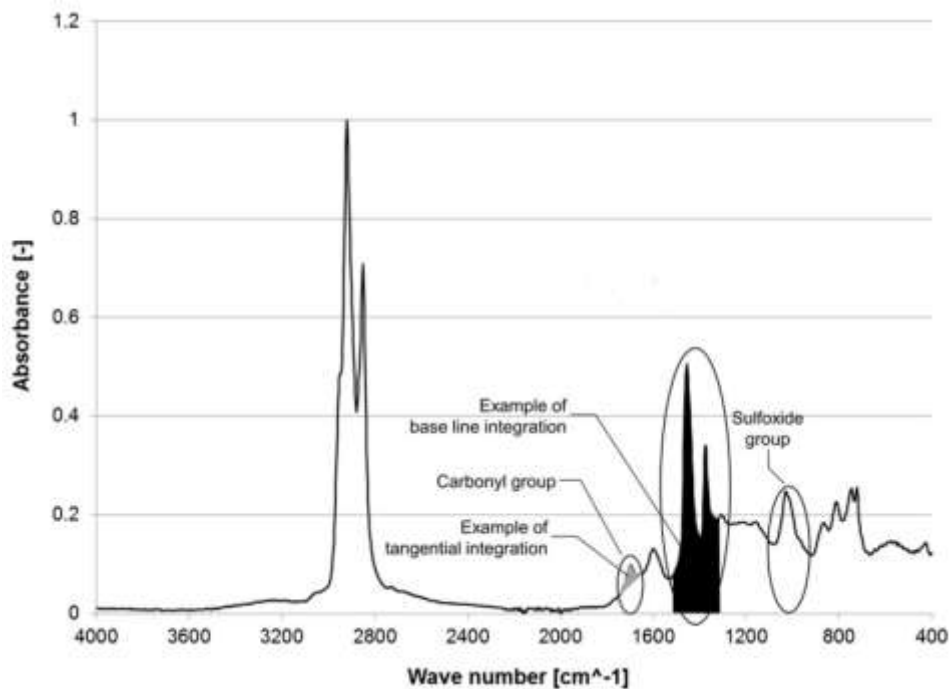


Figure 3.11 Typical FTIR spectrum obtained for long-term aged bitumen, demonstrating key functional groups for oxidation assessment and different band area integration methods. Adapted from [228].

3.5.6 Penetration Test

The penetration value of asphalt binder has been described as an indicator of its consistency, which in turn reflects its rheological properties [141]. Penetration tests were conducted at 25 °C on the samples according to BS EN 1426, using a standard needle, a 100 g weight and 5 second loading time [231]. Measuring this conventional physical property will indicate the hardness or softness of the control and w-binders. It will also aid in selecting a suitable control grade binder to provide good comparison to the w-binders in asphalt formulation and testing. Typical test configuration and the test set-up used is shown in Figure 3.12. The penetration distance was recorded to a tenth of a millimetre. Generally, lower penetration grade bitumens are used in hotter regions, whereas higher penetration grade bitumens are utilised in colder climates [32].

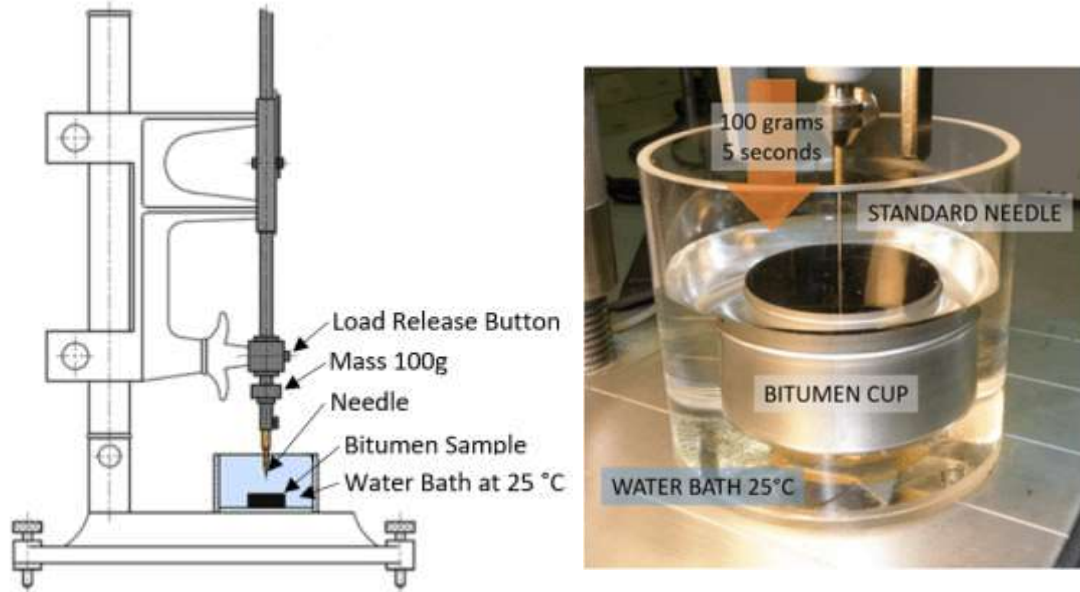


Figure 3.12 The penetration test: configuration and set-up, adapted from [232].

3.6 Binder Performance Tests

3.6.1 Dynamic Shear Rheometer

- **Principle**

The dynamic shear rheometer (DSR) is a piece of dynamic oscillatory test equipment that is used to characterise both the viscous and elastic behaviour of asphalt binders at intermediate to high service temperatures. In the case of the dynamic shear rheometer utilised in this study, an asphalt binder sample is placed between a top oscillating and bottom static plate. A constant strain is applied by moving the top plate to a fixed distance away (B) from the start position (A), back to the start position (A), and then repeated in the other direction at the same fixed distance (C), to move back to the start position again and complete one cycle [167]. This cycle is repeated continuously throughout testing and is further demonstrated in Figure 3.13. The required magnitude of stress to perform these movements is calculated from the required torque [167, 233]. The DSR OMNIC software used the following Equations (6-7) to calculate the stress and strain.

$$\sigma = \frac{F}{A} = \frac{2T}{\pi r^3} \quad (6)$$

$$\gamma = \frac{\theta r}{h} \quad (7)$$

Where σ is the maximum shear stress, F is force, A is area, T is torque, r is radius γ is maximum shear strain θ is deflection angle and h is the gap between the parallel plates.

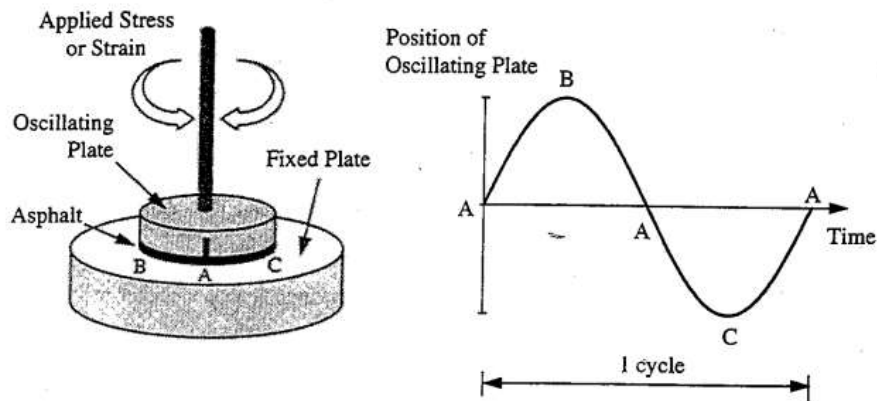


Figure 3.13 Basic principle of the Dynamic Shear Rheometer (DSR), [167].

From this, key rheological parameters may be measured for the asphalt binders at an applied sinusoidal strain and selected test temperatures and loading frequencies, including the complex shear modulus $|G^*|$ and phase angle δ . The complex modulus is typically used to assess a binder's resistance to deformation under repeated shear, such that a high complex modulus indicates a higher resistance to deformation [234, 235]. The phase angle is used for assessing the viscoelastic behaviour of asphalt binders, in which a higher phase angle (90°) indicates more viscous behaviour, while a low phase angle (0°) indicates a more elastic response [234, 235]. The selected sinusoidal strain applied to the asphalt binder during testing is expressed as:

$$\gamma^* = \gamma_o \sin \omega t \quad (8)$$

Where γ^* is the oscillating shear strain, γ_o is the peak shear strain, ω is the angular frequency (rad sec^{-1}) and t is time (seconds). The loading frequency (ω), also known as the angular frequency, is defined as:

$$\omega = 2\pi f \quad (9)$$

Where f is the frequency (Hz) and is the reciprocal of time, t . Sinusoidal stress is the response of the applied sinusoidal strain, however there is typically a time delay observed between the two which causes a lag. This lag is expressed as the phase angle (δ), as seen in Figure 3.14.

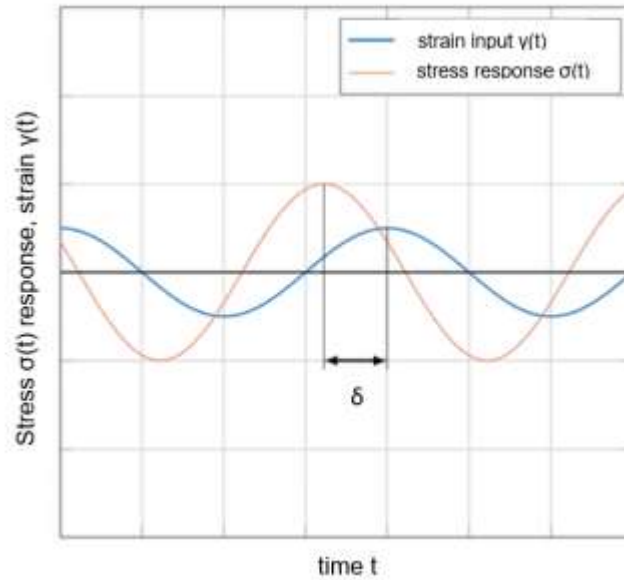


Figure 3.14 Phase lag between the applied sinusoidal strain and stress response, adapted from [236].

The sinusoidal stress response is expressed as:

$$\sigma^* = \sigma_0 \sin(\omega t - \delta) \quad (10)$$

Where σ^* is the oscillating stress response (Pa), σ_0 is the peak stress (Pa) and δ is the phase angle ($^\circ$). Furthermore, the ratio between the stress response and the applied strain is the complex modulus (G^*), which is defined as:

$$G^* = \frac{\sigma^*}{\gamma} = \frac{\sigma_0}{\gamma_0} e^{i\delta} \quad (11)$$

Where G^* is the complex shear modulus (Pa). The absolute function of this parameter can be expressed as the ratio of the peak stress to peak strain:

$$|G^*| = \frac{\sigma_0}{\gamma_0} \quad (12)$$

Which can also be written as:

$$G^* = \left(\frac{\sigma_0}{\gamma_0}\right) \cos \delta + i \left(\frac{\sigma_0}{\gamma_0}\right) \sin \delta \quad (13)$$

And:

$$G^* = G' + iG'' \quad (14)$$

Where G' is the storage modulus (Pa) or the elastic component, which is related to the amount of energy stored in the sample during each testing cycle. G'' is the loss modulus (Pa) or viscous/non-recoverable component and is related to the energy lost during each testing cycle through plastic flow or permanent deformation [167]. From Equation (14), the absolute function of the complex shear modulus can be calculated as the square root of the sum of the square of the storage and loss moduli:

$$|G^*| = \sqrt{(G')^2 + (G'')^2} \quad (15)$$

Additionally, the storage and loss moduli may be expressed as:

$$G' = G^* \cos \delta \quad (16)$$

$$G'' = G^* \sin \delta \quad (17)$$

The ratio of the viscous and elastic components of the complex modulus is equal to the phase angle tangent, written as:

$$\tan \delta = \frac{G''}{G'} \quad (18)$$

Testing temperature and frequency of loading have a significant effect on the G^* and δ of asphalt binders. Such that, they behave as elastic solids (represented by the horizontal arrow in Figure 3.15) at low temperatures. Whereas at high temperatures, they behave as viscous fluids (represented as the vertical arrow in Figure 3.15.) At pavement service temperatures, they simultaneously act like both, thus they are viscoelastic materials.

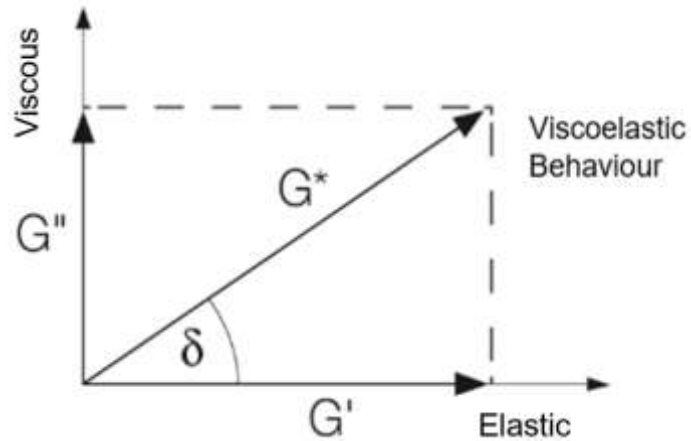


Figure 3.15 Relationship between the complex shear modulus, storage modulus (elastic component), loss modulus (viscous component) and phase angle.

- **Testing Protocol**

Rheological tests were conducted using a Kinexus Dynamic Shear Rheometer (DSR) from Malvern Panalytical. The bitumen samples were prepared according to BS EN 14770 [237]. An 8 mm diameter parallel plate geometry with a 2 mm gap was employed for tests conducted below 30 °C (increased stiffness of samples) due to torque limitations of the DSR [238]. A 25 mm diameter parallel plate geometry with 1 mm gap was utilised for tests above this temperature. The binder samples were heated to and remained at the test temperature for 5 minutes to achieve stability before loading was applied [239]. The DSR test equipment and plate geometries are shown in Figure 3.16.

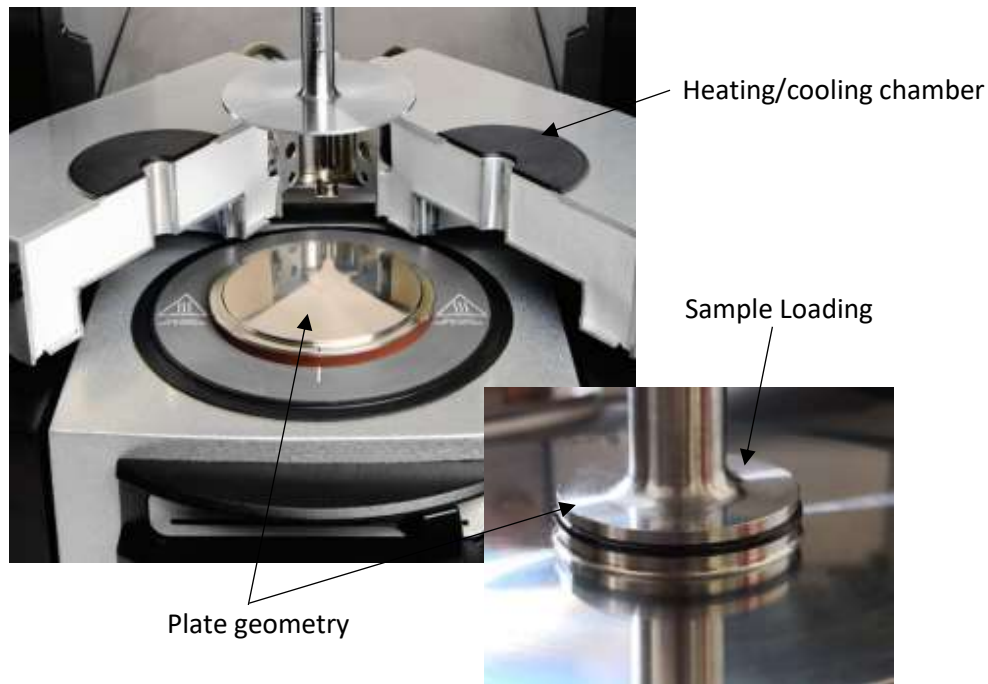


Figure 3.16 DSR test equipment with plate geometries.

3.6.2 Rolling Thin Film Oven Test (RTFO)

Prior to rheological characterisation of the control and w-binders, they were subjected to the rolling thin-film oven (RTFO) test to simulate the short-term aging process (BS EN 12607 [240]). 35 g of each sample was placed into a glass bottle and rotated to create a film of bitumen over their interior surface. Eight bottles containing samples at a time could be placed within the continuously rotating shelf (15 rpm) of the oven. The samples were aged at 163 °C for 85 minutes. Continuous rotating of the sample bottles was to ensure that no surface skin formed on the samples to prevent binder ageing and the air flow into the sample bottles was maintained at 4000 mL/min to ensure proper exposure of the bitumen to the heat and air [241]. The testing oven and sample bottles are shown in Figures 3.17-3.18. The mass loss of the control and w-binders was calculated using their weight prior to and following RTFO ageing, to determine the percentage weight reduction as a result of volatile loss at high temperatures, obtained by:

$$\text{Mass loss} = \frac{\text{Aged mass} - \text{Original mass}}{\text{Original mass}} \times 100 \quad (19)$$



Figure 3.17 RTFO oven.



Figure 3.18 RTFO sample bottles.

3.6.3 Pressure Ageing Vessel (PAV) Test

A portion of the RTFO aged asphalt binders subsequently placed in a pressure ageing vessel (PAV) chamber at to simulate the long-term ageing process (BS EN 14769 [242]). 50 g of each sample was poured into 140 mm diameter pans and placed into the pan holder of the PAV machine (Figures 3.19-3.20.) The control and w-binders were aged at 100 °C and 2.1 MPA for 20 hours. Furthermore, the aged samples were placed into a vacuum oven at 170 °C for 30 minutes at 15 kPa for degassing.



Figure 3.19 PAV sample pan.



Figure 3.20 PAV test set-up.

3.6.4 Frequency Sweep (FS) Test

- **Principle**

A frequency sweep (FS) test enables the viscoelastic properties of a sample to be determined in the undamaged linear viscoelastic (LVE) range. Key rheological parameters can be obtained such as the complex shear modulus (G^*), phase angle (δ) and complex viscosity (η^*). It can be performed at different temperatures for a fixed strain rate and varying loading frequencies. In literature, this testing method has been used to indicate the presence of synergistic effects of modified asphalt binders/mixtures and the effect of modifier materials on the viscoelastic properties [243]. It has been utilised for the selection of optimal dosage of modifier, a common trade-off being enhanced stiffness, which is favourable for rutting resistance but detrimental for fatigue cracking. Its results can indicate when the excess addition of a modifier will deteriorate the properties of the base binder [244].

- **Testing Protocol**

Frequency Sweep (FS) tests were performed according to BS EN 14770 on the unaged and aged (RTFO and RTFO+PAV) binders at 10-70 °C, with 10 °C intervals to obtain the shear complex modulus, phase angle and complex viscosity. Throughout the test, a frequency range of 0.1-25 HZ under a shear strain level of 0.5% were applied. [237].

3.6.4.1 Master Curve Construction

Master curves are constructed from FS data to enable the assessment of a binder's viscoelastic behaviour over an expanded range of loading frequencies. The continuous plot is obtained from isothermal plots that are manually shifted about a reference temperature using shift factors, $a(T)$. In this study, master curves were produced using the Arrhenius shifting factor law and the Christensen and Anderson (CA) Model. The horizontal time-temperature superposition principle (TTSP) shifting of the rheological parameters was modelled using the following Arrhenius and associated Equations (19-20) [245]:

$$\log(a_T) = \frac{-\Delta H}{2.303R} \left(\frac{1}{T} - \frac{1}{T_{ref}} \right) \quad (19)$$

$$a_T = \frac{f_r}{f} \quad (20)$$

Where a_T is the shift factor, R is the universal gas constant, ΔH is the flow activation energy, T is the tested temperature, T_{ref} is the selected reference temperature (40 °C), f is the tested frequency and f_r is the reduced frequency at the reference temperature. For the determination of $|G^*|$, the following CA model was used in Equation (21) [246]:

$$|G^*| = G_g \left[1 + \left(\frac{f_c}{f_r} \right)^{\frac{\log 2}{R}} \right]^{\frac{R}{\log 2}} \quad (21)$$

Where $|G^*|$ is the predicted shear modulus, G_g is the glassy modulus, R is rheological index and f_c is the crossover frequency. The resultant master curve will be a plot of the complex modulus against the reduced frequency on a log-log scale. A typical master curve and its construction is shown in Figure 3.21.

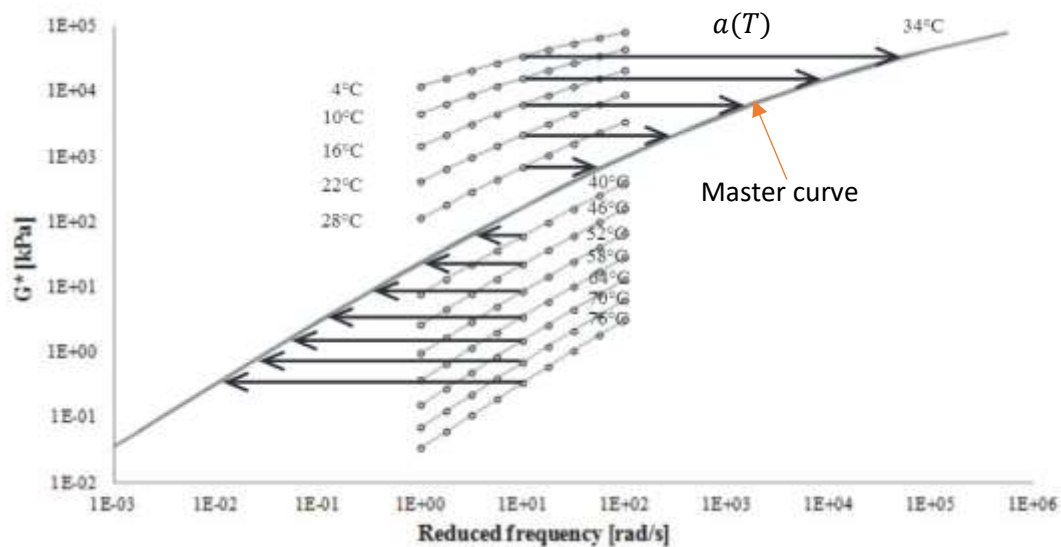


Figure 3.21 A typical master curve and its construction, adapted from [247].

3.6.4.2 Black Diagram

The black diagram is often utilised to identify patterns within datasets that can be influenced by the presence of binder modifiers. For wax modifiers, this data representation can indicate the melting of the wax and whether it occurs within the measured temperature range, as well as the effect on the mechanical properties of the material [197]. Black diagrams were constructed from the FS data over the temperature range of 30-70 °C to evaluate the relationship between $|G^*|$ and δ in the unaged condition for the control and w-binders. If there is a high content of wax, asphaltenes and polymer within the binder, a disjointed curve as opposed to a smooth one is often observed [248]. Typical black diagrams plot $\log |G^*|$ versus δ , as seen in Figure 3.22, for bitumens modified with different chain length Fischer-Tropsch waxes.

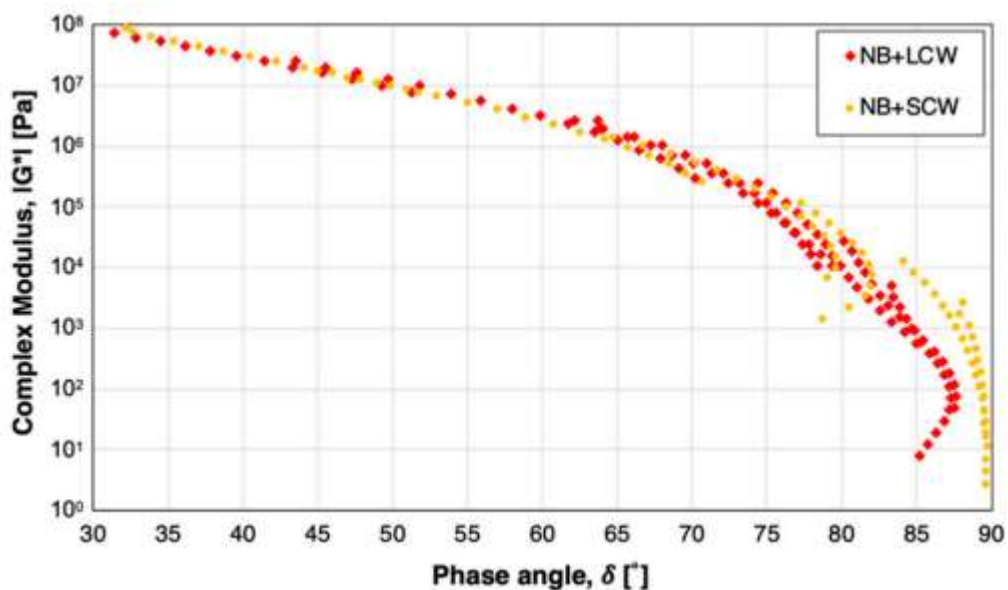


Figure 3.22 A typical black diagram for bitumens modified with different chain length Fischer-Tropsch waxes, [197].

3.6.4.3 Complex Viscosity

Viscosity is one of the most important properties of asphalt binders used as paving materials. Knowledge of binder viscosity provides information about their pumpability, mixability and workability [249]. The complex viscosity (η^*) is a vital

rheological parameter that indicates the change within a materials structure and consistency, in relation to temperature and loading time. This parameter may also be used to indicate an asphalt mixtures resistance to viscoelastic deformation [250].

Non-Newtonian fluids can have a viscosity that is dependent on the applied shear rate and shear stress and have two main categories: shear-thinning (pseudoplastic) fluids and shear-thickening (dilatant) fluids. Highly modified binders especially exhibit non-Newtonian behaviours due to the interaction between the bitumen and the modifier [249]. Cox and Merz stated the empirical relationship that the steady-state viscosity at some shear rate ($\dot{\gamma}$) can be related to the dynamic complex viscosity as follows:

$$|\eta^*(\omega)| = \eta(\dot{\gamma}) \quad (22)$$

Where $|\eta^*(\omega)|$ is the absolute value of the dynamic complex viscosity as a function of angular frequency, and $\eta(\dot{\gamma})$ is the steady-state viscosity as a function of shear rate [251]. This has been found to be applicable in the shear-thinning region of bitumen [252]. In this study, complex viscosity (η^*) values were obtained from the DSR test results over the whole FS test temperature range (10-70 °C.) This was to understand the effect of the pyrolysis waxes on this rheological parameter as well as categorise the non-Newtonian behaviour of the w-binders. It was also used to indicate binder resistances to permanent deformation and determine whether the pyrolysis waxes offer a solution to the workability issues previously seen in polymer modified binders. [134, 165]. A typical isochronal plot of the $\log \eta^*$ versus temperature and log-log plot of the η^* versus ω is shown in Figure 3.23.

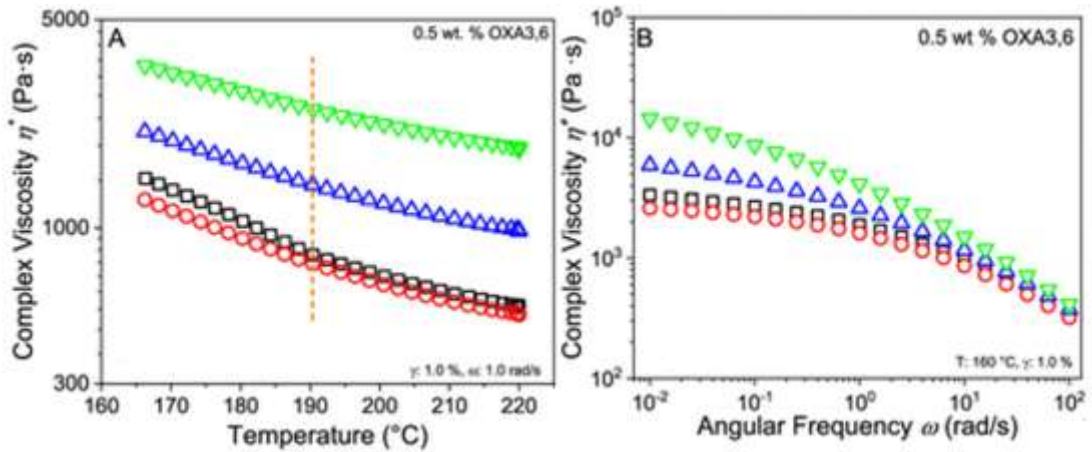


Figure 3.23 A typical isochronal plot of the $\log \eta^*$ versus temperature and log-log plot of the η^* versus ω , [253].

3.6.5 Rutting factor

- **Principle**

The high temperature performance of the RTFO aged control and w-binders was initially going to be characterised by obtaining the non-recoverable creep compliance (J_{nr}) using the multiple stress creep recovery (MSCR) test at 58 °C (BS EN 16659 [254]). During this test, a creep load is applied for 1 s followed by a 9 s recovery time. Each specimen is subjected to 10 cycles with a creep stress of 0.1 kPa, followed by 10 cycles with a creep stress of 3.2 kPa [255]. Due to the results obtained from this test, as will be discussed in Chapter 5, the original Superpave rutting factor was alternatively obtained [256].

With each traffic loading cycle, work is done to deform the pavement surface. A portion of this work is recovered through the elastic component of the surface, while some work is dissipated in the form of deformation and heat [257]. The work dissipated with each loading cycle at a constant stress is expressed as:

$$W_c = \pi \times \sigma_o^2 \left(\frac{1}{G^* / \sin \delta} \right) \quad (23)$$

Where W_c is the work dissipated with each loading cycle; σ_o is the applied stress per loading cycle, G^* is the complex modulus and δ is the phase angle. According to Equation (24), $G^*/\sin \delta$ may be extracted and considered the rutting factor for

predicting the rutting resistance of asphalt binders. This calculation is typically considered as unsuitable for the evaluation of polymer modified binders, as recoverable delayed-elastic deformation is not taken into account [258]. However, it may be acceptable for characterising binders modified with polymer derived products from thermal degradation, such as waxes.

- **Testing Protocol**

In this study, $G^*/\sin\delta$ is extrapolated from the rheological analysis to evaluate the performance of the control and w-binders at higher in-service pavement temperatures. A higher rutting factor indicating superior performance of a binder. Authors in literature have started the $G^*/\sin\delta$ test from 52-64 °C and increased the temperature until the rutting factor is (or less than) 2.2 kPa [17, 255]. Due to the results seen in the MSCR test, in this work a lower starting temperature of 40 °C was selected, increasing in 10°C intervals (10 rad/s, 0.5% shear strain). Figure 3.24 shows a typical plot for the rutting factor as a function of temperature.

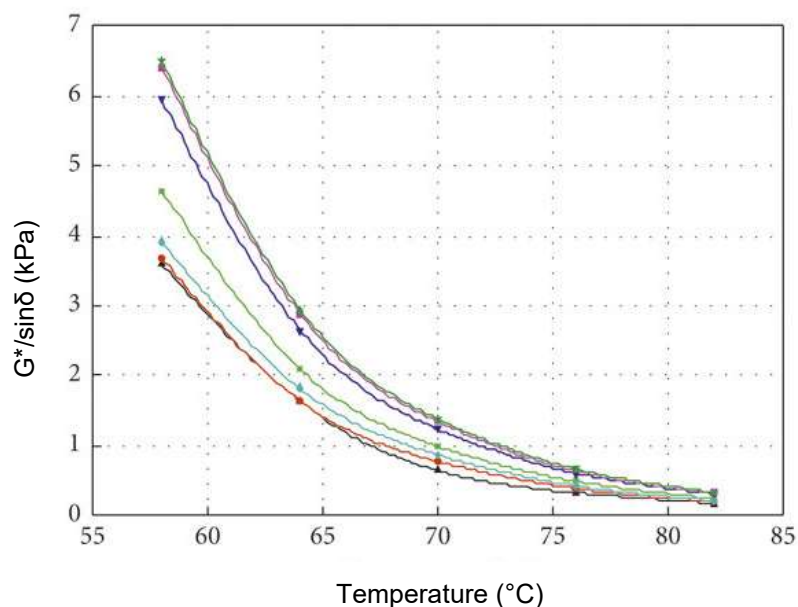


Figure 3.24 Typical plot of $G^*/\sin\delta$ as a function of temperature, adapted from [259].

3.6.6 Shear Fatigue Tests

The accurate characterisation and quantification of the fatigue resistance of asphalt binders is critical for the optimisation of asphalt mixture design and furthermore, the extension of the pavement service life. Two types of shear fatigue tests were performed on the RTFO+PAV aged binders, the linear amplitude sweep (LAS) test and time sweep (TS) test. This was in accordance with the accurate and effective DSR-based crack growth mechanics model (DSR-C) for fatigue crack length prediction, as proposed by Gao et al [239]. The predicted crack growth under a rotational shear force in terms of crack length can serve as a direct evaluation of the bitumens resistance to fatigue cracking.

To overcome the deficiencies of the Superpave fatigue parameter ($G^*\sin\delta$), which does not measure the material in the damaged condition; has poor correlation with the fatigue phenomena that occur in the field; and low applicability for modified binder characterisation, Bahia et al proposed the Time Sweep (TS) test [260]. The Time Sweep (TS) is a repetitive cyclic loading test that has been successfully utilised for defining the fatigue failure of bitumen, from which established the empirical indicators for fatigue failure such as the dissipated energy concept [261]. Despite its good correlation with the asphalt mixture fatigue test, it unfortunately has an excessively long testing time and is unrepeatable. [262] Therefore, Johnson developed the Linear Amplitude Sweep (LAS) test, which quantifies the accelerated fatigue damage of asphalt binders. It involves cyclic loading of the tested sample with a constant frequency and a gradually increasing strain amplitude in order to measure the bitumen damage tolerance [261]. This procedure was later modified further to achieve correlation with the asphalt mixture fatigue test; used to develop fatigue laws based on viscoelastic continuum damage (VECD) mechanics; and became a provisional standard procedure for AASHTO (The American Association of State Highway and Transportation Officials) [261, 263].

3.6.6.1 Linear Amplitude Sweep (LAS) Test

In this study, the LAS test was used to obtain the shear modulus ($|G_0^*|$) and phase angle (δ_0) of the binders in the undamaged condition, performed under strain amplitudes ranging from 0.1% to 15% linearly, at 20 °C and a frequency of 10 Hz. Additionally, from this test a suitable level for the controlled strain could be selected for the TS fatigue damage test. Li et al stated that theoretically, the ($|G_0^*|$) and (δ_0) can be obtained using the average of the $|G^*|$ and δ within the undamaged strain level range of 0.01- 0.8% [264]. However, it is stated that sample-to-sample variation should also be considered. Therefore, these parameters were obtained by averaging the values within the LVE (plateau) region of each LAS curve, as seen in Figure 3.25.

The DSR-C model will be used to evaluate the fatigue performance of the binders in this study. However, the maximum stress (τ_{max}) reached by a sample during the LAS test is a specified criterion of its fatigue life, the peak stress being the yield threshold when the binder is subjected to increasing load [265]. Additionally, a higher peak area indicates a more ductile, tougher binder, indicating that more energy is required to collapse the material. A typical stress versus strain curve obtained from the LAS test is shown in Figure 3.26.

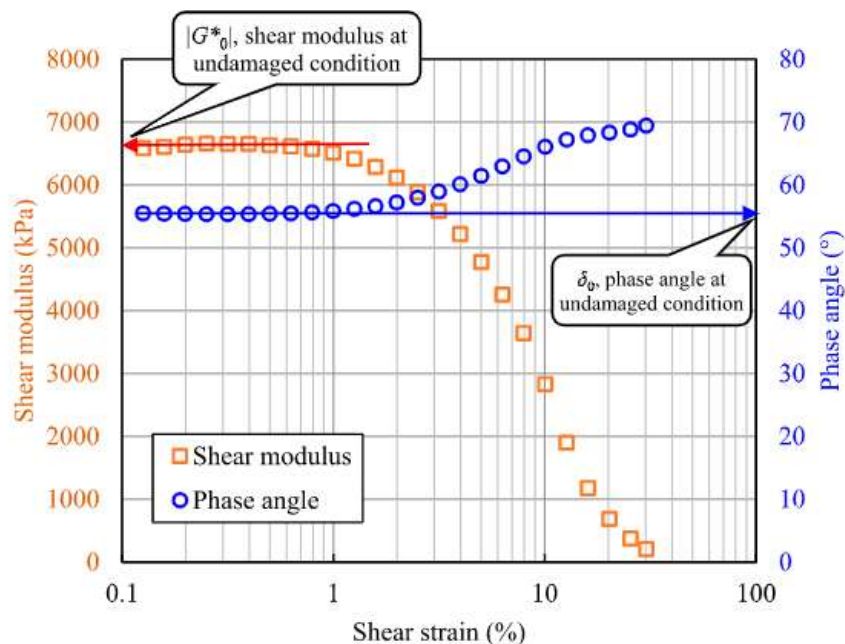


Figure 3.25 The ($|G_0^*|$) and (δ_0) determined from LAS test results, [261].

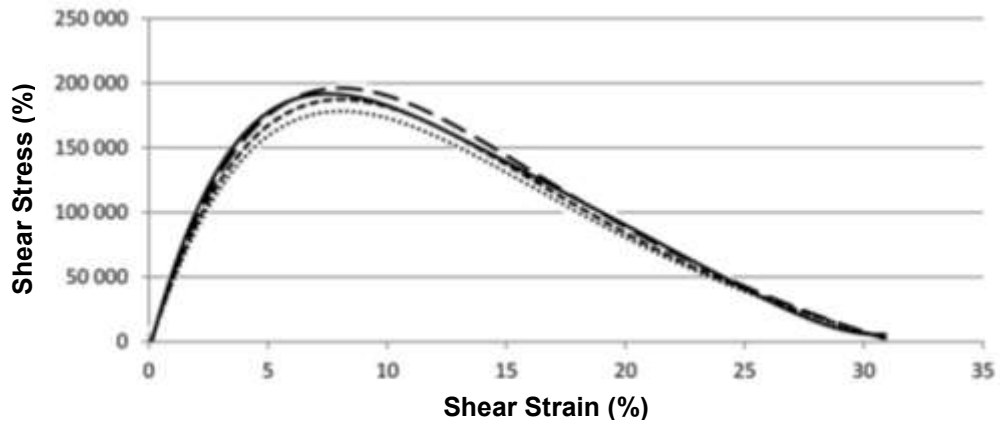


Figure 3.26 A typical stress versus strain curve obtained from the LAS test, [266].

3.6.6.2 Time Sweep (TS) Test

In this study, the TS test was performed to obtain the shear modulus ($|G_N^*|$) and phase angle (δ_N) of the binders with the number of load cycles in the damaged condition. A 5% strain level was utilised with the same test frequency and temperature as employed in the LAS tests. As can be seen in Figure 3.27, the phase angle increases up to a peak during the test and this peak is used to obtain the values for ($|G_N^*|$) and (δ_N), defining the fatigue failure of binders. Additionally, a common criteria used for determining the material failure point in the TS test is the point at which $|G^*|$ reaches 50% of its initial value, $N_{50\%G^*ini}$ [267].

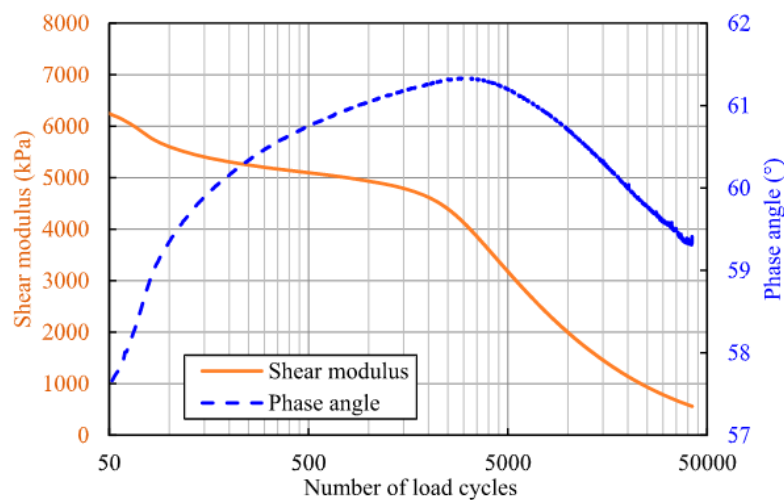


Figure 3.27 Typical results of time sweep (TS) test, from which ($|G_N^*|$) and (δ_N) may be obtained [261].

3.6.6.3 Mechanistic Modelling of Crack Growth

The measured rheological parameters described in Sections 3.6.6.1-3.6.6.2 were used in the DSR-C model defined in Equation (24), to obtain a predicted crack growth length in the Time Sweep test:

$$c = \left[1 - \left(\frac{|G_N^*|/\sin(\delta_N)}{|G_0^*|/\sin(\delta_0)} \right)^4 \right] r_0 \quad (24)$$

Where c is the crack length in a cylindrical bitumen sample; $|G_0^*|$ and δ_0 are the shear modulus and phase angle in the undamaged condition, respectively; $|G_N^*|$ and δ_N are the shear modulus and phase angle at the N th load cycle at the damaged condition respectively; and r_0 is the original radius of the bitumen specimen [239]. From this, pre-defined phases (see Figure 3.28) for crack evolution and propagation may be identified within the generated crack length curves for the control and w-binders. These can give key insights to the relationships between the chemical composition of the binders and fatigue damage tolerance, as will be discussed in the results chapters.

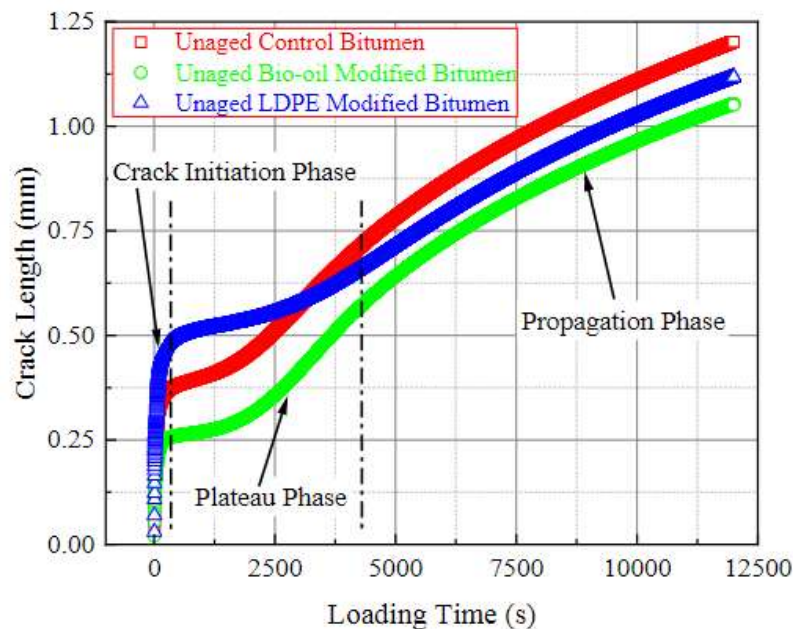


Figure 3.28 Evolutions of crack length for bio-oil modified bitumen, [264].

3.6.7 Dispersity – Optical Microscope

Dispersity describes the extent of fragmentation of a dispersed phase or additive within the bitumen binder. A considered technical limitation for waste plastic modified binders is the ease of dispersity as well as potential to phase separate from the bitumen during static storage, aggregating within the binder. To evaluate the dispersity of the pyrolysis waxes within the neat bitumen, the optical function of an OSTEC RAMOS S120 Raman microscope, using 2592x1944 resolution, 50x magnification, was utilised. The samples were heated and homogenized, stirred to remove air bubbles, and an aliquot of each sample was placed between two 1 mm soda lime glass slides and viewed under the microscope. The microscope equipment and an example of the glass slide samples are in Figures 3.29-3.30.



Figure 3.29 OSTEC RAMOS S120 microscope.



Figure 3.30 Example of glass slide samples.

3.7 Asphalt Mixture Formulation

3.7.1 Asphalt Binder

This phase of the study involved the formulation of three mixtures:

1. Control mixture using 70/100 binder (Control).
2. Test mixture using 40/60 binder + 6wt% pyrolysis wax (PW).
3. Test mixture using 40/60 binder + 6wt% pyrolysis wax + 20wt% RAP (RAP+PW).

The Control mixture utilised a Total Energies UK Azalt® 70/100 penetration grade binder to provide an accurate comparison with the test mixtures, based on the effect of the selected pyrolysis wax on the penetration point value of the 40/60 base binder, as seen in Chapter 5. The grade designation properties of the 70/100 binder are presented in Table 3.3. The PW mixture was formulated using a preblended 40/60 binder with HDPE pyrolysis wax. The method for its production as well as properties can be found in Sections 3.2-3.4. A 6wt% dosage was initially chosen as this is a typical dosage for raw HDPE modification in literature. The RAP+PW mixture uses the same binder as the PW mixture and will provide analysis of the rejuvenation capacity of the pyrolysis wax in a mixture containing RAP. In this way, the wax may reinstate the aged binder's properties to ensure better performance of recycled mixes, while greatly increasing the total amount of recyclables used in asphalt roads.

Table 3.3 Grade designation properties of Azalt® 70/100 asphalt binder.

Property	Units	Grade Designation	Test Method
Penetration @ 25 °C	dmm	70 – 100	EN 1426
Softening Point	°C	43 – 51	EN 1427
Resistance to hardening @ 163 °C	% max +/-	0.8	EN 12607 – 1
- Change in mass	min %	46	
- Retained penetration	min °C	45	
- Softening point after hardening			EN 1427
Flash point	min °C	230	EN 22592
Solubility in Toluene	min % (m/m)	99.0	EN 12592
Kinematic Viscosity @ 135 °C	min mm ² /s	230	EN 12595

3.7.2 Aggregates

A Porphyritic Andesite aggregate from Bardon Hill Quarry, UK was used for the asphalt mixtures formulated in this investigation. The filler was crushed limestone, which was obtained from Tunstead Quarry, Derbyshire, UK. The aggregate grading envelope for an AC14 close surface course was utilized for all mixtures, complying with BS EN 13108-1:2006, the gradation curve is shown in Figure 3.31 (top). This target composition required a binder content (B_{act}) of 5.1%. The target air void content for this design was $4.0 \pm 0.5\%$. The reclaimed asphalt utilised within the RAP+PW mixture was sourced from Colemans Quarry, Somerset, UK, with a 4.1% soluble binder content and particle size distribution that is presented in Figure 3.31 (bottom). The maximum density for each mixture was determined via density pycnometer apparatus according to BS EN 12697-5:2018. From this and the target air voids, the required bulk density of the mixtures could be calculated and subsequently the mass of each mix (BS EN 12697-33:2019) and the coated blend proportions for each component. The resultant composition for each mixture is presented in Appendix A, with the relevant formula.

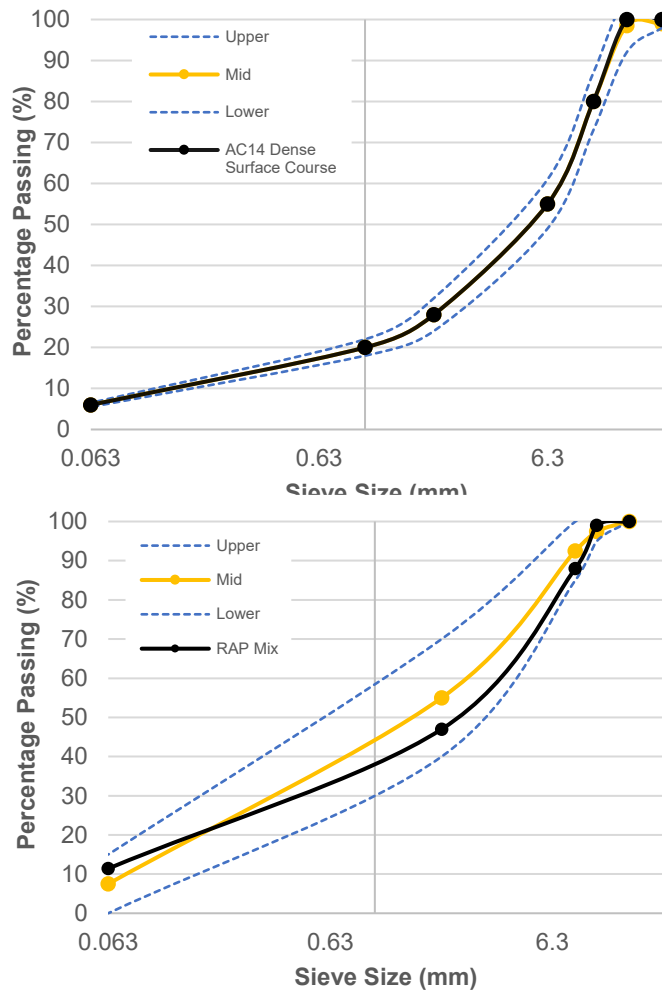


Figure 3.31 (Top) Target particle size distribution of the mixtures used in this investigation; (Bottom) RAP particle distribution.

3.7.3 Mixing and Compaction

The mixing and compaction of the mixtures was carried out according to BS EN 12697-35:2016 and BS EN 12697-33:2019 and at specified temperatures of 190 °C and 170 °C, respectively. Prior to mixing, the aggregate and binders were heated at the specified mixing temperature for 8 and 3 hours, respectively. A uniform mixture of aggregates and binders were produced using a mechanical asphalt mixer, as shown in Figure 3.32 (left). For the RAP mixture, the RAP was heated with the virgin aggregates for at least 3 hours before entering the mixer, as is the typical process for this achievable RAP level [268]. Prior to compaction, the mixtures were subjected to oven ageing to simulate short-term aging at 135 °C for up to 4 hours.

It has been reported in literature that, in addition to the effect of aggregate type and gradation on compaction, concern has often been expressed that certain methods of compaction in the laboratory, such as Marshall compaction, may lead to excessive aggregate degradation [269]. Alternatively, a laboratory roller compactor, as seen in Figure 3.32 (right), was utilised to manufacture 305 x 305 h mm slabs, which were compacted until the desired slab thickness (roughly 40 mm and 60 mm for the slabs to produce 100 Φ and 150 Φ specimens, respectively) was achieved. It has been seen that this compaction method yields test specimens with mechanical properties that more closely simulate those encountered in cores removed from the field [270]. The slabs were dried at room temperature and cored to produce 100 Φ x 40 mm and 150 Φ x 60 mm specimens for volumetric and mechanical testing. The distribution of air voids, determined by BS 12697-6 (Procedure B: Bulk density – Saturated Surface Dry) were calculated for all test mixtures and can be found in Appendix B.



Figure 3.32 (Left) Mechanical asphalt mixer; (Right) Laboratory Roller Compactor.

3.8 Asphalt Mixture Performance Tests

3.8.1 Indirect Tensile Stiffness Modulus (ITSM) Test

The stiffness modulus is an important asphalt mixture property as it indicates its capability to spread applied loads [271]. In this study, the ITSM test was utilised to evaluate the stiffness modulus of the asphalt mixtures using a Cooper servo-hydraulic universal testing machine (UTM-HYD) at Aston University. The test was performed in accordance with BS EN 12697-26:2018 (E), in which cylindrical 100 Φ x 40 mm specimens were subjected to stress-controlled harmonic sinusoidal loading to achieve a maximum tensile strain of 50 $\mu\epsilon$. Under this strain level the specimens were believed in an undamaged or cracked condition. The load frequencies were 0.1, 0.5, 1, 5 and 10 Hz at test temperatures -10, 0, 10, 20 and 30 (± 0.5) $^{\circ}\text{C}$. The specimens were placed vertically with two linear variable transducers (LVDTs) placed diametrically along each side, in order to measure the deformation (Figure 3.33) [272]. Prior to the test, the specimens were preheated at each test temperature for at least 2 hours. At each test temperature, four specimens from each mixture were tested, chosen with small variability in air voids ($<0.6\%$) for the purpose of repeatability. The stiffness modulus $|E^*|$ values were obtained from Dimension software, which calculated this property according to Equation (25):

$$\text{ITSM} = \frac{F \times (v + 0.27)}{z \times h} \quad (25)$$

Where ITSM is the indirect tensile stiffness modulus (MPa), F is the applied load (kN), v is Poisson's ratio, z is the horizontal deformation (mm), and h is specimen thickness (mm). For master curve construction, the sigmoidal dynamic modulus master curve model was applied, as seen in Equation (26). The horizontal time-temperature superposition principle (TTSP) shifting of the rheological parameters was modelled using the following Arrhenius and associated equations (Equations 27-28):

$$\log|E^*| = \delta + \frac{\alpha}{1 + e^{\beta - \gamma(\log(f_r))}} \quad (26)$$

$$\log(a_T) = \frac{-\Delta H}{2.303R} \left(\frac{1}{T} - \frac{1}{T_{ref}} \right) = C \left(\frac{1}{T} - \frac{1}{T_{ref}} \right) \quad (27)$$

$$a_T = \frac{f}{f_r} \quad (28)$$

Where a_T is the shift factor, C is a constant, T is the tested temperature ($^{\circ}\text{C}$), T_{ref} is the selected reference temperature (10°C), f is the tested frequency (Hz) and f_r is the reduced frequency at the chosen reference temperature (Hz). α , β , γ , δ within the sigmoidal dynamic modulus master curve model (Equation (26)) are constant parameters. This master curve fitting method involves the simultaneous variation of the shift factor (C) and these parameters, to fit the most suitable function to the measured points. This optimal value search can be performed by the Solver module of Excel [273, 274]. The generated master curve will look analogous to that produced from the frequency sweep test for the control and w-binders, as seen in *Section 3.6.4.1*.

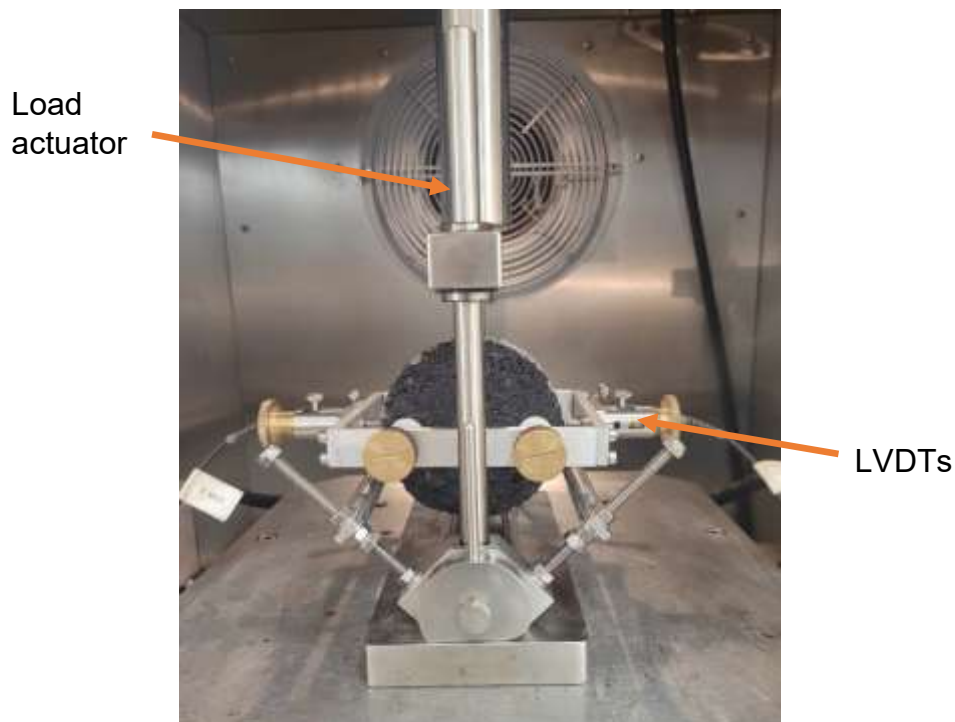


Figure 3.33 The configuration of the ITSM test in the UTM-HDY machine.

3.8.2 Indirect Tensile Fatigue Test (ITFT)

The fatigue performance of the asphalt mixtures can be characterised by the Indirect Tensile Fatigue Test (ITFT) using UTM-HYD machine, performed according to BS EN 12697-24:2018 (E). The cylindrical 100 Φ x 40 mm samples were subjected to a repeated compressive loads with a haversine load signal through the vertical diametrical plane. LVDTs were placed diametrically along each side, in order to measure the deformation (Figure 3.34). A repetition period of 0.1s loading time and 0.4s rest time was applied in stress-controlled mode, the input stress level of 400 kPa was selected. The test temperature was 15 °C with preconditioning of at least 2 hours. 3 specimens with small variability (<1%) in air voids from each mixture were tested. To consider both the tensile strength and strain tolerance of each mixture, the output was expressed in terms of resilient strain amplitude (ϵ_{res}) over cycles N. The energy ratio (E_{ratio}) was also plotted to calculate the number of cycles to failure (peak of the E_{ratio} vs. N curve [275].)

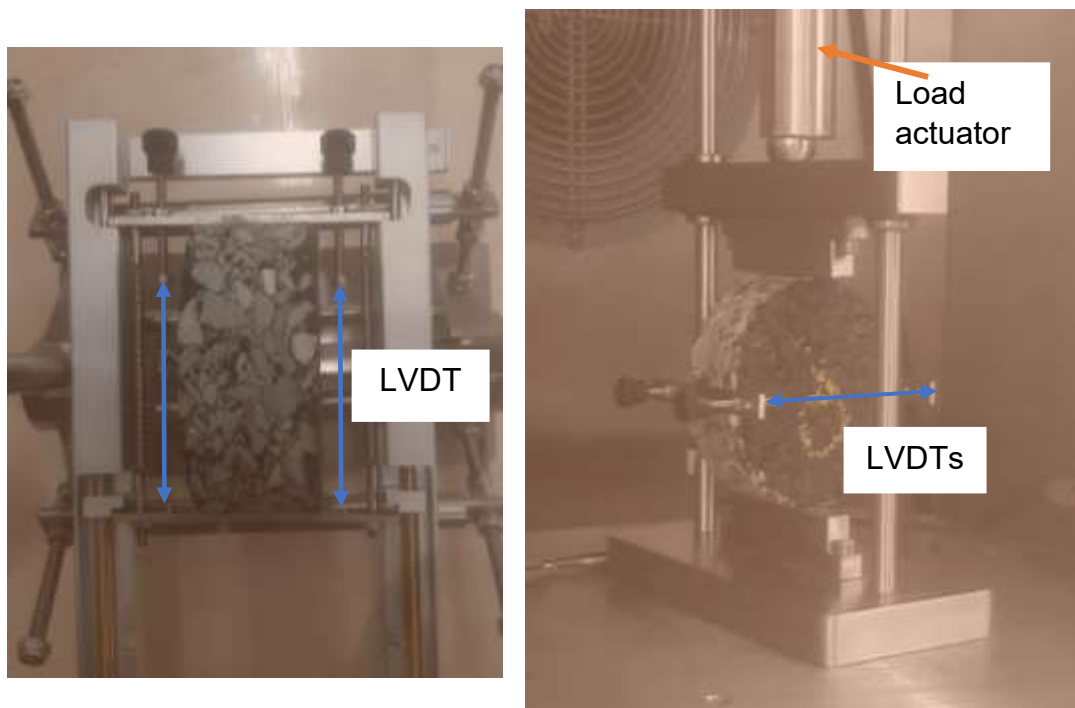


Figure 3.34 The configuration of the ITFT test in the UTM-HYD machine.

3.8.2.1 Mechanistic Modelling of Cracking Damage

A mechanistic model of cracking damage produced by Dr. Yuqing Zhang was utilised to predict the evolution of crack growth under an indirect tensile fatigue load. Employing the relationship between the horizontal tensile stress and vertical load outlined in BS EN 12697-24:2018 (E); equilibrium principle in continuum damage mechanics (CDM); strain energy equilibrium principle based on Griffith fracture theory and the elastic-viscoelastic corresponding principle based on pseudo strain (Schapery); the following simplified cubic equation and corresponding equations were outlined [276]. The horizontal tensile stress, strain, calculated resilient modulus, bond energy and the strain energy release volume can all be determined at different fatigue load cycles using the IDT fatigue test measurements; therefore, the parameters a, b, c, and d were determined. Then, the damage density (an indicator defined as the ratio between the cracked area and total area in the local cracked region,) obtained by solving the cubic equation in Equation (29) and the crack length of the specimen under the IDT fatigue test could be predicted using Equation (30):

$$a\xi^3 + b\xi^2 + c\xi + d = 0 \quad (29)$$

Where:

$$a = 2\Gamma$$

$$b = -4\Gamma - \frac{1}{2} \frac{\sigma_H^2}{E_r} \alpha D$$

$$c = 2\Gamma + \frac{\sigma_H^2}{E_r} \alpha D - \frac{1}{4} \frac{\sigma_H^2}{E_0} \alpha D$$

$$d = \frac{1}{2} \frac{\sigma_H^2}{E_0} \alpha D - \frac{1}{2} \frac{\sigma_H^2}{E_r} \alpha D$$

$$\xi = \frac{ch}{S^A} = \frac{c}{D} \quad (30)$$

Where ξ is the damage density of the specimen; Γ is the bond energy of the materials that is determined using the material surface energy; σ_H is the apparent horizontal tensile stress in the centre part of the specimen along the

vertical direction; which E_r is the resilient modulus of the materials that represents the modulus in the apparent (damaged) configuration; α is the ratio of width of the local cracked region to the diameter of the specimen; D is the diameter of the specimen; E_0 is the initial undamaged resilient modulus ($E_0=E_r(N=1)$); c is the crack length along the vertical direction of the specimen; h is the height of the specimen and S^A is the apparent area which is the total area that the apparent horizontal stress acts on.

3.8.3 Repeated Load Axial Test (RLAT)

The rutting performance of the test mixtures was characterised via uniaxial cyclic compression tests (CCT) in accordance with BS EN 12697-25:2016 (A2). 150 Φ x 60 mm specimens were subjected to a cyclic axial haversine-pulse with rest time. Following a preload of 200 N for 30s, the maximum pulse and minimum rest loads used were 350 kPa and 80 kPa, respectively (0.2s loading pulse with a 1.5s rest period.) The test temperature was 40 °C with preconditioning for at least 4 hours. The specimen was positioned horizontally between a steel upper loading and a lower platen, the contact areas between these were coated in silicone grease (Figure 3.35.) The confined axial stress was applied vertically by the load actuator of the HYD-UTM. Three specimens with small variability in air voids (<1%) from each mixture were tested. The rutting behaviour was evaluated using the average creep rate (f_c), which incorporated the theory of the minimum strain rate ($\mu\epsilon/\text{cycle}$) that is considered more reliable, as it is independent of the initial strain experienced by the mixtures during the RLAT test. This can be calculated using the secondary steady state zone (rate of deformation of the mixture is constant with loading cycle) that is observed in a typical raw data plot of the cumulative axial strain vs. number of cycles N (Figure 3.36.) The slope of the (quasi-linear) steady state zone was obtained between pulse 3000 and 5000, the creep rate was calculated using Equation (31) [7, 277, 278].

$$f_c = \frac{\epsilon_{n1} - \epsilon_{n2}}{n_1 - n_2} \quad (31)$$

Where ε_{n_1} is the accumulated strain at cycle 3000, ε_{n_2} is the accumulated strain at cycle 5000, n_1 is pulse number 3000 and n_2 is pulse number 5000.



Figure 3.35 Configuration of the RLAT test in the UTM-HYD machine.

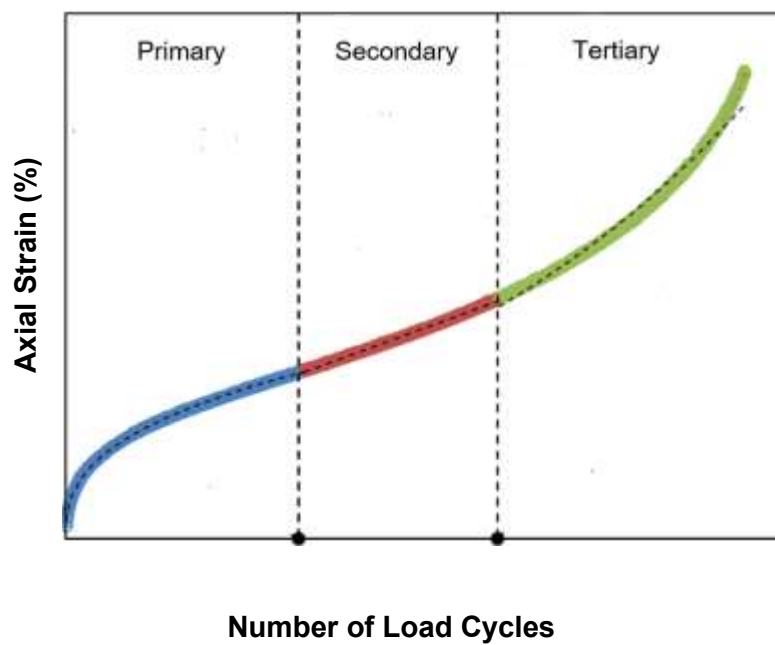


Figure 3.36 Typical raw data from the RLAT for asphalt mixtures.

3.8.4 Indirect Tensile Strength (ITS) Test

The fracture resistance of the mixtures was investigated using the Indirect Tensile Strength (ITS) test in accordance with BS EN 12697-23:2017. According to the standard test conditions, a vertical strain of 51 mm/min was applied diametrically to the cylindrical 100 Φ x 40 mm specimens, which were loaded vertically between two loading strips (Figure 3.37.) The tests were performed at 10 °C and the samples were preheated at the test temperature for at least 2 hours. Three specimens from each test mixture with small variability in air voids (<0.9%) were tested. The indirect tensile strength was calculated from the peak load applied at breaking and the dimensions of the specimen, as seen in Equation (32):

$$ITS = \frac{2P}{\pi DH} \times 1000 \quad (32)$$

Where ITS is the indirect tensile strength (kPa), P is the peak load (N), D is the diameter of the specimen (mm) and H is the height of the specimen (mm).

The ITS tests were also carried out on cylindrical 100 Φ x 40 mm specimens preliminarily subjected to wet conditioning in order to investigate the susceptibility to moisture of each test mixture, in accordance with BS EN 12697-12:2018 (A). The wet subset of three specimens for each test mixture was placed in a water bath at 40 °C for 72 hours. The specimens were then placed at the test temperature of 10 °C for at least 4 hours prior to performing the ITS test as outlined for the dry subset of specimens. From this, the tensile strength ratio (TSR) could be determined using Equation (33) for each mixture. This is a ratio of the tensile strength of the dry, unconditioned specimens to the tensile strength of the wet, conditioned specimens. A higher TSR value typically indicates that the mixture has good resistance to moisture damage [279].

$$TSR = \frac{ITS_{WET}}{ITS_{DRY}} \times 100 \quad (33)$$

Where ITS is the tensile strength ratio (%), ITS_{WET} is the indirect tensile strength of the wet, conditioned specimens (kPa) and ITS_{DRY} is the indirect tensile

strength of the dry, unconditioned specimens (kPa). ITS and resultant TSR results are typically presented in a combined bar and scatter graph chart, respectively (**Figure 3.38.**)



Figure 3.37 Configuration of the ITS test in the UTM-HYD machine.

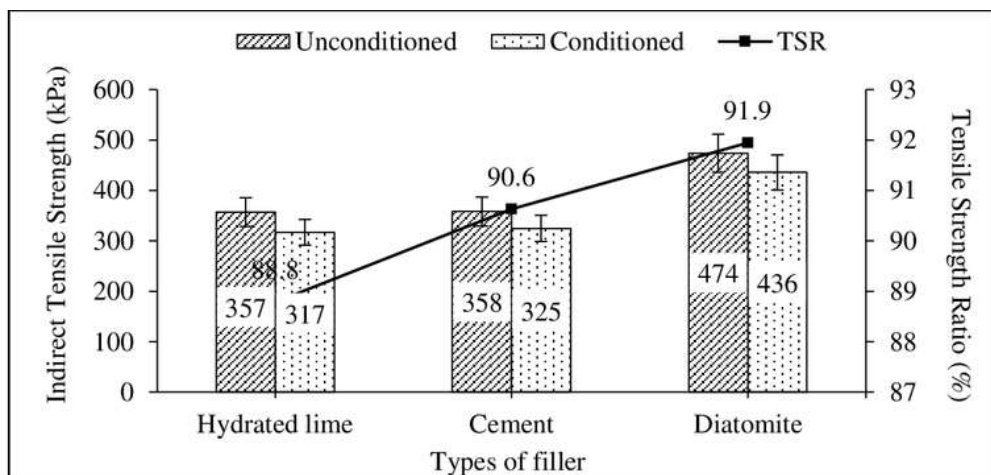


Figure 3.38 Typical data presentation for the ITS and TSR for asphalt mixtures, [280].

3.9 Summary

In this chapter, the materials and methodology implemented throughout this study have been outlined. The thermal pyrolysis of high-density polyethylene in a fixed bed reactor was performed in the 450-550 °C range with two different nitrogen carrier gas flowrates, 2 and 4 L min⁻¹, to study the effect of these process parameters, as well as the resultant vapour residence times on the formation of wax and its chemical and thermal properties. The waxes were characterised using different techniques such as gas-chromatography-mass spectroscopy (GC-MS), Fourier transform infrared (FTIR), thermal gravimetric analysis (TGA) and differential scanning calorimetry (DSC). Thermal conditioning in an ashing oven at 170 °C for 0-6 hours was conducted with a detailed analysis of GC-MS and FTIR at each stage of thermal exposure to further support thermal characterisation results and identify key thermal and oxidative ageing mechanisms. The rheological, chemical, and thermal characterisation of 40/60 asphalt binder modified at 6 and 12 wt% with high-density polyethylene (HDPE) pyrolysis waxes, produced using different process parameters (450, 500 and 550 °C), was performed. This was to establish relationships between the chemical and thermal properties of the waxes and their rheological and mechanical performance, allowing for the selection of an optimal wax to take forward for w-asphalt formulation. For the asphalt mixtures, a 14 mm dense graded asphalt concrete was formulated that utilised porphyritic andesite and limestone aggregates and filler, respectively. A laboratory study was performed to investigate the use of a selected HDPE pyrolysis wax modified binder in a hot-mix asphalt (HMA) mixture and a mixture additionally containing 20% reclaimed asphalt (RAP.) The indirect stiffness modulus test, indirect tensile fatigue test (employing a novel mechanistic model for the prediction of cracking damage,) the repeated load axial test and indirect tensile strength test were performed to determine the resistance of the mixtures to key pavement deterioration modes.

CHAPTER 4: High-Density Polyethylene Pyrolyzed Wax: Mechanism, Thermal Properties, and Ageing Performance

4.1 Overview

Using a fixed bed reactor to obtain wax from the thermal pyrolysis of HDPE, this chapter describes the first phase of the project, in which pyrolysis mechanisms and wax yields are described, and relationships between the process operating parameters and resultant wax chemical and thermal properties are established. The wax thermal ageing properties are investigated with regards to volatile loss, oxidation, and polymerization. This can be linked to the chemical composition of the wax and thus the pyrolysis parameters utilised that result in certain pyrolysis reaction mechanisms. The techniques utilised to assist in this investigation include non-isothermal thermogravimetric analysis (TGA) and differential scanning calorimetry (DSC) to examine the thermal degradation characteristics and melting point ranges of the unaged waxes. Gas Chromatography-Mass Spectroscopy (GC-MS) and Fourier Transform Infrared Spectroscopy (FTIR) are used to quantitatively determine the chemical composition and distribution as well as qualitatively identify the chemical functional groups present in the pyrolysis waxes, respectively. The two latter techniques especially are used to comprehensively analyse the unaged and thermally aged waxes, in order to propose ageing mechanisms that take place. These techniques in conjunction can be used to assess the ageing performance of the waxes, such that optimal waxes can be taken forward to the next phase for blending with bitumen and optimum blending conditions can be suggested.

4.2 Pyrolysis Yields

In this study, the two controllable variables were the pyrolysis temperature and carrier gas flowrate. Initial TGA analysis was performed on the HDPE pellets to determine a suitable temperature range for pyrolysis. The results showed that thermal degradation commenced within the range of 425-500 °C, as seen in Appendix C. Figure 4.1 shows the wax yield with respect to the process conditions described in *Section 3.3*. The yield of wax obtained for HDPE pyrolysis

is higher than that reported by other authors in literature, such as 32 wt% wax in a fixed-bed reactor 500 °C obtained by Al-Salem et al [281]. Nevertheless, Arabiourrutia et al saw a similar yield in a conical spouted bed reactor at 450 °C of 80 wt% [29]. A prominent trend reported in literature is the favouring of secondary cracking reactions at high operating temperatures, which generates more gaseous products and in turn reduces the formation of wax products [29, 57, 104, 110]. This is due to the increased concentration of short radicals from favouring the vaporisation of long chains and as a consequence increasing the rate of this process. In this study, the trend in wax yield with increasing pyrolysis temperature differs to this, such that the wax yield increases with temperature from 75.73-79.46 wt% at 450 °C to 86.53-87.86 wt% at 550 °C. The wax yield is only seen to decrease with temperature from 91.87 wt% at 500 ° to 86.53 wt% at 550 °C at the higher carrier gas flowrate of 4 L min⁻¹.

For HDPE, an initial increase in wax yield at increasing low-moderate operating temperatures (500-600 °C), followed by a yield decrease at higher temperatures (600+ °C) was also reported by Al-Salem et al [281] and was explained as a consequence of the low branched structure of HDPE. For polyolefins with a higher degree of branching (polypropylene), at lower temperatures (450-500 °C), cracking initially takes place in branched chains. At the short residence times achieved by reactor configurations designed for optimised wax production, the cracking of principal chains is low. At temperatures of 450-500 °C, the cracking of HDPE feedstock to gases is favoured, which may later be condensed to pyrolysis oils. Furthermore, it was reported that commingled plastic solid waste (PSW) consisting of mildly branched feedstock (such as HDPE) with 10 wt% of the higher branched PP yielded no wax at 500 °C and produced low yields at 600 and 800 °C [281]. It was attributed to the mildly branched, more crystalline feedstock requiring higher temperatures and residence times [104, 281]. This was consistent with the lower wax yield from HDPE pyrolysis at 500°C and agrees with this work at 450-500 °C.

Another explanation is that a lower residence time as a result of increasing the temperature (as seen in Table 3.2) in the reactor reduces cracking of the feedstock, therefore higher molecular chain hydrocarbons are obtained [74]. A governing factor in the pyrolysis of PO polymers is the residence time of the feedstock material in the reactor; longer residence times typically increase the cracking of primary products to more thermally stable products, favouring the production of oils [282]. Moreover, Park et al reported the non-isothermal pyrolysis of low-density polyethylene (LDPE) at 440 °C in a semi-batch reactor, noting that the retention time increased in the low temperature region and a subsequent increase in ratio of lower molecular weight products [283].

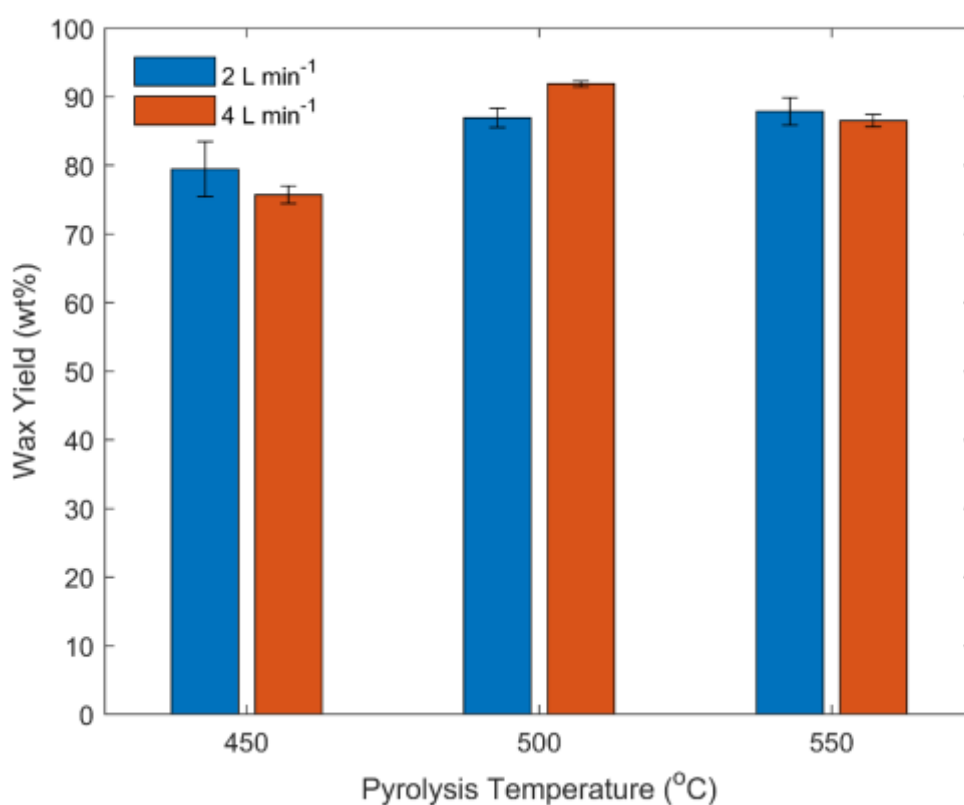


Figure 4.1 Yields (wt%) of wax with respect to the reactor operating conditions.

In terms of the effect of the carrier gas flow rate and subsequent vapour residence times calculated at each temperature, a faster nitrogen flowrate decreased the yield of wax at 450 °C. This could be attributed to the structure of HDPE, which may require more elevated temperatures for higher wax yields to be obtained, as discussed. The only increase in wax yield with an increase carrier gas rate is at 500 °C, whereas the yields are somewhat similar at each flowrate at 550 °C. It

can be comprehended that the effect of the operating temperature and its subsequent vapour residence time had a larger effect on the resultant wax yields. The predominant influence of reactor temperature on the resultant spectrum of pyrolysis products, more so than other process parameters, has been reported by other authors. This is due to the temperature being the key parameter in controlling the cracking mechanisms of the polymer chains [77, 284].

4.3 Wax Chemical Characterisation

4.3.1 FTIR Analysis

Infrared spectra of the waxes obtained at the pyrolysis parameters studied are shown in Figure 4.2. The spectra are analogous to each other and it is noted that they are also comparable to those obtained by Chaala et al for commercial paraffinic wax as well as pyrolysis wax obtained from the vacuum pyrolysis of polyethylene based electric cables [105]. There are two bands corresponding to the stretching of $\text{-CH}_2\text{-}$ groups at 2920 and 2850 cm^{-1} , as well as a doublet seen at 725 cm^{-1} which relates to the skeletal vibrations of these C-H groups. Two shoulders are observed at 2960 and 2900 cm^{-1} which correspond to -CH_3 terminal bond groups. Aguado et al noted that these are much weaker for pyrolytic waxes than for commercial waxes, inferring that the alkyl chains of waxes obtained from pyrolysis are less branched than those produced commercially [104]. Deformation vibrations of these C-H alkyl groups are additionally observed by the bands at 1465 and 1380 cm^{-1} . When comparing the spectra of this study with those produced by Chaala et al for commercial waxes, it is noticed that the waxes obtained from plastic pyrolysis are more unsaturated, the generation of -C=C- olefinic groups explained by the occurrence of radical degradation mechanisms such as β -scission [105]. The bands located at 3040 , 1645 and in the $890\text{-}995\text{ cm}^{-1}$ range correspond to C-H deformation vibrations of olefinic bonds, stretching of conjugated alkene groups and R-CH=CH_2 , trans -CH=CH- and $\text{R}_1\text{R}_2\text{C=CH}_2$ groups, respectively [104].

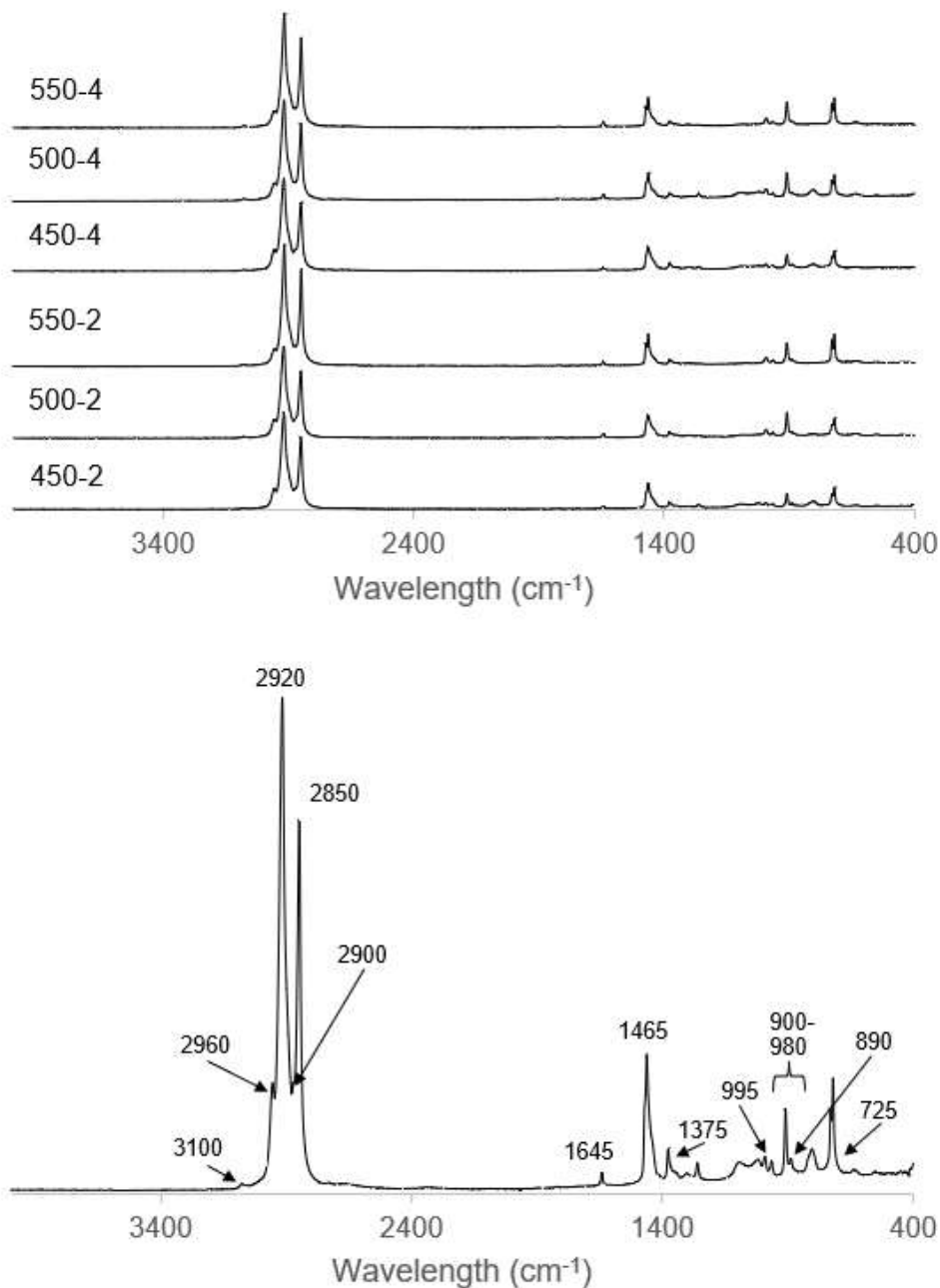


Figure 4.2 FTIR Spectra for HDPE Pyrolysis Waxes. ('450-2' stands for pyrolysis wax produced at 450 °C using a 2 L min⁻¹ nitrogen flowrate, etc.)

4.3.2 GC-MS Analysis

The GC-MS chromatograms produced for the pyrolysis waxes are appended in Appendix D (a-g) and show homologous series of triplets that are typical of HDPE depolymerisation. [285]. Within the spectrum, each triplet is comprised of an α,ω -diene, olefin and paraffin for each carbon number [36]. In addition, trace amounts of branched and cyclic hydrocarbons between the triplets as well as noticeable

peaks for aromatic components, such as benzene and xylene, can be seen at the lower retention times within the spectrum. The mass response factors and thus percentiles were calculated for each component and the peak areas were integrated and totalled for representative categories: gasoline range ($<C_{12}$) and high molecular weight (MW) hydrocarbon ($C_{13}<$) components, as well as the class of hydrocarbons (aromatic, paraffinic, olefinic and diene) present in each sample, as shown in Table 4.1.

Table 4.1 Distribution in weight percentage of hydrocarbons in each pyrolysis wax sample and percentile distribution in gasoline and high MW categories, as well as class of components.

	450-2*	500-2	550-2	450-4	500-4	550-4
Gasoline Range ($<C_{12}$)	25.87	25.76	26.37	22.92	29.93	30.18
High MW ($C_{13}-C_{30}$)	74.13	74.24	73.63	77.08	70.07	69.82
Aromatic	3.38	3.48	2.91	2.45	1.83	2.38
Paraffinic	57.53	39.57	36.70	61.83	38.11	35.53
Olefinic	36.03	49.65	51.38	35.72	54.53	54.79
Diene	3.06	7.29	9.00	0.00	5.53	7.30

*'450-2' stands for pyrolysis wax produced at 450 °C using a 2 L min⁻¹ nitrogen flowrate, etc.

The wax samples were extremely viscous (semi-solid) at room temperature, and the majority of each sample eluted in the higher molecular weight carbon range ($C_{13}-C_{30}$). It is observed that heavy hydrocarbons did not elute with a considerable differentiation from the baseline due to the GC-MS program utilised, as also observed by Al-Salem et al [36]. This should be considered when the heavy components are analysed. However, this program is still considered as suitable as it meets the criteria previously outlined by Lund et al for the analysis of plastic depolymerisation [285]. Kumar and Singh reported the characteristics of heavy hydrocarbon thermal degradation to include poor gasoline selectivity, with a wide distribution of light molecular weight products [86]. The results and chromatograms show that this work is in agreement mainly due to the reactor system operating under thermal (non-catalytic) pyrolysis conditions, therefore fuel production is not favoured. Furthermore, it can be seen that the operating temperature has the most significant effect on the cracking and wax product

composition, rather than the effect of the carrier gas flow rate on volatile residence times in the reactor system.

It is generally established that increasing the pyrolysis temperature results in a reduction of residence time, lowering the extent of cracking reaction rates and thus a generating higher molecular weight compounds (oils and waxes [74]). Noticeably in this work, with the increase in pyrolysis temperature, the percentage of gasoline range hydrocarbons is seen to rise. Specifically, the increased generation of C₆-C₈ aliphatic compounds is noted, such as 1-hexene, 1-heptene and 1-octene. Similar observations have been made; Hernández et al conducted thermal pyrolysis of HDPE in a fluidised bed reactor. Yields of these compounds (especially *n*-hexane) were reported to have increased due to the extension of secondary propagation reactions of intermediate compounds, facilitated by high operating temperatures and low resistance times [286].

In this work, the pyrolysis temperature is seen to have a dominating impact in promoting secondary cracking reactions to generate smaller compounds (C₆-C₈) within the gasoline range. These are further promoted (to an extent) at higher temperatures with lower residence times, reducing the mass% of (C₁₃-C₃₀) wax compounds somewhat. Al Salem et al also saw an initial increase in high molecular weight compounds in the product oil with increasing operating temperature (500-600 °C), for the thermal cracking of HDPE in a fixed bed reactor. However, the authors also saw an increase in gasoline range compounds with the further elevation of bed temperatures (600 °C+) as a consequence of further cracking reactions [92]. The analysis of the wax products confirms mainly aliphatic products comprising of paraffins, olefins and diolefins [287]. The latter possibly a result of propagation intramolecular hydrogen transference and β-scission mechanisms. With the exception of paraffinic compounds being the main product at the lower pyrolysis temperature of 450 °C, with increasing temperature the main product was olefinic, while the amount of diene production increased significantly. Other authors have reported similar for the thermal pyrolysis of HDPE [86, 288]. This work is also in agreement with mechanistic models produced in literature to predict the product distribution of

HDPE pyrolysis in a conical spouted-bed reactor, based on radical mechanisms [289]. The results from such models demonstrated that the fastest reaction and controlling propagation stage in cracking is β -scission for the production of olefins and dienes. The importance of other stages was also emphasised, such as hydrogen abstraction in the role of paraffin and diene production.

Aromatics such as benzene belong to a group of compounds which yield increases by increasing the residence time and temperature [286]. Generally, raising the pyrolysis temperature increases the formation of aromatic hydrocarbons as it promotes the rapid release of radicals which undergo intramolecular exchanges to produce cyclic compounds [92, 290]. Additionally, high residence times and temperatures favour secondary reactions that produce highly reactive gaseous products, allowing for tertiary reactions to form more stable aromatics compounds. In this study, small amounts of benzene, ethyl benzene and xylene were seen in the lower region of the chromatograms. The amount of aromatics in the wax samples varies between 1.83-3.48%, the carrier gas flowrate does not largely affect the yield of cyclic compounds present, however, it is observed that the aromatic yield is higher for the reactions with a 2 L min⁻¹ carrier gas flowrate, corresponding to slightly higher residence times. Overall, a slight decrease in aromatics can be seen as the temperature parameter is increased, suggesting that the effect of temperature and nitrogen flowrate on volatile residence times within the reactor has a larger influence on aromatic production in this reactor system. Jung et al. suggested that the Diels-Alder reaction mechanism followed by dehydrogenation may result in aromatic production from the catalytic pyrolysis of polypropylene/polyethylene [107].

4.4 Wax Thermal Characterisation

4.4.1 TGA Analysis

Representative TGA and DTG thermograms for each pyrolysis wax thermal degradation as a function of pyrolysis conditions (temperature, carrier gas flowrate) are presented in Figure 4.3. HDPE typically shows a two-stage decomposition process; the initial degradation starts at a lower temperature and propagates gradually until the second degradation stage is reached in which a sharp degradation is observed [291]. The pyrolysis of HDPE significantly shortens the initial stage of thermal decomposition in the wax products and the rapid weight loss of hydrocarbons now happens over a wider temperature range, as the pyrolysis has yielded a broad spectrum of small molecular weight hydrocarbons. The maximum degradation of PE is typically achieved within 420-490 °C, whereas this can be seen to happen between 90-460 °C for the pyrolysis waxes.

As the temperature was increased for the pyrolysis, an increase in thermal stability, or a decrease in volatility, of the pyrolysis waxes was observed. This infers that heavier hydrocarbon chains are generated and distilled during the chain scission mechanism at higher pyrolysis temperatures. The effect of carrier gas flowrate on vapour residence time is also seen to influence the thermal properties of the waxes, with the waxes produced using a faster nitrogen flowrate having a slightly higher thermal stability, for the same reason as the higher temperature conditions. These results for thermal stability of the waxes indicate their potential suitability in asphalt pavement applications such as alternative binder materials, as these are incorporated into bitumen at temperatures of 150-170 °C.

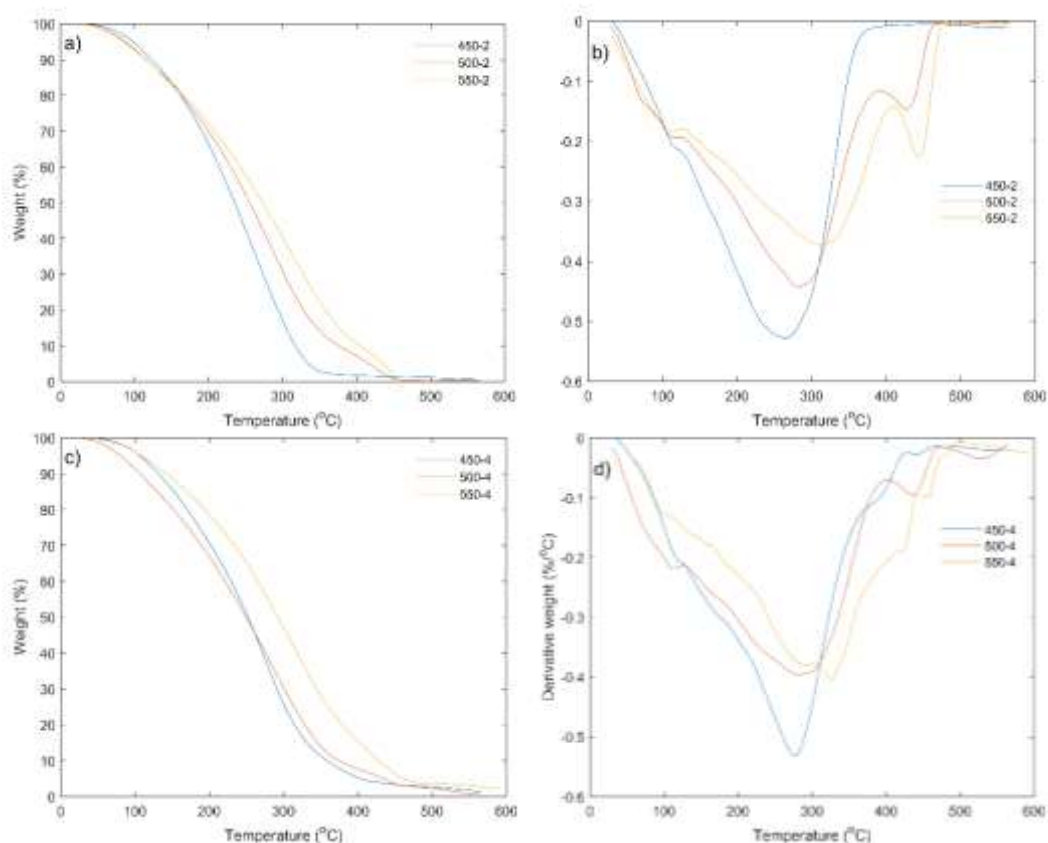


Figure 4.3 Representative TGA and DTG thermograms for each pyrolysis wax thermal degradation as a function of pyrolysis conditions ('450-2' stands for pyrolysis wax produced at 450 °C using a 2 L min⁻¹ nitrogen flowrate, etc.)

4.4.2 DSC Analysis

Waxes are mixtures of different size and nature molecules and therefore do not have a defined characteristic melting point that pure substances have [292]. Therefore, when investigating the melting points of the pyrolysis waxes with DSC, a temperature from which the samples start to melt (onset temperature) and a highest peak indicating the point at which the samples have melted completely were recorded. The onset and peak melting temperatures are recorded in Table 4.2, taken from the endothermic peak identified for the melting of the wax on the DSC thermograms. The melting point values obtained for the HDPE pyrolysis waxes can be compared to commercial paraffin (50-70 °C), microcrystalline (60-91 °C), Barnsdall (70-74 °C) and beeswax (63-70 °C) waxes, as observed by Arabiourrutia et al when characterising waxes produced from the pyrolysis of polyolefins in a conical spouted bed reactor [29].

The same trend in influence of the pyrolysis parameters is seen in these results as those for the TGA analysis. The pyrolysis temperature is seen to have a more definitive impact on the thermal properties of the waxes (as with chemical characterisation.) With increasing process temperature, higher peak melting points can be observed. Additionally, the waxes produced using a higher carrier gas flowrate and thus lower vapour residence time, also have slightly higher melting points than those produced with the lower nitrogen flowrate. In *Section 4.3.2* it was discussed that the rise of process temperature results in an increase gasoline range (<C₁₃) compounds, therefore, containing more lower melting point compounds. The higher melting points seen in the waxes produced at the higher pyrolysis temperatures (500 and 550 °C) will be explained in *Section 4.5.2*, in which further GC-MS and FTIR analysis of the waxes at different stages of thermal (and oxidative) ageing are investigated.

The waxes produced at higher temperatures are more olefinic in nature, containing more unsaturated compounds as a result of the influence of process temperature on the radical mechanisms involved in pyrolysis. Not only do alkenes have slightly higher melting points than alkanes due to stronger intermolecular forces, but they are also more prone to oxidation reactions, as indicated by the number of compounds containing hydroxyl and carbonyl functional groups in Table 4.3, even at the unconditioned stage. The hydroxyl and carbonyl groups present within alcohol molecules require a greater energy to overcome the stronger intermolecular forces of hydrogen bonding, therefore the melting point of alcohols is higher than that of alkanes with the same chain length [293]. Additionally, when further exposed to elevated temperatures in analysis, the more unsaturated waxes may take part in polymerization reactions to form heavier molecules.

Table 4.2 Onset and peak melting points of the pyrolysis waxes using DSC.

Sample	Onset (°C)	Peak (°C)
450-2*	46.84	49.26
500-2	85.25	88.92
550-2	71.22	78.25
450-4	48.02	49.75
500-4	82.21	86.42
550-4	74.18	87.67

*'450-2' stands for pyrolysis wax produced at 450 °C using a 2 L min⁻¹ nitrogen flowrate, etc.

4.5 Thermal Ageing of Waxes

In this study, it has been established that the pyrolysis operating temperature is the dominant parameter that influences the chemical and thermal properties of the wax products in the thermal pyrolysis of HDPE. To further support the thermal characterisation results in *Section 4.4.1 and 4.4.2* and to assess the suitability of the waxes for applications that may involve their incorporation at temperatures above their melting points, such as in asphalt road construction, three of the waxes (450-2, 500-2 and 550-2) were selected for thermal conditioning/ageing and analysis. The mass losses were recorded, and a further detailed analysis of GC-MS chromatograms was conducted at each stage of the thermal conditioning. This included further representative categories for the different molecular weight components within the waxes; diesel (C₄-C₉), gasoline (C₁₀-C₁₉) and wax (C₂₀-C₃₀) fractions. A focus on compounds that are present in trace-small amounts and therefore overlooked in the initial analysis by the peak width integration and identification are also examined to identify possible oxidation products. FTIR analysis was additionally utilised to examine the change in functional groups present at each stage.

4.5.1 Mass Loss

Due to the wax fractions being cooled swiftly from hot vapours to a low temperature (5 °C) after leaving the pyrolysis reactor vessel, they contain lightweight components (<C₁₀) that have boiling points lower than the chosen condition temperature of 170 °C. Significant mass losses from 15.96-21.61% at 1 hour to 28.2-41.49% at 6 hours were observed (Figure 4.4) as a result of the

loss of volatiles. A high mass loss indicates high emissions and therefore detailed information on the low molecular weight hydrocarbons should be evaluated with respect to influence on the environment and exposure. If the effects are substantial, further efforts to reduce this should be considered for potential applications.

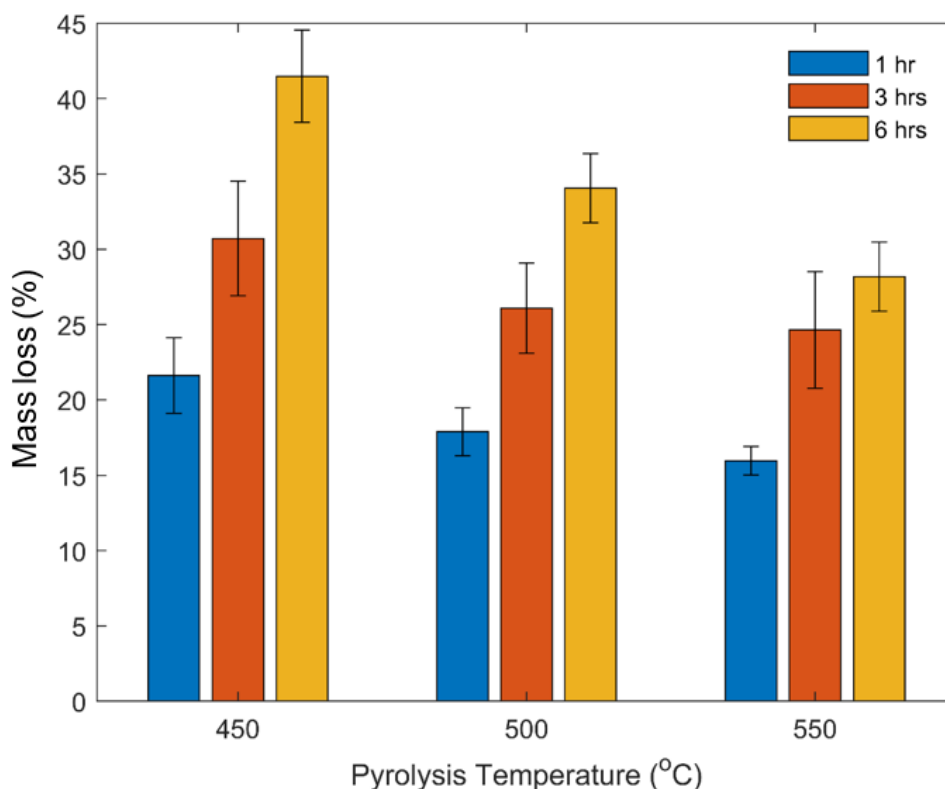


Figure 4.4 Mass loss of pyrolysis waxes with thermal conditioning.

4.5.2 Chemical Characterisation

(In continuation of *Section 4.5.1*) The distribution in weight percentage of molecular weight and class of hydrocarbons in pyrolysis waxes (450-2, 500-2 and 550-2) after thermal conditioning at 170 °C from 0-6 hours is presented in Table 4.3. At all time periods, the mass loss surpasses the initial percentage of compounds with a boiling point below 170 °C, indicating thermal decomposition taking place of the decreasing gasoline range (C₁₀-C₁₉) to lower molecular weight components (C₄-C₉), which are emitted by the samples. In all waxes, an initial significant decrease in diesel (C₄-C₉) fractions is observed within the first hour as the low boiling point components are emitted and lost from the samples. The fractional category is then seen characteristically to increase, assumed to be a

result of the gasoline (C₁₀-C₁₉) fractions beginning to thermally decompose upon extended thermal exposure. The diesel fractions again begin to incrementally decrease at 6 hours as the produced lower molecular weight products of thermal decomposition begin to be emitted and lost from the samples. The heavier wax fraction (C₂₀-C₃₀) is seen to significantly increase, obviously due to the mass % decrease of the diesel and gasoline fractions. However, the increase in wax components is larger than the overall reductions in the other fractional categories and the total mass loss in the wax samples at the end of the thermal conditioning.

Thermal hydrocarbon chemistry involves the degradation of large molecules into smaller ones, but it can also involve the production of heavier molecules [294]. The thermal polymerisation of alkenes within the wax may be a contributing reaction to the substantial increase in heavier molecular weight fractions. A reaction such as this can be evident by the sizable drop in percentage of unsaturated (alkene and diene) compounds present in the waxes from the non-conditioned state to 6 hours of thermal conditioning, and the subsequent increase in mass percentage of larger paraffinic hydrocarbons. The peaks in the GC-MS chromatograms were seen to shift to the right, as seen in Appendix E (a-j). Additionally, in the FTIR spectra presented in Appendix F (a-i), the bands corresponding to olefinic bonds (890, 900-980, 995, 1645 and 3040 cm⁻¹) are all seen to decrease or disappear entirely from the spectra throughout the stages of thermal exposure. In the case of not all unsaturated bonds being located at the terminal position of the hydrocarbon chains, this could contribute to the reduction in the two bands at 2960 and 2900 cm⁻¹ that correspond to -CH₃ terminal groups. The C-H bond stretching of -CH₂- groups at 725, 2850 and 2920 cm⁻¹ are seen to be slightly more elongated in shape but are not significantly changed.

In the case of self-initiated polymerization, the initiating radicals, and mechanisms by which they are formed can be unclear. However, it is noted that the primary and secondary products of paraffin and alkene oxidation, as will be discussed, include hydroperoxides and acids. Hydroperoxide groups are used as initiators in radical polymerization reactions with alkenes as these functional groups can break easily, generating free radicals. Acidic reagents are also

typically used in cationic polymerization by donating a proton to an alkene to yield long-chain carbocations [295, 296]. In the unconditioned waxes, small amounts (2.08-2.52 %) of primary alcohols were detected. This may be attributed to oxidation processes during the cooling of the waxes within the glassware in the instance of oxygen entering the system and upon wax storage prior to analysis. It can be observed in Table 4.3 that when subjected to heat in oxygen for prolonged times, the number of primary alcohols ($C_{10}<$) as well as diols are increased, which is supported by the FTIR spectra in Appendix F (a-i). With increased time of thermal conditioning, the band at 1076 cm^{-1} for primary alcohols significantly increases, while the bands at 2960 and 2900 cm^{-1} for $-CH_3$ terminal bond groups decreased.

Some cycloalkanes with alcohol substituents such as methanol were also identified, such as Cyclododecanemethanol ($C_{13}H_{26}O$.) Additionally, trace amounts of compounds containing carbonyl functional groups were detected, increasing with conditioning time from the initial unconditioned waxes and including larger chain esters and acids especially. Products such as this are common in the thermal oxidation of paraffin wax conducted at $110-140\text{ }^\circ\text{C}$, however, typically with an appropriate catalyst present. This is reported to lead predominantly to the formation of alcohol isomers with the same number of carbon atoms as the initial hydrocarbon molecules, as well as other secondary products including acids, esters, and ketones [293]. The oxidation products identified may also be a result of the oxidation of alkene molecules within the pyrolysis waxes. Alkenes are more susceptible to reactions with oxygen, with the addition of O_2 molecules most commonly occurring to the carbon atom adjacent to the double bond [295]. This produces unstable hydroperoxide molecules that decompose to form two aldehyde or carboxylic acid groups [295]. This can be observed in the FTIR spectra as the reduced CH_3 band, as previously discussed, and the growing band at $1650-1800\text{ cm}^{-1}$ with conditioning time that corresponds to conjugated and aliphatic aldehydes, carboxylic acids, esters, and ketones.

This is similar to the oxidation of bitumen fractions, which produces higher polarity components. The oxidation products from pyrolysis waxes may also increase polar-polar interactions with other active polar sites, thus increasing the

apparent molecular weight of the wax. The occurrence of such ageing mechanisms and resultant formation of higher molecular weight components (C₂₀-C₃₀) resulted in visibly stiffer/harder wax products, with the pyrolysis waxes consisting of a higher distribution of (C₂₀-C₃₀) hydrocarbons having hardened the most after thermal conditioning. An important relationship between the molecular weight of HDPE waxes and the bitumen modifying process has been reported [202]. The molecular weight of the waxes can influence the viscosity, moisture, low and high temperature resistance capacity of PE wax modified asphalt mixtures. Therefore, the influence of these ageing mechanisms will have a significant impact on the pyrolysis wax performance as a bitumen modifier (as already demonstrated by the thermal properties of the waxes, as discussed in Section 4.4.), which will be investigated further in Chapter 5.

Table 4.3 Distribution in weight percentage of molecular weight and class of hydrocarbons in pyrolysis waxes (450-2, 500-2 and 550-2) after thermal conditioning at 170 °C from 0-6 hours.

Ageing time (hour)	450-2				500-2				550-2			
	0	1	3	6	0	1	3	6	0	1	3	6
Diesel (C ₄ -C ₉)	7.19	3.41	6.30	6.19	7.87	3.54	7.56	10.96	10.42	3.18	7.99	15.57
Gasoline (C ₁₀ -C ₁₉)	62.00	44.89	20.31	11.76	56.89	37.11	10.46	1.15	54.38	31.92	10.54	0.00
Wax (C ₂₀ -C ₃₀)	30.81	51.70	73.39	82.04	35.24	59.36	81.98	87.89	35.20	64.90	80.92	84.43
Paraffinic	55.76	59.60	58.95	72.46	34.65	41.35	46.29	61.69	35.89	37.84	42.04	49.49
Olefinic	35.92	31.34	29.35	17.41	48.31	45.73	38.90	23.01	50.24	47.12	40.83	28.68
Diene	2.96	2.64	1.55	0.25	7.09	6.79	4.27	0.00	8.80	8.68	5.96	0.00
Aromatics	3.27	3.57	6.30	6.19	3.39	3.78	8.71	12.86	2.85	3.18	7.99	18.48
Alcohols	2.08	2.30	3.09	2.61	2.52	2.08	1.59	2.45	2.10	2.43	2.83	2.46
Carbonyls	0.00	1.39	0.75	1.07	0.16	0.27	0.24	0.00	0.13	0.74	0.36	0.89

4.6 Summary

The key findings in this chapter are:

1. The fixed-bed reactor vessel produced for this study was efficient for the thermal pyrolysis of HDPE at moderate temperatures (450-550 °C), which allowed for obtaining (in batch mode) a yield of up to 91.87% wax at 500 °C. The melting points of the waxes were within the range of 49-89 °C, corresponding to commercial waxes that are typically used as flow improvers and performance enhancers in hot-mix asphalt, or as low temperature additives in warm-mix asphalt.
2. The waxes produced at higher temperatures were mainly olefinic, due to higher temperatures promoting certain thermal degradation radical mechanisms, such as β -scission. The more olefinic waxes produced at higher temperatures and higher nitrogen flowrates (having the lowest vapour residence times) saw the lowest volatile mass loss. They were observed to be more prone to oxidation and polymerization reactions, the products from each supporting the higher melting point and thermal stability of these waxes.
3. The lowest loss in volatiles was seen for the wax produced at 550 °C, inferring that it would be the optimal wax to blend with asphalt binders. For HMA modification purposes, blending at temperatures lower than 170 °C should be considered to lessen the volatile loss with initial blending and storage of the wax modified binders. In the case of significant volatile loss, further efforts to reduce this should be considered for potential applications.

The relationship between pyrolysis parameters, resultant wax properties and their subsequent performance and compatibility as binder modifiers in hot-mix asphalt is not yet fully realised and will be investigated in the following chapters.

CHAPTER 5: High-Density Polyethylene Pyrolysis Wax in Asphalt Binder 'w-bitumen' Modification

5.1 Overview

In Chapter 4, the final pyrolysis temperature was observed to have a controlling influence on the properties of the pyrolysis waxes. Therefore, three waxes produced at 450, 500 and 550 °C using a constant nitrogen flowrate of 2 L min⁻¹ have been selected for use in this chapter for the production and testing of the w-binders. A penetration grade 40/60 binder was used as the base binder for the pyrolysis wax additives as well as the control binder for comparison. This chapter details the second phase of the project, aiming to provide a baseline of understanding of the interactions between HDPE pyrolysis process parameters, the product wax characteristics and resultant plastic pyrolysis wax modified binder ('w-binder') performance in HMA. The relationships between the chemical and thermal properties of the waxes and their rheological and mechanical performance are explored, allowing for the selection of an optimal wax to take forward for w-asphalt formulation. Furthermore, an extensive investigation using shear fatigue tests and a DSR based crack growth model (DSR-C) is employed. The ageing mechanisms of the w-binders are explored as a continuation of the investigation into the thermal and oxidative stability of the waxes within this application.

5.2 w-Bitumen Rheological Testing

5.2.1 Needle Penetration

The penetration value of asphalt binder has been described as an indicator of its consistency, which in turn reflects its rheological properties [141]. It can be seen in Figure 5.1 that the addition of the pyrolysis waxes resulted in an increase in penetration value, indicating that it tends to increase the softening of the binder, regardless of the pyrolysis parameters utilised to produce the wax and wax dosage. Moreover, the effect of increasing the wax dosage from 6 to 12 wt% led to a further increase in penetration value. This suggests a decrease in

consistency of the w-binders and thus, the resistance to deformation must be closely monitored. Otherwise, the application of the waxes may be considered for the composite modification of high viscosity and low workability binders, such as polymer-modified and rubberized bitumen, or potentially the rejuvenation of reclaimed asphalt (RAP) [197, 297-299]. It is noted that the 450 °C waxes result in the largest increase in penetration, followed by the 500 and 550 °C waxes. The 450 °C wax was much less viscous and softer than the other waxes at room temperature, exhibiting a significantly lower melting temperature range. This can be attributed to its higher content of shorter hydrocarbon chain structures (C₄-C₁₉.) The waxes produced at higher process temperatures were more viscous and harder waxes, with higher melting point ranges due to higher contents of larger chain olefins and paraffins (C₂₀-C₃₀) that may produce more crystalline structures within the binder [33].

In contrast, the addition of commercial wax additives in literature, such as Sasobit ® (Fischer-Tropsch paraffin wax) and polyethylene wax has resulted in the reduction of penetration values. However, this was reported due to the fact that viscosity-reducing additives do not fluidify until fusion, which occurs at temperatures greater than 90 °C, and the penetration test is performed at 25 °C, a temperature at which the additives were seen to increase the stiffness of the binder [300-302].

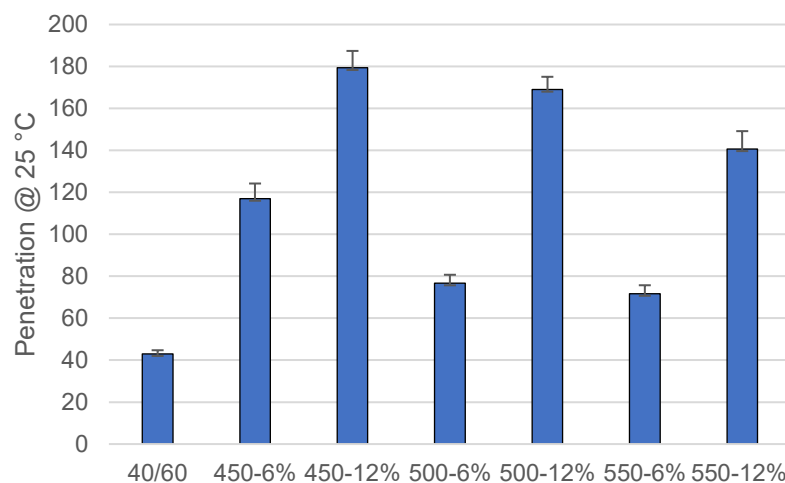


Figure 5.1 Penetration point of the control and wax modified asphalt binders at 25 °C. (450-6%' stands for a 6 wt% dosage of the pyrolysis wax produced at 450 °C.)

5.2.2 Frequency Sweep Test Analysis

The rheological results are plotted in the master curve (isothermal frequency sweeps shifted to a reference temperature) presented in Figure 5.2 for the complex shear modulus ($|G^*|$). The reference temperature is 40 °C and based on the time-temperature superposition principle of viscoelastic materials, low frequency refers to high temperature, etc. The complex modulus is typically used to assess a binder's resistance to deformation under repeated shear, such that a high complex modulus indicates a higher resistance to deformation [234, 235].

The shape of the master curves for the w-binders are identical to the base binder, at both the low and high levels of modification, however, at all temperature and frequency ranges, the $|G^*|$ is decreased when the pyrolysis waxes are mixed with the conventional asphalt binder. This can be observed for all w-binders and their subsequent doses, by the master curve of the $|G^*|$ shifting horizontally towards the right. The sequence of decreasing complex modulus for the binders is 40/60 > 550-6% > 500-6% > 500-12% = 550-12% > 450-6% > 450-12%. In general, with the increase in each of pyrolysis wax, the $|G^*|$ is decreased further. The $|G^*|$ of the wax modified binders decreased in the high temperature-low frequency ranges and with the increase of temperature; showing that at higher temperatures the binders became soft and their resistance to rutting declined. Though, their moduli were lower in the higher frequency range, indicating them superior to the conventional binder in low-temperature, anti-cracking performance. This has been similarly reported in bio-oil modifiers obtained from this thermochemical process [303, 304]. These results differ to that reported by Edwards et al, in which a commercial polyethylene wax (Luwax © by Sasol) exhibited the highest stiffening effects of all the viscosity-reducing modifiers studied at 25-90 °C. This high effect was suggested to be partly due to its narrow melting temperature range when compared to other commercial waxes such as Fischer-Tropsch paraffin or Montan wax, as well as its ability to form a crystal/gel network within the bitumen matrix that improves its elasticity [22].

Not only does the presence of the pyrolysis waxes highly influence the mechanical properties of the binders, but also their chemical composition, namely the hydrocarbon chain lengths present within each wax. In previous chapter, it was established that the waxes produced at higher process temperatures are composed of a higher content of olefinic hydrocarbons. The chemical composition of the waxes shifted to more olefinic when increasing the pyrolysis temperature, due to these process conditions promoting thermal degradation mechanisms, such as β -scission. With the exposure to typical binder mixing and storage temperatures, all waxes were seen to undergo oxidation reactions as well as increase in heavier molecules and become more saturated, explained by polymerization mechanisms. The more olefinic (500 and 550 °C waxes) are slightly more susceptible to these reactions, producing larger and more thermally stable components (supported by their volatilization and thermal degradation behaviour [33].) While all waxes reduce the complex modulus of the bitumen, it can be seen that the 450 °C waxes result in the largest reductions in $|G^*|$, while the waxes produced at 500 and 550 °C give lower reductions. Despite the overall softening action of the higher process temperature waxes, this may be due to the presence of more crystalline structures as a result of longer chain paraffins in the waxes. A significant relationship between the molecular weight (M_w) of low-density polyethylene (LDPE) and HDPE waxes and their performance as bitumen modifiers was commented on by Zhang et al. Waxes with increasing M_w further increased the viscosity, low temperature, and moisture resistances of the modified asphalt. Higher M_w waxes improved the high temperature resistance of the modified mixtures also [202].

Furthermore, the phase angle is used for assessing the viscoelastic behaviour of asphalt binders, in which a higher phase angle (90°) indicates more viscous behaviour, while a low phase angle (0°) indicates a more elastic response [234, 235]. Table 5.1 in *Section 5.6.1* presents the δ of the unaged, RTFO and RTFO+PAV aged control and w-binders at a loading frequency of 1.59 Hz (10 rad/s) for two different temperatures. At 20 °C (in the unaged condition), it is observed that the 450 °C at both modification levels provided a substantial increase in δ , especially at 12 wt% addition (likely due to the additive containing

a higher concentration of light molecular weight components). The 500 and 550 °C waxes provided similar values to the control binder or showed a decrease in δ . At 60 °C, a significant increase in δ of all binders occurs as they become more viscous. The δ values of the w-binders are slightly lower than that of the control binder, indicating a larger elastic component. This may be due to some of the lighter components within the waxes having melted but not all, so the w-binders are not yet tending fully towards viscous behaviour, as will be investigated further in the next *Section 5.2.3*.

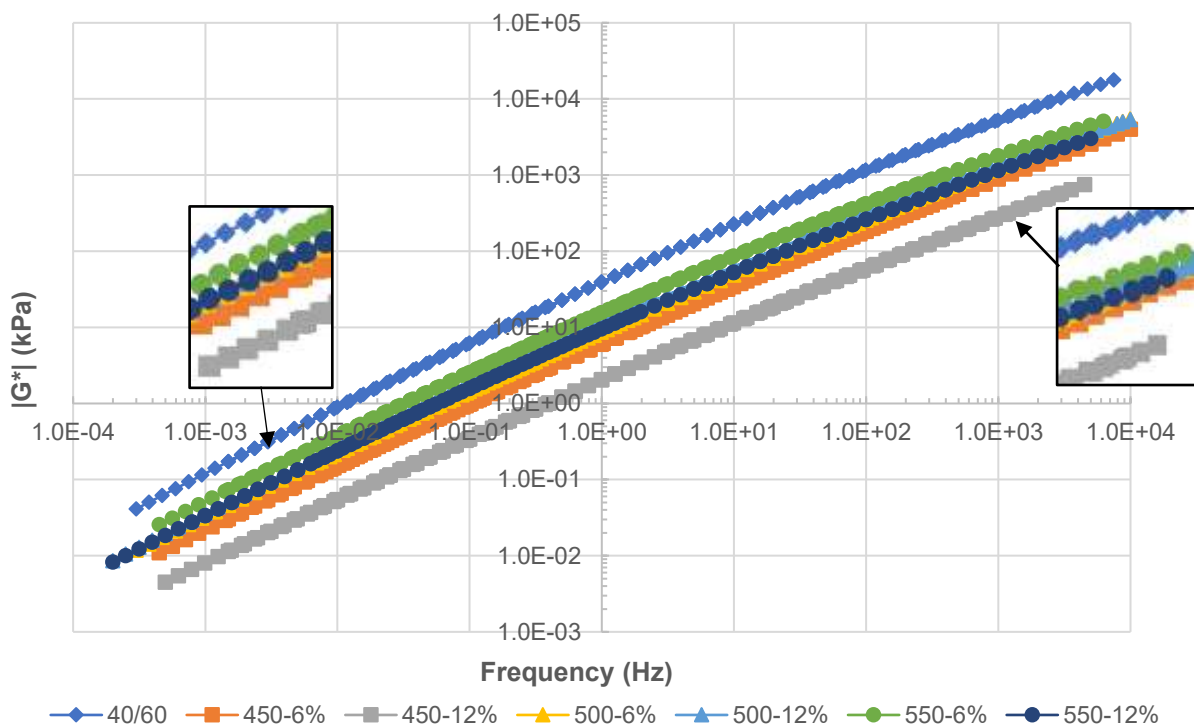


Figure 5.2 Master curves for the complex shear modulus ($|G^*|$) of the control binder and pyrolysis wax modified binders. (450-6%' stands for a 6 wt% dosage of the pyrolysis wax produced at 450 °C.)

5.2.3 Black Space Diagrams

The black space diagram is often utilised to identify patterns within datasets that can be influenced by the presence of binder modifiers. For wax modifiers, this data representation can indicate the melting of the wax and whether it occurs within the measured temperature range, as well as the effect on the mechanical properties of the material [197]. Figure 5.3 shows the frequency sweep results of

the control and w-binders in an ordinary black space diagram, in the temperature range of 30-70 °C (the range in which rheological changes are observed with temperature increase). For all binders studied, an increase in temperature resulted in a decrease in stiffness as well as an increase in viscous response. The presence of the HDPE derived waxes reduces the phase angle of the base binder, and generally, the higher the content of each wax, the higher the reduction in phase angle. An increase in elastic component due to the presence of a polymer network has been reported for plastic modified binders, such as styrene-butadiene-styrene, polyethylene and polypropylene [32, 305]. This behaviour is seen until the inferred point of each wax's fusion, in which the phase angle starts to tend towards viscous behaviour in the same way as the base binder. Especially as the temperature increases, a highly viscous response indicates that the material is becoming more fluidlike [139].

For the neat bitumen blended with 450 °C wax, the curved shape of the datasets obtained are indicative of a binder with the mechanical behaviour that is affected by the presence of a modifier up the temperature ranges of 30-40 °C and 40-50 °C for the 6 and 12% dosages, respectively. The datasets obtained above this temperature range then move asymptotically towards the phase angle value of 90° for a fully viscous response, showing no interference in the mechanical behaviour from the plastic wax. This infers that the melting of this wax and the subsequent softening action of the bitumen happens at 40-50 °C, which agrees with the DSC results for the pyrolysis waxes obtained in *Section 4.4.2* [33].

The 500 and 550 °C w-binders demonstrated a larger reduction in the phase angle and the curved shape of the datasets show that the mechanical response of these binders are still affected by the wax modifier. A fully viscous response was not achieved at 70 °C for the 500 °C wax at a 12% dosage and for the 550 °C wax at both modifier dosages. Flow-improver additives do not fluidify until fusion, which doesn't fully occur above 70 °C for these waxes, as verified by previous DSC results [33]. Desidery et al saw comparable result datasets in their investigation involving the effect of short and long chain Fischer-Tropsch waxes on the viscoelastic properties and performance of bitumen [197].

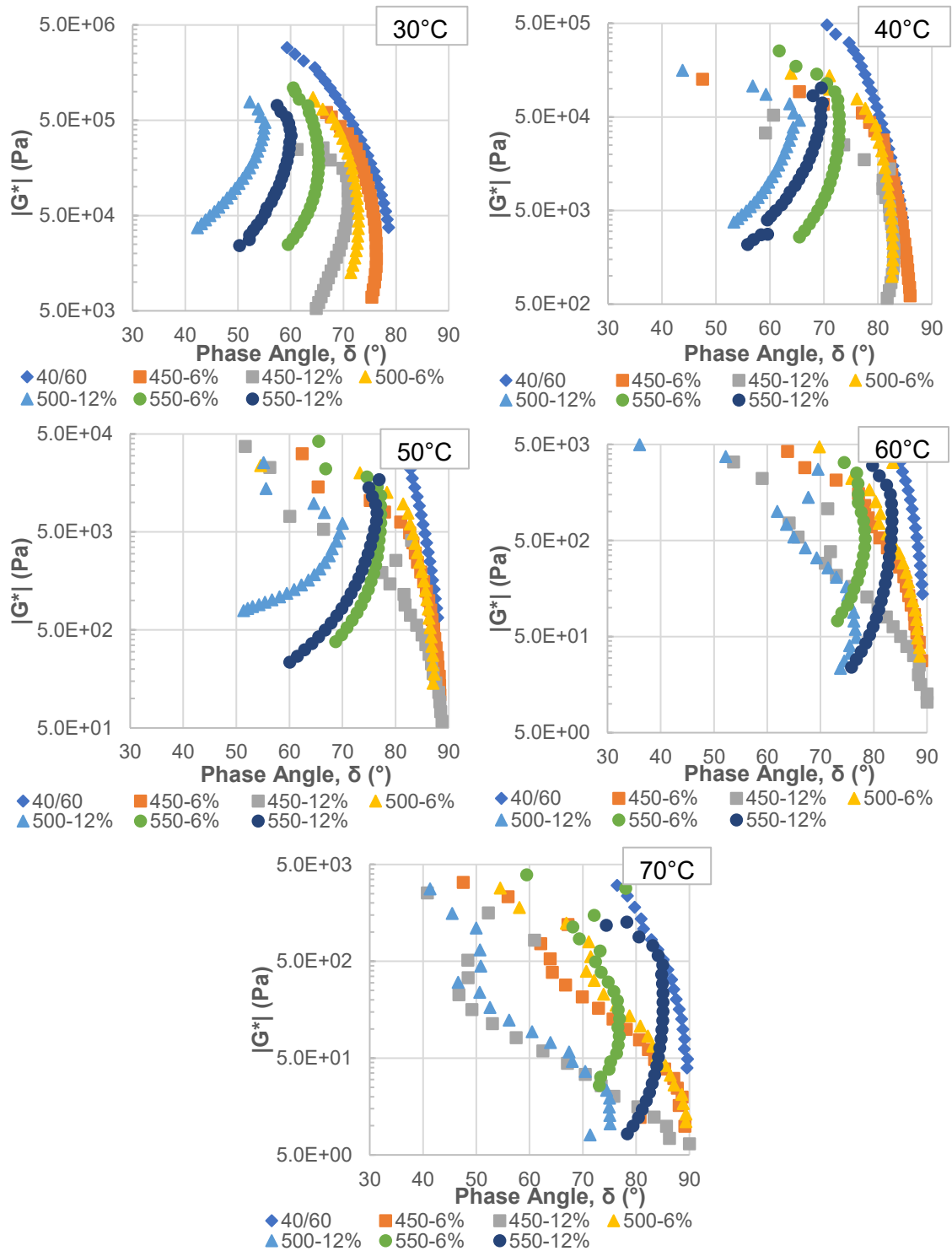


Figure 5.3 Black diagrams of neat and pyrolysis wax blended binders, from 30-70°C utilising frequency sweep test parameters.

5.2.4 Complex Viscosity

The complex viscosity is a vital rheological parameter that indicates the change within a materials structure and consistency, in relation to temperature and loading time. This parameter may also be used to indicate an asphalt mixtures resistance to viscoelastic deformation [250]. The complex viscosity η^* results at test temperatures of 10-70 °C are shown in Figure 5.4. The results indicate that the use of pyrolysis wax additives significantly reduces the complex viscosity of the binders, independent of temperature. The reduction in η^* shows a similar trend to that of $|G^*|$, regarding the wax modifier type and dosage. A frequency dependence was observed which provided evidence for non-Newtonian shear-thinning behaviour, such that, decreasing the oscillation frequency of the applied shear strain resulted in an increase in the binders complex viscosity, which is expressed by $|G^*|/(\sin\delta \cdot \omega)$, (Appendix G) [306].

Within the bitumen matrix, asphaltenes are regarded as randomly orientated particles within the maltene fraction which mainly contribute to a binder's viscosity and may aggregate at rest. At certain temperatures, when the bitumen undergoes shear loading the asphaltenes will transition to an ordered state within the maltenes, causing shear-thinning behaviour. This explanation is extended to the shear-thinning behaviour of wax-modified bitumens by Wang et al., regarding wax as solid particles [249]. The decrease in viscosity indicates that the wax modifiers offer promising solutions to workability issues previously seen in polymer modified binders, increasing binder workability of the binders at typical process temperatures for mixing and compaction [134, 165].

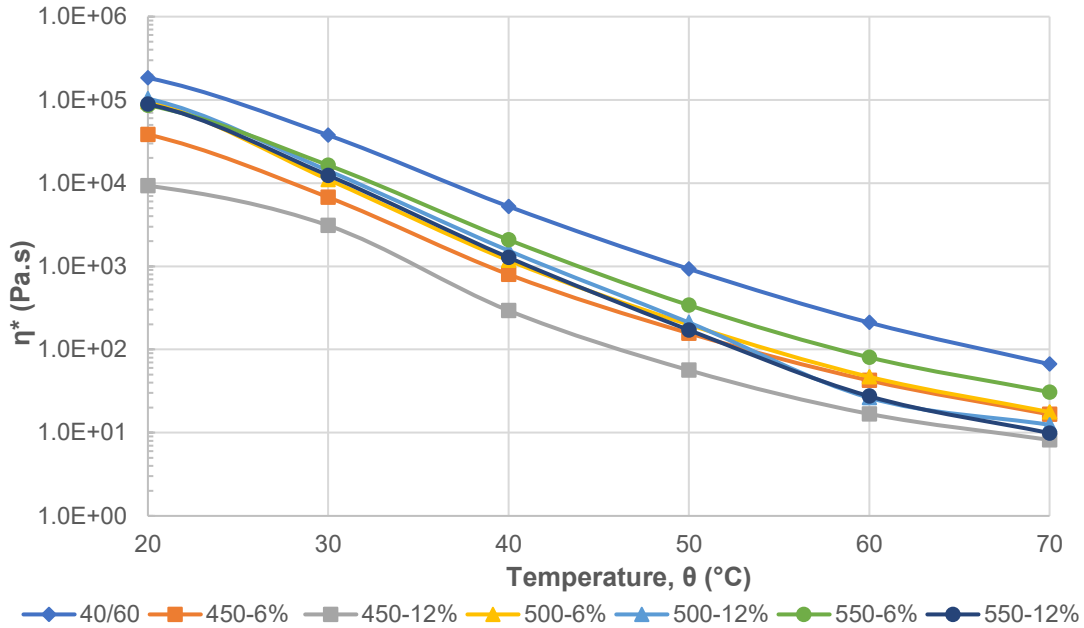


Figure 5.4: Complex viscosity as a function of temperature.

5.3 w-Bitumen Fatigue Performance

5.3.1 LAS and TS Tests

In accordance with the DSR based crack growth model (DSR-C) for fatigue crack length prediction as proposed by Gao et al, the LAS test was used to obtain the undamaged shear modulus ($|G_0^*|$) and phase angle (δ_0) of all RTFO+PAV aged binders [239]. From this, a suitable level for the controlled strain could be selected for the TS fatigue damage test. Li et al stated that theoretically, the ($|G_0^*|$) and (δ_0) can be obtained using the average of the $|G^*|$ and δ within the undamaged strain level range of 0.01- 0.8% [264]. However, it is stated that sample-to-sample variation should also be considered.

Appendix H shows the results of the LAS test at 20 °C and 10 Hz for all tested binders. It can be seen that after RTFO+PAV ageing, the recorded values for $|G^*|$ are significantly higher, indicating much stiffer binders due to the effects of oxidative aging mechanisms. The range of δ is also seen to decrease, moving towards a more elastic behaviour after ageing. The observed trend in the reduction of stiffness of the w-binders with each wax modifier and subsequent dosage is comparable to that of the unaged frequency sweep master curves. The

DSR-C model will be used to evaluate the fatigue performance of the binders in this study, however, the curve of shear stress as a function of shear strain may still be commented on. The maximum stress (T_{max}) reached by a sample during the LAS test is a specified criterion of its fatigue life, the peak stress being the yield threshold when the binder is subjected to increasing load [265]. Additionally, a higher peak area indicates a more ductile, tougher binder, indicating that more energy is required to collapse the material. Regarding Appendix I, depicting the stress-strain curve of the binders produced during previous LAS tests conducted between 0.1-30% strain (10Hz, 20°C), the peak stress is reduced with the addition of the softening pyrolysis waxes. The larger molecular chain waxes (500 and 550 °C at 6% dosage) reduce the peak stress the least and a higher wax modification significantly decreases the peak stress with shear strain. The 550 °C w-binder (6% modification) has the highest peak area, suggesting a more ductile and tougher binder. Additionally, it is noted that in comparison to the control binder curve, the stress response of the wax binders (especially at 6% modification) decreases the least by the end of the applied strain amplitude of the test. Not exhibiting a significant degradation in stress response at the higher levels of strain indicates that these binders are the least damaged and may be subjected to strain amplitude higher than 30%.

The TS test was utilised to obtain ($|G_N^*|$) and (δ_N) at a 5% strain level as determined from the LAS test, performed at 20 °C and 10 Hz for all the tested RTFO+PAV aged binders. The results of which are presented in Appendix J. A common criteria used for determining the material failure point is the point at which $|G^*|$ reaches 50% of its initial value, $N_{50\%G^*ini}$ [267]. The $N_{50\%G^*ini}$ values determined from this test can be seen in Appendix K. To comment, the sequence of decreasing $N_{50\%G^*ini}$ values of the binders is 550-12% > 500-12% > 450-12% > 450-6% > 500-6% > 550-6% > 40/60. This is comparable to the sequence of decreasing $|G^*|$ observed within the frequency sweep and aged fatigue damage tests.

5.3.2 Crack Growth Modelling

Utilising the undamaged and damaged values for the $|G^*|$ and δ , the propagation and length of fatigue cracks could be determined for the RTFO+PAV aged binders when a rotational shear fatigue load is applied. Figure 5.5 depicts the calculated crack growth of the neat and w-binders, as a function of the loading cycle. Li et al showed that crack length evolution can typically be characterised by three phases: initiation of a crack, a plateau in crack length and then its propagation [264]. Figure 5.5 mainly depicts the plateau and propagation phases. Within the plateau phase, the crack growth with loading cycles is slow, which is a result of microstructure restructuring after crack initiation, through the reorganizing of low molecular components (e.g., saturates and aromatics). With binder ageing, the loss of lightweight components would tend to minimise this plateau phase.

It can be observed that in comparison to the control binder, the crack evolution of the aged w-binders is dominated by the plateau phase. Chapter 4 investigated the thermal ageing properties of the wax modifiers used within this study, including volatile loss with heating time [33]. The relationship between the length of the plateau phase in the crack evolution curve ($550^\circ\text{C} > 500^\circ\text{C} > 450^\circ\text{C}$) and extent of volatile loss ($450^\circ\text{C} > 500^\circ\text{C} > 550^\circ\text{C}$) can be observed especially at the higher modification level. Yet overall, it is observed that the trend in crack length correlates strongly to the trend on $|G^*|$ values obtained for the RTFO+PAV aged samples, as seen later in Figure 5.9 (b).

Furthermore, pyrolysis waxes contain light saturated and unsaturated components. A higher saturation of lightweight components within the w-binders from the waxes will increase the extent of microstructure rearrangement available during crack initiation, thus further delaying crack growth. This is comparable to the crack evolution of bio-oil modified bitumen also observed by Li et al [264]. As with bio-oil, the addition of pyrolysis wax significantly decreases the final crack length, rejuvenating and enhancing the fatigue cracking resistance of the binders.

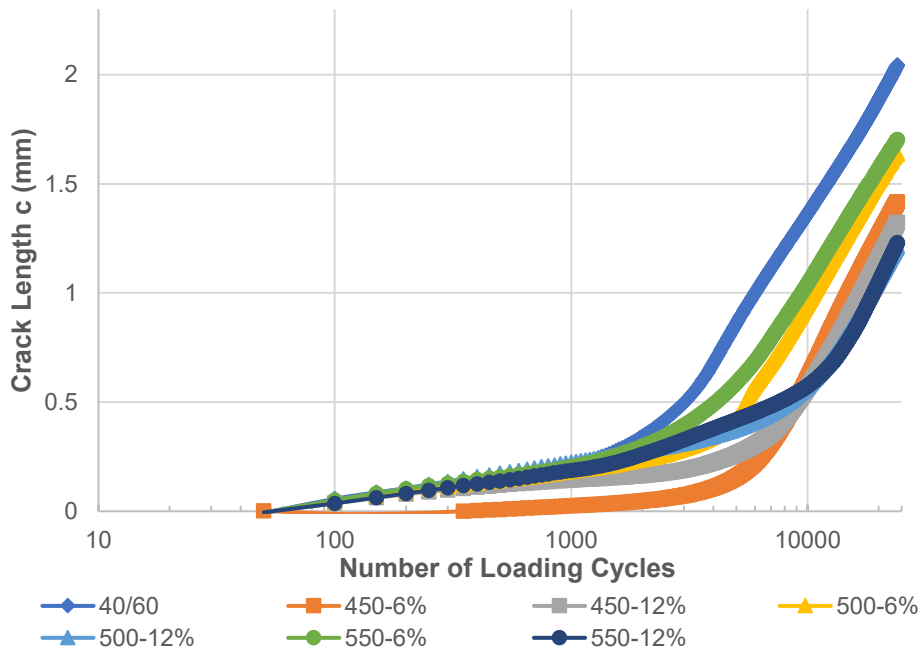


Figure 5.5 Binder crack length evolution curve of the RTFO+PAV aged neat and w-bitumens.

5.4 w-Bitumen High-Temperature Performance

At temperature conditions above 40 °C, the asphalt binders within flexible pavements become softer and more viscous. The main failure mode exhibited at these conditions is permanent deformation or rutting. Rutting mainly occurs due to high volumes of traffic and therefore load repetitions, causing plastic deformation of the materials within the multi-layer pavement structure. The high temperature performance of the RTFO aged binders was initially characterised using the multiple stress creep recovery (MSCR) test at 58 °C (BS EN 16659 [254]) by obtaining the non-recoverable creep compliance (J_{nr}). Observing the accumulated shear strain plots in Appendix L (a-b) (taken from the rSpace software) for the neat, aged binder, inaccurate readings resulted in no obvious strain recovery and dubious results, especially at 3.2 kPa creep stress. This is thought to be due to the softness of the binder, even at a reduced temperature of 52 °C. Due to the observed softening of the w-binder samples, it was thought appropriate to alternatively obtain and comment on the Superpave rutting factor, $|G^*|/\sin\delta$ [256]. This factor is utilised to evaluate the performance of bitumen blended with different modifiers at higher in-service pavement temperatures, with

a higher rutting factor indicating superior performance of a binder. The rutting factors of all RTFO-aged binders were calculated and are exemplified in Figure 5.6.

It can be observed that the rutting factor of the binders sharply decrease due to an increase in the viscous component with increasing temperature, followed by its slow decline after a certain temperature. The ageing of asphalt binders mainly proceeds via volatilization and oxidation mechanisms. The temperature at which the $|G^*|/\sin\delta$ of each binder equalled or was less than 2.2 kPa followed the trend of 40/60 > 550-6% > 450-6% > 500-6% > 550-12% > 500-12% > 450-12%. The 450-12% w-binder had the lowest rutting performance, most likely due to an over-saturation of light components within the w-binder, despite high volatilisation (Figure 5.10.) The same can be inferred for all high modification level wax modifiers, having the lowest rutting performance. The 500-6% and 550-6% w-binders had the highest rutting performance, their rutting factors closest to that of the neat binder, possibly due to their higher affinity for other ageing mechanisms (polymerisation.) The rutting performance of the w-binders shows that the higher pyrolysis temperature waxes especially can have a value-added application in asphalt binders, showing significant improvements in failure resistances such as fatigue damage, while having minor impact on rutting resistance after the short-term ageing that occurs with storage and compaction.

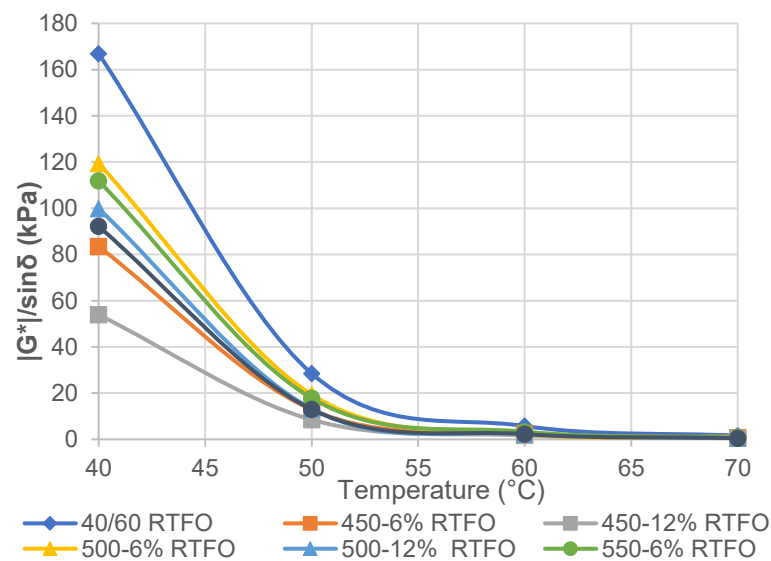


Figure 5.6 The $|G^*|/\sin\delta$ of the neat and w-binders after short-term ageing.

5.5 Chemical Characterisation

5.5.1 Modification Mechanism

The chemical composition of the neat and w-binders was evaluated by means of FTIR Spectroscopy. The main functional chemical groups of the (unaged) neat bitumen are identified in Figure 5.7. In the spectrum, it is observed that the main peaks are located at: 2920 and 2850 cm^{-1} (CH_2 stretch), 2900 and 2690 cm^{-1} (CH_3 stretch), 1600 cm^{-1} ($\text{C}=\text{C}$ stretch), 1465 cm^{-1} (CH_2 bend), 1375 cm^{-1} (CH_3 bend), 1030 cm^{-1} ($\text{S}=\text{O}$ stretch), 700-900 cm^{-1} ($\text{C}-\text{H}$ bend). It has been observed in previous literature that sulfoxides are formed earlier than carbonyls and are present under weak ageing conditions [307]. The same functional groups listed can be seen in Figure 5.8 for the w-binders. No additional peaks were observed yet it is noted the more prominent shoulder at 1700 cm^{-1} for $\text{C}=\text{O}$ and peak at 1030 cm^{-1} for $\text{S}=\text{O}$, which correspond to the chemical composition and ageing processes available to the waxes during its collection, storage and blending with the asphalt binder. This indicates that there are no chemical interactions between the asphalt binder and the waxes. Moreover, this indicates that the pyrolysis waxes consist of similar fractions to those already present in the bitumen, such as natural waxes, inferring that its addition and partial replacement will not negatively impact the recyclability of the resultant asphalt. FTIR analysis of the binders can additionally be utilised to show the chemical functional groups present prior to and after the binder ageing that might occur upon blending, compaction and throughout their service life, which will be investigated in *Section 5.6.3*.

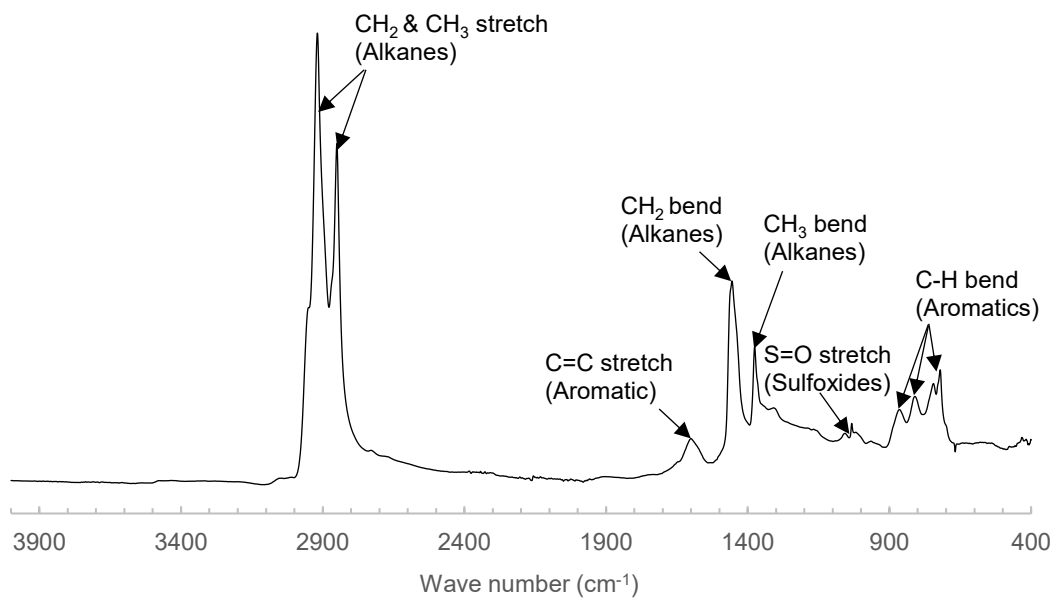


Figure 5.7 Neat bitumen infrared spectrum, identifying main functional chemical groups.

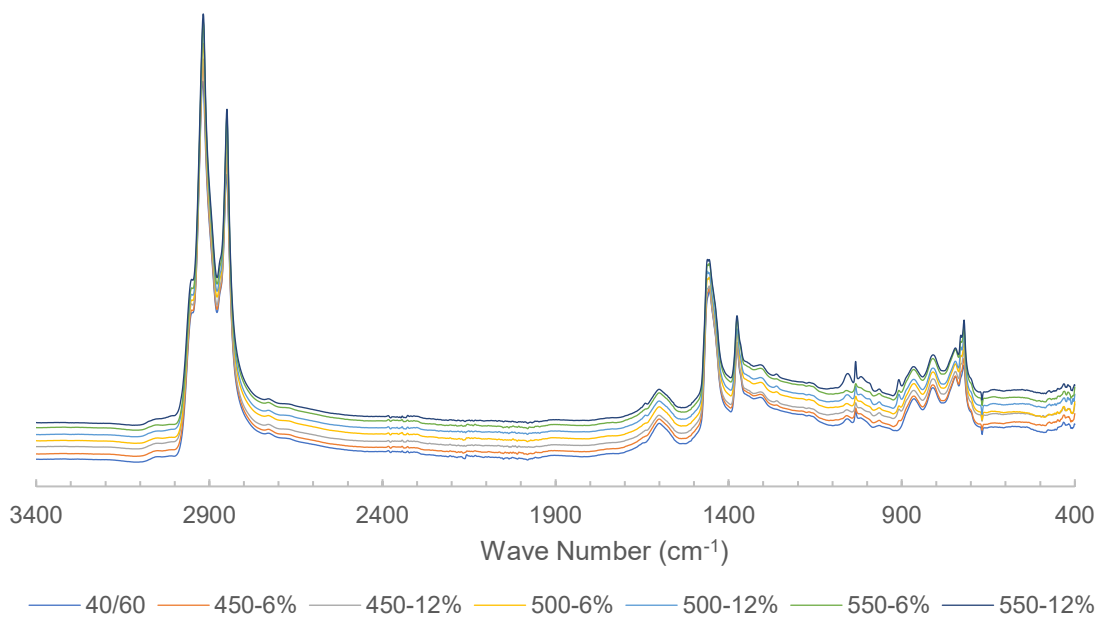


Figure 5.8 FTIR spectra of the unaged neat and w-binders.

5.6 Ageing Performance

5.6.1 Rheological properties of aged w-Binders

Referring to Figure 5.9 (a-b), it can be observed that the $|G^*|$ values of all binders increase after the RTFO and PAV ageing processes. The difference between the complex modulus and subsequent stiffness of the 40/60 binder and the w-binders is much reduced, with some overlapping after the RTFO ageing for the 500-6% binder. However, the evident softening of the binder with the addition of the pyrolysis waxes indicates a resistance to ageing, with similar trends for $|G^*|$ values as observed within the master curve for the unaged w-binders in Figure 5.2.

After the short-term ageing, notable increases in stiffness are seen for the 450-6% and 500-6% w-binders. The 500-6% wax is now slightly stiffer than the 550-6% wax, which was originally the stiffest of the w-binders in the unaged condition, while the 450-6% exhibits similar $|G^*|$ values to the 550-6% binder. This correlates (especially within the high temperature/low frequency region of the master curve) with the described trend in Superpave rutting factors $|G^*|/\sin\delta$ obtained in *Section 5.4* and presented in Figure 5.6. The observed stiffening effects can additionally be related to the extent of volatilization available to each wax type ($450\text{ }^\circ\text{C} > 500\text{ }^\circ\text{C} > 550\text{ }^\circ\text{C}$), which will be discussed further in the next *Section 5.6.2*. The trend in $|G^*|$ values for the RTFO+PAV aged w-binders is similar to that after RTFO ageing, except from the notable stiffening of the 450-12% w-binder after long-term ageing, a result of the substantial mass loss exhibited by this sample. Some correlation can be drawn between this trend (especially within the low temperature/high frequency region of the master curve) and the described trend in the w-binders fatigue performance obtained in *Section 5.3* and presented in Figure 5.5.

Individual values were obtained at a loading frequency of 1.59 Hz (10 rad/s) at two different temperatures for the phase angle of the control and w-binders before and after RTFO and RTFO+PAV ageing, the values are presented in Table 5.1. At 20 °C, all unaged w-binders (apart from the 500-12% sample) have

a larger viscous component than the control binder. They all follow a similar trend with a movement towards more elastic behaviour after ageing. At 60 °C, all binders generally have a more viscous response overall, yet it is observed that the phase angles do decrease (increase in elastic response) or remain at similar values after the RTFO+PAV ageing, in comparison to the unaged condition, with the exception of the 450-12% binder.

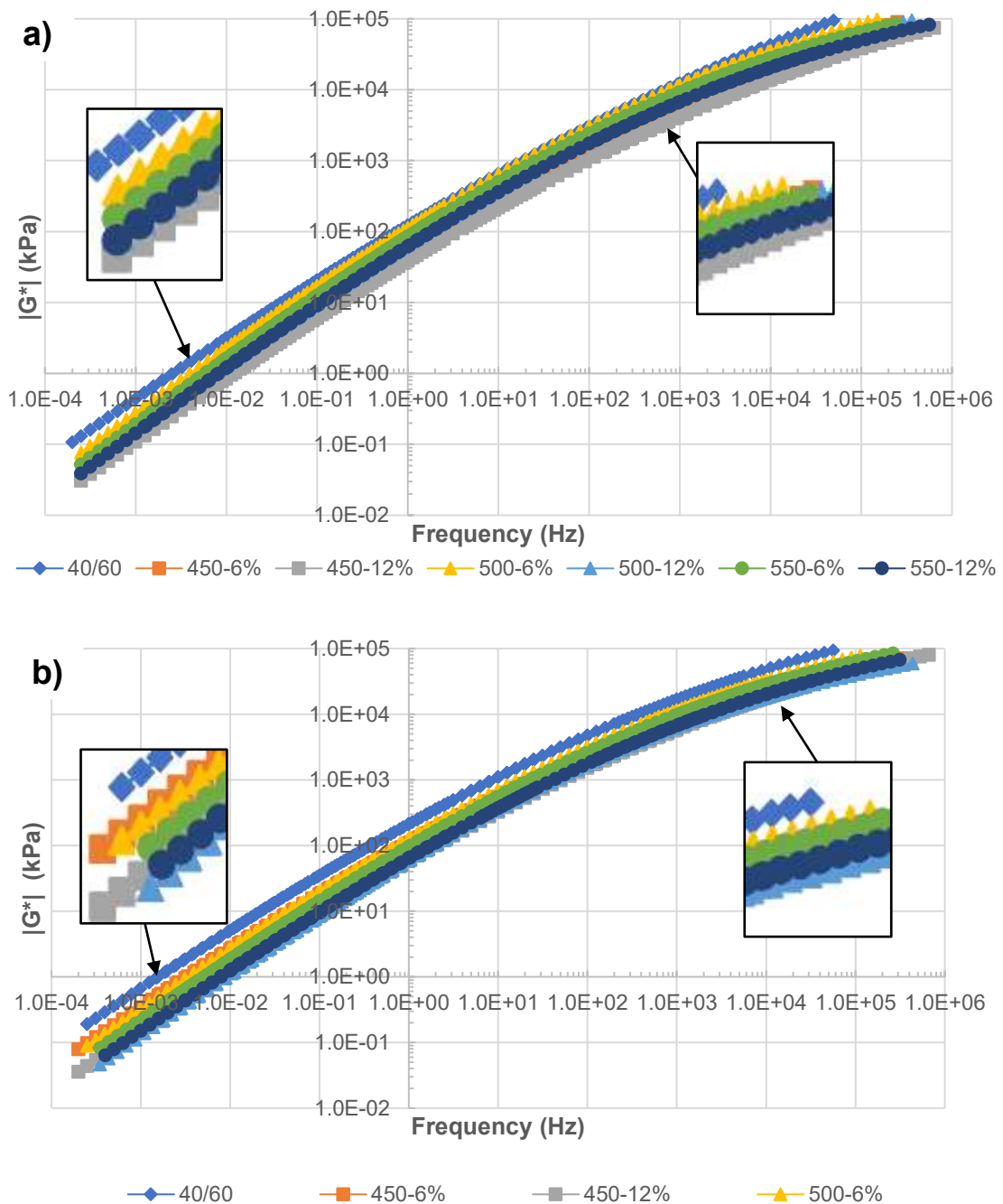


Figure 5.9 Master curve of the $|G^*|$ for the control binder and pyrolysis wax modified binders in the: (a) short-term (RTFO) aged (b) long-term (RTFO+PAV) aged condition.

Table 5.1 Phase angle of neat and w-binders at loading frequency of 1.59 Hz for two different temperatures.

	δ at 20 °C			δ at 60 °C		
	Unaged	RTFO	RTFO+PAV	Unaged	RTFO	RTFO+PAV
40/60	59.08	49.29	48.38	85.96	84.00	82.39
450-6%	63.99	46.20	42.23	82.53	85.11	82.28
450-12%	66.05	46.98	47.83	75.93	85.52	86.14
500-6%	60.51	46.40	42.7	83.68	82.94	82.01
500-12%	46.77	44.69	40.95	71.41	83.4	82.99
550-6%	57.45	47.28	44.32	78.07	83.94	82.92
550-12%	61.98	42.92	38.31	82.70	81.95	81.65

5.6.2 Mass Loss during Ageing

The control and w-binders were aged in an RTFO oven at 163 °C for 85 minutes. According to the Superpave standard and BS EN 12607-1 (ASTM D2872), the mass loss of the asphalt binders after the short-term ageing must not exceed one percent. The mass loss results are presented in Figure 5.10, in which it can be determined that only the control 40/60 binder and 550 °C wax w-binder (at both modification levels) met this requirement. However, it is noted that the 500 °C wax at the lower modification level had a mass loss averaging 0.06 % over the standardised 1 % limit, with a mass loss variance below this. The results indicate that as the neat binder had negligible mass loss, the mass loss is from the pyrolysis waxes. The higher modification w-binders were observed to have the highest mass loss, especially the 450-12% w-binder. The mass loss varied in accordance with and most likely due to an over-saturation of light components within the w-binders. Additionally, the source of the mass loss is the pyrolysis waxes, the trend in these results being comparable to that obtained in *Section 4.5.1* for the thermal ageing and volatile mass loss of the waxes (450 °C > 500 °C > 550 °C), as discussed.

In Figure 5.9 (a) depicting the master curve of the RTFO aged samples attained using the frequency sweep test, the same trend $|G^*|$ reduction and softening of the binders with the addition of pyrolysis wax can still be discerned, however, with an observed increase in $|G^*|$ for all binders as a result of the thermal ageing. The 450 °C waxes are still observed to have the lowest modulus values over the reduced frequency range, despite the highest observed mass loss of volatiles during the short-term ageing. Therefore, it can be deduced that the increased stiffness and over rheological change of the binders is more dependent on the ageing mechanisms apart from volatilization, such as oxidation, as well as other ageing mechanisms that are characteristic to the pyrolysis waxes with thermal ageing. The oxidation mechanisms that occur during the different stages of binder thermal ageing will be investigated using FTIR Spectroscopy and discussed further in the next *Section 5.6.3*.

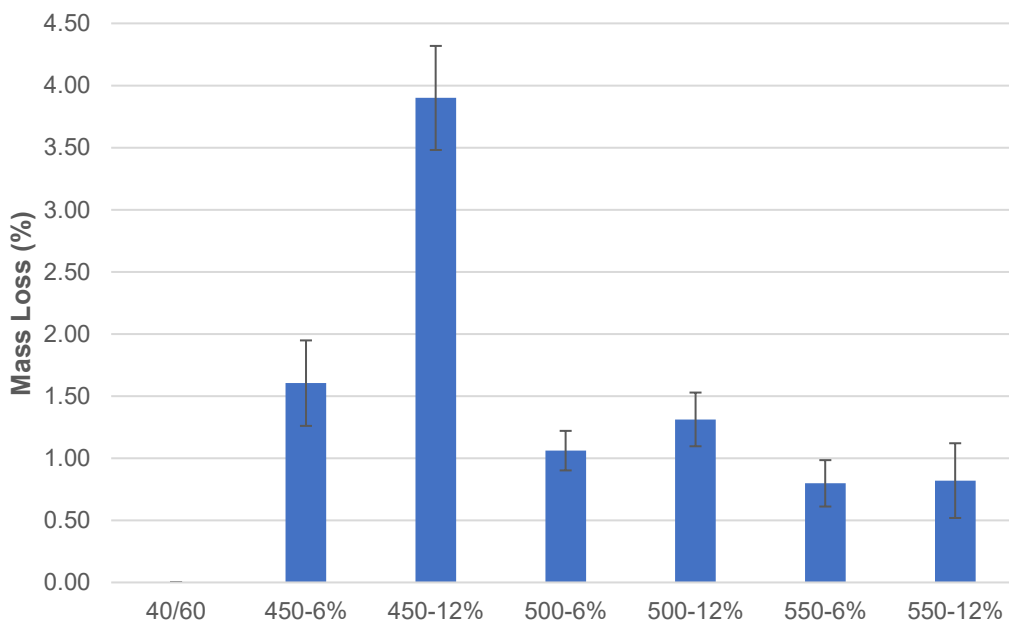


Figure 5.10 The mass loss of the neat and w-binders after RTFO ageing.

5.6.3 Ageing Indexes from FTIR

The ageing mechanisms of bitumen affect its chemical composition and mechanical performance. In an FTIR spectrum for bitumen, the absorbance bands corresponding to carbonyl and sulfoxide functional groups are commonly used as indicators for ageing. Using the obtained spectra (which are shown in

Appendix M and N for further reference), the ageing indices for each sample were calculated. The resultant carbonyl and sulfoxide indices are shown in Figure 5.11 (a-b). It is observed in the results that both indices increased with ageing time. It has been observed in previous literature that under weak ageing conditions, only sulfoxides are initially formed due to sulphur being more reactive with bitumen components than carbon [307]. After RTFO ageing, the sulfoxide index for the neat binder was higher than that of the w-binders. This remained true after the RTFO+PAV ageing, except for the index for the 550-12% binder being significantly higher.

Considering the carbonyl index, the addition of the pyrolysis waxes increases this index to higher values than that of the control binder apart from the 550-6% wax, which is of a similar value. There is a discernible trend for this index, being that the index increases with the increasing degree of modification with pyrolysis wax. This trend remains similar for both the short- and long-term ageing processes. The chemical composition of the waxes produced at higher pyrolysis temperatures are more olefinic and therefore, may tend more to oxidation reactions. The effect of this can be seen for the higher modification binders especially. This effect is observed less within the lower modification w-binders, as the 550-6% w-binder has a lower C=O index, similar to that of the neat binder. The polymerization of unsaturated species within the waxes may account for this. After the RTFO+PAV ageing, only the 550-6% w-binder has a similar index to the neat binder, followed by the 450-6% and 500-6% w-binders. Despite the waxes having similar functional groups to the bitumen, this increase will be due to the waxes increasing the percentage of small molecules and carbonyl functional groups within the binder as a result of their chemical composition. Some authors utilise additional phenolic additives such as lignin, which can neutralize oxygen free radicals lowering the formation of carbonyl compounds [308].

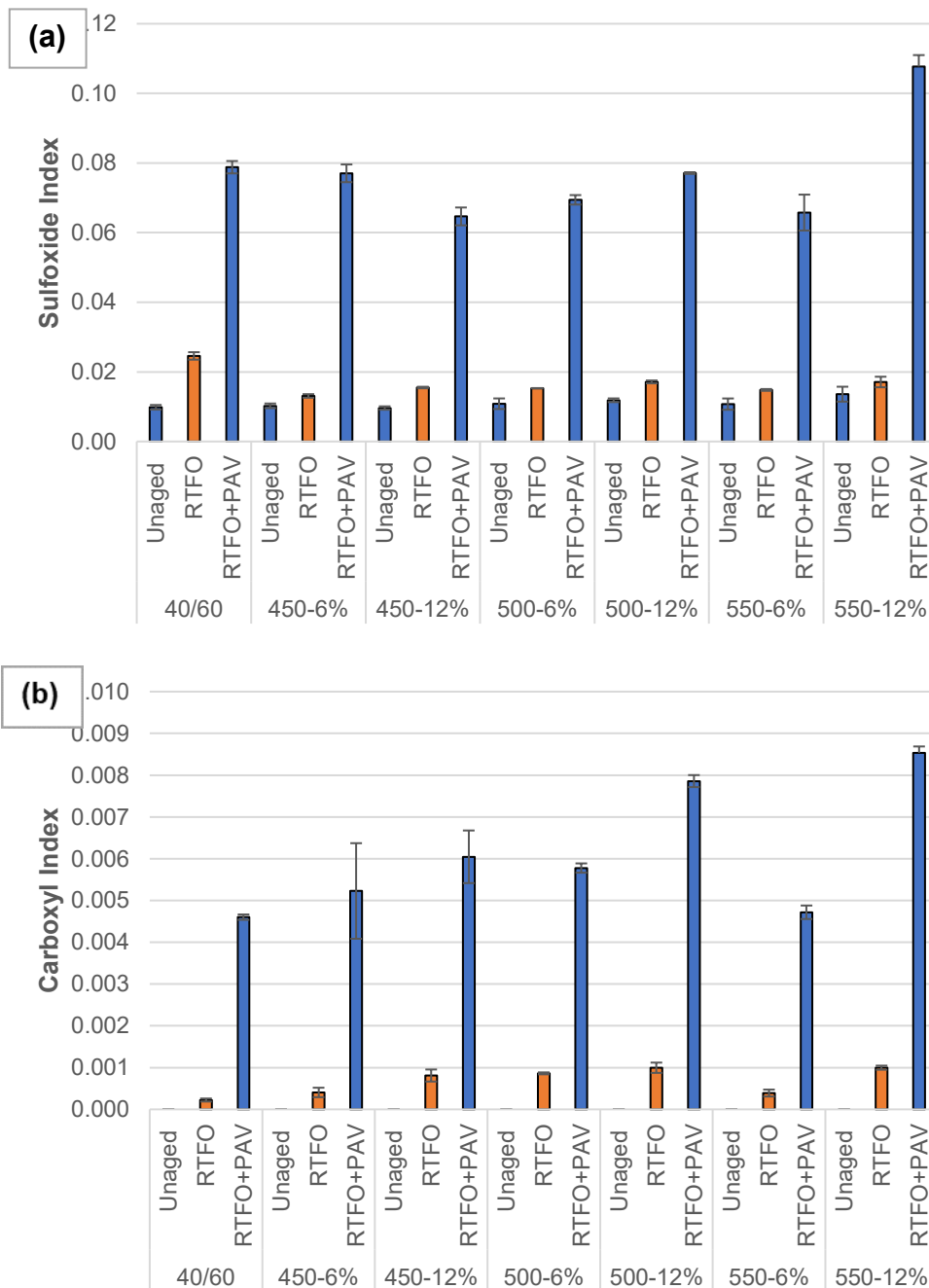


Figure 5.11 Ageing indices of the neat and w-binder at different stages of ageing: (a) Sulfoxide Index, (b) Carbonyl Index.

Overall, from a rheological perspective the pyrolysis waxes function as binder softeners before and after thermal oxidative ageing. They generally reduce the formation of the sulfoxide index, yet due to their own chemical structures increase the carbonyl functional groups present within the binders. However, this is more of an issue within the higher modification w-binders. The lower-level modification binders (such as the 550-6% w-binder) obtained similar C=O indices to that of

the neat bitumen. Upon considering the thermal and oxidative stability of the higher modification w-binders, these are quite unstable and other stabilizing additives may be considered. In terms of volatilization and ageing indices, the 550-6% and 500-6% wax additives had the most stable behaviour and promising results.

5.7 w-Bitumen Dispersity

Dispersity describes the extent of fragmentation of a dispersed phase or additive within the bitumen binder. A concern with waste plastic modified binders is its ease of dispersity as well as potential to phase separate from the bitumen during static storage, aggregating within the binder. Optical microscopy was used to evaluate the dispersity of the waxes within the 40/60 binder after a high-speed shear mixing at 150 °C with a rotation speed of 500 rpm for 15 minutes, in the unaged and aged (RTFO+PAV) condition. From visual analysis, it can be inferred in Figure 5.12 (a-g) that the waxes are well dispersed within the binder after the blending protocol and static storage, with no obvious aggregating and phase separation. This indicates that the mixing time could be potentially reduced to minimise the ageing during mixing. However, it is noted that more small particles are observed within the images for the higher-level modification w-binders.

During ageing, bitumen constituents react with oxygen to form higher molecular weight molecules from unsaturated species, similar polymerization mechanisms have been observed for the pyrolysis waxes. Overall, more particles were observed within all of the sample images after RTFO+PAV ageing, which can be viewed in Appendix O. For the w-binders, some samples such as the 500-12% sample also exhibited particles with a larger diameter. However, in comparison to bitumen modification with the parent polymer (HDPE) in literature, the w-binders are still considered much better dispersed with no very obvious phase separation and therefore are not subject to this technical limitation.

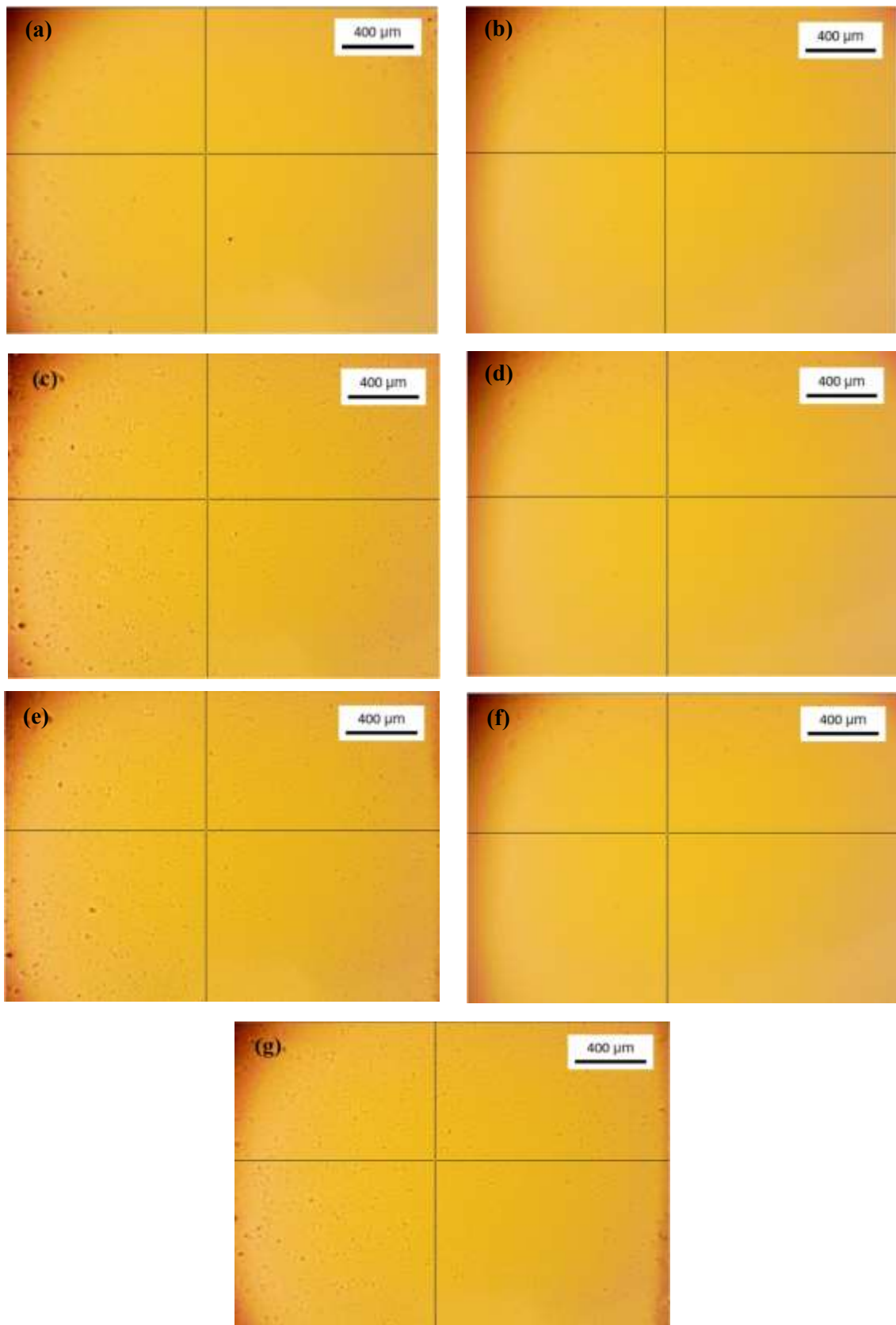


Figure 5.12 Optical microscope images of the control and w-binders for evaluation of dispersity in the unaged condition: (a) 40/60, (b) 450-6%, (c) 450-12%, (d) 500-6%, (e) 500-12%, (f) 550-6%, (g) 550-12%.

5.8 Summary

In this chapter, a comprehensive laboratory study has been performed to characterize and compare the rheological, mechanical, chemical, and ageing properties of a 40/60 asphalt binder modified at 6 and 12 wt% with HDPE pyrolysis waxes, produced using different process parameters (450, 500 and 550 °C). The following findings have been obtained:

1. The HDPE pyrolysis wax additives increase the penetration point and soften the asphalt binder, reducing the complex viscosity. These characteristics are more pronounced for the higher modification level (12 wt%) w-binders. They are also more pronounced for the 450-6% and 450-12% w-binders, due to the 450 °C wax being softer and less viscous as a result of its chemical composition. The addition of pyrolysis wax substantially reduces the overall fatigue crack length, rejuvenating and enhancing the crack resistance of the binders. The higher modification level binders and binders with softer wax additives (450 °C) reduces the final fatigue crack length the most, however, these have the largest negative impact on the rutting factor.
2. The 500 and 550 °C (harder, more viscous) waxes at the lower modification level (6wt%) were observed to have similar performance characteristics, improving fatigue resistance while affecting the rutting factor the least. This performance was attributed to the waxes chemical composition as a result of specific pyrolysis mechanisms, allowing for lower volatilization and the polymerization of unsaturated species to produce larger molecules during thermal ageing. There was a considerable amount of binder stiffening for the 450-6% and 450-12% w-binders, as a result of high volatile mass loss with ageing. Only the 40/60 binder and 550 °C wax w-binder (at both modification levels) had a mass loss under 1%. The 500-6% w-binder had a mass loss averaging 0.06 % over the standardised 1 % limit, with a mass loss variance below this.
3. All w-binders were observed to soften the base asphalt binder after RTFO+PAV ageing and reduced the sulfoxide ageing index. Due to the chemical structures of the waxes, they increase the amount of carbonyl

functional groups within the binder and thus the carbonyl ageing index. However, this is more of an issue within the higher modification w-binders. The lower-level modification binders (especially 550-6% w-binder) obtained similar C=O indices to that of the neat bitumen. Good dispersity of all pyrolysis waxes within the binder (high-speed shear mixed at 150 °C with a rotation speed of 500 rpm for 15 minutes) was observed with no obvious phase separation, both in the unaged and aged (RTFO+PAV) condition. Therefore, reducing this prominent technical limitation associated with plastic modified bitumen.

The findings of this experimental chapter may act as a baseline and be translated to other pyrolysis configurations for the processing of HDPE (and other plastics, as well as waste) with the knowledge that certain wax properties relate to specific bitumen additive performance characteristics. Furthermore, considering performance trade-offs between fatigue and rutting resistance as well as ageing resistance and stability, the 550-6% w-binder is the most suitable to be taken forward to further investigate its suitability in HMA asphalt formulation.

CHAPTER 6: Pyrolysis Wax Binder Additives from High-Density Polyethylene in Hot Mix and Reclaimed Asphalt Mixtures

6.1 Overview

This chapter details a laboratory performance investigation of HMA mixtures with the incorporation of high-density polyethylene (HDPE) wax that has been obtained via thermal pyrolysis and up to 20% RAP. It describes the third phase of this study, aiming to provide a baseline of understanding of the relationships between HDPE pyrolysis process parameters, the product wax characteristics and resultant plastic pyrolysis wax modified binder and mixture performance as well as that when RAP is used in the wax modified mixture. The pyrolysis HDPE wax contains lower molecular weight constituents than commercial wax additives, potentially allowing it to act as a temperature lowering additive for mixtures containing RAP, while acting as a rejuvenator for the aged RAP binder, due to its chemical composition. Furthermore, this baseline of understanding may then be applied for waxes from waste plastics, further increasing the amount of recyclable material within flexible pavements to approach a circular economy. Mixture resistances to the key modes of failure within HMA are investigated using standard procedures including mixtures' stiffness, fatigue, rutting, fracture, and moisture susceptibility.

6.2 Compatibility

The air voids of an asphalt mixture are an important parameter that will affect performance throughout its service life. A mixture should contain enough air voids to prevent bleeding in hot environments, yet have low enough air voids to not affect rutting resistance and prevent permeability of water and air [309, 310]. Mixture design and compaction factors that can affect the air voids within HMA have been observed to include: low filler and insufficient binder content in the mixture design, the compact effort and environment such as pressure, number of passes, temperature (including cessation temperature) presence of moisture [311-313].

The target air void content for the test mixtures within this study was 4%. This was not achieved for any of the mixtures produced using the selected compaction method, as can be seen in Figure 6.1. In this figure, the air void content for all 20 specimens (100 Φ x 40 mm and 150 Φ x 60 mm) from each mixture were rounded to the nearest integer so that the frequency could be calculated for each air void level within the range achieved (7-11%.) The roller compactor is set to compact to a preset specimen thickness and the mass of the material is proportioned accordingly, further studies are required to assess the reliability of this method. Higher air void content indicates a lower resistance to plastic flow and rutting. It is also a prominent observation within literature that permeability increases rapidly as the void content increases above 8% [314, 315].

The results obtained suggest that the addition of plastic wax within the asphalt binder of the PW mixture slightly improves workability, as shown by the lower air void mean in Table 6.1. Both test mixtures PW and RAP+PW have a significantly tighter range than the control mixture. The RAP+PW mixture containing plastic pyrolysis wax and RAP had the highest frequency of specimens with the lowest air void content (7%) within the range of air voids observed for the mixtures. This test mixture additionally had no specimens over 8% air voids, as well as the lowest mean and range. Generally, the addition of RAP has been seen to increase voids with its increasing content, however, the addition of reclaimed asphalt with rejuvenating agents and warm mix asphalt (WMA) additives such as polyethylene waxes have been seen to reduce the void content in comparison to control mixtures [198]. It is noted that the frequency of specimens above 8% air voids is slightly higher for the PW mixture than the Control mixture, suggesting the possibility of a greater susceptibility to air and moisture especially, which will be investigated further in *Section 6.6*.

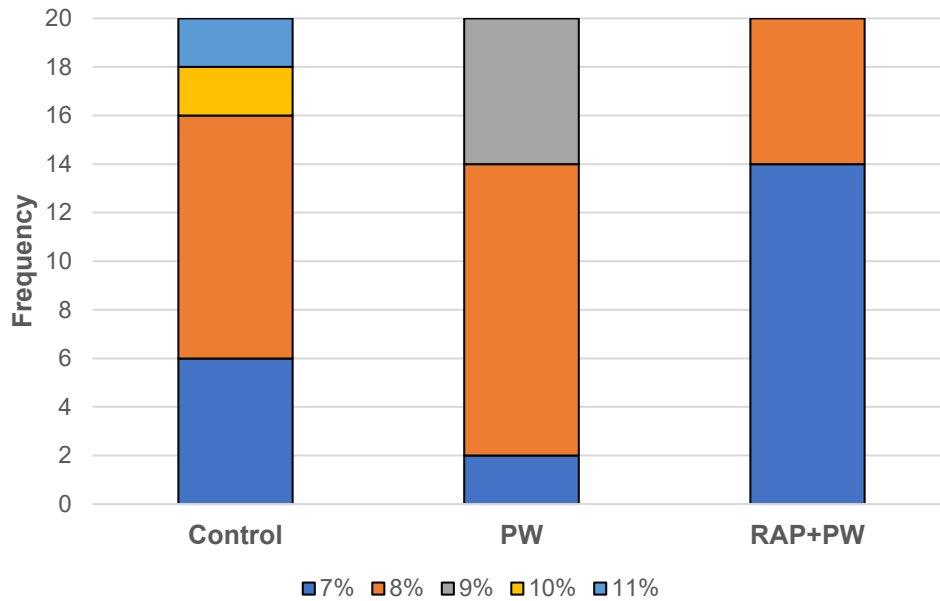


Figure 6.1 Frequency distribution of air void content of the control and test mixtures.

Table 6.1 Descriptive statistics for the air void content of the control and test mixtures.

Descriptive Statistics	Mixture		
	Control	PW	RAP+PW
Mean	8.24	8.13	7.24
Median	7.80	7.95	7.2
Range	4.1	1.9	1.8
Standard Deviation	1.14	0.55	0.47
Confidence Level (95%)	0.50	0.24	0.21

3.3 Indirect Tensile Stiffness Modulus Test (ITSM)

Figure 6.2 illustrates the master curve of the ITSM for the control and test mixtures. The reference temperature to shift the data points is 10 °C and based on the time-temperature superposition principle of viscoelastic material, low frequency refers to high temperature and vice versa. The ITSM is typically used to assess the deformation resistance of asphalt mixtures, such that a higher stiffness modulus value indicates that the ability of the mixture to spread the load is higher [316]. A lower stiffness modulus indicates a higher resistance to fatigue, while stiffer mixtures have greater resistance to permanent deformation [272, 317].

It can be seen that the stiffness modulus value for the PW mixture is decreased in comparison to the Control mixture. The incorporation of plastic pyrolysis wax, which has been observed to act as a softening and viscosity-reducing additive in the same way as WMA additives, reduces the stiffness modulus of the mixture over the whole temperature and frequency range. In the hot temperature/ low frequency region, ITSM: Control = RAP+PW > PW, whereas in the low temperature/ high frequency region, ITSM: Control > PW > RAP+PW. At 20 °C, the trend of the ITSM of the mixtures is RAP+PW > Control > PW. Studies have shown that the incorporation of RAP into HMA will make the mixture stiffer and more brittle due to the addition of aged binder [25]. A high stiffness will improve rutting resistance, yet negatively impact the fatigue performance of the mixture. However, the stiffness modulus of the RAP+PW mixture was similar to that of the Control mixture in the high temperature/ low frequency region, suggesting similar rutting performance. Additionally, the RAP+PW mixture had the lowest stiffness modulus in the low temperature/ high frequency region, demonstrating that the pyrolysis plastic wax may act as a sufficient softening and rejuvenating agent to mitigate the adverse effects to fatigue resistance of high RAP content in HMA mixtures.

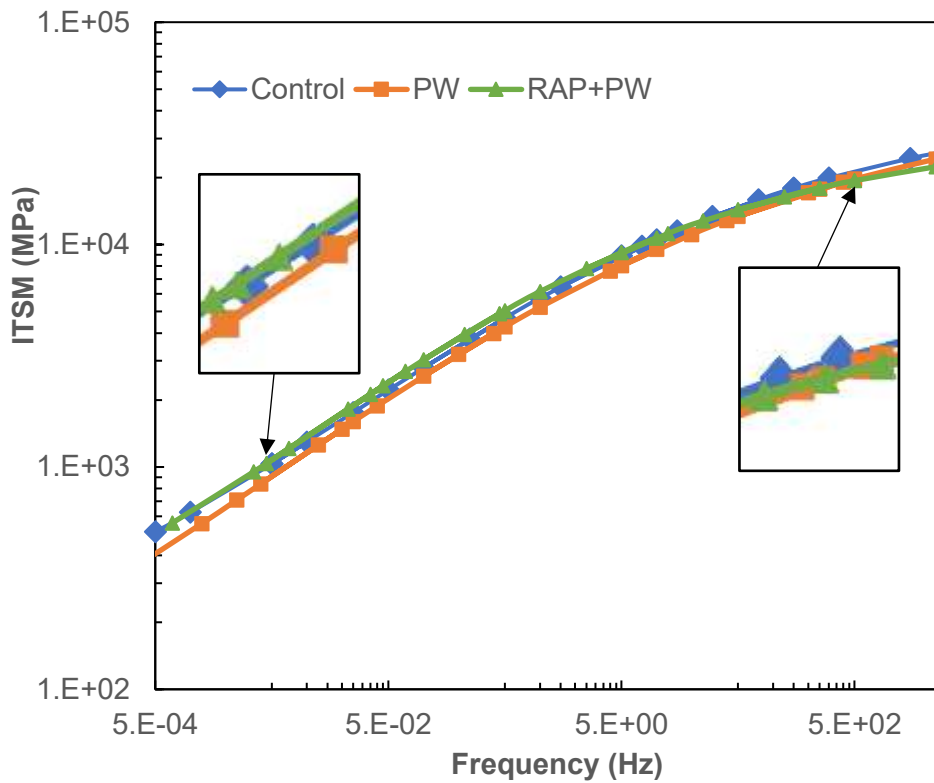


Figure 6.2 ITSM master curves for the stiffness modulus of the control and test mixtures.

3.4 Indirect Tensile Fatigue Test (ITFT)

As can be seen in Appendix P, the resilient strain amplitude (ϵ_{res}) and energy ratio (E_{ratio}) were plotted as a function of the number of cycles (N). The E_{ratio} plot was utilised to calculate the number of cycles to failure, N_f , which is the peak of the resultant E_{ratio} vs. N curve. The average N_f calculated for each mixture is presented in Figure 6.3, in which it can be inferred that the addition of the plastic pyrolysis wax binder additive enhances the tensile resistance of a HMA mixture. The additive led to a x 1.3 higher fatigue fracture resistance, with a higher strain at failure to the Control mixture. Furthermore, in comparison to the Control mixture, the RAP+PW mixture had a x 2.5 higher fatigue fracture resistance and a significantly higher strain at failure in comparison to the other mixtures. This supports that the pyrolysis plastic wax acts as an efficient rejuvenating agent for

the old RAP binder, allowing for superior fatigue performance despite the high content of RAP used within this HMA mixture.

Additionally, the damage density (ξ) and predicted evolution of crack growth (c) of the mixtures when subjected to an indirect tensile fatigue load are plotted in Figure 6.4. As $c = \xi \times D$ and the diameter of all mixture specimens are similar values, the shape of the crack length curve is analogous to that of the damage density curve. The number of cycles does not begin at zero as it took a different number of cycles for the target maximum stress to be achieved for each mixture. In the crack initiation phase ($N < 1,000$), it can be seen that the curves for the PW and RAP+PW mixtures have significant overlapping, while the curves for the Control mixture also overlap, yet they have a slightly higher damage density and crack growth as a result of its higher stiffness. Both curves for all of the mixtures are dominated by a plateau phase, in which the growth of accumulated damage density and crack growth is slow with loading cycles. Within both plots, the trend within this propagation phase is $\text{RAP+PW} > \text{PW} > \text{Control}$, for both damage density and crack evolution.

In the damage mechanics crack growth model for waste-derived asphalt binders proposed by Li et al., it is stated that a plateau phase is due to the restructuring of the microstructure via the rearrangement of light components, following crack initiation [264]. It is evidenced in the ITSM results (*Section 6.3*) observed in Chapter 5 (*Sections 5.3, 5.6*), that despite long-term ageing, the mixtures containing binders modified with the pyrolysis plastic wax have a lower stiffness and extended fatigue life. This can be attributed to the waxes containing a high amount of lower molecular weight saturated and unsaturated components that are available for rearrangement after crack initiation. Therefore, the higher amount of lighter components within the PW and RAP+PW prolong the propagation and increase in accumulated damage density with cycles. The PW and RAP+PW mixtures can also have a higher final damage density and predicted crack length prior to the total failure of the specimen. Overall, the results indicate the extension of fatigue life when pyrolysis wax is used within HMA and especially as a rejuvenating agent for RAP.

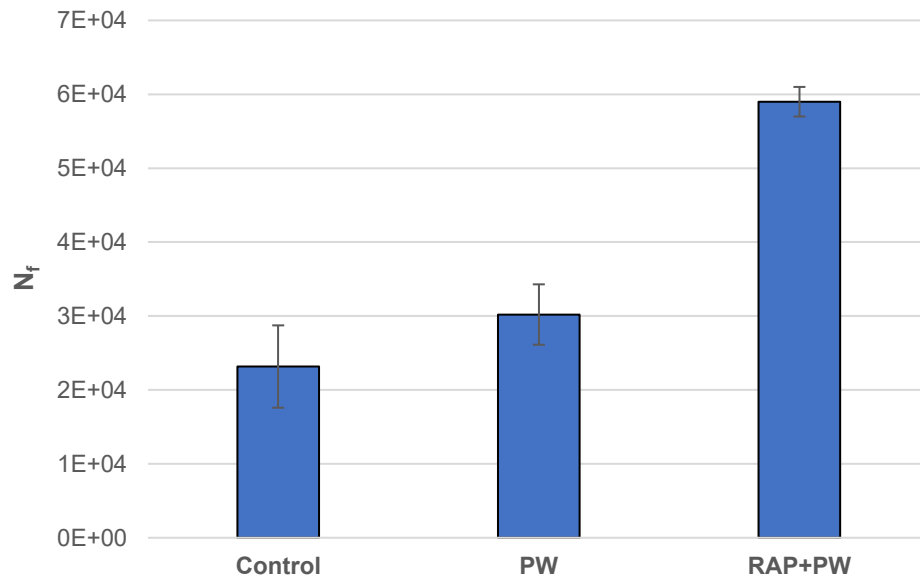


Figure 6.3 The average number of cycles to failure (N_f) for each mixture, determined by the peak of the E_{ratio} vs. N curve.

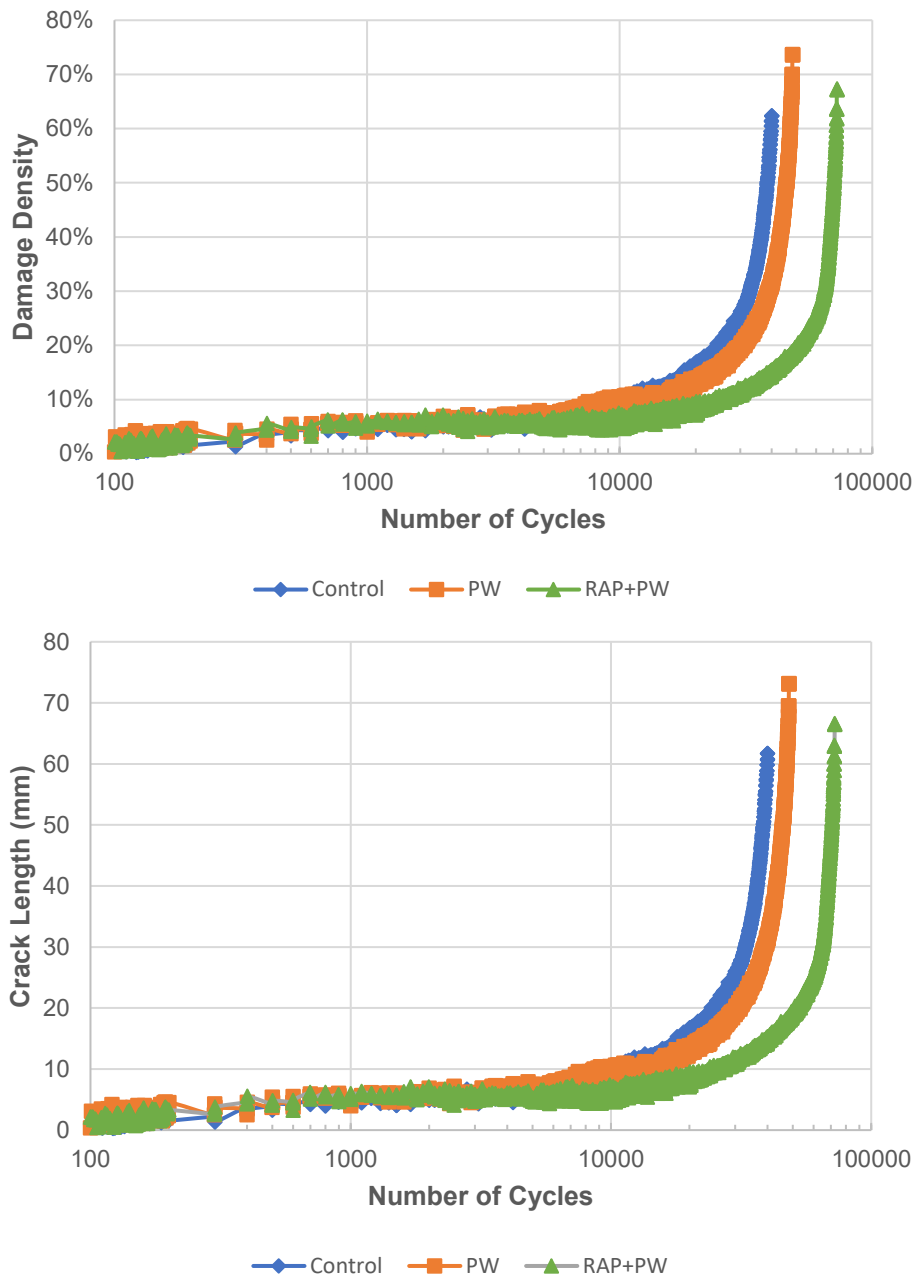


Figure 6.4 (Top) The damage density (ξ); (Bottom) The predicted evolution of crack growth (c) of the mixtures when subjected to an indirect tensile fatigue load.

3.5 Repeated Load Axial Tests (RLAT)

A key parameter obtained from the RLAT test is the cumulative axial strain (%), which can be plotted as a function of the number of load cycles to produce a

creep curve, as seen in Figure 6.5. A higher accumulated axial strain for a mixture typically indicates a lower resistance to rutting [318]. Previously, authors have stated that if the axial strain of a mixture exceeds 2%, it is considered to have poor resistance to rutting [270]. According to Figure 6.5, only the RAP+PW mixture was below this threshold, having superior rutting resistance to the Control and PW mixtures. These two mixtures have a poorer rutting resistance, with a 3.21 and 3.23 % axial strain at cycle 5000, respectively.

It is noted that the mixture design (Appendix A) for the Control and PW mixtures contain a higher proportion of virgin binder (+ wax additive). Previous studies in literature have shown that mixtures with a higher binder content generally have a higher susceptibility to rutting [319, 320]. This is due to the reduction in friction between the aggregate particles due to thicker binder film coating them, therefore, the binder will be carrying loads more than the aggregate structures [319]. Even so, as seen in Chapter 5 (*Section 5.4*), the softness of the control and pyrolysis wax modified binders made them unsuitable to have their rutting behaviour characterised by the multiple stress creep recovery (MSCR) test. Despite this, it can be seen that all mixtures do not reach the tertiary stage of a typical creep curve, in which strain accumulates rapidly, increasing the deformation rate and indicating sample failure. Therefore, the Control and PW mixtures do have an axial strain above the 2% threshold, most likely due to their lower stiffness modulus in comparison to the RAP+PW mixture. Yet it would require more loading pulses for all mixtures to enter the tertiary zone of the creep curve and exhibit permanent deformation damage.

The trend of the creep rate (f_c) that incorporates the minimum strain rate of the mixtures are presented in Figure 6.6 and observed to be Control > PW > RAP+PW. The strain rate vs. number of load cycles is also depicted in Appendix Q, demonstrating the same trend. This parameter indicates the rate of change in the rutting performance of the mixtures [32]. The RAP+PW mixture has the lowest strain rate, supporting its superior rutting resistance. The Control mixture does have the largest strain rate, yet the highest variance of the PW mixture is a similar value to the average of the Control mixture. The findings indicate that the plastic

pyrolysis wax binder additive does offer valued benefits to fatigue performance, while not significantly or adversely affecting the rutting performance. Additionally, incorporating pyrolysis plastic wax and RAP into HMA produces a superior mixture in terms of both fatigue and rutting performance, while increasing the proportion of recycled materials within the mixture.

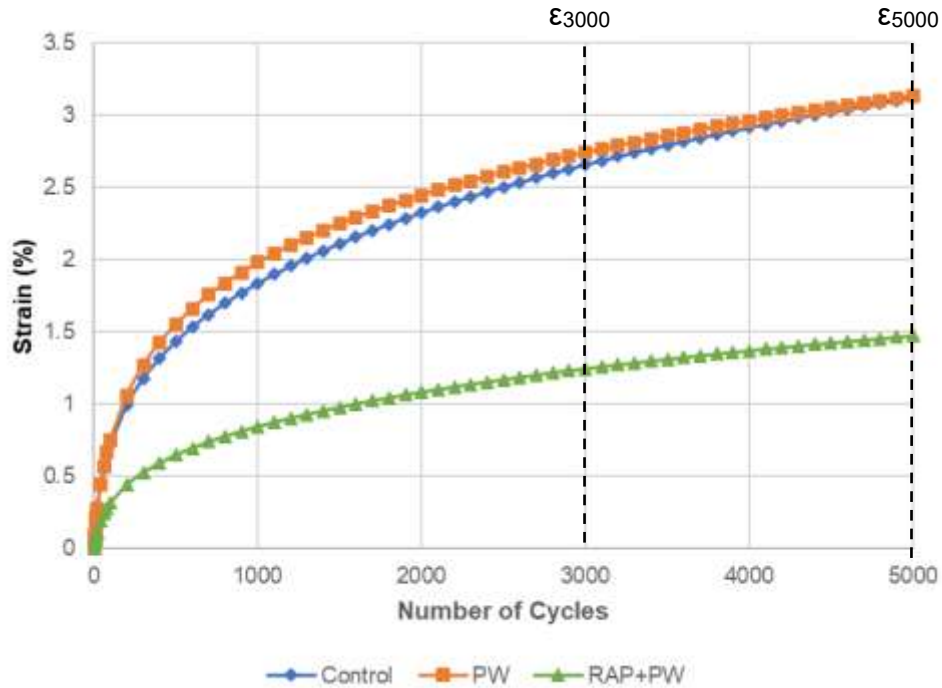


Figure 6.5 Averaged RLAT results of the control and test mixtures at test temperature 40 °C.

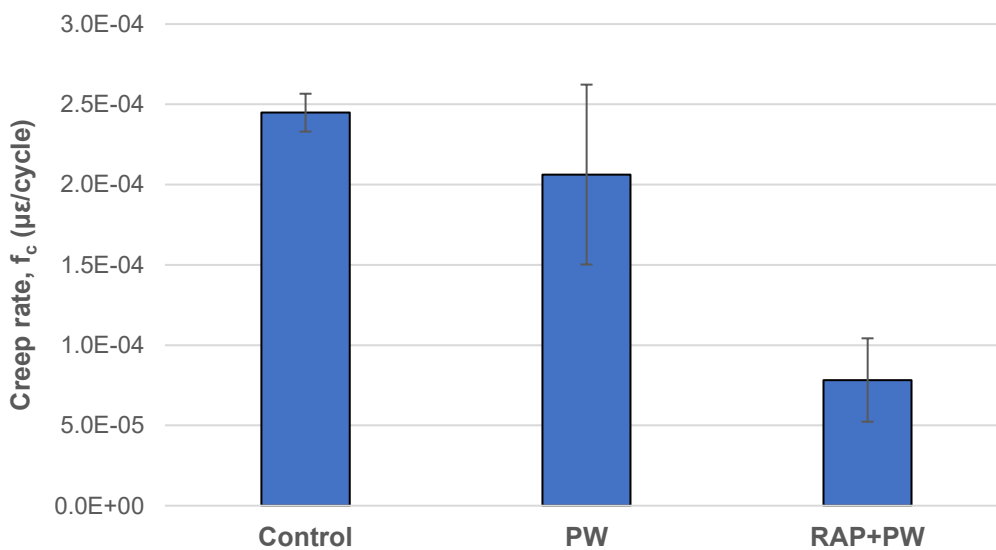


Figure 6.6 Calculated creep rate, f_c of the control and test mixtures.

3.6 Indirect Tensile Fatigue (ITS) Test & Moisture Resistance

Figure 6.7 shows the ITS of the dry and wet condition as well as the TSR values for each mixture. The observed trend in ITS in both conditions is mixture $RAP+PW > Control > PW$. The ITS of the Control and PW mixtures can be seen to have a small decrease in the wet condition, while statistically, there is no difference in the ITS value of the RAP+PW mixture after wet conditioning.

Comparing the Control and PW mixtures, the ITS and TSR is decreased for the PW mixture containing the plastic pyrolysis wax binder additive. Authors in literature have observed an increased TSR value with increasing commercial wax addition and have attributed this increase in moisture resistance to the hydrophobic characteristics of organic waxes. However, the waxes ability to decrease the adhesion between the binder and aggregated can negate this [321, 322]. In this case, there is at 1.64% drop in the TSR value of the PW mixture in comparison to the Control mixture. The drop is very small and could be attributed to the increased diffusion of moisture as a result of the higher frequency of specimens with an air void content of 8%, as discussed in *Section 6.2*, which could be attributed to factors such as mixture design and compaction method. Despite this, overlapping in the ITS lower variance of the Control mixture and upper variance of the PW mixture as well as the very small drop (<2%) in TSR value would suggest that the effect of the wax modifier binder additive has very little impact on fracture resistance and moisture susceptibility.

The RAP+PW mixture had the highest fracture and moisture resistance, indicated by the highest average ITS values in both conditions and highest TSR value of 101.00%. Adding the RAP positively influenced the moisture resistance of the HMA, which is indicated by the slightly increased ITS in the wet condition. Explanations for this in literature include the increase in asphalt-coated aggregates, which are insensitive to the effect of water due to the existing bituminous film, as well as the percentage of aged binder increases the strength of the mixture [323, 324].

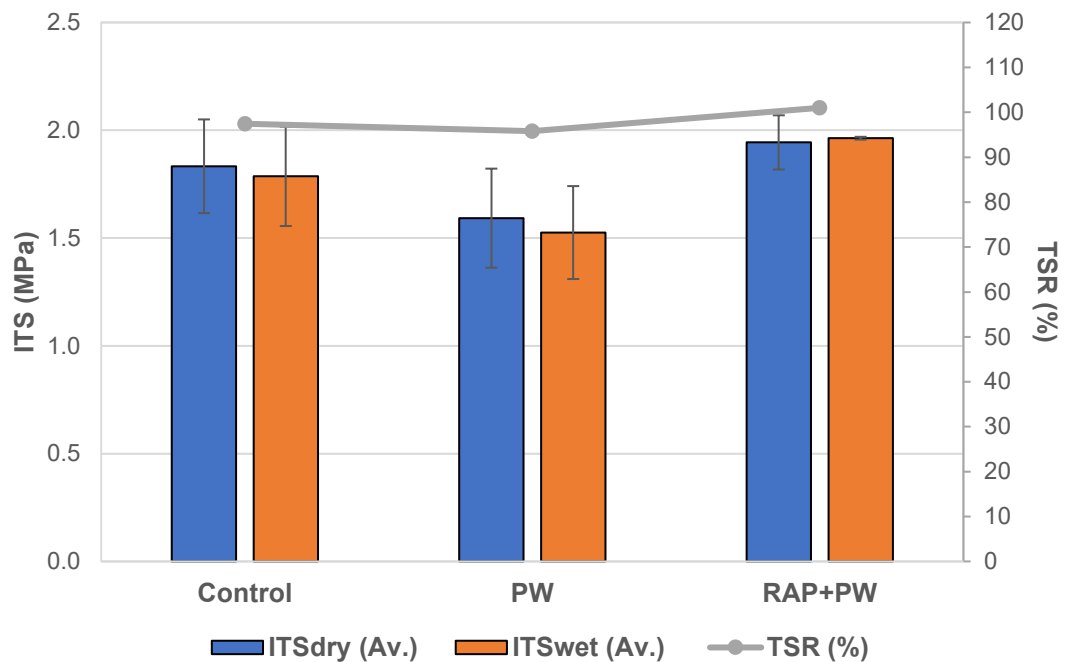


Figure 6.7 Average ITS values of unconditioned (dry) and conditioned (wet) specimens from each mixture and TSR values.

6.7 Summary

This chapter investigates the use of HDPE pyrolysis wax modified binders in a HMA mixture and a mixture additionally containing 20% reclaimed asphalt. As part of achieving circular economy goals within sustainable infrastructure, this was to greatly increase the total amount of recyclables used within asphalt flexible pavements, while improving vital failure resistances. The main findings were:

1. The compatibility results suggest that the addition of plastic pyrolysis wax within the asphalt binder slightly improves mixture workability, as shown by the lower air void mean achieved. Both mixtures containing plastic wax and RAP + plastic wax had a significantly tighter air void range than the control mixture. The stiffness of the mixture containing RAP + plastic wax had the lowest stiffness modulus in the low temperature/ high frequency region of the ITSM master curve, demonstrating that the pyrolysis plastic wax may function as a sufficient softening and rejuvenating agent to mitigate the adverse effects to fatigue resistance of high RAP content in HMA mixtures. This was further

supported by the ITFT test, in which the N_f and ϵ_{res} at failure were superior for the mixtures containing plastic pyrolysis wax and RAP plus the wax additive. The plastic wax additive improved the fatigue resistance by x 1.3, while the RAP + plastic wax improved the fatigue resistance by x 2.5, in comparison to the control mixture.

2. A novel mechanistic model for the prediction of cracking damage was further employed to present the evolution of the cracking performance within each mixture. The plastic wax and RAP + plastic wax mixtures demonstrated a lower initial damage density and crack growth initiation, followed by prolonged accumulated damage and crack propagation phases before specimen failure, in comparison to the control mixture.
3. The control mixture and pyrolysis plastic wax mixtures had a poorer rutting resistance than the mixture containing RAP + plastic wax, yet it was determined that the pyrolysis plastic wax binder additive did not adversely affect the rutting performance of the mixture, when compared to the control mixture. Both mixtures containing the plastic wax additive and RAP + plastic wax had lower creep rates than the control mixture. The effect of the plastic wax binder additive had very little impact on fracture resistance and moisture susceptibility. The RAP + plastic wax mixture had the highest fracture and moisture resistance.

CHAPTER 7: Conclusions and Recommendations

7.1 Conclusions

In this research study, the effect of waxes generated from the thermal pyrolysis of HDPE were investigated in terms of the rheological, mechanical, chemical, and thermal performance characteristics of modified binders and asphalt mixtures. The key conclusions produced from this work are as follows:

1. Six types of pyrolysis wax were produced from the thermal pyrolysis of HDPE in a fixed bed reactor, using temperatures and carrier gas flowrates of 450-550 °C and 2 and 4 L min⁻¹, respectively. The melting point ranges of the pyrolysis waxes were compared to commercial paraffin and microcrystalline waxes typically used in WMA technologies. Chemical characterisation of the waxes showed that, in comparison to commercial waxes studies in literature, the waxes in this study were more olefinic in nature. This is through the promotion of certain degradation mechanisms such as β -scission, as a result of the pyrolysis system and parameters applied.
2. The more olefinic waxes, which were produced at higher temperatures and carrier gas flowrates (lowest vapour residence times,) saw the lowest volatile mass loss during the wax ageing experiments. They were observed to be prone to oxidation and polymerization reactions, similar to those observed for the thermal and oxidative ageing of bitumen components.
3. For HMA modification purposes, blending at temperatures lower than 170 °C should be considered to lessen the volatile loss with initial blending and storage of the wax modified binders.
4. Three waxes produced at 450, 500 and 550 °C and a set carrier gas flowrate (2 L min⁻¹) were taken forward for w-binder production, blending at 500 rpm and 150 °C for 15 minutes using a high shear mixer. Two wax modification levels: lower (6 wt%) and higher (12 wt%), were utilised to determine optimum dosage. HDPE pyrolysis wax additives increase the penetration point and soften the asphalt binder, reducing the complex viscosity. These characteristics are more pronounced for the higher modification level (12 wt%) w-binders.

5. The addition of HDPE pyrolysis wax substantially reduces the overall fatigue crack length, rejuvenating and enhancing the crack resistance of the binders. The higher modification level binders and binders with softer wax additives (450 °C) reduces the final fatigue crack length the most, however, these have the largest negative impact on the rutting factor.
6. The harder, more viscous waxes produced at higher process temperatures (500 and 550 °C) provided enhanced cracking resistance while affecting the rutting factor the least. This was attributed to the chemical composition of these waxes as a result of specific pyrolysis mechanisms, allowing for lower volatilization and the polymerization of unsaturated species to produce larger molecules during thermal ageing.
7. The thermal and oxidative stability of the higher modification w-binders were unstable and other stabilizing additives may be considered. The lower dose (6 wt%) of pyrolysis waxes produced at higher process temperatures demonstrated the most stable thermal behaviour with promising results. Even so, the use of additional phenolic additives that neutralize oxygen free radicals to lower the formation of carbonyl compounds could be considered.
8. The use of plastic-derived products such as this for bitumen modification negates prominent technical limitations associated with polymer-modified bitumen, such as poor workability and modifier dispersion.
9. An optimum wax and dose (HDPE pyrolysis wax produced at 550 °C, 6 wt% dose) was taken forward for w-asphalt modification. It was additionally used in conjunction with 20% RAP, to evaluate its capacity as a rejuvenating agent. The compatibility results suggest that the addition of pyrolysis wax within the asphalt binder slightly improves mixture workability.
10. The stiffness modulus of the RAP mixture with pyrolysis wax demonstrated that the pyrolysis wax may act as a sufficient softening and rejuvenating agent to mitigate the adverse effects to fatigue resistance of high RAP content in HMA mixtures.
11. The pyrolysis wax additive improved the fatigue resistance by x 1.3, while the RAP + pyrolysis wax improved the fatigue resistance by x 2.5, in comparison to the control mixture. The mechanics model for the prediction of cracking damage demonstrated a lower initial damage density and crack growth

initiation, followed by prolonged accumulated damage and crack propagation phases before specimen failure for the mixtures containing pyrolysis wax and RAP.

12. The w-asphalt mixture containing pyrolysis wax and 20% RAP demonstrated the highest rutting resistance. As opposed to the w-binder high temperature performance results, it was determined that the HDPE pyrolysis wax additive did not adversely affect the rutting performance of the w-asphalt mixtures, when compared to the control mixture.
13. The HDPE pyrolysis wax + 20% RAP mixture had the highest fracture and moisture resistance. The effect of the HDPE pyrolysis wax additive had very little impact on fracture resistance and moisture susceptibility of the w-asphalt mixtures.
14. Modified HMA mixtures with enhanced or unaffected resistance to the key failure modes studied were achieved using HDPE pyrolysis wax solely and in conjunction with reclaimed asphalt. This application of plastic pyrolysis waxes could help to reduce the amount of virgin and non-renewable materials used for HMA production, while increasing the amount of recyclable material. It may lead to potential cost, emission and energy saving for the industry, with respect to the use of secondary materials. Also the lower temperature and faster blending times, in comparison to polymer-modified bitumen especially. These findings may be applied for waxes from waste plastics, further increasing the amount of recyclable material within flexible pavements to approach a circular economy.

7.2 Recommendations

This study provides a novel contribution to outlining the full potential of thermal pyrolysis products from polyolefin plastics, such as HDPE, in the modification of bitumen and subsequent HMA (+RAP) mixtures. In the interest of product and process optimisation, it establishes key relationships between the pyrolysis process parameters, the chemical and thermal properties/mechanisms of the wax modifiers and the rheological and mechanical performance of the modified binders/mixtures. Additionally, the research aims of producing modified HMA

mixtures with enhanced or unaffected resistance to the key failure modes studied were achieved using HDPE pyrolysis wax solely and in conjunction with reclaimed asphalt. However, there are some areas that merit further investigation to continue the production of effective research. Recommendations for future studies are suggested as follows:

1. Perform further high temperature performance tests on the control and w-binders using a revised MSCR test to obtain creep compliance values. This would provide more appropriate analysis for modified binders as opposed to the rutting factor.
2. Study the low temperature thermal cracking performance of the w-binders via bending beam rheometer as well as apply further conventional tests such as softening point to achieve further understanding of the temperature susceptibility.
3. Further investigation into the storage stability of the w-binders, perhaps using the cigar tube separation/toothpaste test.
4. A study into the effect of ultraviolet exposure on the physiochemical properties of the w-binders.
5. Evaluate the method of laboratory roller compaction to assess its reliability to achieve target specimen dimensions and air voids, as opposed to gyratory compaction.
6. Perform the ITFT in strain-controlled mode, as the initiation and propagation of fatigue cracking is more stable and better replicated to provide an even more reliable cracking damage prediction results. Repeating this test and cracking damage analysis at different stresses/strains, temperatures, and frequencies to provide further model verification for viscoelastic materials.
7. Expand the study findings to other polyolefin plastics and waste plastics to study the effects of co-pyrolysis, as well as contaminants and colourants on the product wax.
8. A study on the Life Cycle Cost Analysis (LCCA) of pyrolysis wax (+RAP) modified bitumen/asphalt is recommended to evaluate its effectiveness based on cost and life cycle. Further study should investigate the Life Cycle Assessment (LCA) analysis for measuring the cost and environmental impact.

9. Investigation into the role of lower molecular weight waxes or distilled oils from HDPE pyrolysis as fluxing agents.
10. Further exploration into RAP + plastic pyrolysis waxes modified asphalt, testing different percentages of RAP. Additionally, a study on the rejuvenating effects and interactions between the pyrolysis waxes and aged RAP binder/aggregates.

References

- [1] S. Dharmaraj *et al.*, "Pyrolysis: An effective technique for degradation of COVID-19 medical wastes," *Chemosphere*, vol. 275, pp. 130092-130092, 2021, doi: 10.1016/J.CHEMOSPHERE.2021.130092.
- [2] C. Abdy, Y. Zhang, J. Wang, Y. Yang, I. Artamendi, and B. Allen, "Pyrolysis of polyolefin plastic waste and potential applications in asphalt road construction: A technical review," *Resources, Conservation and Recycling*, vol. 180, p. 106213, 2022, doi: <https://doi.org/10.1016/j.resconrec.2022.106213>.
- [3] C. J. Tsai, M. L. Chen, K. F. Chang, F. K. Chang, and I. F. Mao, "The pollution characteristics of odor, volatile organochlorinated compounds and polycyclic aromatic hydrocarbons emitted from plastic waste recycling plants," *Chemosphere*, vol. 74, no. 8, pp. 1104-1110, 2009, doi: <https://doi.org/10.1016/j.chemosphere.2008.10.041>.
- [4] J. R. Jambeck *et al.*, "Plastic waste inputs from land into the ocean," *Science*, vol. 347, no. 6223, pp. 768-771, 2015, doi: 10.1126/science.1260352.
- [5] R. Verma, K. S. Vinoda, M. Papireddy, and A. N. S. Gowda, "Toxic Pollutants from Plastic Waste- A Review," *Procedia Environmental Sciences*, vol. 35, pp. 701-708, 2016, doi: <https://doi.org/10.1016/j.proenv.2016.07.069>.
- [6] J. A. Onwudili, N. Insura, and P. T. Williams, "Composition of products from the pyrolysis of polyethylene and polystyrene in a closed batch reactor: Effects of temperature and residence time," *Journal of Analytical and Applied Pyrolysis*, vol. 86, no. 2, pp. 293-303, 2009, doi: 10.1016/j.jaap.2009.07.008.
- [7] E. Gaudenzi, F. Canestrari, and X. Lu, "Performance Assessment of Asphalt Mixture Produced with a Bio-Based Binder," *Materials*, vol. 14, no. 4, p. 918, 2021, doi: <https://doi.org/10.3390/ma14040918>.
- [8] N. Su, F. Xiao, J. Wang, L. Cong, and S. Amirkhanian, "Productions and applications of bio-asphalts – A review," *Construction and Building Materials*, vol. 183, pp. 578-591, 2018, doi: <https://doi.org/10.1016/j.conbuildmat.2018.06.118>.
- [9] M. A. Raouf and R. C. Williams, "Temperature and shear susceptibility of a nonpetroleum binder as a pavement material," *Transportation Research Record*, 2010, doi: 10.3141/2180-02.

- [10] L. Brasileiro, F. Moreno-Navarro, R. Tauste-Martínez, J. Matos, and M. Rubio-Gámez, "Reclaimed Polymers as Asphalt Binder Modifiers for More Sustainable Roads: A Review," *Sustainability*, vol. 11, no. 3, pp. 646-646, 2019, doi: 10.3390/su11030646.
- [11] B. P. Grady, "Waste plastics in asphalt concrete: A review," *SPE Polymers*, vol. 2, no. 1, pp. 4-18, 2021, doi: 10.1002/PLS2.10034.
- [12] P. Ahmedzade, A. Fainleib, T. Günay, and O. Grygoryeva, "Modification of bitumen by electron beam irradiated recycled low density polyethylene," *Construction and Building Materials*, vol. 69, pp. 1-9, 2014, doi: 10.1016/j.conbuildmat.2014.07.027.
- [13] A.I. Al-Hadidy and Y. Q. Tan, "Effect of polyethylene on life of flexible pavements," *Construction and Building Materials*, vol. 23, no. 3, pp. 1456-1464, 2009, doi: 10.1016/J.CONBUILDMAT.2008.07.004.
- [14] Y. Becker, M. P. Méndez, and Y. Rodríguez, "Polymer Modified Asphalt," *Vision Technologica*, vol. 9, no. 1, pp. 39-50, 2001.
- [15] M. Zaumanis and V. Haritonovs, "Research on properties of warm mix asphalt," *Sci J Riga Tech Univ Constr Sci*, vol. 11, pp. 77-84, 2010.
- [16] M. Sukhija and N. Saboo, "A comprehensive review of warm mix asphalt mixtures-laboratory to field," *Construction and Building Materials*, vol. 274, pp. 121781-121781, 2021, doi: 10.1016/J.CONBUILDMAT.2020.121781.
- [17] T. Ling, Y. Lu, Z. Zhang, C. Li, and M. Oeser, "Value-added application of waste rubber and waste plastic in asphalt binder as a multifunctional additive," *Materials*, vol. 12, no. 8, pp. 16-19, 2019, doi: 10.3390/ma12081280.
- [18] H. Fazaeli, H. Behbahani, A.A. Amini, J. Rahmani, and G. Yadollahi, "High and Low Temperature Properties of FT-Paraffin-Modified Bitumen," *Advances in Materials Science and Engineering*, vol. 2012, p. 406791, 2012, doi: 10.1155/2012/406791.
- [19] SASOL. "Sasobit REDUX Product information." Sasol Performance Chemicals.
https://www.sasobit.com/files/downloads/PDF_070722/0433SAS-Sasobit_Redux-BR_en_LR_1 (accessed 31/05/21.)
- [20] H. Yu, Z. Leng, and Z. Gao, "Thermal analysis on the component interaction of asphalt binders modified with crumb rubber and warm mix additives," *Construction and Building Materials*, vol. 125, pp. 168-174, 2016, doi: 10.1016/J.CONBUILDMAT.2016.08.032.
- [21] M. Nakhaei, A.D. Darbandi Olia, A. Akbari Nasrekani, and P. Asadi, "Rutting and moisture resistance evaluation of polyethylene wax-modified asphalt mixtures," *Petroleum Science and Technology*, vol. 34, no. 17-18, pp. 1568-1573, 2016, doi: 10.1080/10916466.2016.1212209.
- [22] Y. Edwards, "Influence of waxes on polymer modified mastic asphalt performance," in *"4th Eurasphalt and Eurobitumen Congress"*, Copenhagen, Denmark, 2008: European Asphalt Pavement Association (EAPA), p. 6.
- [23] Y. Kim, J. Lim, M. Lee, S. Kwon, S. Hwang, and L. Wei, "Comprehensive Evaluation of Polymer-Modified SMA Mixture Produced with New Polyethylene Wax-Based WMA Additive with Adhesion Promoter," in *"Transportation Research Board 92nd Annual Meeting"*, Washington DC, United States, 2013, p. 8.

- [24] W. Wang, J. Chen, Y. Sun, B. Xu, J. Li, and J. Liu, "Laboratory performance analysis of high percentage artificial RAP binder with WMA additives," *Construction and Building Materials*, vol. 147, pp. 58-65, 2017/08/30/ 2017, doi: <https://doi.org/10.1016/j.conbuildmat.2017.04.142>.
- [25] C. Zhang, Q. Ren, Z. Qian, and X. Wang, "Evaluating the Effects of High RAP Content and Rejuvenating Agents on Fatigue Performance of Fine Aggregate Matrix through DMA Flexural Bending Test," (in eng), *Materials (Basel)*, vol. 12, no. 9, May 9 2019, doi: 10.3390/ma12091508.
- [26] A. Copeland, "Reclaimed Asphalt Pavement in Asphalt Mixtures: State of the Practice," 2011, FHWA-HRT-11-021: Turner-Fairbank Highway Research Center: McLean, VA, USA, pp. 1-5.
- [27] W. Mogawer, "Development of Balanced & Eco-Friendly Thin Lift Asphalt Mixtures Incorporating Sustainable Materials," in *International Pavement Preservation Conference*, University of Massachusetts Dartmouth, 2012.
- [28] N. Tran, A. Taylor, and R. Willis, "Effect of Rejuvenator on Performance Properties of HMA Mixtures with High RAP and RAS Contents," 2012.
- [29] M. Arabiourrutia, G. Elordi, G. Lopez, E. Borsella, J. Bilbao, and M. Olazar, "Characterization of the waxes obtained by the pyrolysis of polyolefin plastics in a conical spouted bed reactor," *Journal of Analytical and Applied Pyrolysis*, vol. 94, pp. 230-237, 2012, doi: 10.1016/j.jaap.2011.12.012.
- [30] L. Quesada, M. C. d. Hoces, M. A. Martín-Lara, G. Luzón, and G. Blázquez, "Performance of Different Catalysts for the In Situ Cracking of the Oil-Waxes Obtained by the Pyrolysis of Polyethylene Film Waste," *Sustainability*, vol. 12, no. 13, pp. 1-15, 2020.
- [31] N. A. Abdul Raman, M. R. Hainin, N. Abdul Hassan, and F. N. Ani, "A Review on the Application of Bio-oil as an Additive for Asphalt," *Journal Teknologi*, vol. 72, no. 5, 2015, doi: 10.11113/jt.v72.3948.
- [32] N. M. Zakaria, "Characterisation of bitumen and asphalt mixture with recycled waste plastic (RWP) modified binder," *Thesis*, pp. 1-341, 2020.
- [33] C. Abdy, Y. Zhang, J. Wang, Y. Cheng, I. Artamendi, and B. Allen, "Investigation of high-density polyethylene pyrolyzed wax for asphalt binder modification: Mechanism, thermal properties, and ageing performance," *Journal of Cleaner Production*, vol. 405, p. 136960, 2023, doi: <https://doi.org/10.1016/j.jclepro.2023.136960>.
- [34] European Commission, "New Circular Economy Strategy - Environment," ed, 2010.
- [35] European Commission, "Introducing the EU's green city tool – A treasure trove of sustainable urban planning tips," ed, 2019.
- [36] S.M. Al-Salem, Y. Yang, J. Wang, and G. A. Leeke, "Pyro-Oil and Wax Recovery from Reclaimed Plastic Waste in a Continuous Auger Pyrolysis Reactor," *Energies*, vol. 13, no. 8, pp. 2040-2040, 2020, doi: 10.3390/en13082040.
- [37] PlasticsEurope Deutschland, "Plastics - the Facts 2019," 2019. [Online]. Available: <https://www.plasticseurope.org/en/resources/market-data> (accessed 19/02/21.)
- [38] J. Hopewell, R. Dvorak, and E. Kosior, "Plastics recycling: Challenges and opportunities," in *Philosophical Transactions of the Royal Society B: Biological Sciences* vol. 364, ed: Royal Society, 2009, pp. 2115-2126.

- [39] S. Dharmaraj *et al.*, "Pyrolysis: An effective technique for degradation of COVID-19 medical wastes," *Chemosphere*, vol. 275, pp. 130092-130092, 2021, doi: 10.1016/J.CHEMOSPHERE.2021.130092.
- [40] S. D. Anuar Sharuddin, F. Abnisa, W. M. A. Wan Daud, and M. K. Aroua, "A review on pyrolysis of plastic wastes," in *Energy Conversion and Management* vol. 115, ed: Elsevier Ltd, 2016, pp. 308-326.
- [41] European Commission, "Plastic waste shipments: new EU rules on importing and exporting plastic waste," ed, 2020.
- [42] F. Simon, "Recyclers fret as EU plastic waste export ban comes into force," *EURACTIV*, 2021.
- [43] L. Delva, L. Cardon, and K. Ragaert, "Evaluation of post-consumer mixed polyolefines and their injection moulded blends with virgin polyethylene," *Environmental Engineering and Management Journal*, 2018, doi: 10.30638/eemj.2018.043.
- [44] V. Lore, E. Du Bois, H. Sara, V. K. Karen, and R. Kim, "*Design from recycling*," Alive. Active. Adaptive: International Conference on Experiential Knowledge and Emerging Materials, EKSIG 2017, 2017, pp. 129-143.
- [45] K. Ragaert, L. Delva, and K. Van Geem, "Mechanical and chemical recycling of solid plastic waste," *Waste Management*, vol. 69, pp. 24-58, 2017, doi: 10.1016/j.wasman.2017.07.044.
- [46] J. Santos, A. Pham, P. Stasinopoulos, and F. Giustozzi, "Recycling waste plastics in roads: A life-cycle assessment study using primary data," *Science of The Total Environment*, vol. 751, pp. 141842-141842, 2021, doi: 10.1016/J.SCITOTENV.2020.141842.
- [47] Z. N. Kalantar, M. R. Karim, and A. Mahrez, "A review of using waste and virgin polymer in pavement," *Construction and Building Materials*, vol. 33, pp. 55-62, 2012, doi: 10.1016/J.CONBUILDMAT.2012.01.009.
- [48] X. Yu, N. A. Burnham, and M. Tao, "Surface microstructure of bitumen characterized by atomic force microscopy," in *Advances in Colloid and Interface Science* vol. 218, ed: Elsevier B.V., 2015, pp. 17-33.
- [49] A. S. Bale, "Potential Reuse of Plastic Waste in Road Construction: A Review," *International Journal of Advances in Engineering & Technology (IJAET)*, vol. 2, pp. 233-236, 2011.
- [50] J. Simon, "A Zero Waste hierarchy for Europe," in "Zero Waste Europe," 2019. [Online]. Available: <https://zerowasteurope.eu/2019/05/press-release-a-zero-waste-hierarchy-for-europe/> (Accessed 21/06/2020.)
- [51] S. M. Al-Salem, P. Lettieri, and J. Baeyens, "Recycling and recovery routes of plastic solid waste (PSW): A review," *Waste Management*, vol. 29, no. 10, pp. 2625-2643, 2009, doi: 10.1016/j.wasman.2009.06.004.
- [52] A. Brems, R. Dewil, J. Baeyens, and R. Zhang, "Gasification of plastic waste as waste-to-energy or waste-to-syngas recovery route," *Natural Science*, 2013, doi: 10.4236/ns.2013.56086.
- [53] F. Vilaplana and S. Karlsson, "Quality concepts for the improved use of recycled polymeric materials: A review," in *Macromolecular Materials and Engineering*, ed, 2008.
- [54] S. M. Al-Salem, P. Lettieri, and J. Baeyens, "The valorization of plastic solid waste (PSW) by primary to quaternary routes: From re-use to energy and chemicals," in *Progress in Energy and Combustion Science* vol. 36, ed: Pergamon, 2010, pp. 103-129.

- [55] A. Antelava *et al.*, "Plastic Solid Waste (PSW) in the Context of Life Cycle Assessment (LCA) and Sustainable Management," *Environmental Management*, vol. 64, no. 2, pp. 230-244, 2019, doi: 10.1007/s00267-019-01178-3.
- [56] V. A. González-González, G. Neira-Velázquez, and J. L. Angulo-Sánchez, "Polypropylene chain scissions and molecular weight changes in multiple extrusion," *Polymer Degradation and Stability*, 1998, doi: 10.1016/S0141-3910(96)00233-9.
- [57] S. M. Al-Salem, A. Antelava, A. Constantinou, G. Manos, and A. Dutta, "A review on thermal and catalytic pyrolysis of plastic solid waste (PSW)," *Journal of Environmental Management*, vol. 197, pp. 177-198, 2017, doi: 10.1016/j.jenvman.2017.03.084.
- [58] E. A. Williams and P. T. Williams, "Analysis of products derived from the fast pyrolysis of plastic waste," *Journal of Analytical and Applied Pyrolysis*, vol. 40-41, pp. 347-363, 1997, doi: 10.1016/S0165-2370(97)00048-X.
- [59] N. Patni, P. Shah, S. Agarwal, and P. Singhal, "Alternate Strategies for Conversion of Waste Plastic to Fuels," *ISRN Renewable Energy*, vol. 2013, 2013, doi: 10.1155/2013/902053.
- [60] S. L. Wong, N. Ngadi, T. A. T. Abdullah, and I. M. Inuwa, "Current state and future prospects of plastic waste as source of fuel: A review," in *Renewable and Sustainable Energy Reviews* vol. 50, ed: Elsevier Ltd, 2015, pp. 1167-1180.
- [61] B. Kunwar, H. N. Cheng, S. R. Chandrashekar, and B. K. Sharma, "Plastics to fuel: a review," *Renewable and Sustainable Energy Reviews*, vol. 54, pp. 421-428, 2016, doi: 10.1016/j.rser.2015.10.015.
- [62] R. Khatun, H. Xiang, Y. Yang, J. Wang, and G. Yildiz, "Bibliometric analysis of research trends on the thermochemical conversion of plastics during 1990–2020," *Journal of Cleaner Production*, vol. 317, pp. 128373-128373, 2021, doi: 10.1016/J.JCLEPRO.2021.128373.
- [63] P. J. Donaj, W. Kaminsky, F. Buzeto, and W. Yang, "Pyrolysis of polyolefins for increasing the yield of monomers' recovery," *Waste Management*, vol. 32, no. 5, pp. 840-846, 2012, doi: 10.1016/j.wasman.2011.10.009.
- [64] L. S. Diaz-Silvarrey, K. Zhang, and A. N. Phan, "Monomer recovery through advanced pyrolysis of waste high density polyethylene (HDPE)," *Green Chemistry*, vol. 20, no. 8, pp. 1813-1823, 2018, doi: 10.1039/c7gc03662k.
- [65] N. Horvat, "Tertiary polymer recycling: study of polyethylene thermolysis as a first step to synthetic diesel fuel," *Fuel*, vol. 78, pp. 459-470, 1999, doi: 10.1016/s0016-2361(98)00158-6.
- [66] I. de Marco, B. M. Caballero, A. López, M. F. Laresgoiti, A. Torres, and M. J. Chomón, "Pyrolysis of the rejects of a waste packaging separation and classification plant," *Journal of Analytical and Applied Pyrolysis*, vol. 85, no. 1-2, pp. 384-391, 2009, doi: 10.1016/j.jaap.2008.09.002.
- [67] G. Lopez, M. Artetxe, M. Amutio, J. Bilbao, and M. Olazar, "Thermochemical routes for the valorization of waste polyolefinic plastics to produce fuels and chemicals. A review," in *Renewable and Sustainable Energy Reviews* vol. 73, ed: Elsevier Ltd, 2017, pp. 346-368.
- [68] F. Abnisa and W. M. A. Wan Daud, "A review on co-pyrolysis of biomass: An optional technique to obtain a high-grade pyrolysis oil," *Energy*

- Conversion and Management*, vol. 87, pp. 71-85, 2014, doi: 10.1016/j.enconman.2014.07.007.
- [69] PlasticsEurope, "Polyolefins," in *PlasticsEurope*, ed, 2021.
- [70] American Chemistry Council, "Plastic Packaging Resins," in *American Chemistry Council*, ed, 2021.
- [71] J. Aguado, D. P. Serrano, and J. M. Escola, "Fuels from waste plastics by thermal and catalytic processes: A review," *Industrial and Engineering Chemistry Research*, 2008, doi: 10.1021/ie800393w.
- [72] E. Butler, G. Devlin, D. Meier, and K. McDonnell, "A review of recent laboratory research and commercial developments in fast pyrolysis and upgrading," in *Renewable and Sustainable Energy Reviews*, ed, 2011.
- [73] R. W. J. Westerhout, J. Waanders, J. A. M. Kuipers, and W. P. M. Van Swaaij, "Recycling of polyethylene and polypropene in a novel bench-scale rotating cone reactor by high-temperature pyrolysis," *Industrial and Engineering Chemistry Research*, 1998, doi: 10.1021/ie970704q.
- [74] A. Adrados, I. de Marco, B.M. Caballero, A. López, M.F. Laresgoiti, and A. Torres, "Pyrolysis of plastic packaging waste: A comparison of plastic residuals from material recovery facilities with simulated plastic waste," *Waste Management*, vol. 32, no. 5, pp. 826-832, 2012, doi: 10.1016/j.wasman.2011.06.016.
- [75] B. Csukás, M. Varga, N. Miskolczi, S. Balogh, A. Angyal, and L. Bartha, "Simplified dynamic simulation model of plastic waste pyrolysis in laboratory and pilot scale tubular reactor," *Fuel Processing Technology*, vol. 106, pp. 186-200, 2013, doi: 10.1016/j.fuproc.2012.07.024.
- [76] M. S. Qureshi, A. Oasmaa, and C. Lindfors, "Thermolysis of plastic waste: Reactor comparison," 2019. [Online]. Available: https://dc.engconfintl.org/pyroliq_2019 (Accessed 31/05/2021.)
- [77] S. Kumar and R. K. Singh, "Recovery of hydrocarbon liquid from waste high density polyethylene by thermal pyrolysis," *Brazilian Journal of Chemical Engineering*, vol. 28, no. 4, pp. 659-667, 2011, doi: 10.1590/S0104-66322011000400011.
- [78] W. C. McCaffrey, M. R. Kamal, and D. G. Cooper, "Thermolysis of polyethylene," *Polymer Degradation and Stability*, vol. 47, no. 1, pp. 133-139, 1995, doi: 10.1016/0141-3910(94)00096-Q.
- [79] S. V. Papuga, P. M. Gvero, and L. M. Vukić, "Temperature and time influence on the waste plastics pyrolysis in the fixed bed reactor," *Thermal Science*, vol. 20, no. 2, pp. 731-741, 2016, doi: 10.2298/TSCI141113154P.
- [80] D. P. Serrano, J. Aguado, J. M. Escola, and E. Garagorri, "Performance of a continuous screw kiln reactor for the thermal and catalytic conversion of polyethylene-lubricating oil base mixtures," *Applied Catalysis B: Environmental*, 2003, doi: 10.1016/S0926-3373(03)00024-9.
- [81] D. P. Serrano, J. Aguado, G. Vicente, and N. Sánchez, "Effects of hydrogen-donating solvents on the thermal degradation of HDPE," *Journal of Analytical and Applied Pyrolysis*, 2007, doi: 10.1016/j.jaap.2006.07.001.
- [82] A. Marcilla, Á. N. García, and M. del Remedio Hernández, "Thermal Degradation of LDPE-Vacuum Gas Oil Mixtures for Plastic Wastes Valorization," *Energy & Fuels*, vol. 21, no. 2, pp. 870-880, 2007, doi: 10.1021/ef0605293.

- [83] S. C. Oh, D. I. Han, H. Kwak, S. Y. Bae, and K. H. Lee, "Kinetics of the degradation of polystyrene in supercritical acetone," *Polymer Degradation and Stability*, 2007, doi: 10.1016/j.polymdegradstab.2007.04.009.
- [84] M. Artetxe, G. Lopez, M. Amutio, G. Elordi, J. Bilbao, and M. Olazar, "Cracking of High Density Polyethylene Pyrolysis Waxes on HZSM-5 Catalysts of Different Acidity," *Industrial and Engineering Chemistry Research*, vol. 52, no. 31, pp. 10637-10645, 2013, doi: 10.1021/IE4014869.
- [85] L. Quesada, M. C. de Hoces, M. A. Martín-Lara, G. Luzón, and G. Blázquez, "Performance of different catalysts for the in situ cracking of the oil-waxes obtained by the pyrolysis of polyethylene filmwaste," *Sustainability (Switzerland)*, 2020, doi: 10.3390/su12135482.
- [86] S. Kumar and R. K. Singh, "Thermolysis of High-Density Polyethylene to Petroleum Products," *Journal of Petroleum Engineering*, vol. 2013(6), p. 987568, 2013, doi: 10.1155/2013/987568.
- [87] Y. Sakata, M. A. Uddin, and A. Muto, "Degradation of polyethylene and polypropylene into fuel oil by using solid acid and non-acid catalysts," *Journal of Analytical and Applied Pyrolysis*, vol. 51, no. 1-2, pp. 135-155, 1999, doi: 10.1016/S0165-2370(99)00013-3.
- [88] A. López, I. de Marco, B. M. Caballero, M. F. Laresgoiti, A. Adrados, and A. Aranzabal, "Catalytic pyrolysis of plastic wastes with two different types of catalysts: ZSM-5 zeolite and Red Mud," *Applied Catalysis B: Environmental*, 2011, doi: 10.1016/j.apcatb.2011.03.030.
- [89] Y. Kodera, Y. Ishihara, and T. Kuroki, "Novel process for recycling waste plastics to fuel gas using a moving-bed reactor," *Energy and Fuels*, 2006, doi: 10.1021/ef0502655.
- [90] Y. Yang, Y. Zhang, E. Omairey, J. Cai, F. Gu, and A. V. Bridgwater, "Intermediate pyrolysis of organic fraction of municipal solid waste and rheological study of the pyrolysis oil for potential use as bio-bitumen," *Journal of Cleaner Production*, vol. 187, pp. 390-399, 2018, doi: 10.1016/j.jclepro.2018.03.205.
- [91] S. M. Al-Salem *et al.*, "Non-isothermal degradation kinetics of virgin linear low density polyethylene (LLDPE) and biodegradable polymer blends," *Journal of Polymer Research*, vol. 25, no. 5, pp. 111-111, 2018, doi: 10.1007/s10965-018-1513-7.
- [92] S. M. Al-Salem, "Thermal pyrolysis of high density polyethylene (HDPE) in a novel fixed bed reactor system for the production of high value gasoline range hydrocarbons (HC)," *Process Safety and Environmental Protection*, vol. 127, pp. 171-179, 2019, doi: 10.1016/j.psep.2019.05.008.
- [93] M. L. Mastellone, F. Perugini, M. Ponte, and U. Arena, "Fluidized bed pyrolysis of a recycled polyethylene," *Polymer Degradation and Stability*, vol. 76, no. 3, pp. 479-487, 2002, doi: 10.1016/S0141-3910(02)00052-6.
- [94] N. Miskolczi, A. Angyal, L. Bartha, and I. Valkai, "Fuels by pyrolysis of waste plastics from agricultural and packaging sectors in a pilot scale reactor," *Fuel Processing Technology*, 2009, doi: 10.1016/j.fuproc.2009.04.019.
- [95] T. Stclair-Pearce and D. Garbett, "Plastic Waste Thermal Cracking New Energy Investment Business Plan," 2018.
- [96] Renewlogy, "Renew Phoenix – Renewlogy," ed, 2018.

- [97] finnCap, "New wave of tech companies grows to tackle plastic pollution," ed, 2019.
- [98] Plastic Energy, "Technology - Plastic Energy," ed, 2020.
- [99] S. Nanda and F. Berruti, "Thermochemical conversion of plastic waste to fuels: a review," *Environmental Chemistry Letters*, vol. 19, no. 1, pp. 123-148, 2021, doi: 10.1007/S10311-020-01094-7.
- [100] V. K. Soni, G. Singh, B. K. Vijayan, A. Chopra, G. S. Kapur, and S. S. V. Ramakumar, "Thermochemical Recycling of Waste Plastics by Pyrolysis: A Review," *Energy and Fuels*, vol. 35, no. 16, pp. 12763-12808, 2021, doi: 10.1021/ACS.ENERGYFUELS.1C01292.
- [101] S. J. Pickering, "Recycling technologies for thermoset composite materials—current status," *Composites Part A: Applied Science and Manufacturing*, vol. 37, no. 8, pp. 1206-1215, 2006, doi: 10.1016/j.compositesa.2005.05.030.
- [102] M. Solis and S. Silveira, "Technologies for chemical recycling of household plastics – A technical review and TRL assessment," in *Waste Management* vol. 105, ed: Elsevier Ltd, 2020, pp. 128-138.
- [103] P. T. Benavides, P. Sun, J. Han, J. B. Dunn, and M. Wang, "Life-cycle analysis of fuels from post-use non-recycled plastics," *Fuel*, vol. 203, pp. 11-22, 2017, doi: 10.1016/j.fuel.2017.04.070.
- [104] R. Aguado, M. Olazar, M.J. San José, B. Gaisán, and J. Bilbao, "Wax formation in the pyrolysis of polyolefins in a conical spouted bed reactor," *Energy and Fuels*, vol. 16, no. 6, pp. 1429-1437, 2002, doi: 10.1021/ef020043w.
- [105] A. Chaala, H. Darmstadt, and C. Roy, "Vacuum pyrolysis of electric cable wastes," *Journal of Analytical and Applied Pyrolysis*, vol. 39, no. 1, pp. 79-96, 1997, doi: 10.1016/S0165-2370(96)00964-3.
- [106] H. Bockhorn, A. Hornung, U. Hornung, and D. Schawaller, "Kinetic study on the thermal degradation of polypropylene and polyethylene," *Journal of Analytical and Applied Pyrolysis*, vol. 48, no. 2, pp. 93-109, 1999, doi: 10.1016/S0165-2370(98)00131-4.
- [107] S.H. Jung, M.H. Cho, B.S. Kang, and J. S. Kim, "Pyrolysis of a fraction of waste polypropylene and polyethylene for the recovery of BTX aromatics using a fluidized bed reactor," *Fuel Processing Technology*, vol. 91, no. 3, pp. 277-284, 2010, doi: 10.1016/j.fuproc.2009.10.009.
- [108] R. Miandad, M. A. Barakat, M. Rehan, A. S. Aburiazzaiza, I. M. I. Ismail, and A. S. Nizami, "Plastic waste to liquid oil through catalytic pyrolysis using natural and synthetic zeolite catalysts," *Waste Management*, vol. 69, pp. 66-78, 2017, doi: 10.1016/j.wasman.2017.08.032.
- [109] M. Predel and W. Kaminsky, "Pyrolysis of mixed polyolefins in a fluidised-bed reactor and on a pyro-GC/MS to yield aliphatic waxes," *Polymer Degradation and Stability*, vol. 70, no. 3, pp. 373-385, 2000, doi: 10.1016/S0141-3910(00)00131-2.
- [110] P.T. Williams and E. A. Williams, "Fluidised bed pyrolysis of low density polyethylene to produce petrochemical feedstock," *Journal of Analytical and Applied Pyrolysis*, vol. 51, no. 1-2, pp. 107-126, 1999, doi: 10.1016/S0165-2370(99)00011-X.
- [111] F. T. Ademiluyi, E. O. Oboho, and D. J. Akpan, "The effect of pyrolysis temperature and time, on the properties of polyethylene wax and hydrocarbon gases produced from waste polyethylene sachets," *ARP*

- Journal of Engineering and Applied Sciences*, vol. 8, no. 7, pp. 557-562, 2013.
- [112] L. I. Jixing, "Study on the Conversion Technology of Waste Polyethylene Plastic to Polyethylene Wax," *Energy Sources*, vol. 25, no. 1, pp. 77-82, 2003, doi: 10.1080/00908310290142136.
- [113] K. Murata, K. Sato, and Y. Sakata, "Effect of pressure on thermal degradation of polyethylene," *Journal of Analytical and Applied Pyrolysis*, vol. 71, no. 2, pp. 569-589, 2004, doi: 10.1016/j.jaap.2003.08.010.
- [114] T. V. Mathew. "Lecture notes in Transportation Systems Engineering," Indian Institute of Technology Bombay. [Online.] Available: https://www.civil.iitb.ac.in/tvm/1100_LnTse/401_InTse/plain/plain.html (accessed 17/05/2022.)
- [115] M. M. A. Aziz, M. T. Rahman, M. R. Hainin, and W. A. W. A. Bakar, "An overview on alternative binders for flexible pavement," *Construction and Building Materials*, vol. 84, pp. 315-319, 2015, doi: 10.1016/j.conbuildmat.2015.03.068.
- [116] BSOL, *BS 3690-2: Bitumens for building and civil engineering. Specification for bitumens for industrial purposes.*, 1989.
- [117] M. Holý and E. Remišová, "Analysis of influence of bitumen composition on the properties represented by empirical and viscosity test," *Transportation Research Procedia*, vol. 40, pp. 34-41, 2019, doi: <https://doi.org/10.1016/j.trpro.2019.07.007>.
- [118] M. R. Nivitha, E. Prasad, and J. M. Krishnan, "Transitions in unmodified and modified bitumen using FTIR spectroscopy," *Materials and Structures/Materiaux et Constructions*, vol. 52, no. 1, pp. 1-11, 2019, doi: 10.1617/s11527-018-1308-7.
- [119] S. Weigel and D. Stephan, "The prediction of bitumen properties based on FTIR and multivariate analysis methods," *Fuel*, vol. 208, pp. 655-661, 2017, doi: 10.1016/j.fuel.2017.07.048.
- [120] M. Holý and E. Remisova, "Characterization of Bitumen Binders on the Basis of Their Thermo-Viscous Properties," *Slovak Journal of Civil Engineering*, vol. 27, pp. 25-31, 2019, doi: 10.2478/sjce-2019-0004.
- [121] D. Grossegger, "Investigation of Aged, Non-aged Bitumen and their Bitumen Fractions," 2015.
- [122] P. Redelius, "Asphaltenes in bitumen, what they are and what they are not," vol. 10, pp. 25-43, 2009, doi: 10.1080/14680629.2009.9690234.
- [123] F. Zheng, Q. Shi, G. S. Vallverdu, P. Giusti, and B. Bouyssiere, "Fractionation and Characterization of Petroleum Asphaltene: Focus on Metalopetroleomics," *Processes*, vol. 8, no. 11, doi: 10.3390/pr8111504.
- [124] Federal Highway Administration, "Using Falling Weight Deflectometer Data with Mechanistic-Empirical Design and Analysis, Volume iii: Guidelines for Deflection Testing, Analysis and Interpretation," FHWA-HRT-16-011, 2017. [Online]. Available: <https://www.fhwa.dot.gov/publications/research/infrastructure/pavements/16011/004.cfm> (accessed 17/05/2022.)
- [125] A. Cocurullo, G. Airey, A. Collop, and C. Sangiorgi, "Indirect tensile versus two-point bending fatigue testing," presented at the Institution of Civil Engineers-Transport, 2008.
- [126] M. M. A. Aziz, "A Short Review on Partial Replacement of Asphalt Binder with Crumb Rubber," *Journal Teknologi*, 2016.

- [127] F. T. S. Aragão, Y.-R. Kim, and L. D, "Research on Fatigue of Asphalt Mixtures and Pavements in Nebraska," 2008.
- [128] Z. Zhao, F. Xiao, and S. Amirkhanian, "Recent applications of waste solid materials in pavement engineering," *Waste Management*, vol. 108, pp. 78-105, 2020, doi: 10.1016/J.WASMAN.2020.04.024.
- [129] M. Porto, P. Caputo, V. Loise, S. Eskandarsefat, B. Teltayev, and C. O. Rossi, "Bitumen and bitumen modification: A review on latest advances," *Applied Sciences (Switzerland)*, vol. 9, no. 4, 2019, doi: 10.3390/app9040742.
- [130] D. Lesueur, "The colloidal structure of bitumen: Consequences on the rheology and on the mechanisms of bitumen modification," in *Advances in Colloid and Interface Science* vol. 145, ed, 2009, pp. 42-82.
- [131] H. R. Radeef *et al.*, "Enhanced Dry Process Method for Modified Asphalt Containing Plastic Waste," *Frontiers in Materials*, vol. 8, pp. 247-247, 2021, doi: 10.3389/FMATS.2021.700231/BIBTEX.
- [132] P. Lastra-González, M. A. Calzada-Pérez, D. Castro-Fresno, Á. Vega-Zamanillo, and I. Indacochea-Vega, "Comparative analysis of the performance of asphalt concretes modified by dry way with polymeric waste," *Construction and Building Materials*, vol. 112, pp. 1133-1140, 2016, doi: 10.1016/J.CONBUILDMAT.2016.02.156.
- [133] M. T. Awwad and L. Shbeeb, "The use of polyethylene in hot asphalt mixtures," *American Journal of Applied Sciences*, vol. 4, no. 6, pp. 390-396, 2007, doi: 10.3844/AJASSP.2007.390.396.
- [134] S. Tapkin, "The effect of polypropylene fibers on asphalt performance," *Building and Environment*, vol. 43, no. 6, pp. 1065-1071, 2008, doi: 10.1016/J.BUILDENV.2007.02.011.
- [135] E. Ahmadinia, M. Zargar, M. R. Karim, M. Abdelaziz, and P. Shafigh, "Using waste plastic bottles as additive for stone mastic asphalt," *Materials and Design*, vol. 32, no. 10, pp. 4844-4849, 2011, doi: 10.1016/J.MATDES.2011.06.016.
- [136] S. E. Zoorob and L. B. Suparma, "Laboratory design and investigation of the properties of continuously graded Asphaltic concrete containing recycled plastics aggregate replacement (Plastiphalt)," *Cement and Concrete Composites*, vol. 22, no. 4, pp. 233-242, 2000, doi: 10.1016/S0958-9465(00)00026-3.
- [137] Y. M. Alghrafy, S. M. El-Badawy, and E. S. M. Abd Alla, "Rheological and environmental evaluation of sulfur extended asphalt binders modified by high- and low-density polyethylene recycled waste," *Construction and Building Materials*, vol. 307, pp. 125008-125008, 2021, doi: 10.1016/J.CONBUILDMAT.2021.125008.
- [138] N. M. Zakaria, "Characterisation of bitumen and asphalt mixture with recycled waste plastic (RWP) modified binder," University of Nottingham, 2020.
- [139] M. Murphy, M. O'Mahony, C. Lycett, and I. Jamieson, "Bitumens modified with recycled polymers," *Materials and Structures* 2000 33:7, vol. 33, no. 7, pp. 438-444, 2000, doi: 10.1007/BF02480663.
- [140] M. Attaelmanan, C. P. Feng, and A.-H. Ai, "Laboratory evaluation of HMA with high density polyethylene as a modifier," *Construction and Building Materials*, vol. 25, no. 5, pp. 2764-2770, 2011, doi: 10.1016/j.conbuildmat.2010.12.037.

- [141] R. Yu, C. Fang, P. Liu, X. Liu, and Y. Li, "Storage stability and rheological properties of asphalt modified with waste packaging polyethylene and organic montmorillonite," *Applied Clay Science*, vol. 104, pp. 1-7, 2015, doi: <https://doi.org/10.1016/j.clay.2014.11.033>.
- [142] D. Casey, C. McNally, A. Gibney, and M. D. Gilchrist, "Development of a recycled polymer modified binder for use in stone mastic asphalt," *Resources, Conservation and Recycling*, vol. 52, no. 10, pp. 1167-1174, 2008, doi: 10.1016/J.RESCONREC.2008.06.002.
- [143] A. Ait-Kadi, B. Brahim, and M. Bousmina, "Polymer blends for enhanced asphalt binders," *Polymer Engineering and Science*, vol. 36, no. 12, pp. 1724-1733, 1996, doi: 10.1002/pen.10568.
- [144] S. Hinislioglu and E. Agar, "Use of waste high density polyethylene as bitumen modifier in asphalt concrete mix," *Materials Letters*, vol. 58, no. 3-4, pp. 267-271, 2004, doi: 10.1016/S0167-577X(03)00458-0.
- [145] C. Fang, P. Liu, R. Yu, and X. Liu, "Preparation process to affect stability in waste polyethylene-modified bitumen," *Construction and Building Materials*, vol. 54, pp. 320-325, 2014, doi: 10.1016/J.CONBUILDMAT.2013.12.071.
- [146] M. E. Abdullah, N. A. Ahmad, R. P. Jaya, N. A. Hassan, H. Yaacob, and M. R. Hainin, "Effects of Waste Plastic on the Physical and Rheological Properties of Bitumen," *IOP Conference Series: Materials Science and Engineering*, vol. 204, no. 1, pp. 012016-012016, 2017, doi: 10.1088/1757-899X/204/1/012016.
- [147] M. A. Dalhat and H. I. Al-Abdul Wahhab, "Performance of recycled plastic waste modified asphalt binder in Saudi Arabia," vol. 18, no. 4, pp. 349-357, 2015, doi: 10.1080/10298436.2015.1088150.
- [148] Y. M. Alghrafi, E. S. M. Abd Alla, and S. M. El-Badawy, "Rheological properties and aging performance of sulfur extended asphalt modified with recycled polyethylene waste," *Construction and Building Materials*, vol. 273, pp. 121771-121771, 2021, doi: 10.1016/J.CONBUILDMAT.2020.121771.
- [149] A.-R. I. Al-Hadidy, "Evaluation of Pyrolysis Polypropylene Modified Asphalt Paving Materials," *AL-Rafdain Engineering Journal (AREJ)*, vol. 14, no. 2, pp. 36-50, 2006, doi: 10.33899/RENGJ.2006.46555.
- [150] K. Al-Ghannam, "Study on the Rheological Properties of Asphalt, Effect of Modification Process on the Homogeneity of the System," *Thesis*, 1996.
- [151] G. Polacco, S. Berlincioni, D. Biondi, J. Stastna, and L. Zanzotto, "Asphalt modification with different polyethylene-based polymers," *European Polymer Journal*, vol. 41, no. 12, pp. 2831-2844, 2005, doi: 10.1016/j.eurpolymj.2005.05.034.
- [152] F. Cardone, G. Ferrotti, F. Frigio, and F. Canestrari, "Influence of polymer modification on asphalt binder dynamic and steady flow viscosities," *Construction and Building Materials*, vol. 71, pp. 435-443, 2014, doi: 10.1016/j.conbuildmat.2014.08.043.
- [153] M. Naskar, T. K. Chaki, and K. S. Reddy, "Effect of waste plastic as modifier on thermal stability and degradation kinetics of bitumen/waste plastics blend," *Thermochimica Acta*, vol. 509, no. 1-2, pp. 128-134, 2010, doi: 10.1016/J.TCA.2010.06.013.
- [154] F. Moghadas Nejad, M. Gholami, K. Naderi, and M. Rahi, "Evaluation of rutting properties of high density polyethylene modified binders," *Materials*

- and Structures/Materiaux et Constructions*, vol. 48, no. 10, pp. 3295-3305, 2015, doi: 10.1617/S11527-014-0399-Z.
- [155] K. L. Roja, A. Rehman, M. Ouederni, S. K. Krishnamoorthy, A. Abdala, and E. Masad, "Influence of polymer structure and amount on microstructure and properties of polyethylene-modified asphalt binders," *Materials and Structures/Materiaux et Constructions*, vol. 54, no. 2, 2021, doi: 10.1617/S11527-021-01683-0.
- [156] S. Amirkhanian, "Investigations of Rheological Properties of Asphalt Binders Modified with Scrap Polyethylenes," Sustainability Plastics Industry Association, 2018.
- [157] K. Ghuzlan, G. Al-Khateeb and Y. Qasem, "Rheological Properties of Polyethylene-Modified Asphalt Binder," *Athens Journal of Technology & Engineering*, no. 2, p. 75-88, 2015, doi: 10.30958/ajte.2-2-1.
- [158] J. Zhang *et al.*, "Enhancement of rutting resistance and fatigue behavior of asphalt mixtures modified by recycled waste polymer components," [Online.] Available: <https://core.ac.uk/download/pdf/323357979.pdf> (accessed 04/05/22.)
- [159] U. Isacson and X. Lu, "Testing and appraisal of polymer modified road bitumens—state of the art," *Materials and Structures 1995 28:3*, vol. 28, no. 3, pp. 139-159, 1995, doi: 10.1007/BF02473221.
- [160] M. E. Abdullah *et al.*, "Effect of Waste Plastic as Bitumen Modified in Asphalt Mixture," in *MATEC Web of Conferences 103, 09018 (2017) ISCEE*, 2016, doi: 10.1051/matecconf/201710309018.
- [161] S. Hınısliođlu, H. N. Aras, and O. Ünsal Bayrak, "Effects of high density polyethylene on the permanent deformation of asphalt concrete," *Indian Journal of Engineering & Material Sciences*, vol. 12, pp. 456-460, 2005.
- [162] S. Tapkin, Ü. Uşar, A. Tuncan, and M. Tuncan, "Repeated creep behavior of polypropylene fiber-reinforced bituminous mixtures," *Journal of Transportation Engineering*, vol. 135, no. 4, pp. 240-249, 2009, doi: 10.1061/(ASCE)0733-947X(2009)135:4(240).
- [163] S. Tapkin, A. Çevik, and Ü. Uşar, "Accumulated strain prediction of polypropylene modified marshall specimens in repeated creep test using artificial neural networks," *Expert Systems with Applications*, vol. 36, no. 8, pp. 11186-11197, 2009, doi: 10.1016/J.ESWA.2009.02.089.
- [164] S. W. Goh and Z. You, "A simple stepwise method to determine and evaluate the initiation of tertiary flow for asphalt mixtures under dynamic creep test," *Construction and Building Materials*, vol. 23, no. 11, pp. 3398-3405, 2009, doi: 10.1016/J.CONBUILDMAT.2009.06.020.
- [165] M. Napiah, N. Z. Habib, and I. Kamaruddin, "Creep Behavior of Polyethylene Modified Bituminous Mixture," *APCBEE Procedia*, vol. 9, pp. 202-206, 2014, doi: 10.1016/J.APCBEE.2014.01.036.
- [166] F. Moghadas Nejad, A. Azarhoosh, and G. H. Hamedi, "Effect of high density polyethylene on the fatigue and rutting performance of hot mix asphalt - a laboratory study," *Road Materials and Pavement Design*, vol. 15, no. 3, pp. 746-756, 2014, doi: 10.1080/14680629.2013.876443.
- [167] W. K. Brown *et al.*, "Hot Mix Asphalt Materials, Mixture Design, and Construction," 2009.
- [168] S. Köfteci, "Effect of HDPE Based Wastes on the Performance of Modified Asphalt Mixtures," *Procedia Engineering*, vol. 161, pp. 1268-1274, 2016, doi: 10.1016/j.proeng.2016.08.567.

- [169] T. Abdel-Wahed, G. Moussa, and A. Abdel-Raheem, "Investigating the Moisture Susceptibility of Asphalt Mixtures Modified with High-Density Polyethylene," *JES. Journal of Engineering Sciences*, 2020, doi: 10.21608/JESAUN.2020.39052.1001.
- [170] S. Haider, I. Hafeez, Jamal, and R. Ullah, "Sustainable use of waste plastic modifiers to strengthen the adhesion properties of asphalt mixtures," *Construction and Building Materials*, vol. 235, pp. 117496-117496, 2020, doi: 10.1016/J.CONBUILDMAT.2019.117496.
- [171] R. Bajpai, M. Allah Khan, O. Bin Sami, P. Kumar Yadav, and P. Kumar Srivastava, "A Study on the Plastic Waste Treatment Methods for Road Construction," *International Journal of Advance Research*, 2017.
- [172] A.-H. A. Ibrahim, "Laboratory investigation of aged HDPE-modified asphalt mixes," *International Journal of Pavement Research and Technology*, vol. 12, no. 4, pp. 364-369, 2019, doi: 10.1007/s42947-019-0043-y.
- [173] A. Pérez-Lepe, F. J. Martínez-Boza, and C. Gallegos, "High temperature stability of different polymer-modified bitumens: A rheological evaluation," *Journal of Applied Polymer Science*, vol. 103, no. 2, pp. 1166-1174, 2007, doi: 10.1002/APP.25336.
- [174] J. Zhu, "Storage Stability and Phase Separation Behaviour of Polymer-Modified Bitumen," 2016.
- [175] G. Polacco, J. Stastna, D. Biondi, and L. Zanzotto, "Relation between polymer architecture and nonlinear viscoelastic behavior of modified asphalts," *Current Opinion in Colloid & Interface Science*, vol. 11, no. 4, pp. 230-245, 2006, doi: 10.1016/J.COCIS.2006.09.001.
- [176] E. Masad, K. L. Roja, A. Rehman, and A. Abdala, "A Review of Asphalt Modification Using Plastics: A Focus on Polyethylene," *Texas A&M University*, vol. 1, no. 1, pp. 1-26, 2020, doi: 10.13140/RG.2.2.36633.77920.
- [177] M. García-Morales, P. Partal, F. J. Navarro, and C. Gallegos, "Effect of waste polymer addition on the rheology of modified bitumen," *Fuel*, vol. 85, no. 7-8, pp. 936-943, 2006, doi: 10.1016/j.fuel.2005.09.015.
- [178] C. Giavarini, P. De Filippis, M. L. Santarelli, and M. Scarsella, "Production of stable polypropylene-modified bitumens," *Fuel*, vol. 75, no. 6, pp. 681-686, 1996, doi: 10.1016/0016-2361(95)00312-6.
- [179] P.-H. Yeh, Y.-H. Nien, J.-H. Chen, W.-C. Chen, and J.-S. Chen, "Thermal and rheological properties of maleated polypropylene modified asphalt," *Polymer Engineering & Science*, vol. 45, no. 8, pp. 1152-1158, 2005, doi: 10.1002/PEN.20386.
- [180] A. Chakraborty and S. Mehta, "Utilization & Minimization Of Waste Plastic In Construction Of Pavement : A Review," in "Sapna Mehta International Journal of Engineering Technology Science and Research," 2017, vol. 4. [Online]. Available: www.ijetsr.com (accessed 01/07/2021.)
- [181] P. R. Heikkilä, V. Väänänen, M. Hämeilä, and K. Linnainmaa, "Mutagenicity of bitumen and asphalt fumes," *Toxicology in Vitro*, vol. 17, no. 4, pp. 403-412, 2003, doi: 10.1016/S0887-2333(03)00045-6.
- [182] A. L. Andrady, "The plastic in microplastics: A review," *Marine Pollution Bulletin*, vol. 119, no. 1, pp. 12-22, 2017, doi: 10.1016/J.MARPOLBUL.2017.01.082.

- [183] I. Rodríguez-Fernández, M. C. Cavalli, L. Poulidakos, and M. Bueno, "Recyclability of Asphalt Mixtures with Crumb Rubber Incorporated by Dry Process: A Laboratory Investigation," *Materials* 2020, vol. 13, no. 12, pp. 2870-2870, 2020, doi: 10.3390/MA13122870.
- [184] S. Köfteci, P. Ahmedzade, and B. Kultayev, "Performance evaluation of bitumen modified by various types of waste plastics," *Construction and Building Materials*, vol. 73, pp. 592-602, 2014, doi: 10.1016/j.conbuildmat.2014.09.067.
- [185] J. Santos, J. Bryce, G. Flintsch, A. Ferreira, and B. Diefenderfer, "A life cycle assessment of in-place recycling and conventional pavement construction and maintenance practices," vol. 11, no. 9, pp. 1199-1217, 2014, doi: 10.1080/15732479.2014.945095.
- [186] F. G. Praticò, M. Giunta, M. Mistretta, and T. M. Gulotta, "Energy and Environmental Life Cycle Assessment of Sustainable Pavement Materials and Technologies for Urban Roads," *Sustainability* 2020, vol. 12, no. 2, pp. 704-704, 2020, doi: 10.3390/SU12020704.
- [187] J. Zhu, B. Birgisson, and N. Kringos, "Polymer modification of bitumen: Advances and challenges," *European Polymer Journal*, vol. 54, no. 1, pp. 18-38, 2014, doi: 10.1016/J.EURPOLYMJ.2014.02.005.
- [188] C. Oreto *et al.*, "Life Cycle Assessment of Sustainable Asphalt Pavement Solutions Involving Recycled Aggregates and Polymers," 2021, doi: 10.3390/ma14143867.
- [189] M. I. Souliman, M. Mamlouk, and A. Eifert, "Cost-effectiveness of Rubber and Polymer Modified Asphalt Mixtures as Related to Sustainable Fatigue Performance," *Procedia Engineering*, vol. 145, pp. 404-411, 2016, doi: 10.1016/J.PROENG.2016.04.007.
- [190] R. Dong, M. Zhao, and N. Tang, "Characterization of crumb tire rubber lightly pyrolyzed in waste cooking oil and the properties of its modified bitumen," *Construction and Building Materials*, vol. 195, pp. 10-18, 2019, doi: 10.1016/J.CONBUILDMAT.2018.11.044.
- [191] O. Kolokolova, "Biomass Pyrolysis and Optimisation for Bio-bitumen," *Thesis*, University of Canterbury, 2013.
- [192] A.I. Al-Hadidy and Y. Q. Tan, "Mechanistic approach for polypropylene-modified flexible pavements," *Materials & Design*, vol. 30, no. 4, pp. 1133-1140, 2009, doi: 10.1016/J.MATDES.2008.06.021.
- [193] J. P. Mofokeng, A. S. Luyt, T. Tábi, and J. Kovács, "Comparison of injection moulded, natural fibre-reinforced composites with PP and PLA as matrices," *Journal of Thermoplastic Composite Materials*, vol. 25, no. 8, pp. 927-948, 2012, doi: 10.1177/0892705711423291.
- [194] B. Tajeddin and L. C. Abdulah, "Thermal Properties of High Density Polyethylene-Kenaf Cellulose Composites," vol. 18, no. 5, pp. 257-261, 2010, doi: 10.1177/096739111001800503.
- [195] F. C. G. Martinho, L. G. Picado-Santos, F. M. S. Lemos, M. A. N. D. A. Lemos, and E. R. F. Santos, "Using Plastic Waste in a Circular Economy Approach to Improve the Properties of Bituminous Binders," *Applied Sciences*, vol. 12, no. 5, 2022, doi: 10.3390/app12052526.
- [196] Y. Edwards, "Influence of waxes on bitumen and asphalt concrete mixture performance," *Thesis*, KTH Royal Institute of Technology, 2005.

- [197] L. Desidery and M. Lanotte, "Effect of Waste Polyethylene and Wax-Based Additives on Bitumen Performance.," *Polymers* vol. 13, no. 21, p. 3733, 2021, doi: 10.3390/polym13213733.
- [198] T. Valentová, L. Benešová, J. Mastný, and J. Valentin, "Effect of new type of synthetic waxes on reduced production and compaction temperature of asphalt mixture with reclaimed asphalt," *IOP Conference Series: Materials Science and Engineering*, vol. 236, no. 1, 2017, doi: 10.1088/1757-899X/236/1/012019.
- [199] Y. Kim, J. Lim, and M. Lee, "Comprehensive Evaluation of Polymer-Modified SMA Mixture Produced with New Polyethylene Wax-Based WMA Additive with Adhesion Promoter," in *"Transportation Research Board 92nd Annual Meeting"*, Washington DC, United States, 2013, p. 8.
- [200] L. Shang and S. Wang, "Pyrolysed Wax from Recycled Crosslinked Polyethylene as a Warm-Mix Asphalt (WMA) Additive for Crumb-Rubber-Modified Asphalt," *Progress in Rubber Plastics Recycling Technology* vol. 27, no. 3, pp. 133-144, 2011, doi: 10.1177/147776061102700301.
- [201] A. Diab, C. Sangiorgi, R. Ghabchi, M. Zaman, and A. M. Wahaballa, "Warm Mix Asphalt (WMA) technologies: Benefits and drawbacks—a literature review," 2016.
- [202] Y. Zhang, Q. Song, Q. Lv, and H. Wang, "Influence of different polyethylene wax additives on the performance of modified asphalt binders and mixtures," *Construction and Building Materials*, vol. 302, pp. 124115-124115, 2021, doi: 10.1016/J.CONBUILDMAT.2021.124115.
- [203] EAPA, "The Circular Economy of Asphalt. EAPA Technical Review," 2022. [Online]. Available: <https://eapa.org/> (accessed 31/07/21.)
- [204] EAPA, "Asphalt in Figures," 2020. [Online]. Available: <eapa.org/download/13774/> (accessed 31/07/21.)
- [205] M. Zaumanis and R. B. Mallick, "Review of very high-content reclaimed asphalt use in plant-produced pavements: state of the art," *International Journal of Pavement Engineering*, vol. 16, no. 1, pp. 39-55, 2015, doi: 10.1080/10298436.2014.893331.
- [206] H. F. Haghshenas, Y.-R. Kim, G. Nxengiyumya, S. R. Kommididi, and S. Amelian, "Research on High-RAP Asphalt Mixtures with Rejuvenators – Phase II," 2019.
- [207] Y. Guan, L. Geng, S. Zhang, W. Zhou, and G. Jin, "Design and performance investigation on dense graded anti-sliding ultra-thin wearing course material," *Functional Pavement Design - Proceedings of the 4th Chinese-European Workshop on Functional Pavement Design, CEW 2016*, pp. 1203-1212, 2016, doi: 10.1201/9781315643274-127.
- [208] M. Gong, J. Yang, J. Zhang, H. Zhu, and T. Tong, "Physical–chemical properties of aged asphalt rejuvenated by bio-oil derived from biodiesel residue," *Construction and Building Materials*, vol. 105, pp. 35-45, 2016, doi: 10.1016/J.CONBUILDMAT.2015.12.025.
- [209] M. A. Raouf and C. R. Williams, "General Rheological Properties of Fractionated Switchgrass Bio-Oil as a Pavement Material," vol. 11, pp. 325-353, 2011, doi: 10.1080/14680629.2010.9690337.
- [210] T. Wang *et al.*, "Rheological properties of aged bitumen rejuvenated by polymer modified bio-derived rejuvenator," *Construction and Building Materials*, vol. 298, pp. 123249-123249, 2021, doi: 10.1016/J.CONBUILDMAT.2021.123249.

- [211] A. Kumar and R. Choudhary, "Use of Waste Tyre Pyrolytic Products for Asphalt Binder Modification," 2020, doi: 10.1515/ijpeat-2016-0031.
- [212] I. Cosentino, L. Restuccia, G. A. Ferro, and J. M. Tulliani, "Influence of pyrolysis parameters on the efficiency of the biochar as nanoparticles into cement-based composites," in *Procedia Structural Integrity*, 2018, vol. 13, pp. 2132-2136, doi: 10.1016/j.prostr.2018.12.194.
- [213] X. Yang, Z. You, and Q. Dai, "Performance evaluation of asphalt binder modified by bio-oil generated from waste wood resources," *International Journal of Pavement Research and Technology*, 2013, doi: 10.6135/ijprt.org.tw/2013.6(4).431.
- [214] K. H. Lee and S. C. Oh, "Thermal and catalytic degradation of pyrolytic waxy oil in a plug flow reactor," *Journal of Analytical and Applied Pyrolysis*, vol. 93, pp. 19-23, 2012, doi: 10.1016/J.JAAP.2011.09.002.
- [215] A. Tukker, H. de Groot, L. Simons and S. Wieggersma, "Chemical recycling of plastic waste: PVC and other resins," European Commission, DG III, Final Report, STB-99-55 Final, Delft, The Netherlands.
- [216] BaleBid, "World's First Commercial Plastic Waste To Wax Plant Opens," 2019. [Online.] Available: <https://www.balebid.com/forum/post/worlds-first-commercial-plastic-waste-to-wax-plan/936?page=1> (accessed 03/05/2021.)
- [217] Chemistry Libretexts, "Gas Chromatography," 2021. [Online.] Available: [https://chem.libretexts.org/Bookshelves/Analytical_Chemistry/Supplemental_Modules_\(Analytical_Chemistry\)/Instrumentation_and_Analysis/Chromatography/Gas_Chromatography#:~:text=Gas%20chromatography%20is%20one%20of,%2Dliquid%20chromatography%20\(GLC\)](https://chem.libretexts.org/Bookshelves/Analytical_Chemistry/Supplemental_Modules_(Analytical_Chemistry)/Instrumentation_and_Analysis/Chromatography/Gas_Chromatography#:~:text=Gas%20chromatography%20is%20one%20of,%2Dliquid%20chromatography%20(GLC)) (accessed 17/05/2021.)
- [218] E. Waś, T. Szczesna, and H. Rybak-Chmielewska, "Efficiency of GC-MS method in detection of beeswax adulterated with paraffin," *Journal of Apicultural Science*, vol. 60, 2016, doi: 10.1515/jas-2016-0012.
- [219] J. Szulejko, Y.H. Kim, and K. H. Kim, "Method to predict gas chromatographic response factors for the trace-level analysis of volatile organic compounds based on the effective carbon number concept," *Journal of separation science*, vol. 36, pp. 3356-3365, 2013, doi: 10.1002/jssc.201300543.
- [220] M. N. Islam and M. R. A. Beg, "Fixed Bed Pyrolysis of Waste Plastic for Alternative Fuel Production," *Journal of Energy & Environment*, 2004.
- [221] Adnan, J. Shah, and M. R. Jan, "Effect of polyethylene terephthalate on the catalytic pyrolysis of polystyrene: Investigation of the liquid products," *Journal of the Taiwan Institute of Chemical Engineers*, vol. 51, pp. 96-102, 2015, doi: 10.1016/j.jtice.2015.01.015.
- [222] S. Salaudeen, S. Al-Salem, S. Sharma, and A. Dutta, "Pyrolysis of High-Density Polyethylene in a Fluidized Bed Reactor: Pyro-Wax and Gas Analysis," *Industrial & Engineering Chemistry Research*, vol. 60, 2021, doi: 10.1021/acs.iecr.1c03373.
- [223] D. S. Rahman, K. Hawboldt, R. Helleur, and S. Macquarrie, "Pyrolysis of waste plastic fish bags (polyethylene and polypropylene) to useable fuel oil," Research Report, Memorial University of Newfoundland, St. John's, Newfoundland and Labrador, 2018.
- [224] Hitachi. "Principle of Differential Scanning Calorimetry (DSC)." [Online.] Available: <https://www.hitachi->

- hightech.com/global/en/knowledge/analytical-systems/thermal-analysis/basics/dsc.html (accessed 17/05/2021.)
- [225] C. Leyva-Porras *et al.*, "Application of Differential Scanning Calorimetry (DSC) and Modulated Differential Scanning Calorimetry (MDSC) in Food and Drug Industries," *Polymers*, vol. 12, no. 1, 2019, doi: 10.3390/polym12010005.
- [226] F. B. Benjamin, "Investigation of Asphalt Pavement Mixture Blending Utilizing Analytical Chemistry Techniques," 2013.
- [227] J. Lamontagne, P. Dumas, V. Mouillet, and J. Kister, "Comparison by Fourier transform infrared (FTIR) spectroscopy of different ageing techniques: application to road bitumens," *Fuel*, vol. 80, no. 4, pp. 483-488, 2001, doi: [https://doi.org/10.1016/S0016-2361\(00\)00121-6](https://doi.org/10.1016/S0016-2361(00)00121-6).
- [228] B. Hofko *et al.*, "FTIR spectral analysis of bituminous binders: reproducibility and impact of ageing temperature," *Materials and Structures/Materiaux et Constructions*, vol. 51, no. 2, 2018, doi: 10.1617/s11527-018-1170-7.
- [229] C. P. Joseph, "A Review of the Fundamentals of Asphalt Oxidation: Chemical, Physicochemical, Physical Property, and Durability Relationships," *Transportation research circular*, 2009.
- [230] X. Yang, Z. You, and J. Mills-Beale, "Asphalt Binders Blended with a High Percentage of Biobinders: Aging Mechanism Using FTIR and Rheology," *Journal of Materials in Civil Engineering*, vol. 27, no. 4, p. 04014157, 2015, doi: 10.1061/(ASCE)MT.1943-5533.0001117.
- [231] BSOL, *BS EN 1426:2015 Bitumen and bituminous binders. Determination of needle penetration.*, 2015.
- [232] L. Noferini, "Performance and durability of asphalt mixtures made with RAP," 2016.
- [233] J.C. Petersen *et al.*, "Binder Characterisation and Evaluation Volume 4: Test Methods," 4 ed: SHRP-A-370, Strategic Highways Research Program, National Research Council, Washington, DC., 1994.
- [234] S. Nizamuddin, H. A. Baloch, M. Jamal, S. Madapusi, and F. Giustozzi, "Performance of waste plastic bio-oil as a rejuvenator for asphalt binder," *Science of The Total Environment*, vol. 828, p. 154489, 2022, doi: <https://doi.org/10.1016/j.scitotenv.2022.154489>.
- [235] R. Zhang, Z. You, H. Wang, M. Ye, and Y. K. Yap, "The impact of bio-oil as rejuvenator for aged asphalt binder," *Construction and Building Materials*, vol. 196, pp. 134-143, 2019, doi: 10.1016/j.conbuildmat.2018.10.168.
- [236] M. Kraus, M. Niederwald, M. Dr.-Ing, and G. Siebert, "Rheological modelling of linear viscoelastic materials for strengthening in bridge engineering," 2016.
- [237] BSOL, *BS EN 14770 Bitumen and bituminous binders - Determination of complex shear modulus and phase angle - Dynamic Shear Rheometer (DSR.)*, 2012.
- [238] J. D. B. Carrión, "Design and characterisation of reclaimed asphalt mixtures with biobinders," *Thesis*, University of Nottingham, 2017.
- [239] Y. Gao, L. Li, and Y. Zhang, "Modeling Crack Propagation in Bituminous Binders under a Rotational Shear Fatigue Load using Pseudo J-Integral Paris' Law," *Transportation Research Record: Journal of the*

- Transportation Research Board*, vol. 2674, 2020, doi: <https://doi.org/10.1177/0361198119899151>.
- [240] BSOL, *BS EN 12607 Bitumen and bituminous binders. Determination of the resistance to hardening under influence of heat and air. RTFOT method.*, 2014.
- [241] G. D. Airey, "State of the Art Report on Ageing Test Methods for Bituminous Pavement Materials," *International Journal of Pavement Engineering*, vol. 4, no. 3, pp. 165-176, 2003, doi: 10.1080/1029843042000198568.
- [242] BSOL, *BS EN 14769 Bitumen and bituminous binders. Accelerated long-term ageing conditioning by a Pressure Ageing Vessel (PAV).*, 2012.
- [243] R. S. Souza, L. L. Y. Visconte, A. L. N. Da Silva, and V. G. Costa, "Thermal and Rheological Formulation and Evaluation of Synthetic Bitumen from Reprocessed Polypropylene and Oil," *International Journal of Polymer Science*, 2018, doi: 10.1155/2018/7940857.
- [244] I. Mahali and C. Sahoo, "Rheological characterization of Nanocomposite modified asphalt binder," *International Journal of Pavement Research and Technology*, vol. 12, pp. 589-594, 2019, doi: 10.1007/s42947-019-0070-8.
- [245] G. D. Airey, J. R. A. Grenfell, A. Apeageyi, A. Subhy, and D. Lo Presti, "Time dependent viscoelastic rheological response of pure, modified and synthetic bituminous binders," *Mechanics of Time-Dependent Materials*, vol. 20, no. 3, pp. 455-480, 2016, doi: 10.1007/s11043-016-9295-y.
- [246] N. I. M. Yusoff, "Modelling the Linear Viscoelastic Rheological Properties of Bituminous Binders," *Thesis*, University of Nottingham, 2012.
- [247] E. Santagata, O. Baglieri, L. Tsantilis, and D. Dalmazzo, "Rheological Characterization of Bituminous Binders Modified with Carbon Nanotubes," *Procedia - Social and Behavioral Sciences*, vol. 53, pp. 546-555, 2012, doi: <https://doi.org/10.1016/j.sbspro.2012.09.905>.
- [248] G. Airey, "Use of Black Diagrams to Identify Inconsistencies in Rheological Data," *Road Materials and Pavement Design*, vol. 3, pp. 403-424, 2002, doi: 10.1080/14680629.2002.9689933.
- [249] H. Wang, X. Liu, P. Apostolidis, and T. Scarpas, "Non-Newtonian Behaviors of Crumb Rubber-Modified Bituminous Binders," *Applied Sciences*, vol. 8, no. 10, doi: 10.3390/app8101760.
- [250] G. a. I. M. Mazurek, "Relaxation Modulus of SMA with Polymer Modified and Highly Polymer Modified Bitumen," *Procedia Engineering*, vol. 172, pp. 731-738, 12 2017, doi: 10.1016/j.proeng.2017.02.093.
- [251] N. Saboo and P. Kumar, "Use of flow properties for rheological modeling of bitumen," *International Journal of Pavement Research and Technology*, vol. 9, 2016, doi: 10.1016/j.ijprt.2016.01.005.
- [252] L. Shan, Y. Tan, and Y. Richard Kim, "Applicability of the Cox–Merz relationship for asphalt binder," *Construction and Building Materials*, vol. 37, pp. 716-722, 2012, doi: <https://doi.org/10.1016/j.conbuildmat.2012.07.020>.
- [253] R. Marroquin-Garcia, N. Leone, L. G. D. Hawke, D. Romano, C. H. R. M. Wilsens, and S. Rastogi, "Suppression in Melt Viscosity of the Homogeneously Mixed Blends of Polypropylene (iPP–UHMWiPP) in the Presence of an Oxalamide," *Macromolecules*, vol. 55, no. 7, pp. 2574-2587, 2022, doi: 10.1021/acs.macromol.1c02042.

- [254] BSOL, *BS EN 16659 Bitumen and Bituminous Binders. Multiple Stress Creep and Recovery Test (MSCRT)*., 2016.
- [255] J. Yu, Z. Ren, Z. Gao, Q. Wu, Z. Zhu, and H. Yu, "Recycled Heavy Bio Oil as Performance Enhancer for Rubberized Bituminous Binders," *Polymers*, vol. 11, no. 5, p. 800, 2019, doi: 10.3390/polym11050800.
- [256] *ASTM D6373-16 Specification for Performance Graded Asphalt Binder*., 2016.
- [257] F. L. Roberts, P. S. Kandhal, E. R. Brown, D. Y. Lee, and T. W. Kennedy, "Hot Mix Asphalt Materials, Mixture Design, and Construction," *National Asphalt Pavement Association Research and Education Foundation*, ed. 2, 1996.
- [258] Y. Li *et al.*, "Anti-rutting performance evaluation of modified asphalt binders: A review," *Journal of Traffic and Transportation Engineering (English Edition)*, vol. 8, no. 3, pp. 339-355, 2021, doi: <https://doi.org/10.1016/j.jtte.2021.02.002>.
- [259] Y. Sun, J.-C. Yue, R. Wang, R.-X. Li, and D.-C. Wang, "Investigation of the Effects of Evaporation Methods on the High-Temperature Rheological and Fatigue Performances of Emulsified Asphalt Residues," *Advances in Materials Science and Engineering*, vol. 2020, pp. 1-12, 2020, doi: 10.1155/2020/4672413.
- [260] H. Hanson, M. Zeng, H. Zhai, M. Khatri, and R. Anderson, "Characterization of Modified Asphalt Binders in Superpave Mix Design," TRB, National Research Council, Washington, D. C., 2001.
- [261] Y. Zhang and Y. Gao, "Predicting crack growth in viscoelastic bitumen under a rotational shear fatigue load," *Road Materials and Pavement Design*, pp. 1-20, 2019, doi: 10.1080/14680629.2019.1635516.
- [262] C. M. Johnson, "Estimating asphalt binder fatigue resistance using an accelerated test method," *Thesis*, University of Nottingham, 2010.
- [263] C. Hintz and H. Bahia, "Simplification of linear amplitude sweep test and specification parameter," *Transportation Research Record*, 2013, doi: 10.3141/2370-02.
- [264] L. Li, Y. Gao, and Y. Zhang, "Fatigue cracking characterisations of waste-derived bitumen based on crack length," *International Journal of Fatigue*, vol. 142, p. 105974, 2021, doi: <https://doi.org/10.1016/j.ijfatigue.2020.105974>.
- [265] K. Blazejowski, M. Wójcik-Wiśniewska, W. Baranowska, P. Ostrowski, R. Černý, and P. Jisa, "Fatigue Performance of Bituminous Binders Tested by Linear Amplitude Sweep Test," in *The 5th International Symposium on Asphalt Pavements & Environment (APE)*, p. 385-394, 2020, doi: 10.1007/978-3-030-29779-4_38.
- [266] A. Foroutan Mirhosseini, A. Kavussi, M. H. Jalal Kamali, M. M. Khabiri, and A. Hassani, "Evaluating fatigue behavior of asphalt binders and mixes containing Date Seed Ash," *Journal of Civil Engineering and Management*, vol. 23, no. 8, pp. 1164-1175, 2017, doi: 10.3846/13923730.2017.1396560.
- [267] N. Tabatabaee and H. A. Tabatabaee, "Multiple Stress Creep and Recovery and Time Sweep Fatigue Tests: Crumb Rubber Modified Binder and Mixture Performance," *Transportation Research Record*, vol. 2180, no. 1, pp. 67-74, 2010, doi: 10.3141/2180-08.

- [268] EAPA, "Industry Statement on the recycling of asphalt mixes and use of waste of asphalt pavements," in *European Asphalt Pavement Association*, Brussels, Belgium, 2005.
- [269] G. D. Airey, A. C. Collop, S. E. Zoorob, and R. C. Elliott, "The influence of aggregate, filler and bitumen on asphalt mixture moisture damage," *Construction and Building Materials*, vol. 22, no. 9, pp. 2015-2024, 2008, doi: <https://doi.org/10.1016/j.conbuildmat.2007.07.009>.
- [270] I. Widyatmoko, "Mechanistic-empirical mixture design for hot mix asphalt pavement recycling," *Construction and Building Materials*, vol. 22, no. 2, pp. 77-87, 2008, doi: <https://doi.org/10.1016/j.conbuildmat.2006.05.041>.
- [271] A. Sreeram, Z. Leng, R. K. Padhan, and X. Qu, "Eco-friendly paving materials using waste PET and reclaimed asphalt pavement," *HKIE Transactions*, vol. 25, no. 4, pp. 237-247, 2018, doi: 10.1080/1023697X.2018.1534617.
- [272] T. Baghaee Moghaddam, M. Soltani, and M. R. Karim, "Experimental characterization of rutting performance of Polyethylene Terephthalate modified asphalt mixtures under static and dynamic loads," *Construction and Building Materials*, vol. 65, pp. 487-494, 2014, doi: <https://doi.org/10.1016/j.conbuildmat.2014.05.006>.
- [273] C. Toth and J. Ureczky, "Determination of master curves for asphalt mixtures by means of IT-CY tests¹," *Periodica Polytechnica Civil Engineering*, vol. 54, p. 137, 2010, doi: 10.3311/pp.ci.2010-2.09.
- [274] F. Zhang, L. Wang, C. Li, and Y. Xing, "Predict the Phase Angle Master Curve and Study the Viscoelastic Properties of Warm Mix Crumb Rubber-Modified Asphalt Mixture," *Materials*, vol. 13, p. 5051, 2020, doi: 10.3390/ma13215051.
- [275] M. Pasetto, A. Baliello, E. Pasquini, and L. Poulikakos, "Dry Addition of Recycled Waste Polyethylene in Asphalt Mixtures: A Laboratory Study," (in eng), *Materials (Basel)*, vol. 15, no. 14, 2022, doi: 10.3390/ma15144739.
- [276] R. A. Schapery, "Correspondence principles and a generalized J integral for large deformation and fracture analysis of viscoelastic media," *International Journal of Fracture*, vol. 25, no. 3, pp. 195-223, 1984, doi: 10.1007/BF01140837.
- [277] G. D. Airey, "Fundamental Binder and Practical Mixture Evaluation of Polymer Modified Bituminous Materials," *International Journal of Pavement Engineering*, vol. 5, no. 3, pp. 137-151, 2004, doi: 10.1080/10298430412331314146.
- [278] J. M. Gibb, "Evaluation of resistance to permanent deformation in the design of bituminous paving mixtures," *Thesis*, University of Nottingham, 1998.
- [279] A. V. Tiwari and Y. R. M. Rao, "Study of plastic waste mixed bituminous concrete using dry process for road construction," *Selected Scientific Papers - Journal of Civil Engineering*, vol. 13, no. 1, pp. 105-112, 2019, doi: 10.1515/sspjce-2018-0024.
- [280] N. Mohd Shukry *et al.*, "Effect of various filler types on the properties of porous asphalt mixture," *IOP Conference Series: Materials Science and Engineering*, vol. 342, p. 012036, 2018, doi: 10.1088/1757-899X/342/1/012036.

- [281] S.M. Al-Salem and A. Dutta, "Wax Recovery from the Pyrolysis of Virgin and Waste Plastics," *Industrial & Engineering Chemistry Research*, vol. 60, no. 22, pp. 8301-8309, 2021, doi: 10.1021/acs.iecr.1c01176.
- [282] F. J. Mastral, E. Esperanza, C. Berrueco, M. Juste, and J. Ceamanos, "Fluidized bed thermal degradation products of HDPE in an inert atmosphere and in air–nitrogen mixtures," *Journal of Analytical and Applied Pyrolysis*, vol. 70, no. 1, pp. 1-17, 2003, doi: [https://doi.org/10.1016/S0165-2370\(02\)00068-2](https://doi.org/10.1016/S0165-2370(02)00068-2).
- [283] J.J. Park, K. Park, J.W. Park, and D. C. Kim, "Characteristics of LDPE pyrolysis," *Korean Journal of Chemical Engineering*, vol. 19, no. 4, pp. 658-662, 2002, doi: 10.1007/BF02699313.
- [284] R.W.J. Westerhout, J. Kuipers, and V. Swaij, "Experimental Determination of the Yield of Pyrolysis Products of Polyethylene and Polypropene. Influence of Reaction Conditions," *Industrial & Engineering Chemistry Research*, vol. 37, pp. 841-847, 1998.
- [285] L.M. Lund, P.M.L. Sandercock, G.J. Basara, and C. C. Austin, "Investigation of various polymeric materials for set-point temperature calibration in pyrolysis-gas chromatography-mass spectrometry (Py-GC-MS)," *Journal of Analytical and Applied Pyrolysis*, vol. 82, no. 1, pp. 129-133, 2008, doi: 10.1016/j.jaap.2008.02.002.
- [286] M.D.R. Hernández, A. Gómez, A.N. García, J. J. Agulló, and A. Marcilla, "Effect of the temperature in the nature and extension of the primary and secondary reactions in the thermal and HZSM-5 catalytic pyrolysis of HDPE," *Applied Catalysis A: General*, vol. 317, no. 2, pp. 183-194, 2007, doi: <https://doi.org/10.1016/j.apcata.2006.10.017>.
- [287] P. T. Williams and E. A. Williams, "Interaction of Plastics in Mixed-Plastics Pyrolysis," *Energy & Fuels*, vol. 13, no. 1, pp. 188-196, 1999, doi: 10.1021/ef980163x.
- [288] J. F. Mastral, C. Berrueco, and J. Ceamanos, "Theoretical prediction of product distribution of the pyrolysis of high density polyethylene," *Journal of Analytical and Applied Pyrolysis*, vol. 80, no. 2, pp. 427-438, 2007, doi: <https://doi.org/10.1016/j.jaap.2006.07.009>.
- [289] S.F. Ghasr and H. Abedini, "Predicting the distribution of thermal pyrolysis of high density polyethylene products using a mechanistic model," *Modeling Earth Systems and Environment*, vol. 3, no. 1, p. 40, 2017, doi: 10.1007/s40808-017-0309-9.
- [290] M. Seeger and E. M. Barrall, "Pyrolysis–gas chromatographic analysis of chain branching in polyethylene," *Journal of Polymer Science: Polymer Chemistry Edition*, vol. 13, no. 7, pp. 1515-1529, 1975, doi: 10.1002/pol.1975.170130704.
- [291] R. Miandad *et al.*, "Catalytic pyrolysis of plastic waste: Moving toward pyrolysis based biorefineries," *Frontiers in Energy Research*, vol. 7, pp. 1-27, 2019, doi: 10.3389/fenrg.2019.00027.
- [292] A. Dwivedi, "Studies In Properties Of Different Waxes Using DSC And Correlating These With The Properties Obtained by Conventional Methods.," in *CHEMCON*, Haldia West Bengal, 2017, p. 7.
- [293] S.J. Purohit and M. Pradhan, "Paraffin Oxidation Studies," *International Journal of Engineering Innovations and Research* vol. 2, no. 1, p. 75, 2013.

- [294] P. E. Savage, "Mechanisms and kinetics models for hydrocarbon pyrolysis," *Journal of Analytical and Applied Pyrolysis*, vol. 54, no. 1, pp. 109-126, 2000, doi: [https://doi.org/10.1016/S0165-2370\(99\)00084-4](https://doi.org/10.1016/S0165-2370(99)00084-4).
- [295] X. Liu, *Organic Chemistry I*. Kwantlen Polytechnic University, 2021, p. Chapter 10.6.
- [296] S. C. Moldoveanu, "Chapter 6 - Pyrolysis of Peroxy Compounds," in *Pyrolysis of Organic Molecules (Second Edition)*, S. C. Moldoveanu Ed.: Elsevier, 2019, pp. 311-319.
- [297] H. Lee *et al.*, "Laboratory Evaluation and Field Implementation of Polyethylene Wax-Based Warm Mix Asphalt Additive in USA," *International Journal of Pavement Research and Technology*, vol. 6, no. 5, 2013.
- [298] L. Shang, S. Wang, Y. Zhang, and Y. Zhang, "Pyrolyzed wax from recycled cross-linked polyethylene as warm mix asphalt (WMA) additive for SBS modified asphalt," *Construction and Building Materials*, vol. 25, no. 2, pp. 886-891, 2011, doi: <https://doi.org/10.1016/j.conbuildmat.2010.06.097>.
- [299] H. Kim, K.-D. Jeong, M. Lee, and S.-J. Lee, "Effect of FT Paraffin Wax Contents on Performance Properties of Crumb Rubber–Modified Asphalt Binders," *Journal of Materials in Civil Engineering*, vol. 27, p. 04015011, 2015, doi: 10.1061/(ASCE)MT.1943-5533.0001267.
- [300] A. M. Rodríguez-Alloza, J. Gallego, and I. Pérez, "Study of the effect of four warm mix asphalt additives on bitumen modified with 15% crumb rubber," *Construction and Building Materials*, vol. 43, pp. 300-308, 2013, doi: <https://doi.org/10.1016/j.conbuildmat.2013.02.025>.
- [301] H. Fazaeli, A. A. Amini, F. M. Nejad, and H. Behbahani, "Rheological properties of bitumen modified with a combination of FT paraffin wax (sasobit®) and other additives," *Journal of Civil Engineering and Management*, vol. 22, no. 2, pp. 135-145, 2016, doi: 10.3846/13923730.2014.897977.
- [302] Y. Edwards, Y. Tasdemir, and U. Isacsson, "Rheological effects of commercial waxes and polyphosphoric acid in bitumen 160/220 – high and medium temperature performance," *Construction and Building Materials*, vol. 21, no. 10, pp. 1899-1908, 2007, doi: <https://doi.org/10.1016/j.conbuildmat.2006.07.012>.
- [303] U. Sahib, Z. Syed Bilal Ahmed, and A. Akhlaq, "Evaluating the Properties of Bio-oil Modified Bitumen Derived from Cotton Stalk Waste," in *Proceedings of the International Conference on Engineering, Technology and Social Science (ICONETOS 2020)*, 2021: Atlantis Press, pp. 599-606, doi: <https://doi.org/10.2991/assehr.k.210421.087>.
- [304] J. Gao, H. Wang, Z. You, M. R. M. Hasan, Y. Lei, and M. Irfan, "Rheological behavior and sensitivity of wood-derived bio-oil modified asphalt binders," *Applied Sciences (Switzerland)*, 2018, doi: 10.3390/app8060919.
- [305] L. Jiqing Zhu, J. Lundberg, L. He and Guannan, "Extending the Black diagram of bitumen to three dimensions," *Construction and Building Materials*, vol. 349, p. 128727, 2022, doi: <https://doi.org/10.1016/j.conbuildmat.2022.128727>.
- [306] A. B. Bazyleva, M. D. A. Hasan, M. Fulem, M. Becerra, and J. M. Shaw, "Bitumen and Heavy Oil Rheological Properties: Reconciliation with

- Viscosity Measurements," *Journal of Chemical & Engineering Data*, vol. 55, no. 3, pp. 1389-1397, 2010, doi: 10.1021/je900562u.
- [307] R. Jing, A. Varveri, X. Liu, A. Scarpas, and S. Erkens, "Ageing effect on chemo-mechanics of bitumen," *Road Materials and Pavement Design*, vol. 22, no. 5, pp. 1044-1059, 2021, doi: 10.1080/14680629.2019.1661275.
- [308] M. Fakhri and M. A. Norouzi, "Rheological and ageing properties of asphalt bio-binders containing lignin and waste engine oil," *Construction and Building Materials*, vol. 321, p. 126364, 2022, doi: <https://doi.org/10.1016/j.conbuildmat.2022.126364>.
- [309] A. Zaltuom, "A Review Study of The Effect of Air Voids on Asphalt Pavement Life," 2018, pp. 618-625.
- [310] E. R. Brown, "Density of Asphalt Concrete - How Much Is Needed?," in *The 69th Annual Meeting of the Transportation Research Board*, Washington, DC, 1990, vol. No. 90-3: National Center for Asphalt Technology.
- [311] I. John, R. Mugume, and L. Muhwezi, "Effect of Filler and Binder Contents on Air Voids in Hot-Mix Asphalt for Road Pavement Construction," *Open Journal of Civil Engineering*, vol. 11, pp. 255-289, 2021, doi: 10.4236/ojce.2021.113016.
- [312] E. Masad, E. Kassem, A. Chowdhury, and Z. You, "A Method for Predicting Asphalt Mixture Compacability and its Influence on Mechanical," 2023.
- [313] C. R. Foster, "A Study of Cessation Requirements for Constructing Hot Mix Asphalt Pavements," *Highway Research Board*, no. 316, pp. 70-75, 1970.
- [314] Z. Ernest, "Compaction Studies of Asphalt Concrete Pavement as Related to the Water Permeability Test," *Highway Research Board bulletin*, 1962.
- [315] G. A. Huber and G. H. Heiman, "Effect of Asphalt Concrete Parameters on Rutting Performance: A Field Investigation," in *Association of Asphalt Paving Technologists*, vol. 56, pp. 33-61, 1987.
- [316] N. Bala, M. Napiah, and I. Kamaruddin, "Effect of nanosilica particles on polypropylene polymer modified asphalt mixture performance," *Case Studies in Construction Materials*, vol. 8, pp. 447-454, 2018, doi: <https://doi.org/10.1016/j.cscm.2018.03.011>.
- [317] G. W. Maupin, "Relationship of fatigue to the tensile stiffness of asphaltic concrete : final report on phase 1, laboratory investigation," (in English), Tech Report 1972.
- [318] Y. Ali, M. Irfan, S. Ahmed, and S. Ahmed, "Empirical Correlation of Permanent Deformation Tests for Evaluating the Rutting Response of Conventional Asphaltic Concrete Mixtures," *Journal of Materials in Civil Engineering*, 2017, doi: 10.1061/(ASCE)MT.1943-5533.0001888#sthash.vElbrHiP.dpuf.
- [319] S. Tayfur, H. Ozen, and A. Aksoy, "Investigation of rutting performance of asphalt mixtures containing polymer modifiers," *Construction and Building Materials*, vol. 21, no. 2, pp. 328-337, 2007, doi: <https://doi.org/10.1016/j.conbuildmat.2005.08.014>.
- [320] D. Gardete, L. P. Santos, and J. Pais, "Permanent Deformation Characterization of Bituminous Mixtures using Laboratory Tests," *Road*

- Materials and Pavement Design*, vol. 9, no. 3, pp. 537-547, 2008, doi: 10.1080/14680629.2008.9690132.
- [321] A. Mokhtari, H. Behbahani, and A. Ghortekola, "Effect of Commercial Wax and Typical Additives on Moisture Susceptibility of SMA Mixtures," *Journal of Applied Sciences*, vol. 11, pp. 3708-3716, 2011, doi: 10.3923/jas.2011.3708.3716.
- [322] F. Merusi, A. Caruso, R. Roncella, and F. Giuliani, "Moisture Susceptibility and Stripping Resistance of Asphalt Mixtures Modified with Different Synthetic Waxes," *Transportation Research Record*, vol. 2180, no. 1, pp. 110-120, 2010, doi: 10.3141/2180-13.
- [323] P. Georgiou and A. Loizos, "Characterization of Sustainable Asphalt Mixtures Containing High Reclaimed Asphalt and Steel Slag," (in eng), *Materials (Basel)*, vol. 14, no. 17, 2021, doi: 10.3390/ma14174938.
- [324] I. Al-Qadi *et al.*, "Determination of Usable Residual Asphalt Binder in RAP," 2023.

Appendices

Appendix A

The maximum density (BS EN 12697-5:2018), bulk density (BS EN 12697-33:2019) calculations with the resultant composition for each mixture.

- Formula for **Maximum Density (Mg/m³)** according to **BS EN 12697-5:2018:**

$$\rho_{mv} = \frac{m_2 - m_1}{10^6 x V_p - (m_3 - m_2) / \rho_w}$$

Where ρ_{mv} is maximum density (Mg/m³); m_1 is the mass of the empty pycnometer and head piece (g); m_2 is the mass of the sample, pycnometer and head piece (g); m_3 is the mass of the sample, pycnometer and water (g); V_p is the volume of the pycnometer (m³) and ρ_w is the density of the water at water bath temperature, 25.2 °C (0.9971 Mg/m³).

- Formulae for **Bulk Density** and **Mass of Slab**, according to BS EN 12697-33:2019:

$$V_A = 1 - \left(\frac{\rho_{mv}}{\rho_{bd}} \right)$$

Where V_A is air void content (%); ρ_{mv} is maximum density (Mg/m³) and ρ_{bd} is bulk density (Mg/m³). (In general, $\rho = m/V$.)

$$m_S = V_S x \rho_{mv} x \left(\frac{100 - V_A}{100} \right)$$

Where m_S is the slab mass (g); V_S is the slab mould volume (m³); ρ_{mv} is maximum density (Mg/m³) and V_A is the air void content (%). From this, the coated blend proportions of the mix components were determined, as can be seen in Table A1.

Table A1: Coated blend proportions for the control and test mixtures.

	A	B	C
RAP	0	0	20
14 mm	19.9	19.9	19.9
10 mm	30.4	30.4	24.7
6 mm	9.5	9.5	7.6
Dust	33.4	33.4	22.9
Limestone Filler	1.7	1.7	0.7
Binder	5.1	5.1	4.3

Appendix B

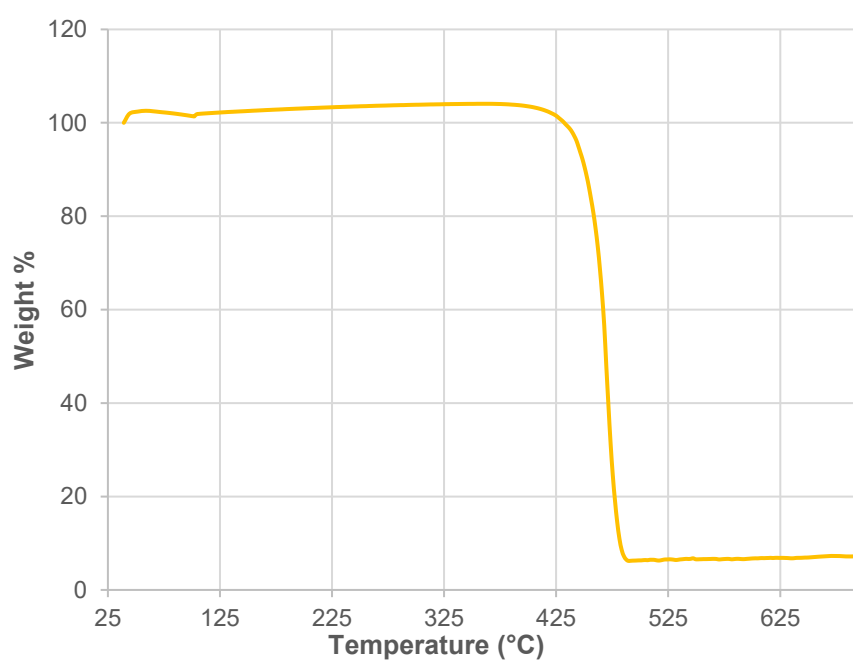
The distribution of air voids, determined by BS 12697-6 (Procedure B: Bulk density – Saturated Surface Dry) for mixture specimens.

Specimen ID	Control	PW	RAP+PW
A	8.3	7.2	6.9
B	7.7	9.1	7.2
C	7.1	7.7	7.4
D	8.3	7.4	7.2
E	7.8	8	7.2
F	7.4	7.8	7
G	7.4	8.2	6.6
H	6.9	8.8	6.7
I	8.2	8.5	7.8
J	7.9	8.2	7.3
K	7.8	9	7.9
L	8.1	7.7	8.3
M	7.8	7.9	7.3
N	7.8	7.9	6.5
O	7.4	8.2	6.9
P	7.4	7.6	7.8
Q	10.6	8.9	7.5

R	11	8.9	7.7
S	9.8	7.9	6.7
T	10	7.7	6.9

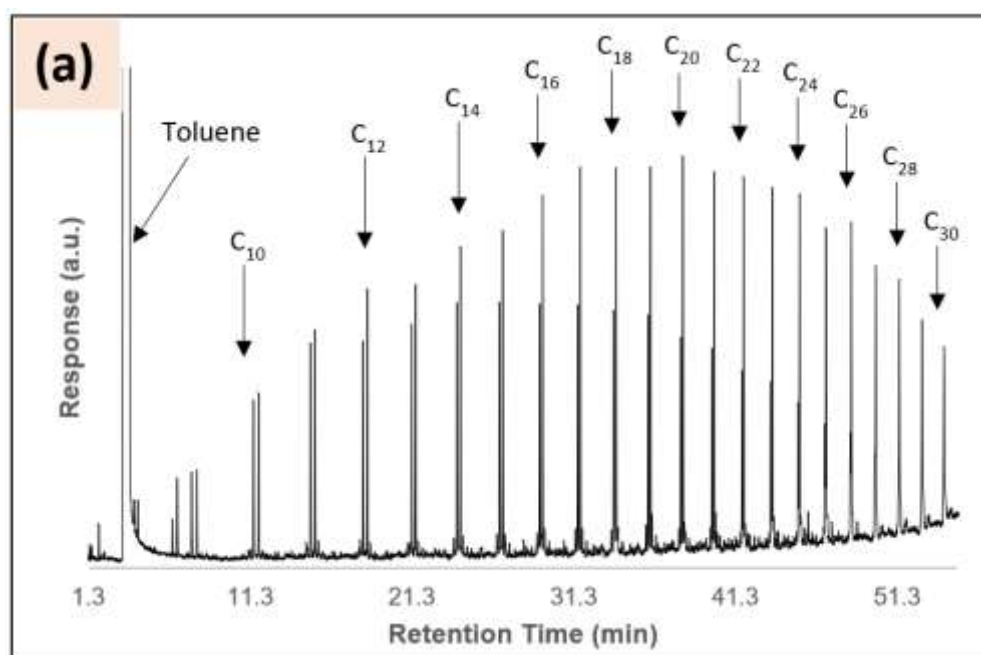
Appendix C

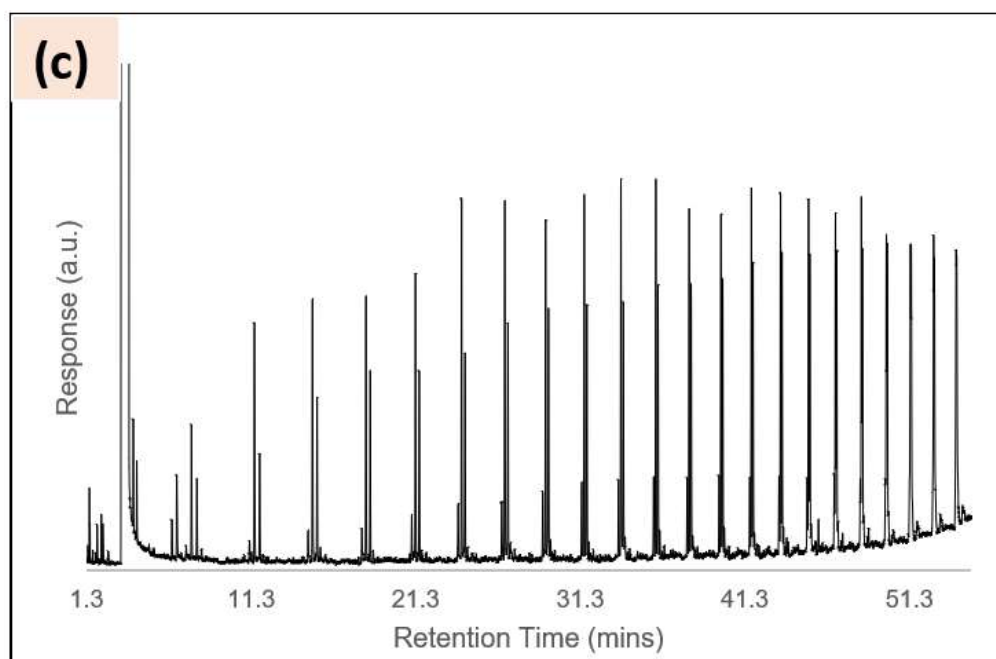
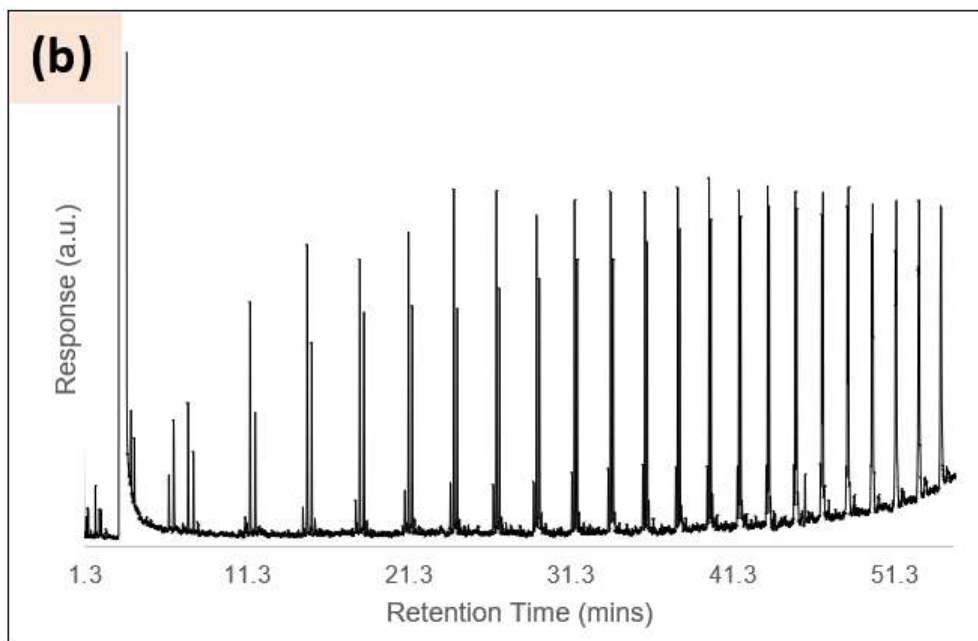
TGA results for HDPE pellets to determine an appropriate temperature range for thermal pyrolysis.

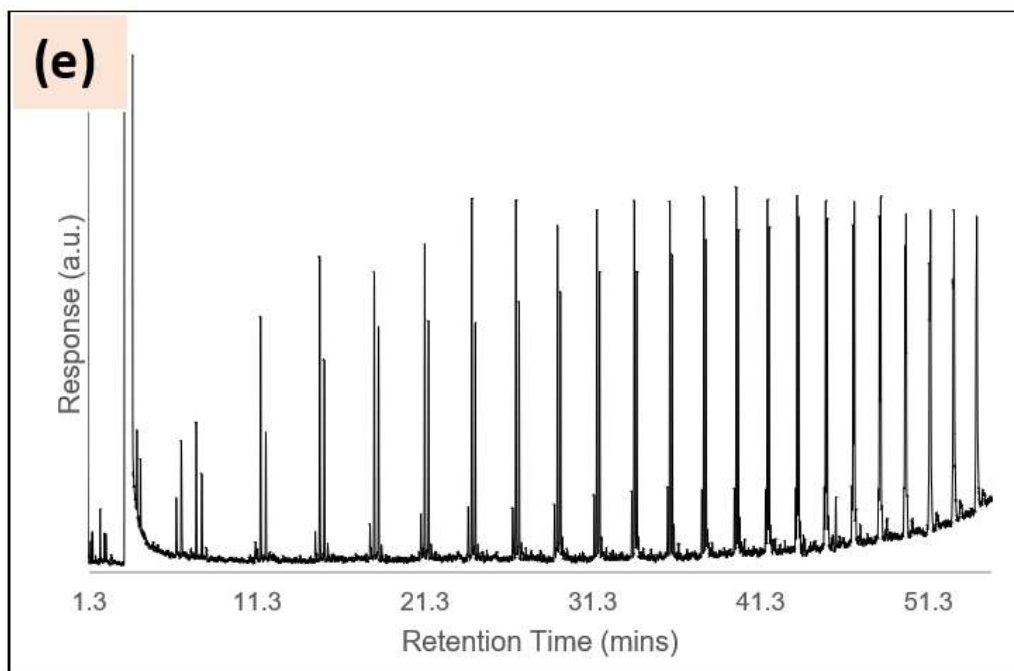
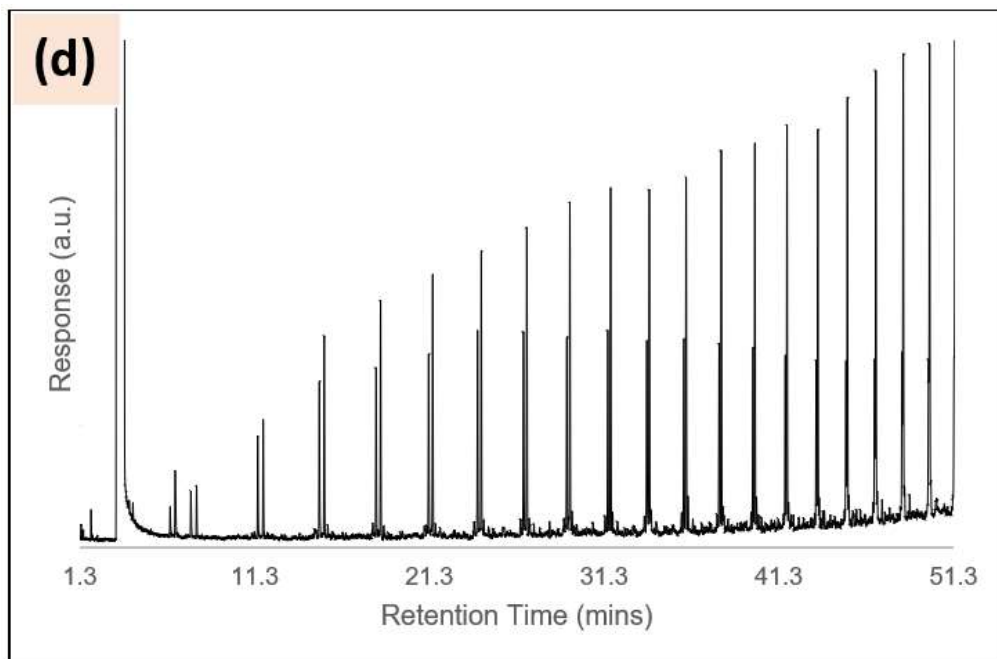


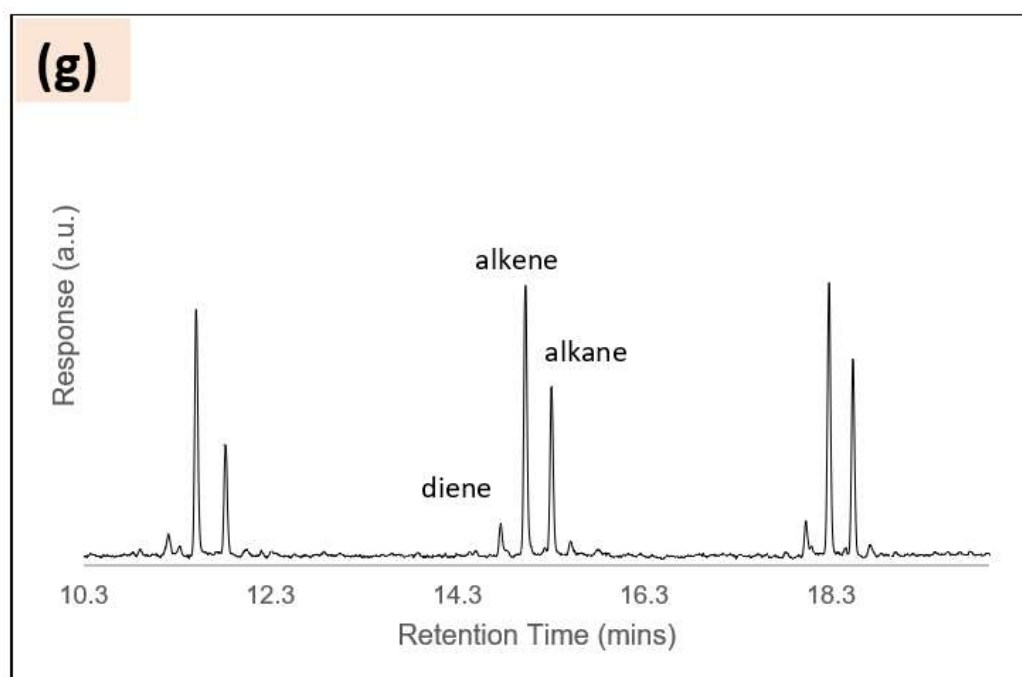
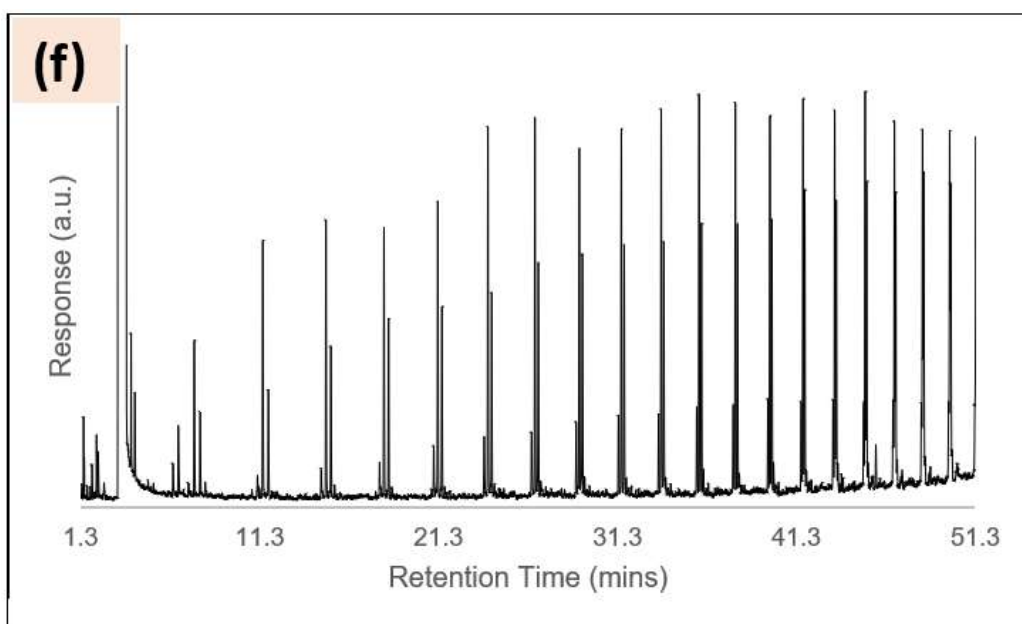
Appendix D

GC-MS chromatograms for (a) 450-2 (450 °C, 2 L/min N₂ flowrate) wax, (b) 500-2 (500 °C, 2 L/min N₂ flowrate) wax, (c) 550-2 (550 °C, 2 L/min N₂ flowrate) wax, (d) 450-4 (450 °C, 4 L/min N₂ flowrate) wax, (e) 500-4 (500 °C, 4 L/min N₂ flowrate) wax, (f) 550-4 (550 °C, 4 L/min N₂ flowrate) wax, (g) Chromatogram depicting homologous series of triplets which is indicative of PE depolymerisation.



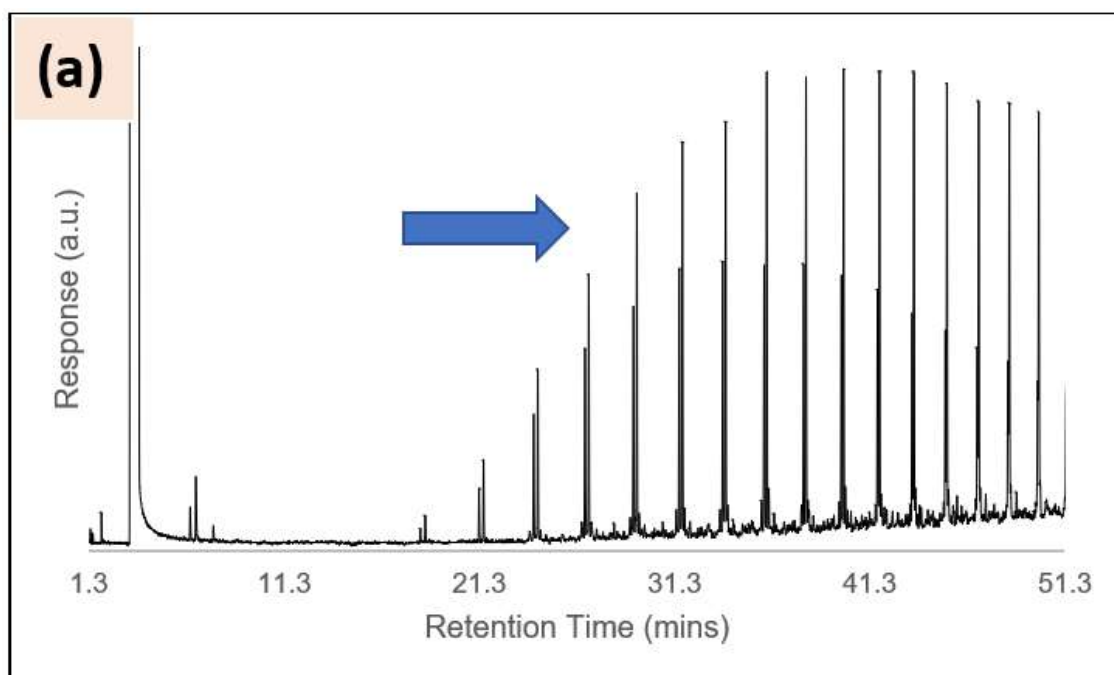


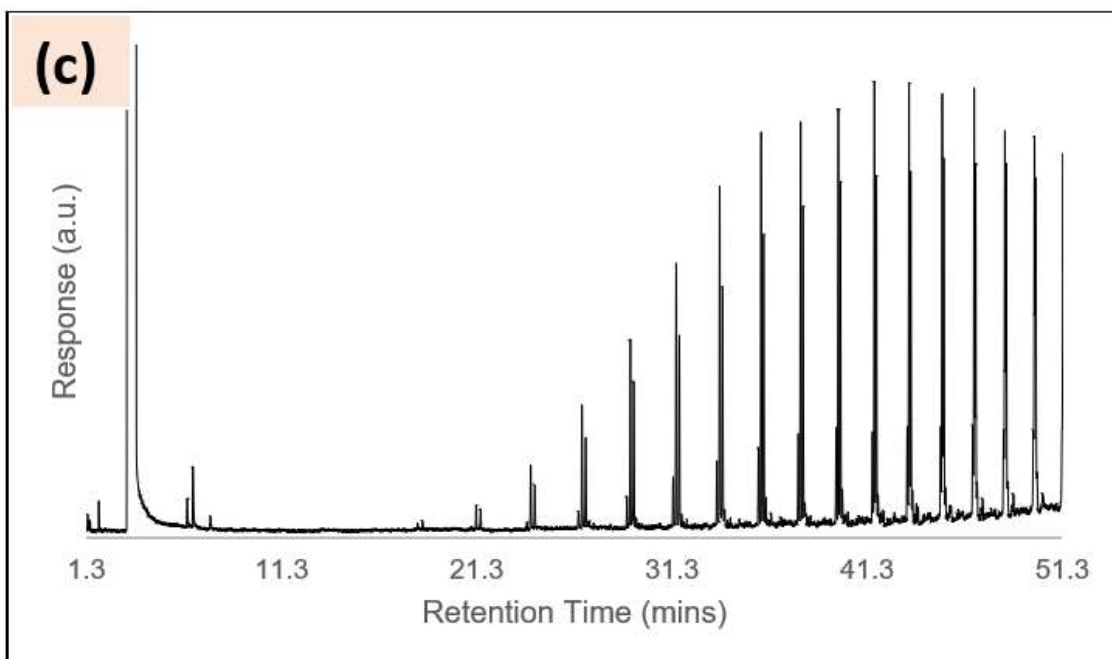
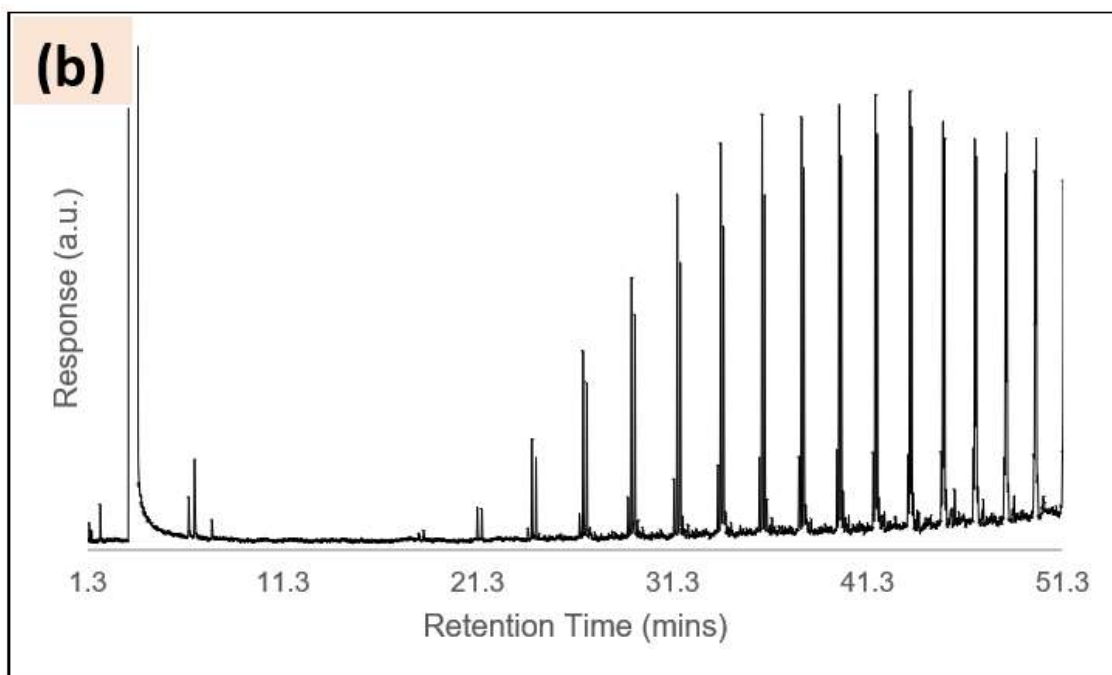


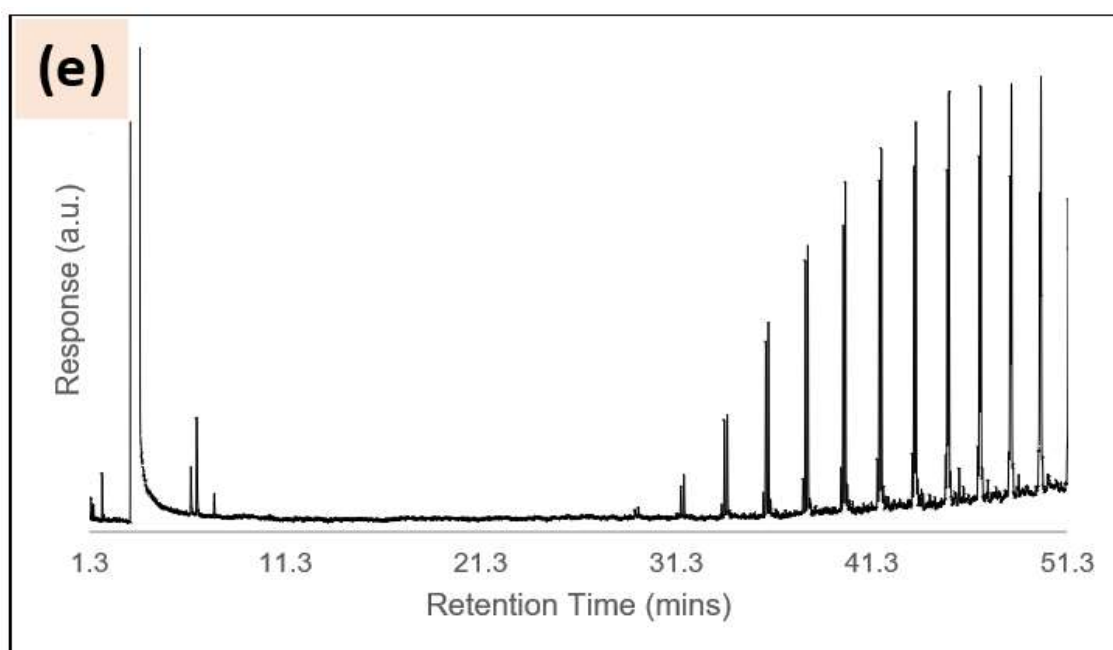
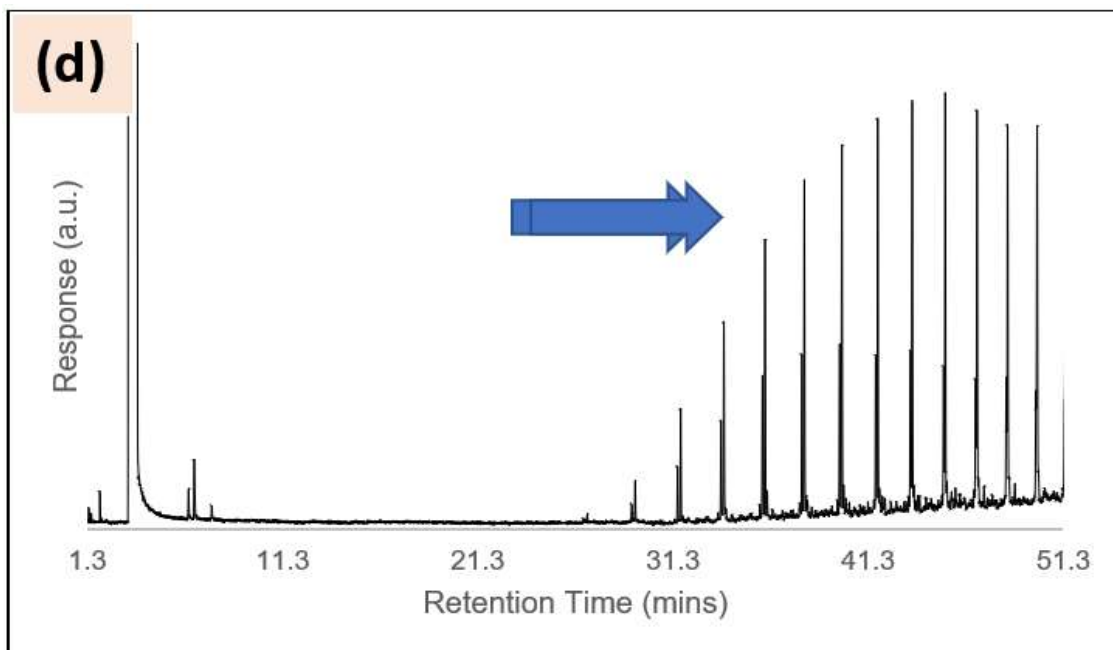


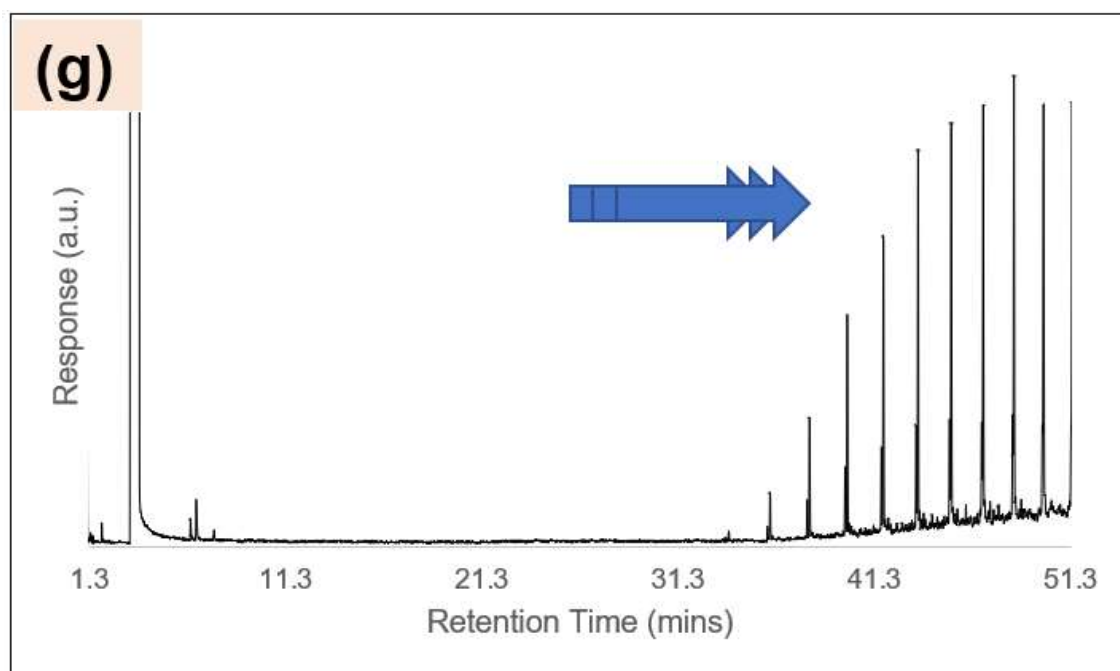
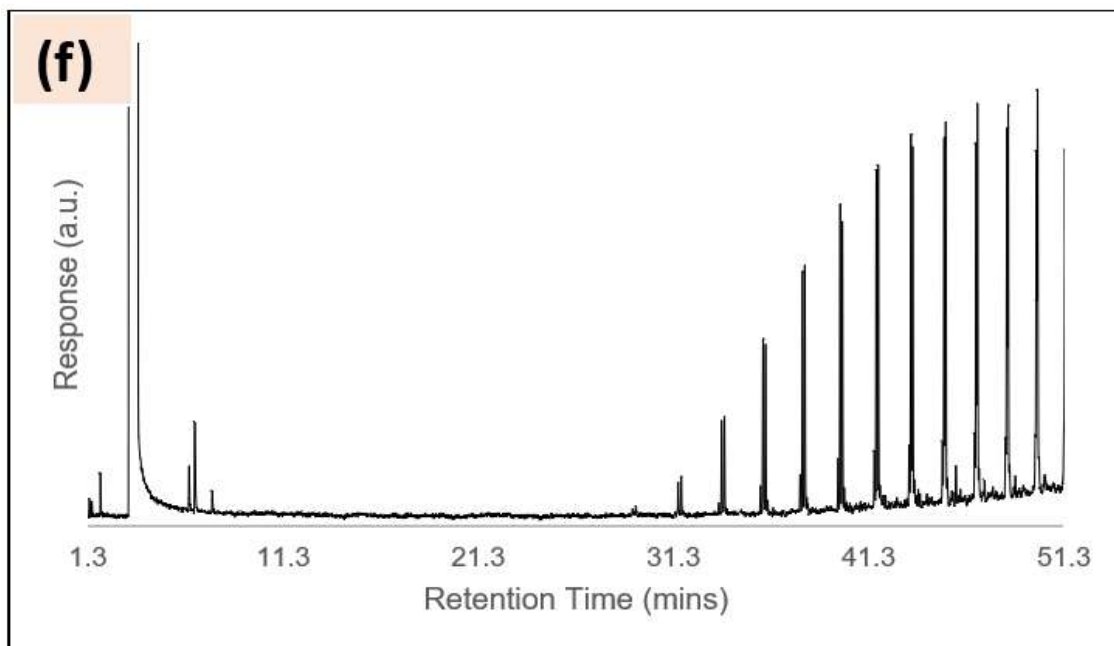
Appendix E

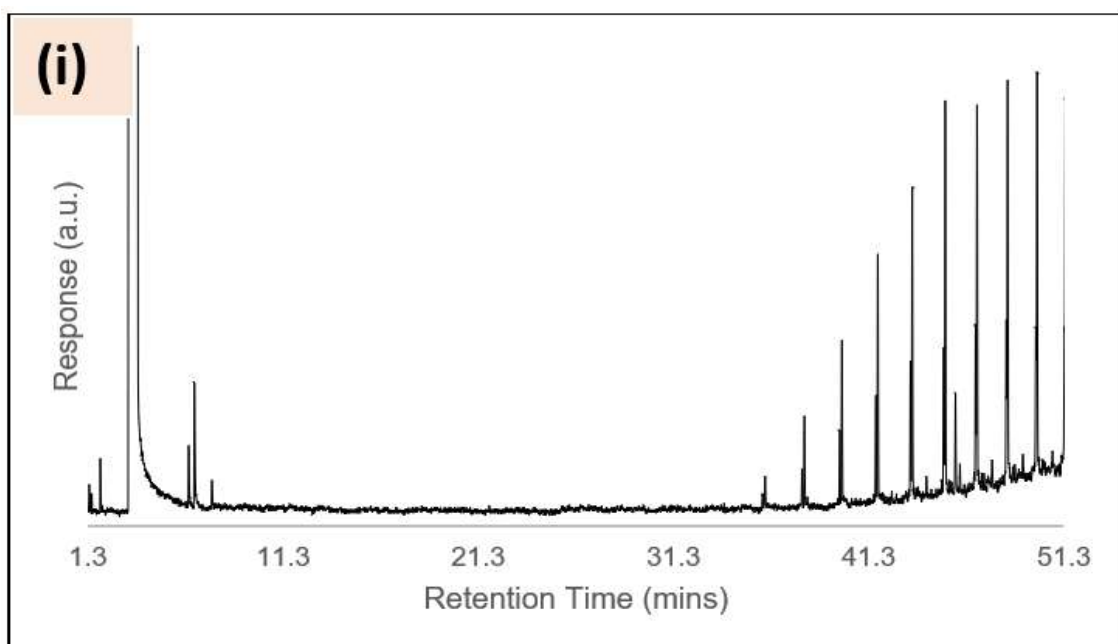
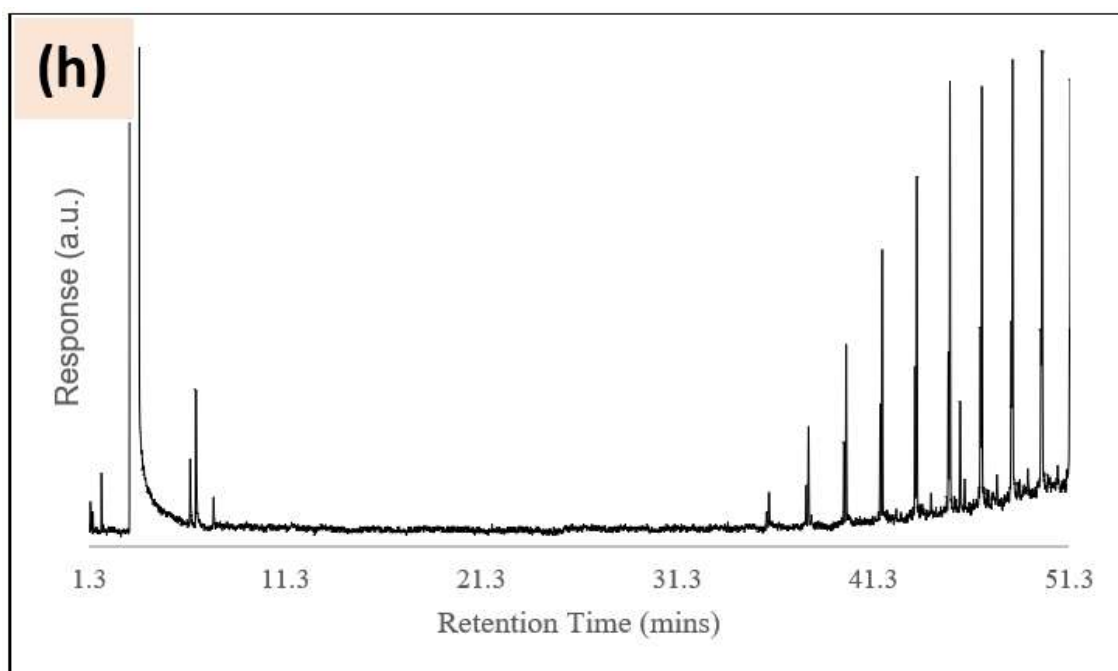
GC-MS chromatograms for (a) 450-2 wax, 1 hour @ 170°C, (b) 500-2 wax, 1 hour @ 170°C, (c) 550-2 wax, 1 hour @ 170°C, (d) 450-2 wax, 3 hours @ 170°C, (e) 500-2 wax, 3 hours @ 170°C, (f) 550-2 wax, 3 hours @ 170°C, (g) 450-2 wax, 6 hours @ 170°C, (h) 500-2 wax, 6 hours @ 170°C, (i) 550-2 wax, 6 hours @ 170°C, (j) Chromatogram depicting the alcohol and carbonyl containing compounds between triplets as a result of oxidation reactions.

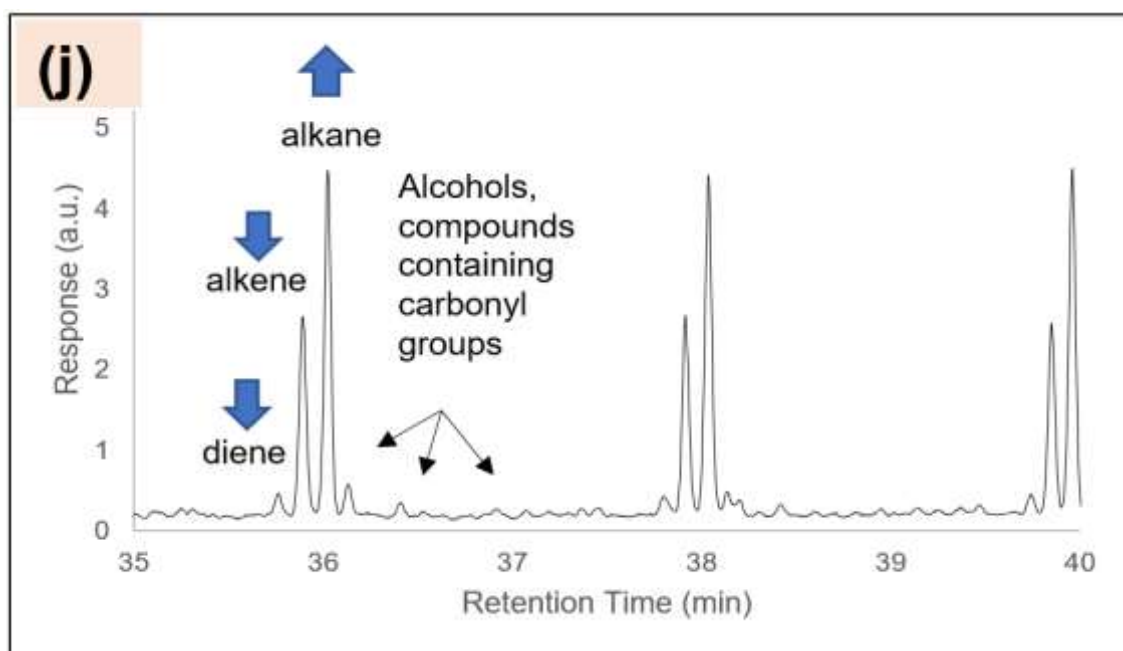






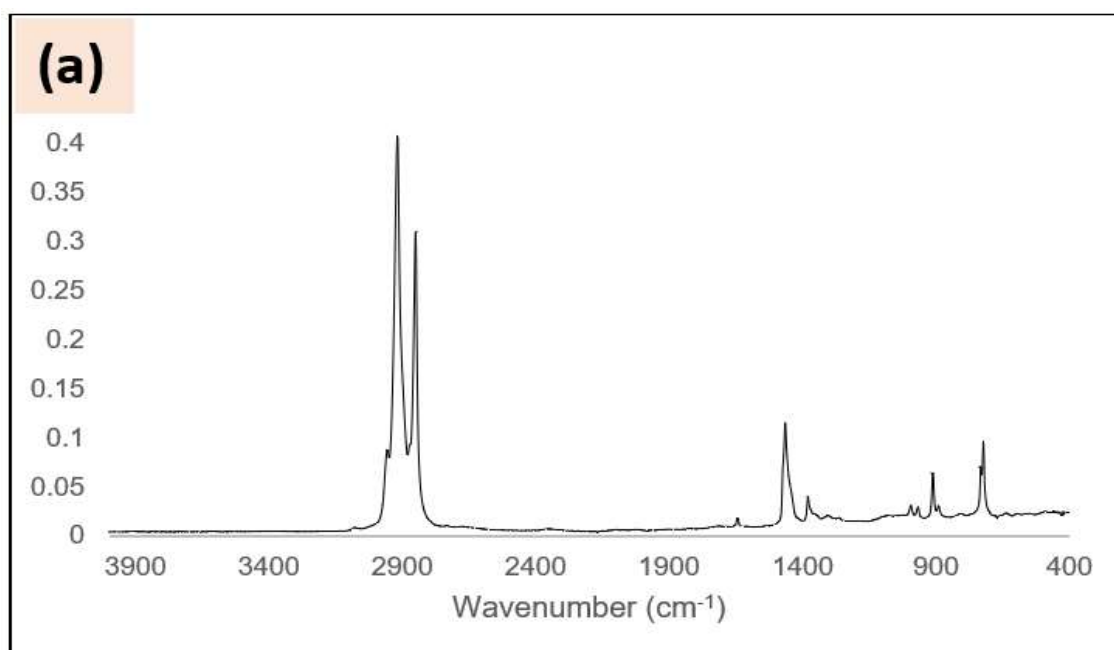


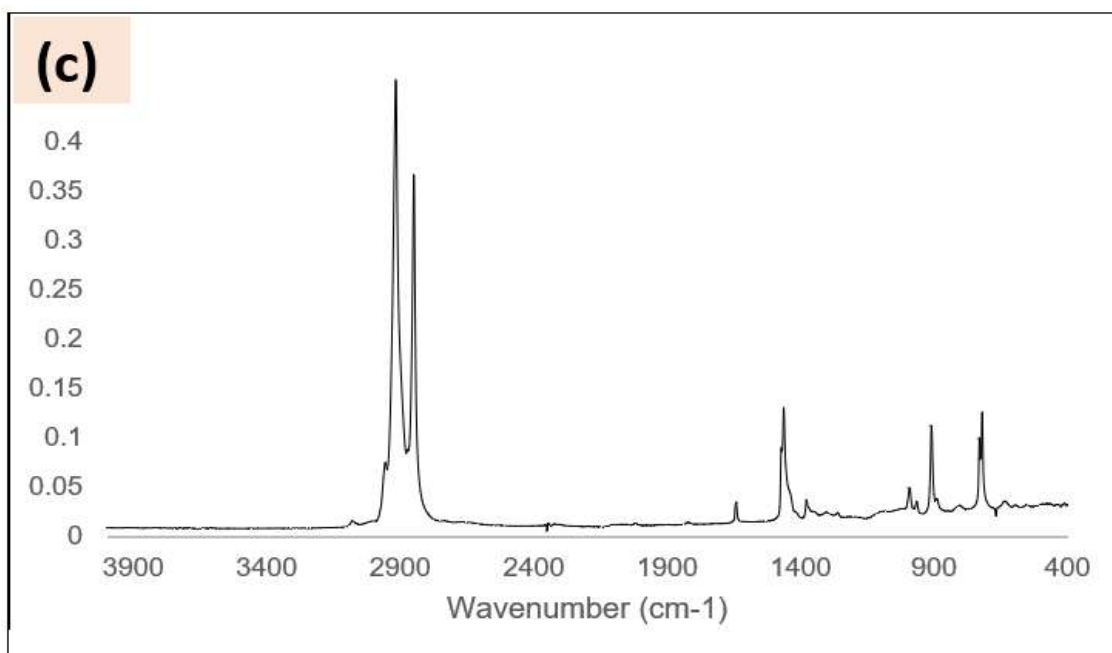
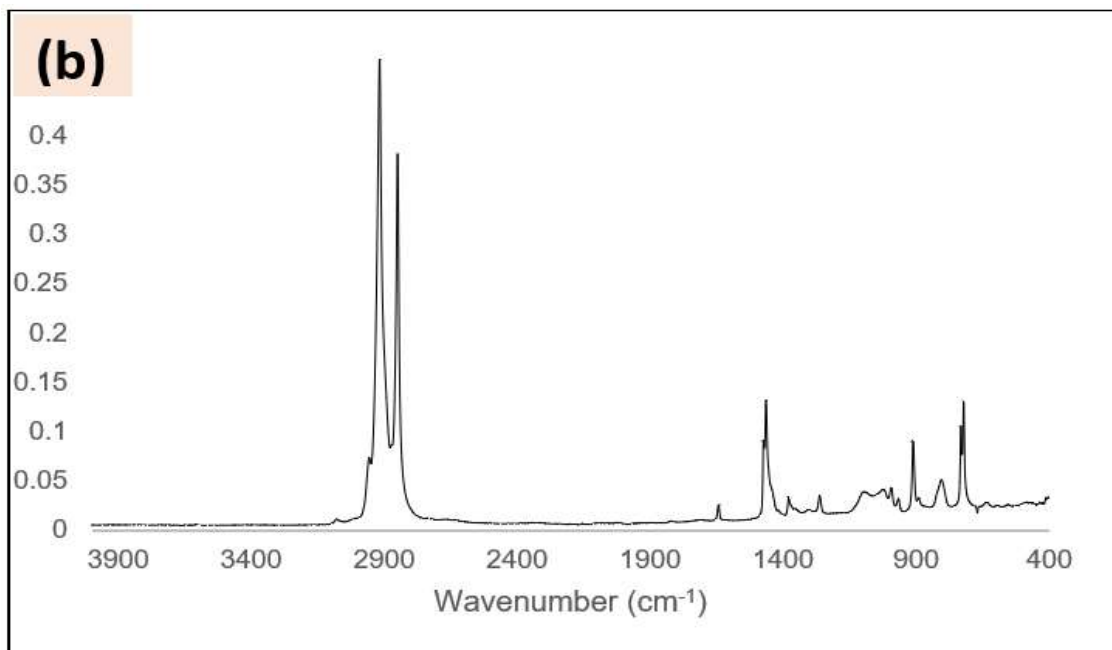


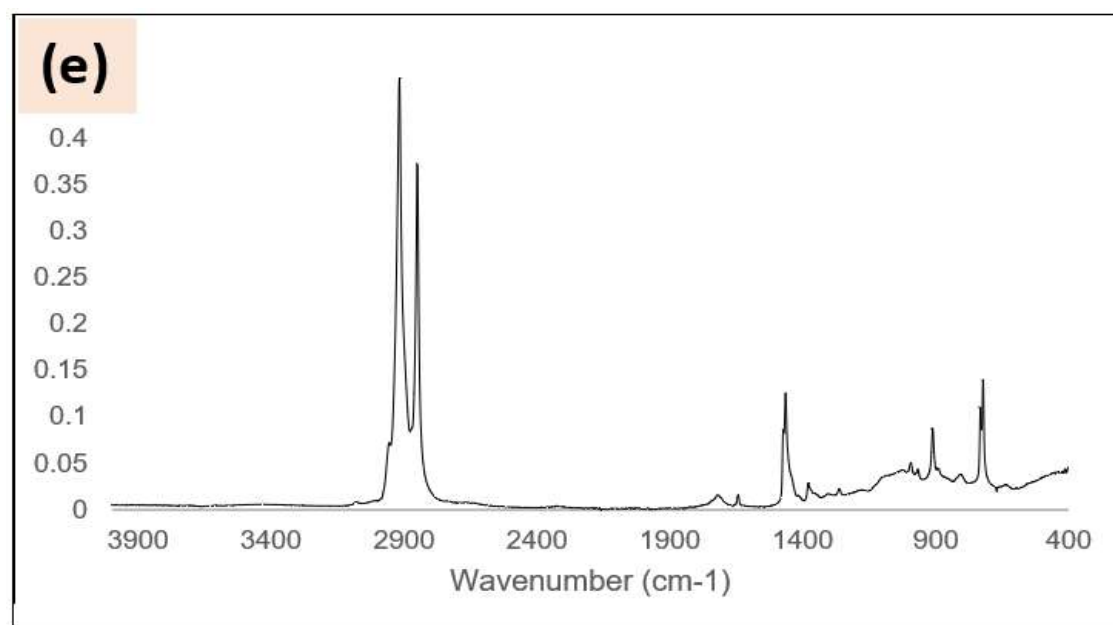
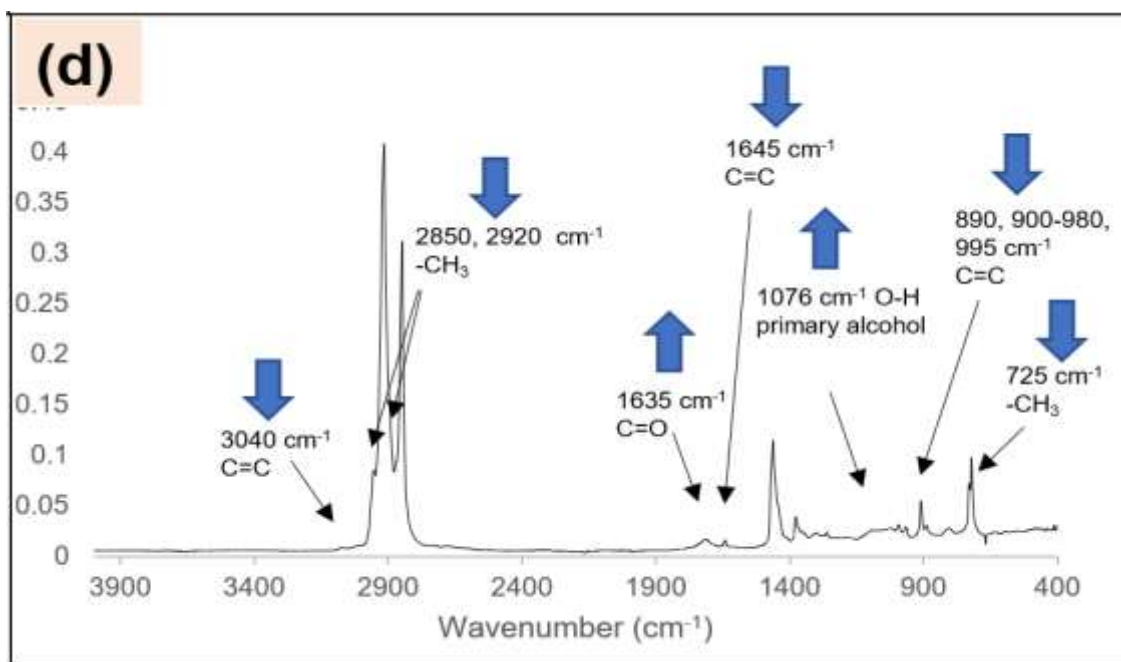


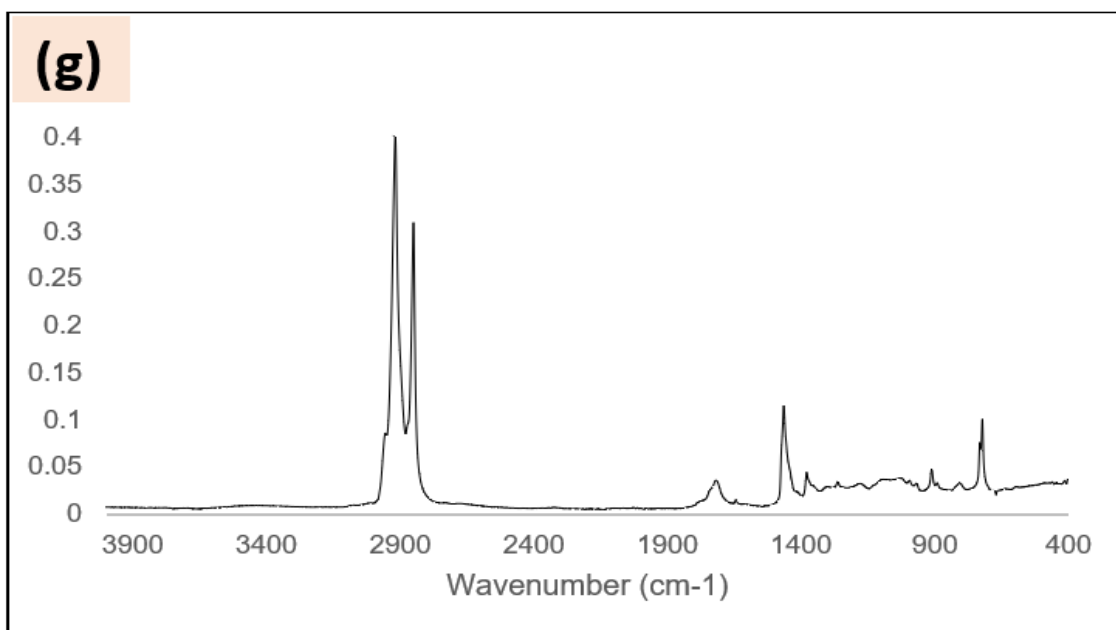
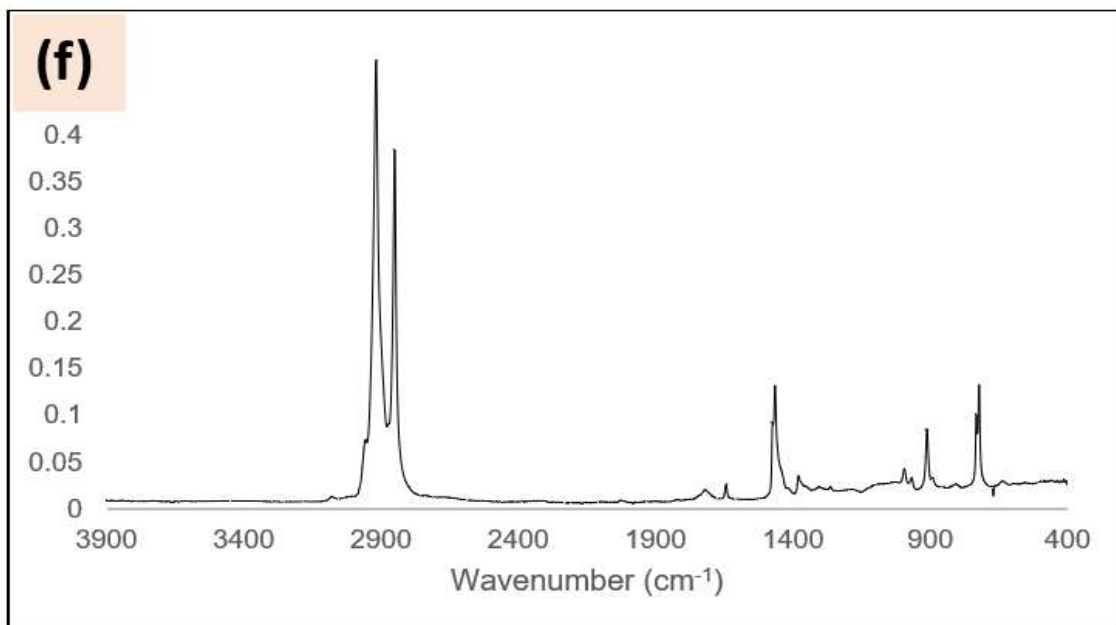
Appendix F

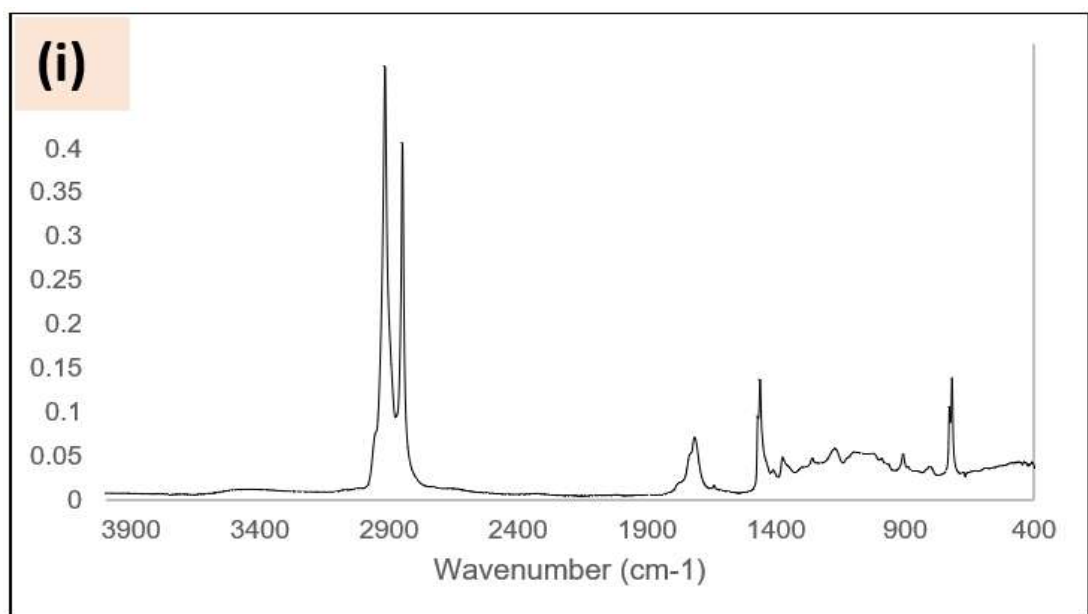
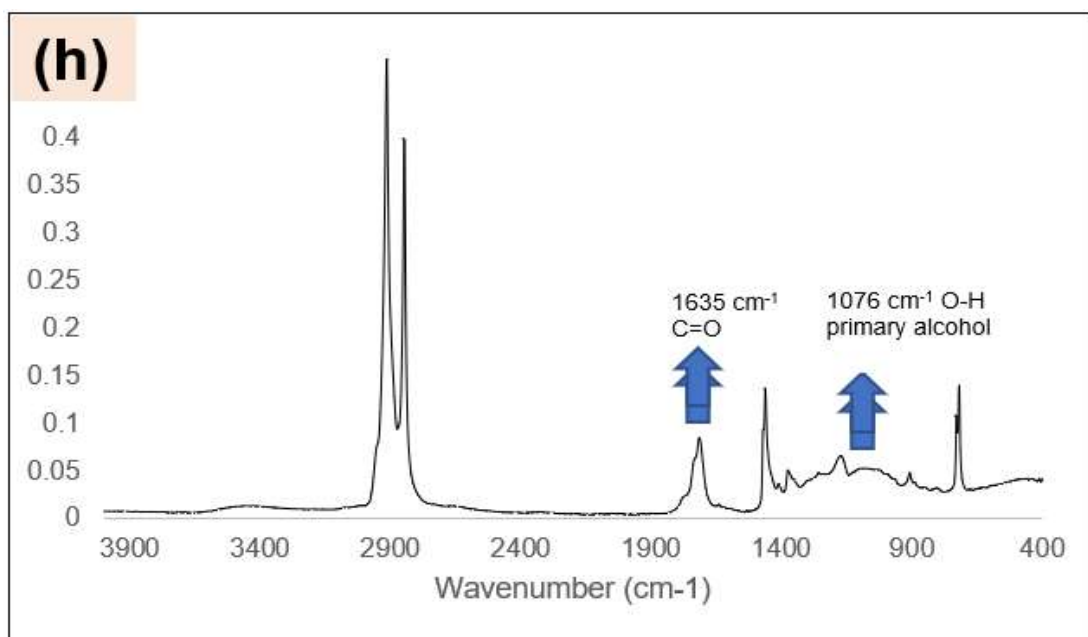
FTIR spectrum for (a) 450-2 wax, 1 hour @ 170°C, (b) 500-2 wax, 1 hour @ 170°C, (c) 550-2 wax, 1 hour @ 170°C, (d) 450-2 wax, 3 hours @ 170°C, (e) 500-2 wax, 3 hours @ 170°C, (f) 550-2 wax, 3 hours @ 170°C, (g) 450-2 wax, 6 hours @ 170°C, (h) 500-2 wax, 6 hours @ 170°C, (i) 550-2 wax, 6 hours @ 170°C.





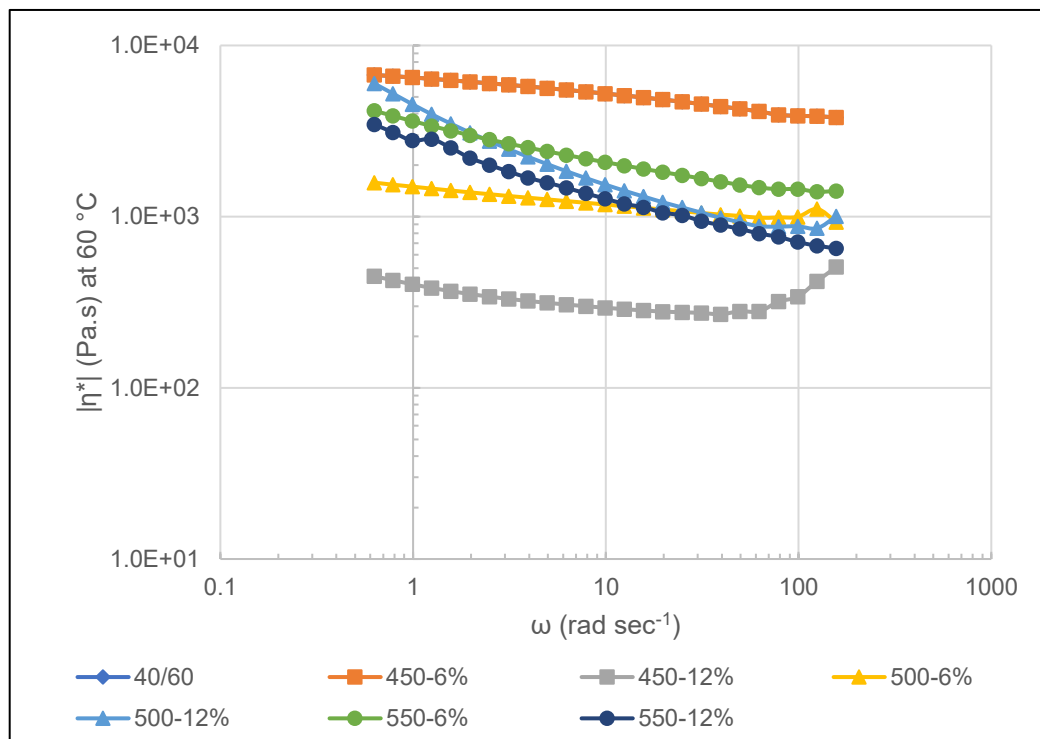
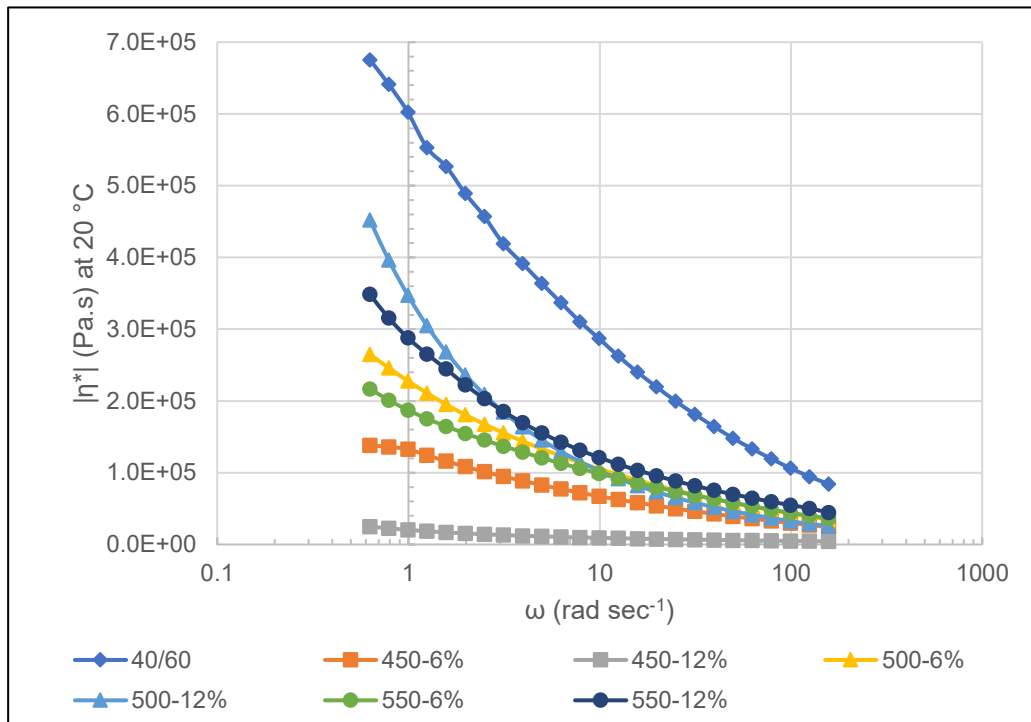






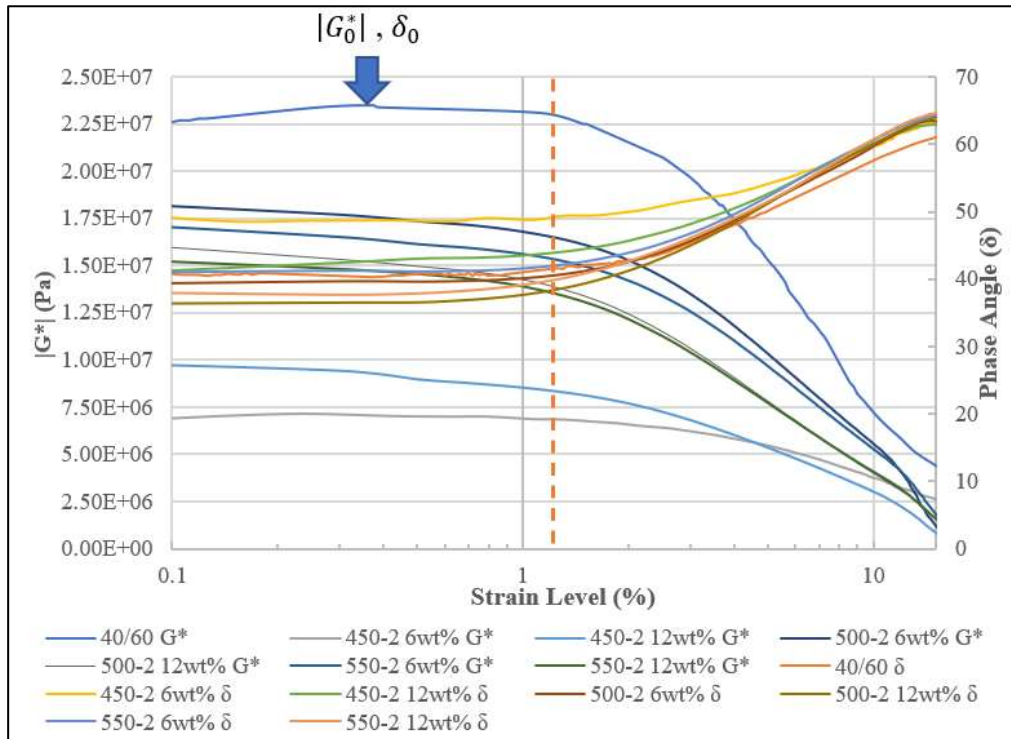
Appendix G

Complex viscosity as a function of oscillation (angular) frequency at 20 and 60 °C.



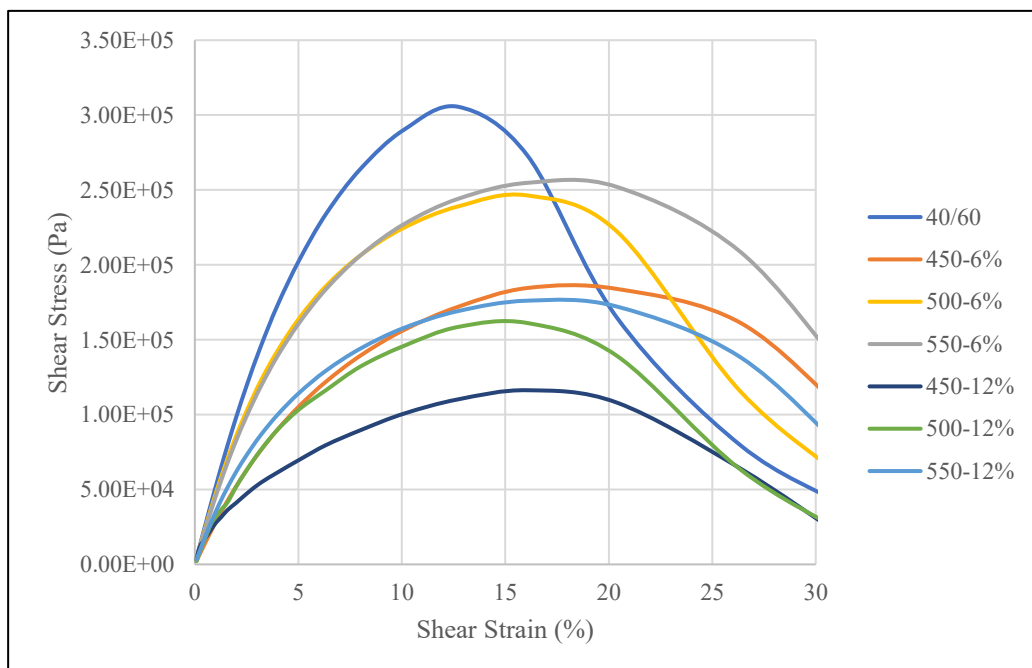
Appendix H

LAS test at 20 °C and 10 Hz used to obtain the ($|G_0^*|$) and (δ_0) of the RTFO+PAV aged binders in the undamaged condition.



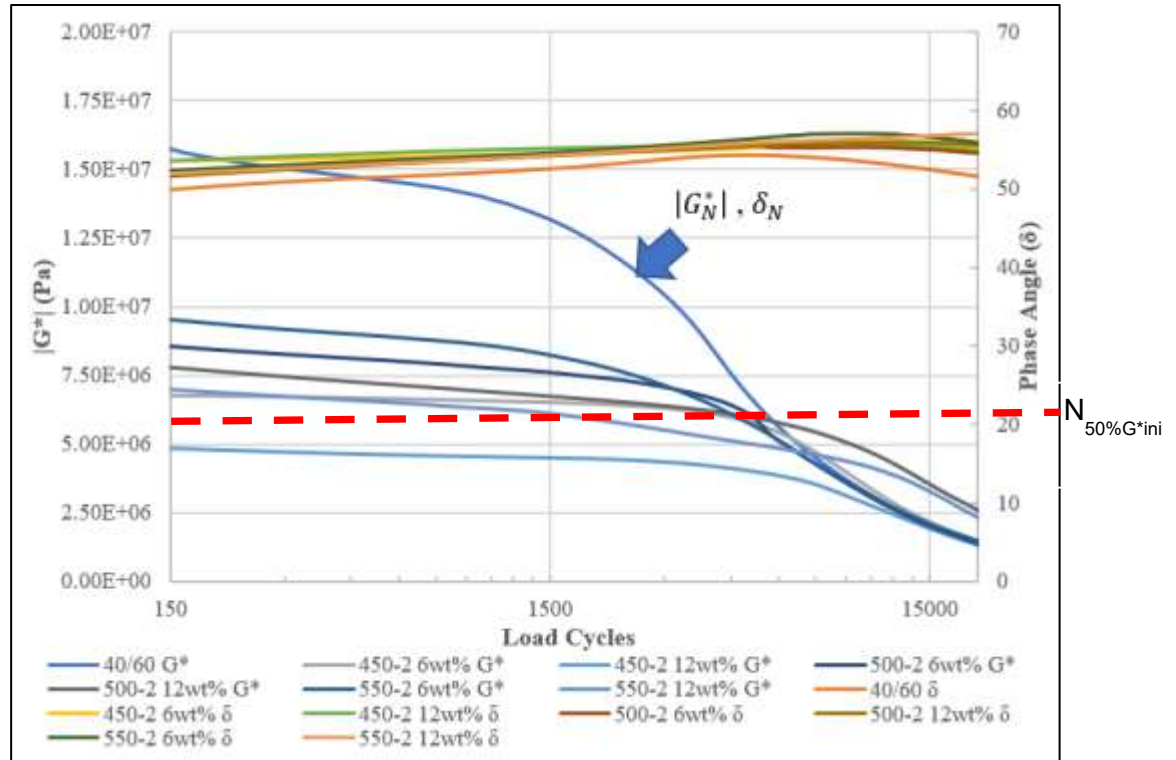
Appendix I

Stress versus strain curve from the LAS test conducted at 20 °C.



Appendix J

TS test at 20 °C, 10 Hz and 5% strain used to obtain the ($|G_N^*|$) and (δ_N) of the RTFO+PAV aged binders in the damaged condition.



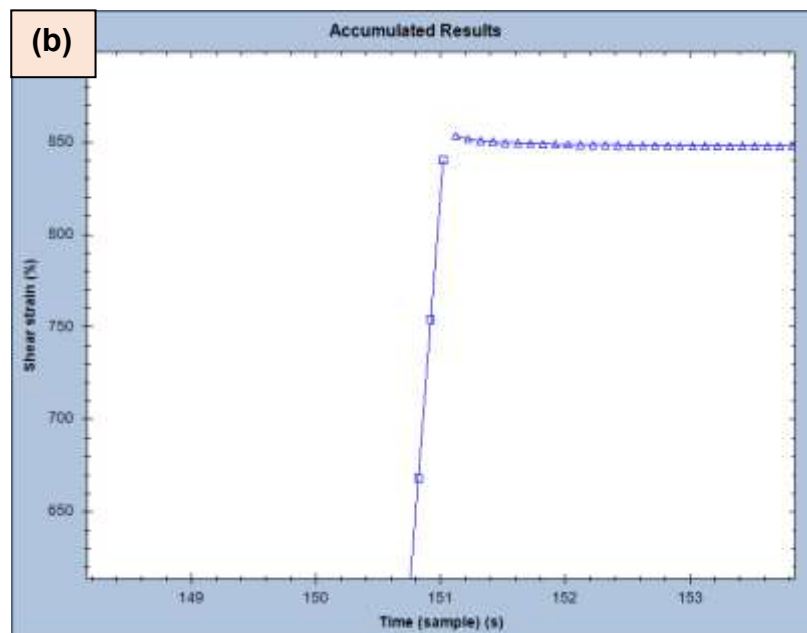
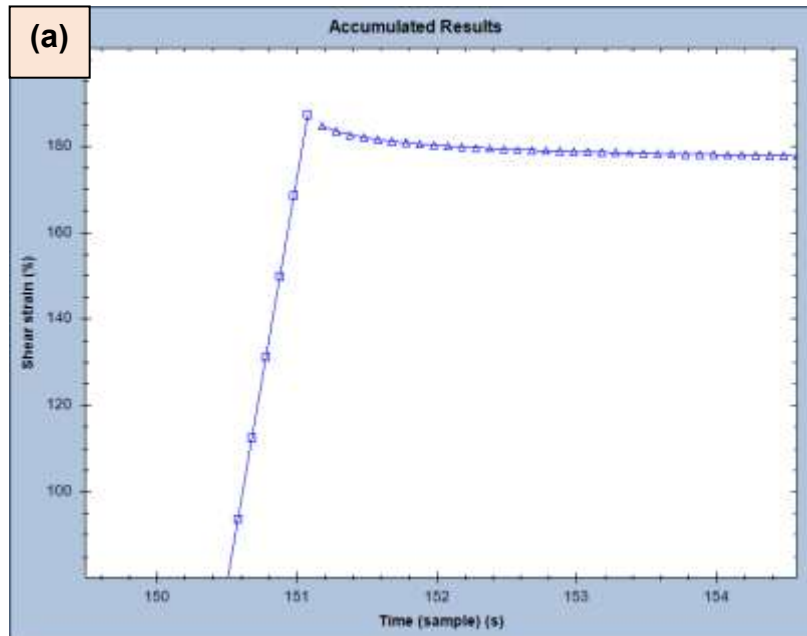
Appendix K

$N_{50\%G^*ini}$ values of the binders studied, determined from the TS test.

Binder	$N_{50\%G^*ini}$
40/60	4,100
450-6%	10,500
450-12%	11,850
500-6%	7,300
500-12%	13,150
550-6%	6,400
550-12%	13,600

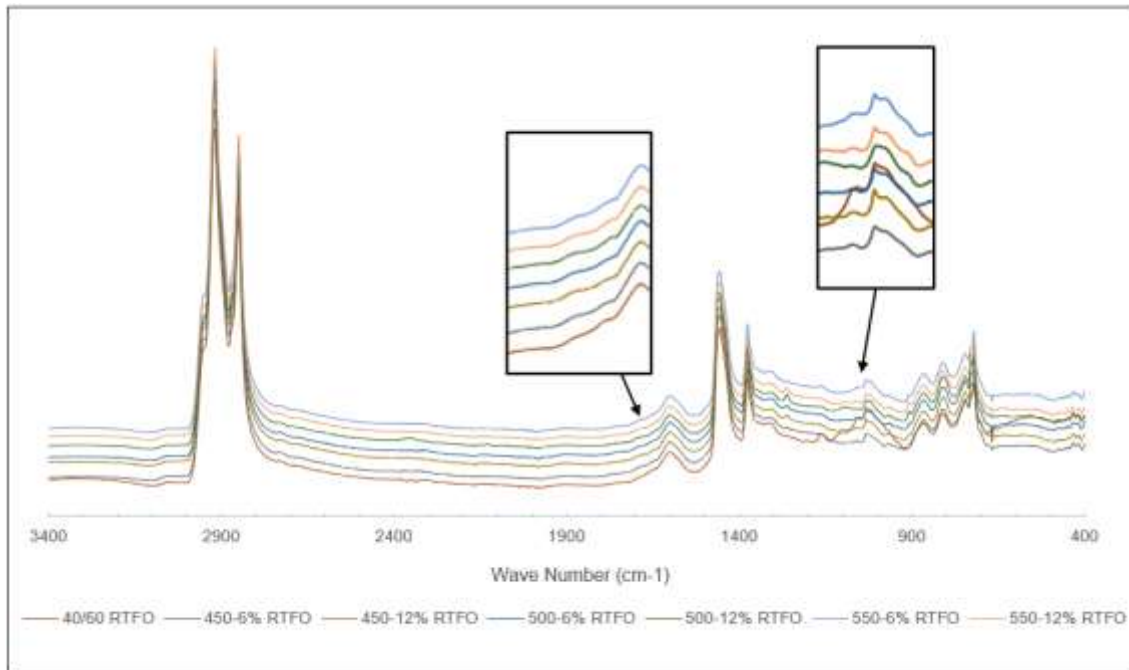
Appendix L

Example accumulated shear strain plots (taken from rSpace) from the MSCR test performed at 52 °C for the RTFO aged 40/60 binder: a) 0.1 kPa b) 3.2 kPa.



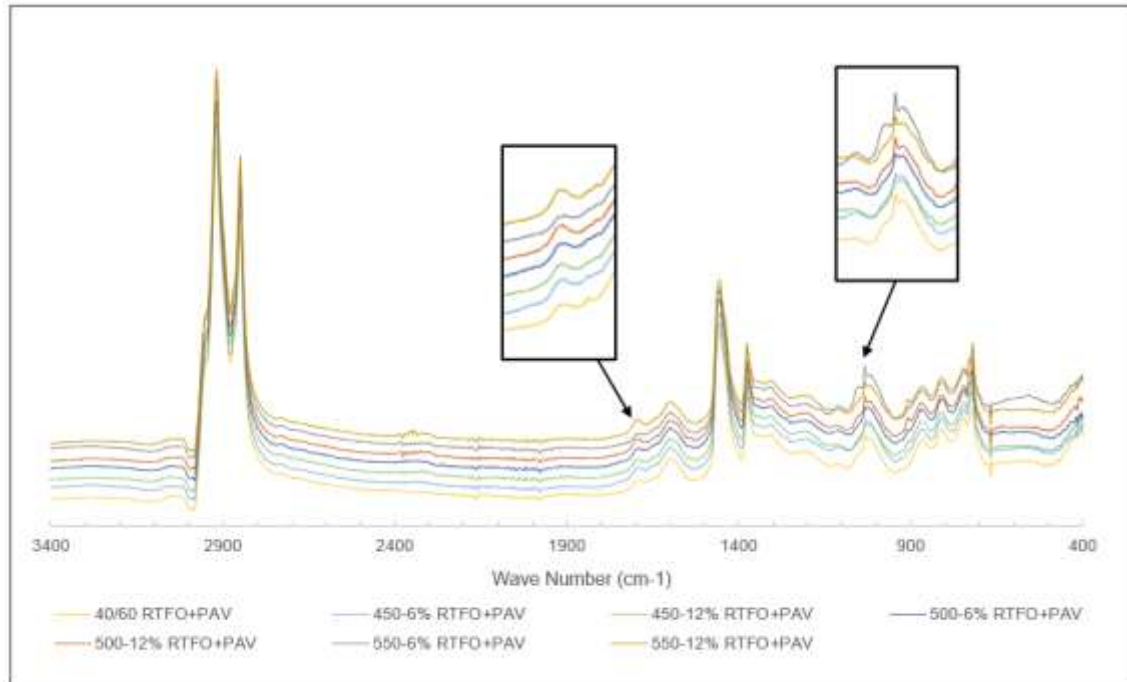
Appendix M

FTIR spectra of the short-term (RTFO) aged control and w-binders, with a focus on the C=O (1700 cm^{-1}) and S=O (1030 cm^{-1}) peaks.



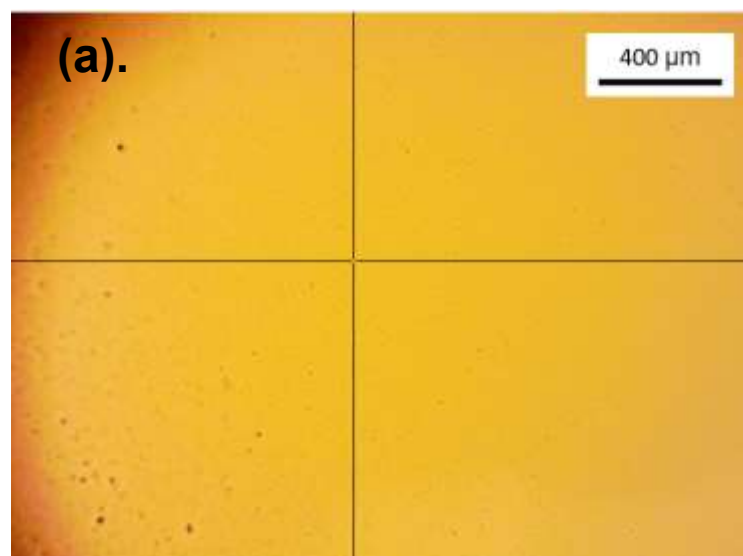
Appendix N

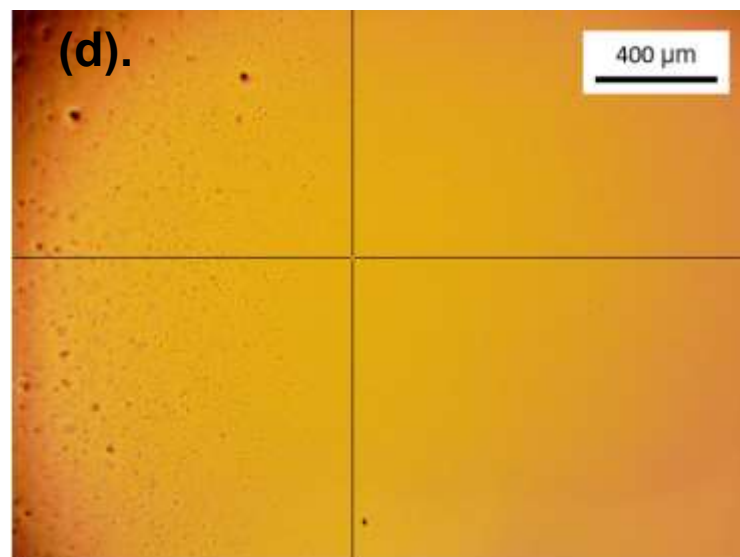
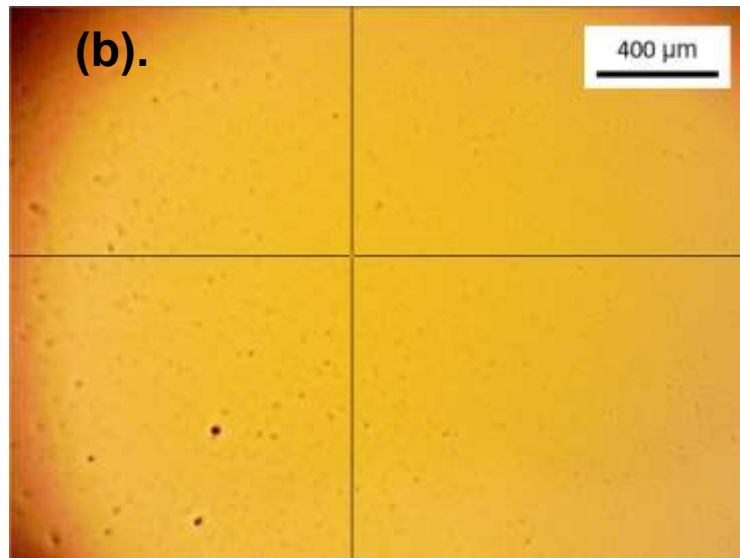
FTIR spectra of the long-term (PAV) aged control and w-binders, with a focus on the C=O (1700 cm^{-1}) and S=O (1030 cm^{-1}) peaks.

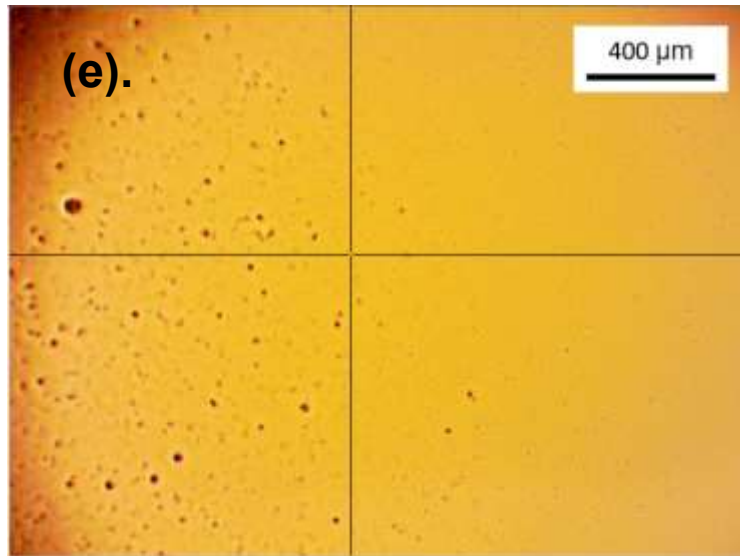


Appendix O

Optical microscope images of the control and w-binders for evaluation of dispersity in the aged (RTFO+PAV) condition: (a) 40/60, (b) 450-6%, (c) 450-12%, (d) 500-6%, (e) 500-12%, (f) 550-6%, (g) 550-12%.

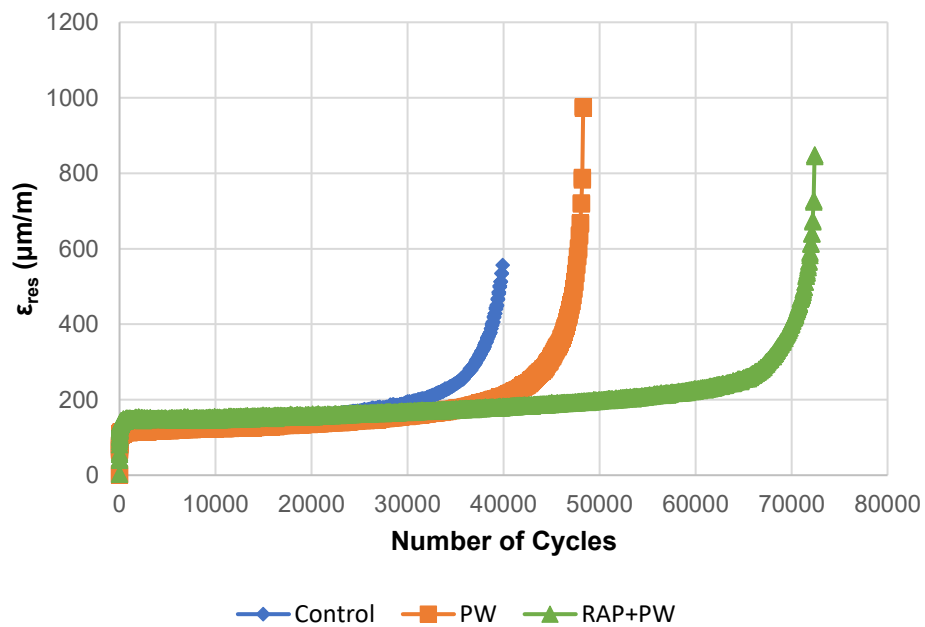
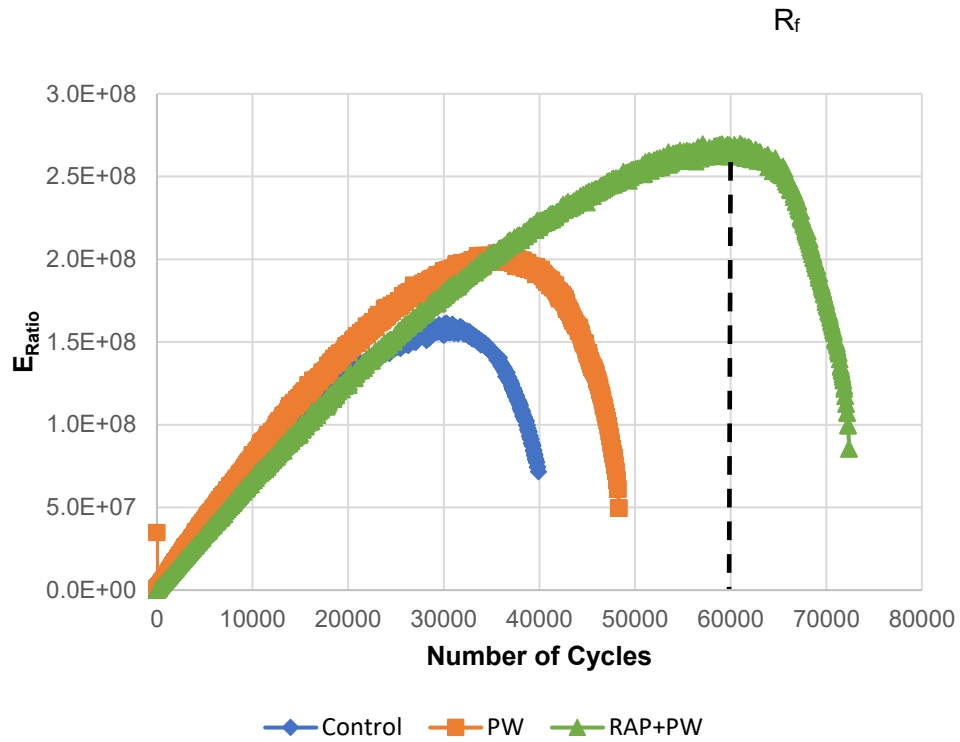






Appendix P

The resilient strain amplitude (ϵ_{res}) and energy ratio (E_{ratio}) plotted as a function of the number of cycles (N) from the ITFT test.



Appendix Q

The strain rate vs. number of load cycles from the RLAT test.

